Johannes Zschocke
K. Michael Gibson
Garry Brown
Eva Morava
Verena Peters *Editors*

JIMD Reports

Volume 13

SSIEM

Springer

JIMD Reports
Volume 13

Johannes Zschocke · K. Michael Gibson
Editors-in-Chief

Garry Brown · Eva Morava
Editors

Verena Peters
Managing Editor

JIMD Reports
Volume 13

Springer

SSIEM

ISSN 2192-8304 ISSN 2192-8312 (electronic)
ISBN 978-3-642-54148-3 ISBN 978-3-642-54149-0 (eBook)
DOI 10.1007/978-3-642-54149-0
Springer Heidelberg New York Dordrecht London

Contents

JIMD Reports
DOI 10.1007/8904_2013_262

INVITED ARTICLES

Newborn Screening for Glutaric Aciduria-II: The New England Experience

I. Sahai · C.L. Garganta · J. Bailey · P. James · H.L. Levy · M. Martin · E. Neilan · C. Phornphutkul · D.A. Sweetser · T.H. Zytkovicz · R.B. Eaton

Received: 03 June 2013 / Revised: 27 July 2013 / Accepted: 02 September 2013 / Published online: 5 November 2013

Abstract Newborn screening (NBS) using tandem mass spectrometry (MS/MS) permits detection of neonates with Glutaric Aciduria-Type II (GA-II). We report follow-up of positive GA-II screens by the New England Newborn Screening Program.

Methods: 1.5 million infants were screened for GA-II (Feb 1999–Dec 2012). Specialist consult was suggested for infants with two or more acylcarnitine elevations suggestive of GA-II.

Results: 82 neonates screened positive for GA-II, 21 weighing > 1.5 kg and 61 weighing ≤ 1.5 kg. Seven (one weighing < 1.5 kg), were confirmed with GA-II. Four of these had the severe form (died < 1 week). The other three have a milder form and were identified because of newborn screening. Two (ages > 5 years) have a G-Tube in place, had multiple hospitalizations and are slightly hypotonic. The third infant remains asymptomatic (9 months old). Two GA-II carriers were also identified. The remaining positive screens were classified as false positives (FP). Six infants (> 1.5 kg) classified as FP had limited diagnostic work-up. Characteristics and outcomes of all specimens and neonates with a positive screen were reviewed, and marker profiles of the cases and FP were compared to identify characteristic profiles.

Conclusion: In addition to the severe form of GA-II, milder forms of GA-II and some GA-II carriers are identified by newborn screening. Some positive screens classified as FP may be affected with a milder form of the disorder. Characteristic GA-II profiles, quantified as GA-II indexes, may be utilized to predict probability of disorder and direct urgency of intervention for positive screens.

Communicated by: Piero Rinaldo, MD, PhD

Competing interests: None declared

I. Sahai · J. Bailey · T.H. Zytkovicz · R.B. Eaton
New England Newborn Screening Program, University of Massachusetts Medical School, Jamaica Plain, MA, USA

I. Sahai · M. Martin · T.H. Zytkovicz · R.B. Eaton
Department of Pediatrics, University of Massachusetts Medical School, Worcester, MA, USA

I. Sahai · D.A. Sweetser
Department of Pediatrics, Massachusetts General Hospital, Boston, MA, USA

I. Sahai · P. James · H.L. Levy · E. Neilan · D.A. Sweetser
Department of Pediatrics, Harvard Medical School, Boston, MA, USA

C.L. Garganta
Department of Pathology and Laboratory Medicine, Tufts Medical Center, Boston, MA, USA

P. James · H.L. Levy · E. Neilan
Department of Medicine, Boston Children's Hospital, Boston, MA, USA

M. Martin
Department of Pediatrics, University of Massachusetts Medical Center, Worcester, MA, USA

C. Phornphutkul
Department of Pediatrics, Rhode Island Hospital, Brown University, Providence, RI, USA

I. Sahai (✉)
305 South St,
Jamaica Plain 02130 MA, USA
e-mail: inderneel.sahai@umassmed.edu

Abbreviations

C0	Free carnitine
C10	Decanoylcarnitine
C10OH	Hydroxydecanoylcarnitine
C14	Tetradecanoylcarnitine
C14:1	Tetradecenoylcarnitine
C2	Acetylcarnitine
C3	Propionylcarnitine

C4	Butyrylcarnitine
C5	Isovalerylcarnitine
C5DC	Glutarylcarnitine
C5OH	Hydroxyisovalerylcarnitine
C6	Hexanoylcarnitine
C8	Octonoylcarnitine
DOL	Day of life
ETF	Electron transfer flavoprotein
ETF-DH	Electron transfer flavoprotein dehydrogenase
FAOD	Fatty acid oxidation defects
FP	False positive
GA-II	Glutaric aciduria-type II
MADD	Multiple acyl-CoA dehydrogenase deficiency
MCAD	Medium chain acyl-CoA dehydrogenase deficiency
MS/MS	Tandem mass spectrometry
NBS	Newborn screening
NENSP	New England Newborn Screening Program
NICU	Neonatal intensive care unit
OOR	Out of range
SCAD	Short-chain acyl-CoA dehydrogenase deficiency
TP	True positive
TPN	Total parental nutrition
VLBW	Very low birth weight
VLCADD	Very long chain acyl-CoA dehydrogenase deficiency

Introduction

Glutaric Aciduria Type II (GA-II; also known as multiple acyl-CoA dehydrogenase deficiency or ethylmalonic-adipic aciduria; OMIM 231680) is an autosomal recessive disorder of fatty acid oxidation and amino acid metabolism (Frerman and Goodman 2001). The underlying etiology is a functional deficiency of the electron transport flavoprotein (ETF, comprised of the alpha and beta subunits; ETFA, ETFB 130410) or electron transfer flavoprotein dehydrogenase (ETF-DH; EC 1.5.5.1), caused by mutations in any one of the *ETFA*, *ETFB*, or *ETFDH* genes (Goodman et al. 2002; Olsen et al. 2007).

GA-II can present as either a severe neonatal form with or without congenital anomalies, or as a milder late-onset disease (Al-Essa et al. 2000; Bohm et al. 1982; Curcoy et al. 2003; de Visser et al. 1986; Loehr et al. 1990; Rhead et al. 1987). Individuals with the severe neonatal form usually present within 24–48 h after birth with severe metabolic abnormalities (nonketotic hypoglycemia, metabolic acidosis, hyperammonemia, lactic acidosis), hypotonia, hepatomegaly, and cardiomegaly, and have a rapidly fatal course. Individuals with the mild form can present at any age with episodic illness (lethargy, vomiting, abdominal pain, hepatomegaly, cardiomegaly, rhabdomyolysis, ataxia) and metabolic abnormalities worsened by catabolic stress. Treatment for the severe form is ineffective. Treatment for the milder form consists of dietary modifications and supplementation with riboflavin and carnitine (Frerman and Goodman 2001)

In the severe form of the disease, a diagnosis can usually be made based on characteristic urine organic acid (UOA) and plasma acylcarnitine (PAC) profiles (Frerman and Goodman 2001). In the milder form, characteristic biochemical profiles may be exhibited only during an acute metabolic crisis. In such cases, enzymatic analysis or molecular studies may be required to make a definitive diagnosis.

Tandem mass spectrometry (MS/MS) makes it feasible to measure numerous acylcarnitines in dried blood spots enabling screening for several fatty acid oxidation defects (FAOD) and organic acidurias (OA) (Millington et al. 1990). GA-II is also detected by newborn screening (NBS). We report the experience of the New England Newborn Screening Program (NENSP) in identifying individuals at risk for GA-II, diagnostics of the positive screens, and long-term outcomes of confirmed cases born in MA, ME, RI, NH, and VT (defined "region" for this report).

Methods and Population

The NENSP has been routinely analyzing acylcarnitines and amino acid markers on NBS dried blood spot specimens since 1999. Screening specimens are obtained between 24–72 h of birth. For infants in the neonatal intensive care units (NICU) and very low birth weight infants (VLBW; Weight $\leq$ 1.5 kg), additional specimens are requested at 2 weeks, 1 month, and at discharge. The laboratory procedure, as previously reported (Zytkovicz et al. 2001), involves extraction from the dried blood spots into a methanol solution with stable isotope-labeled internal standards with butylation prior to analysis by MS/MS. Measurement of C2 acylcarnitine was added in 2002.

Positive screening results wherein one or more markers exceed a defined cutoff are communicated to the primary care provider with recommendations for management (which may include referral to a metabolic specialist). Diagnostic testing is performed under the guidance of the specialist. The NENSP and partner states track all positive screens from the region until resolution of diagnosis (short-term follow-up), as determined by the specialist, and tracks confirmed cases periodically to obtain long-term follow-up information. The final diagnosis and results of confirmatory studies are provided to the NENSP by the specialists. The long-term follow-up information is usually obtained from

the metabolic specialist and occasionally from the primary care provider. Data elements collected include date of last specialty visit, treatment, growth parameters, episodes of metabolic crises, biochemical abnormalities, hospitalizations, and disorder-related clinical sequelae (developmental delays, hypotonia, cardiomyopathy). Information about false negatives is obtained by the NENSP by surveying metabolic specialists periodically.

Consultation with a specialist has always been recommended for all positive screens with elevations of two or more acylcarnitines suggestive of a GA-II profile, regardless of the results of a follow-up screen (if performed). However, contact algorithms have evolved during the study period. Since July 2006, the NENSP has been sorting positive screens into categories ("2006 algorithm") based on a GA-II Index: (1) "High Risk" for GA-II are elevations of two or more acylcarnitines in conjunction with a GA-II Index [C4xC5 x C8xC14]/ [C0xC3] value of $\geq$ 0.005 and (2) "Risk" for GA-II are elevations of two or more acylcarnitines, but GA-II Index is $<$ 0.005. For "High Risk" results, an urgent consultation with a specialist is recommended; for "Risk" results a non-urgent consultation is suggested. The NENSP does not have separate cutoff values for the acylcarnitines at different ages, and specimens collected beyond 30 days of life are not stratified by risk.

The cohort for this report is limited to all infants born in the defined region and screened using MS/MS by the NENSP from February 1, 1999, to December 31, 2012. A retrospective review of the NENSP data was performed and neonates with a screening profile suggestive of GA-II, in a specimen collected within the first 30 days of life, were identified. A "GA-II profile" is defined as an elevation of two or more acylcarnitines associated with at least two distinct flavin-containing acyl-CoA dehydrogenase enzymes involved in GA-II. Among the markers screened by the NENSP, these would include acylcarnitines from the following groups: (i) C4, (ii) C5, (iii) C5DC, (iv) C8, C6, C10, (v) C12, C14:1, C14. Elevations of two or more acylcarnitines consistent with another specific disorder are excluded; for example, elevation of C8, C6 with C10OH would suggest medium-chain acyl-CoA dehydrogenase deficiency (MCADD; OMIM 201450). Diagnostic and long-term follow-up data were analyzed. Short-term and long-term outcomes were analyzed for neonates with a newborn screening profile suggestive of GA-II

Results

Approximately 1.5 million neonates in the cohort received MS/MS screens. Figure 1 summarizes the characteristics and outcomes of all specimens and neonates found to have multiple acylcarnitine elevations with a "GA-II profile" in at least one specimen collected within 30 days of birth. The first out-of-range (OOR) specimen for each baby is shown, and whether this was the "initial" specimen (all collected 24–72 h of age) or "not initial" (all collected as per routine rescreening protocol). Of the 82 infants with a "GA-II profile," 21 had birth weights $>$ 1.5 kg. In 20, the OOR result was seen in the initial screen and only one had an initial normal followed by and an OOR result. Sixty-one specimens were from VLBW infants. In 11 VLBW infants, the OOR result was seen in the initial specimen, and in the other 50 infants on a subsequent screen. Follow-up screening specimens were received from several neonates after the OOR result, and their results are shown as either normal, abnormal (if any acylcarnitine was out-of-range), or not available. All follow-up specimens were received within a week of the OOR result. Infants are classified as True Positives (TP; Confirmed GA-II), Carriers, and False Positives (FP; Not GA-II or GA-II carriers) based on the assessment of the treating physician. The data of the FPs were reviewed to determine the extent of their diagnostic evaluations, and those with limited diagnostic evaluations are shown as incomplete work-up. All confirmed GA-II cases and carriers had an OOR GA-II profile on the initial specimen. We are aware of no false negative newborn screens for GA-II in the study cohort.

The clinical presentations and confirmatory studies performed on the cases and carriers of GA-II are summarized in Table 1. Table 2 shows the concentrations of relevant acylcarnitines in all confirmed GA-II cases, carriers, and the 12 FP neonates $>$ 1.5 kg with an OOR result on the initial screen.

In our cohort, a total of seven cases of GA-II and 2 GA-II carriers were identified. Four of the seven cases had the severe neonatal form and are deceased. Three of these infants had malformations and a severe FAOD was clinically suspected even before an NBS screen was obtained. In the fourth neonate (Case 2) a metabolic disorder had not been considered until results of NBS became available. Three of the seven cases have a milder form of the disorder. Case 5 is notable because the characteristic biochemical profiles were not present in the diagnostic work-up in the neonatal period, and GA-II was eventually confirmed in the 2nd year of life. In this case, screening results suggesting a risk for GA-II were reported on day of life (DOL) 6. UOA and a repeat screen were normal. However, PACs revealed mild elevations of long-chain acylcarnitines and thus a diagnosis of very long chain acyl-CoA dehydrogenase deficiency (VLCAD; OMIM 201475) was entertained. Treatment in the form of avoidance of fasting and a high-carbohydrate, low-fat diet was initiated. The infant had several episodes of dehydration and hypoglycemia in the first 6 months of life, and elevations of urinary ethylmalonic acid were noted at 6 months of age. In vitro fibroblast testing for FAODs was

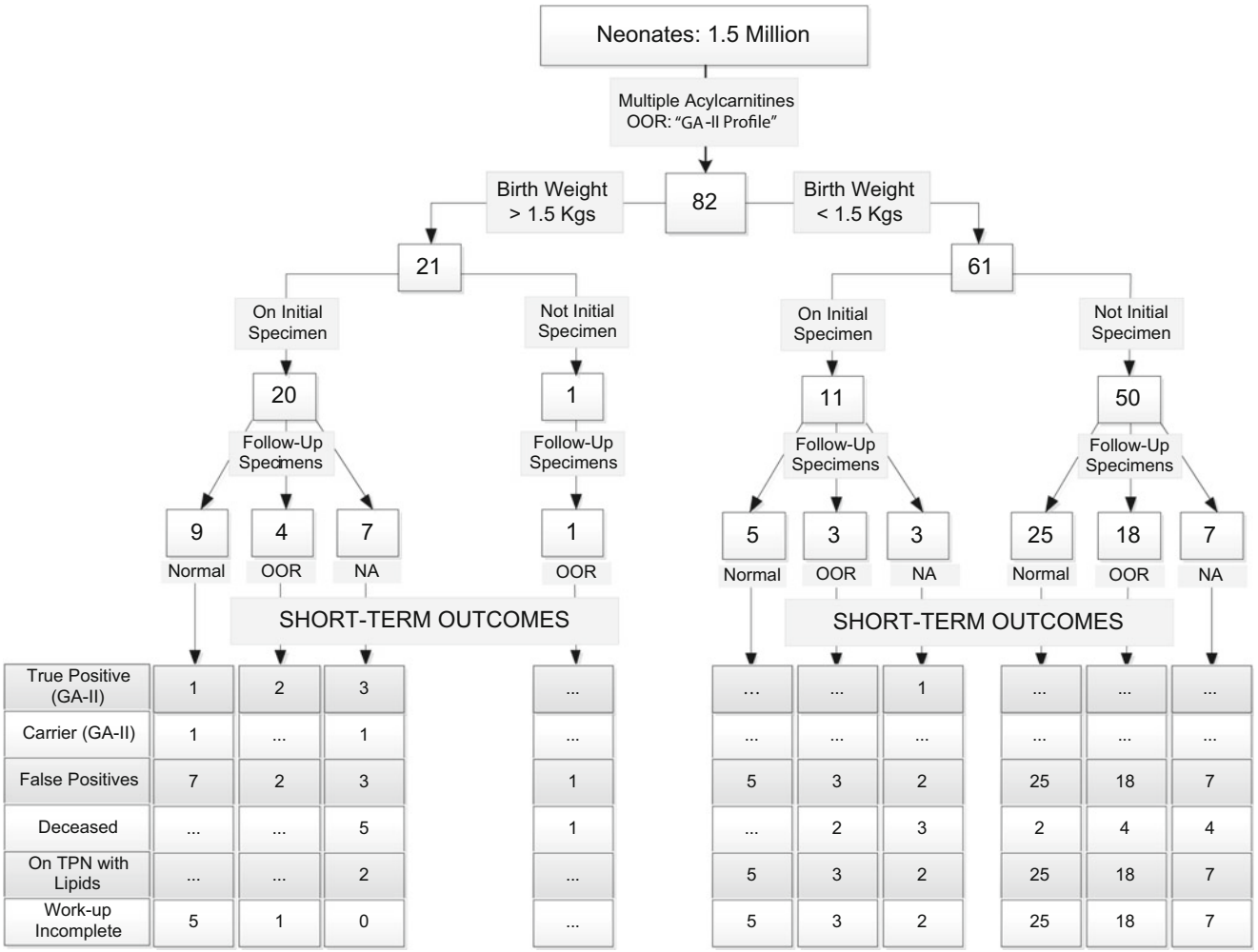

Fig. 1 Characteristics and outcomes of all specimens and neonates found to have multiple acylcarnitine elevations with a "GA-II profile" in at least one specimen collected within 30 days of birth. Consultation with a specialist is recommended for all out-of range (OOR) screens with acylcarnitines suggestive of a GA-II profile, regardless of the results of a follow-up screen (if performed). Initial specimens were all collected at 24 to72 h of age and those shown as "Not Initial" specimens were collected at 72 h to 30 days of age. "Not Initial" specimens were collected as per routine rescreening protocols and the initial screens from these neonates were in range. False positives with limited work-up are shown as work-up incomplete. Please see text for details

reported as "consistent" with short-chain acyl-CoA dehydrogenase deficiency (SCAD; OMIM 201470) and the child was diagnosed with SCAD. At 1-and-1/2 years of age, UOA revealed a profile consistent with GA-II, eventually confirmed by repeat enzymatic studies. A mutation analysis was not pursued for SCAD, and it is feasible that the child harbors one or more alterations in the SCAD gene in addition to the documented mutations in the ETFDH gene. Two infants (Cases 8 and 9) were classified as GA-II carriers, based on the results of confirmatory testing, and remain asymptomatic.

Twelve of the 20 infants > 1.5 kg with an OOR result on the initial screen were classified as FP. Six were FP based on negative results of evaluations beyond initial biochemical testing (Cases 10–15). One neonate was found to have pathogenic alterations in one copy each of the MCAD and VLCAD genes. MCAD and VLCAD carriers have been detected by screening and the coincidental presence of carrier status for both could result in the multiple acylcarnitine pattern seen in this case. Whether it would lead to a clinical phenotype due to synergestic heterozygosity has not been established, but the increased C2 acylcarnitine in NBS suggests significant capacity for fasting and the individual remains asymptomatic (4 years old). The other five OOR results were attributed to non-metabolic causes such as renal or respiratory failure. Hemolysis or jaundice was reported in all five. The only neonate weighing > 1.5 kg who had a normal initial screen followed by an OOR result (mild elevations of C0, C5, C8) on a subsequent screen was on total parenteral nutrition (TPN) at time of specimen collection. Routine laboratory investigations and diagnostic UOA and PAC were normal. The infant was diagnosed with

Table 1 Clinical information and results of diganotic studies of all cases and carriers of Glutaric Aciduria Type II (GA-II) identified by the New England Newborn Screening Program in the defined cohort during the period February 1999 through December 2012

	Clinical presentation		Confirmatory studies				Additional information
ID	Prenatal and Birth history	Neonatal course	Urinary organic acids & acylglycines	Plasma acylcarnitines	Molecular analysis	Enzymatic studies	Autopsy findings
1	Born at 31 weeks gestation following premature rupture of membranes. Apgars 6 & 9*; Wt 1.3 kg. Agenesis of corpus callosum, complex heart defects, cleft lip & palate, enlarged echogenic kidneys and bilateral clubfeet noted at initial prenatal visit (2 weeks prior to delivery). Maternal history of a previous fetal demise at 28 weeks gestation with similar anomalies; she also had a healthy 6 year old son	Lethargic & hypotonic at birth and required endotracheal intubation. Metabolic acidosis noted that initially responded to acetate supplementation. Acute decompensation with hypotension, apnea and hypoglycemia developed on DOL 4. Investigations revealed hypoketotic hypoglycemia, hyperammonemia, metabolic acidosis, elevated CK. The hypoglycemia responded to increased IV glucose, but hyperammonemia & metabolic acidosis persisted. A severe FAOD (GA-II/CPT-II) suspected. Based on grim prognosis, ventilator support withdrawn and neonate died on DOL 7. NBS results, indicating a high risk for GA-II, were reported on DOL 7 after baby was deceased	Markedly increased lactic acid & glutaric acids. Mildly increased ethylmalonic acid, 2-hydroxyglutaric acid & its lactone, and isovalerylglycine	Elevations of acylcarnitine species of all chain lengths	. . .	. . .	Extensive lipid deposition in the heart, muscle, liver and kidneys. Bilateral cleft lip and palate, cardiomegaly with 2 small muscular ventriculoseptal defects, diffusely cystic kidneys with features of acute tubular necrosis.
2	Born at term. Apgars 9 & 9*; Wt 3.2 kg. Placental abruption during delivery suspected. No dysmorphic features noted	Pale and jittery few hours after birth with glucose of 10 mg/dl. Given dextrose bolus, and maintenance intravenous (IV) dextrose continued for 48 h. Was under observation in hospital and appeared to be doing well, when neonate turned pale and collapsed while being fed,	. . .	. . .	. . .	ETF Activity < 0.1 nmol/min/mg (Controls 0.8–2.4). Skin sample for fibroblast culture obtained post mortem	Extensive lipid deposition in heart, muscles, renal tubules and adrenal cortex. Marked thymic involution.

(continued)

Table 1 (continued)

	Clinical presentation		Confirmatory studies				Additional information
ID	Prenatal and Birth history	Neonatal course	Urinary organic acids & acylglycines	Plasma acylcarnitines	Molecular analysis	Enzymatic studies	Autopsy findings
		8 h after discontinuation of IV dextrose. NBS specimen collected a few hours prior to death indicated a high risk for GA-II					
3	Delivered at 37 weeks of gestation due to IUGR. Apgars 7 & 8*; Wt 2.1 kg. Bilateral echogenic kidneys had been noted at 22 weeks, and IUGR & oligohydramnios noted at 32-weeks of gestation. Hypertelorism & low set ears noted at birth	Developed respiratory distress and seizures within an hour of birth and was extremely hypotonic and required endotrac heal intubation. Investigations revealed hypoketotic hypoglycemia, hyperammonemia, metabolic acidosis. A severe FAOD (GA-II/ CPT-II) suspected. Head ultrasound revealed calcification in vessels around the midbrain. An echocardiogram revealed severe left ventricular dysfunction. Metabolic acidosis and hypotension refractory to treatment and baby died on DOL 2. The NBS results, indicating a high risk for GA-II, were reported after baby was deceased	Markedly increased ethylmalonic, glutaric, 2-hydroxyglutaric and adipic acids. Mildly increased methylsuccinic, suberic, sebacic, 5-hydroxyhexanoic & 7-hydroxyoctanoic acids and isovaleryl, 2-methylbutyryl & hexanoylglycines	Elevations of multiple acylcarnitine species (C4, C5, C6, C12, C14, C16, C12:1, C14:1, C14:2, C18, C18:1) suggestive of GA-II	ETFDH Gene: Two muations identified [c.121C>T: p. R41X; c.1648_1649delCT : p.L550VfsX4] Confirmed to be in trans	…	Extensive lipid deposition in heart, muscles and adrenal cortex. Marked thymic involution. Pulmonary hypoplasia, bilobed lungs, renal dysplasia, particularly medullary with dilated tubules and cysts, focal polymicrogyria in the cerebrum and fetal osteosclerosis.
4	Born 37 weeks of gestation. Apgars 8 & 9*. Wt 3.2 kg. Hydrocephalus noted at 22 weeks of gestation. Head ultrasound at birth revealed prominent cystic areas adjacent to lateral ventricles with surrounding leukomalacia in addition to the hydrocephalus. Frontal	Feeding poorly on DOL-1 and had mild hypoglycemia that resolved with dextrose bolus. Lethargic and hypotonic on DOL-2, with severe hypoketotic hypoglycemia, hyperammonemia and metabolic acidosis. Hypoglycemia and	Markedly increased lactic, ethylmalonic, methylsuccinic, glutaric & 2-hydroxyglutaric acids with mildly increased 3-hydroxybutyric, saturated & unsaturated dicarboxylic acids and isovaleryl, butyryl, hexanoyl & suberylglycines	…	…	…	

	bossing, large anterior fontanelle and hypertelorism reported	metabolic acidosis resolved quickly with IV glucose, but hyperammonemia persisted. A severe FAOD (GA-II/CPT-II) suspected. Supportive measures initiated but neonate died on DOL-7. The NBS results, indicating a high risk for GA-II were reported on DOL-4					
							Follow-Up Information
5	Born 6 days post due date. Apgars 9 & 9*; Wt 3.6 kg. No dysmorphic features	No clinical issues were noted and was discharged home on DOL 3. NBS results suggesting high risk for GA-II were reported on DOL 6 and metabolic work-up initiated by specialist. The organic acid analysis was normal as was a follow-up screen collected on DOL 7. Plasma acylcarnitines revealed mild elevations of long chain acylcarnitines so a diagnosis of VLCAD suspected. Treatment (avoidance of fasting, a high carbohydrate and low fat) initiated for FAOD	During Illness at 1-1/2 years: Markedly increased ethylmalonic and adipic acids. Mildly increased methylsuccinic & 3-hydoxydicarboxylic acids and isovaleryl, butyryl, hexanoyl & suberylglycines	During Illness at 1-1/2 years: Elevations of multiple acylcarnitine species (C4, C5, C5DC, C6, C8, C10, C12, C14:2, C14:1, C14, C16) suggestive of GA-II	ETGDH Gene: Two mutations identified [c.121C>T : p.R41x; c.1448C>T : p.P483L] Confirmed to be in trans	ETF-DQ 1.4 nmol/min/mg (Controls 6.5–12.4)	Infant had 3 hospital admissions for dehydration and hypoglycemia in the first 6-months of life. Supplemental G-Tube feeding was initiated at 6 months of life. Elevations of ethylmalonic acid were noted in the urine during a hospitalization at 6 months of age, and skin samples for enzymatic studies on fibroblasts were sent out. These were supportive of SCAD and infant was diagnosed with SCAD. During another admission at 1-1/2 years of age laboratory findings suggestive of GA-II. Repeat enzymatic studies were performed and diagnosis

(continued)

Table 1 (continued)

	Clinical presentation		Confirmatory studies				Additional information
ID	Prenatal and Birth history	Neonatal course	Urinary organic acids & acylglycines	Plasma acylcarnitines	Molecular analysis	Enzymatic studies	Autopsy findings
							confirmed. Riboflavin was initiated. Child continues to have episodes of biochemical abnormalities but frequency has decreased with age. Currently>10 years, child has mild hypotonia and difficulties with sustained activities but otherwise is doing well. Growth measurements are at the 50th %ile for age.
6	Born at term. Apgars 9 & 9*; Wt 3.7 kg. No dysmorphic features	Pallor and tachypnea noted at 25 h after birth attributed to an intrauterine bleed. Symptoms resolved quickly with a few hours of IV hydration and was discharged home on DOL 3. NBS results suggesting high risk for GA-II were reported on DOL 6 and metabolic work-up initiated by specialist on the same day	Markedly increased ethylmalonic & glutaric acids. Mildly increased isovaleryl, hexanoyl & suberylglycines	Elevations of multiple acylcarnitine species (C4, C5, C6, C8, C10:1, C10, C12, C14, C16, C12:1, C14:1, C14:2) suggestive of GA-II	ETFDH Gene: Two muations identified [c.1082A>G: p. Y361C; c.1648_1649delCT: p.L550VfsX4] Confirmed to be in trans	. . .	Treatment (avoidance of fasting, a high carbohydrate and low fat diet, carnitine and riboflavin) initiated. Supplemental G-Tube feeding initiated in 2nd year of life. Has a history of frequent episodes of biochemical abnormalities (abnormal PAC, UOA, CK and LFT's) necessitating hospital admissions during minor illnesses but

							frequency has decreased with age (Current age>5 years). In addition has low energy levels and mild hypotonia but is otherwise doing well. Growth measurements are at the 50 th %ile for age.
7	Born at term. Apgars 9 & 9*; Wt 3.4 kg. No dysmorphic features	No clinical issues. NBS results suggesting high risk for GA-II were reported on DOL 4 and readmitted for diagnostic work-up. Mild hpoglycemia and abnormal LFT's and CK noted on admission	Mildly increased ethylmalonic, glutaric, 2-hydroxyglutaric, methylsuccinic, suberic, sebacic & adipic acids and isovaleryl, 2-methylbutyryl & hexanoylglycines	Elevations of multiple acylcarnitine species (C4, C5, C6, C8, C10, C12, C14, C14:1) suggestive of GA-II	ETFDH Gene: Two mutations identified [c.250G>A:p.A84T; c.1110C>G:pG370G (Predicted to create novel splice donor site)]	. . .	Treatment (avoidance of fasting, a high carbohydrate and low fat diet, carnitine and riboflavin) initiated. Infant is doing well; current age 9 months.
8	Born at term. Apgars 9 & 9*; Wt 2.9 kg. No dysmorphic features	No clinical issues. NBS results suggesting risk for GA-II were reported on DOL 4 and neonate readmitted for diagnostic work-up. Mild hypoglycemia and abnormal LFT's and CK noted on admission	No unusual organic acids detected	Mild elevations of multiple acylcarnitine species (C8, C10, C12, C14, C14:1)	ETGDH Gene: One mutation identified [858 G>A:p.W286X]. ETFA & ETFB: No mutations identified	ETF-DQ 0.70 nmol/min/mg (Controls 0.8–2.4); ETF 2.3 nmol/min/mg (Controls 0.79–2.1)	Asymptomatic. Current age 3 years.
9	Born at term. Apgars 9 & 9*; Wt 3.8 kg. No dysmorphic features	No clinical issues. NBS results suggesting risk for GA-II were reported on DOL 5 and metabolic work-up initiated by specialist the next day	No unusual organic acids detected	Normal	ETFB Gene: One variant identified [P94TfsX21]. ETFA and ETFDH: No mutations	. . .	Asymptomatic. Current age 1-1/2 years.

CPT-II Carnitine palmitoyl transferase deficiency-Type II, *DOL* Day of life, *FAOD* Fatty acid oxidation defect, *IV* Intravenous, *SCAD* Short chain acyl CoA dehydrogenase deficiency, *VLCAD* Very long chain acyl CoA dehydrogenase deficiency

*At 1 and 5 min respectively

a mitochondrial complex III deficiency (OMIM 124000) due to pathogenic mutations in the BCS1L gene following extensive diagnostic studies in view of severe hypotonia and seizures since birth. Mitochondrial disease has been reported to mimic long-chain FAODs and it is possible that a GA-II profile could be seen in infants with mitochondrial disease who are receiving intravenous lipids. Six infants (Cases 16–21) had incomplete evaluation. In two of these neonates classified as FP who had an OOR screen on initial specimen, a repeat NBS was done but no further diagnostic work-up was performed. In an additional 4 of these 6 neonates, molecular studies and enzymatic analyses had not been pursued if initial biochemical testing (UOA or PAC) was not consistent with GA-II, even when no other condition/s was identified to explain the OOR screening result.

A "GA-II profile" was found in the initial specimen for 11 VLBW infants, including 1 infant confirmed to have GA-II (Case 1), and in later specimens after an initial normal screen in 50 VLBW infants. The 60 VLBW infants other than Case 1 were classified as FP based on limited evaluation, but GA-II was not on the differential of the treating physicians based on the clinical picture. These 60 infants were on TPN with lipids at the time of specimen collection. The markers most commonly responsible for the "GA-II" profile included C5 ($n = 58$), C8 ($n = 46$), C4 ($n = 32$), and C5DC (+C10OH; $n = 27$). Free carnitine (C0) was also elevated in 32 neonates, probably a result of carnitine supplementation. OOR C0, C5, and C8 were the most common combination. An elevation of C14 or the other long-chain acylcarnitines was not found in the VLBW infants.

Table 3 shows the clinical status, outcomes, and GA-II Index [C4xC5 x C8 x C14]/ [C0xC3] (and its z-score) on all babies >1.5 kg with a GA-II profile on the initial specimen. All confirmed cases (1–7) had a z-score higher than 7 while all confirmed FP (10–15) and carriers (8–9) had a z-score < 6. None of the VLBW infants on TPN with incomplete work-up had an index z-score of > 2 (data not shown). The only VLBW baby with a high GA-II index was confirmed to have GA-II (Case 1). Three of the six FP that have not had complete diagnostic work-up (16, 17, 21) had a z-score > 6. One was noted to have speech delays at 6 years. The other two are apparently asymptomatic and have no history of documented hypoglycemia at their current ages of 8 years and 9 months.

Discussion

Seven cases of GA-II were identified in our cohort. Four had the severe form and died within a week of life. These neonates were symptomatic or deceased when NBS results were reported. Although NBS was not helpful in preventing mortality associated with the severe form, it aided clinicians in arriving at a final diagnosis, which is extremely helpful for family counseling.

For the milder forms of GA-II, a diagnosis of GA-II was pursued primarily because of NBS. Case 6 had exhibited transient hypoglycemia in the neonatal period that may have been related to GA-II, but was overlooked because it resolved quickly with a few hours of intravenous hydration. In Case 5, confirming a diagnosis of GA-II was a challenge because the characteristic biochemical abnormalities presented only in the second year of life, while previous investigations had prompted a diagnosis of SCAD. Notably all markers on the repeat NBS specimen in this infant were in range, and normal acylcarnitine levels during confirmation of abnormal NBS have been encountered in other FAODs (Browning et al. 2005). If active diagnostic work-up was not being pursued in these infants, a diagnosis of GA-II could have been easily missed or delayed. Our report documents two infants where no biochemical testing was pursued when a repeat NBS was normal, thus it is feasible that some milder cases of GA-II may be dismissed as FP.

Since riboflavin-derived cofactors are essential for the function of the flavin-containing acyl-CoA dehydrogenase enzymes, a maternal riboflavin deficiency can present with a biochemical and clinical phenotype similar to GA-II (Chiong et al. 2007). No cases of maternal riboflavin deficiency were identified in the cohort of this report; however, the maternal riboflavin status was studied in only a subset (6 of 21 of neonates > 1.5 kg) of positive screens.

A comparison of the confirmed TP with the confirmed FP (Table 2) shows that in addition to the elevations of the expected markers in varying degrees, the severe forms of GA-II have decreased levels of Free carnitine (C0), acetylcarnitine (C2), propionylcarnitine (C3), and hydroxyisovalerylcarnitine (C5OH). Low C0 concentrations are expected to be a secondary deficiency, and have been previously reported (Di Donato et al. 1986). We have observed lower C2 and C3 concentrations in other long-chain FAODs also and are not completely unexpected. The production of acetyl-CoA and thereby its carnitine conjugate (C2) is impaired in FAODs and probably accounts for the lower C2 concentrations. Similarly, it is likely that a large portion of the propionyl-CoA and its carnitine conjugate (C3) in neonates comes from beta-oxidation of odd chain fatty acids, and thus the lower C3 concentrations observed in the severe FAOD. We had observed lower concentrations of C5OH in isovaleric acidemia previously (Sahai 2011). We hypothesized that while it is known that the accumulated 3-methylcrotonyl-CoA is reversibly

Table 2 Concentrations of relevant markers and their z-scores (calculated using log normalized population). Shown here are all GA-II cases (1–7), carriers (8–9) and the false positive specimens (10–21) from defined cohort weighing > 1.5 kg who has an out-of-range screen from GA-II on initial specimen. Among the false positives, cases 16–21 are those infants which we consider as not having had complete diagnostic evaluation

Marker	C0		C2		C3		C4		C5		C5OH		C6		C8		C10		C5DC		C14:1		C14		C16	
Mean	22.8		22.5		1.71		0.31		0.16		0.11		0.05		0.08		0.11		0.04		0.15		0.24		3.07	
Cut-Off	≤ 7		…		≥ 4.5		≥ 1.9		≥ 1.2		≥ 0.8		≥ 0.29		≥ 0.5		≥ 0.8		≥ 0.21		≥ 0.7		≥ 1		≥ 9	
ID	value	z-score	value	z-score	value	z-score	value	z-score	value	z-score	value	z-score	value	z-score	value	z-score	value	z-score	value	z-score	value	z-score	value	z-score	value	z-score
1	7.8	**-3.1**	4.6	**-4.7**	0.08	**-8.1**	**3.32**	**6.7**	**6.7**	**11.4**	0.03	**-3.9**	0.15	**3.4**	0.15	2.1	0.32	2.8	**0.47**	**6.2**	0.37	2.35	**1.5**	**5.9**	8.64	**3.04**
2	8.7	**-2.8**	…	…	0.38	**-4.0**	**2.59**	**6.0**	**6.87**	**11.5**	0.05	-2.3	**0.43**	**6.6**	0.43	5.8	0.75	**5.0**	0.18	**3.8**	**1.32**	**5.62**	**4.01**	**9.0**	**10.3**	**3.56**
3	**5.1**	**-4.4**	3.0	**-6.0**	0.11	**-7.3**	**4.58**	**7.7**	**5.26**	**10.7**	0.04	**-3.0**	0.24	**4.8**	0.12	1.3	0.15	0.8	**0.85**	**7.7**	0.22	1.01	0.78	**3.8**	**11.75**	**3.95**
4	**5.2**	**-4.3**	3.1	**-5.9**	0.06	**-8.9**	**3.16**	**6.6**	**3.33**	**9.3**	0.03	**-3.9**	0.18	**4.0**	0.18	2.7	0.35	**3.0**	**0.57**	**6.7**	0.47	**2.96**	**2.01**	**6.8**	6.87	2.37
5	52.0	2.4	…	…	2.1	0.5	**3.08**	**6.5**	0.89	**5.2**	0.12	0.2	**0.77**	**8.4**	**1.56**	**10.4**	**3.15**	**8.7**	**0.27**	**4.8**	**4.8**	**8.94**	**6.64**	**10.7**	**13.3**	**4.31**
6	37.8	1.5	37.0	1.5	2.15	0.6	**13.3**	**10.7**	**2.28**	**8.1**	0.14	0.7	**2.72**	**12.2**	**3.5**	**13.3**	**3.41**	**8.9**	**0.42**	**6.0**	**3.26**	**7.95**	**5.52**	**10.1**	**13.3**	**4.31**
7	17.9	-0.7	28.9	0.7	2.14	0.6	0.85	2.9	0.31	1.9	0.13	0.5	0.27	**5.2**	**0.62**	**7.1**	**1.4**	**6.6**	0.17	**3.7**	**2.49**	**7.25**	**2.27**	**7.2**	5.68	1.81
8	23.4	0.1	30.0	0.9	2.21	0.7	1.01	**3.4**	0.35	2.3	0.12	0.2	0.14	**3.2**	0.34	**5.0**	0.78	**5.1**	**0.24**	**4.5**	**0.93**	**4.72**	0.77	**3.7**	5.73	1.84
9	21.5	-0.2	39.6	1.7	1.48	-0.4	0.37	0.5	0.14	-0.5	0.11	0.0	0.16	**3.6**	0.28	**4.3**	0.47	**3.8**	**0.21**	**4.2**	0.66	**3.84**	**1.04**	**4.7**	6.78	2.33
10	48.0	2.2	63.7	**3.1**	**4.52**	2.6	0.61	1.9	0.35	2.3	0.2	1.8	**0.36**	**6.1**	0.8	**8.0**	1	**5.7**	**0.29**	**5.0**	**0.85**	**4.49**	**1.22**	**5.2**	7.9	**2.78**
11	126.6	**5.0**	116.9	**4.9**	**17.7**	**6.2**	**2.13**	**5.5**	**1.69**	**7.2**	0.37	**3.6**	**0.37**	**6.1**	0.28	**4.3**	0.21	1.7	0.06	1.1	0.48	**3.02**	**1.04**	**4.7**	**12.7**	**4.17**
12	61.6	2.9	59.9	2.9	**10.05**	**4.7**	**2.5**	**5.9**	0.63	**4.1**	0.27	2.6	0.11	2.5	0.12	1.3	0.14	0.7	0.06	1.1	0.37	2.35	0.82	**3.9**	**10.96**	**3.74**
13	100.5	**4.3**	51.6	2.5	**9.9**	**4.7**	**2.4**	**5.8**	**3.23**	**9.2**	0.38	**3.7**	0.15	**3.4**	0.32	**4.8**	0.15	0.8	0.07	1.5	0.16	0.19	0.17	-1.1	2.08	-1.1
14	48.0	2.2	44.0	2.0	2.24	0.7	0.74	2.5	**1.3**	**6.4**	0.2	1.8	0.6	**7.6**	0.6	**7.0**	0.72	**4.9**	**0.24**	**4.5**	0.32	1.97	0.34	1.1	2.6	-0.5
15	26.5	0.4	38.4	1.6	2.17	0.6	0.76	**2.6**	0.32	2.0	0.18	1.4	0.22	**4.6**	0.41	**5.6**	0.67	**4.7**	**0.31**	**5.2**	**0.87**	**4.55**	**1.18**	**5.1**	8.54	**3.01**
16	25.6	0.3	21.5	-0.1	2.21	0.7	**2.46**	**5.9**	**2.79**	**8.7**	0.14	0.7	**0.85**	**8.7**	**1.58**	**10.5**	**2.33**	**7.9**	**0.32**	**5.3**	**1.38**	**5.73**	**2.24**	**7.2**	6.04	1.99
17	41.5	1.7	32.9	1.1	2.43	0.9	1.42	**4.3**	0.41	2.8	0.17	1.3	**0.7**	**8.1**	**1.9**	**11.1**	**3.25**	**8.8**	**0.28**	**4.9**	**1.49**	**5.93**	**1.61**	**6.1**	5.9	1.92
18	24.8	0.2	33.7	1.2	1.49	-0.4	0.39	0.7	0.25	1.3	0.1	-0.3	0.2	**4.3**	**0.58**	**6.9**	**0.88**	**5.4**	0.12	**2.8**	**0.95**	**4.77**	0.62	**3.0**	4.8	1.32
19	48.2	2.2	58.8	2.9	**14.3**	**5.6**	**1.93**	**5.2**	**1.22**	**6.2**	0.24	2.3	0.22	**4.6**	0.14	1.8	0.13	0.5	0.06	1.1	0.32	1.97	0.42	1.8	5.22	1.56
20	40.6	1.7	44.2	2.0	2.7	1.2	0.7	2.3	0.36	2.4	0.15	0.9	0.15	**3.4**	0.23	**3.6**	0.3	2.6	0.16	**3.5**	0.66	**3.84**	0.83	**4.0**	**9.49**	**3.32**
21	25.0	0.3	38.0	1.6	2.6	1.1	1.15	**3.7**	0.4	2.7	0.11	0.0	0.2	**4.3**	0.44	**5.9**	0.88	**5.4**	**0.21**	**4.2**	**1.1**	**5.15**	0.91	**4.3**	6.7	2.30

Acylcarnitine concentrations that exceed the cut-off and z-scores that exceed 3 are shown in bold

Table 3 Clinical information and the NENSP GA-II Index shown here for all GA-II cases and Infants weighing > 1.5 kg with for GA-II initial specimen

Case ID	Results of follow-up screen	Status at time of specimen collection		Follow-up Information /Diagnosis	NENSP GA-II Index [C4xC5xC8xC14]/ [C0xC3]	
		Feeding	Clinical		Value	Z-Score[a]
1	…	IV Fluids with Dextrose	Symptomatic	GA-II . Deceased	**8.062**	**16.52**
2	…	Breast Milk & Formula	Transient Hypoglycemia	GA-II . Deceased	**9.291**	**16.71**
3	…	IV Fluids with Dextrose	Symptomatic	GA-II . Deceased	**4.051**	**15.62**
4	…	Breast Milk & Formula	Symptomatic	GA-II . Deceased	**12.132**	**17.06**
5	Normal	Breast Milk & Formula	Asymptomatic	GA-II; Initial work-up suggested SCAD.	**0.260**	**12.03**
6	Abnormal	Breast Milk & Formula	Transient Hypoglycemia	GA-II	**7.209**	**16.38**
7	Abnormal	Breast Milk & Formula	Asymptomatic	GA-II	**0.010**	**7.72**
8	…	Breast Milk & Formula	Asymptomatic	GA-II Carrier	0.002	5.51
9	Normal	Breast Milk	Asymptomatic	GA-II Carrier	0.000	3.77
10	Abnormal	Breast Milk	Asymptomatic	MCAD & VLCAD Carrier	0.001	4.70
11	…	IV Fluids with Dextrose	Severe Hemolysis	Hemoglobin HE Disease	0.000	3.76
12	Normal	Formula	Cardiomyopathy, Polycythemia, Hemolysis.	Hypoxic event in utero. Significant maternal issues during pregnancy (Morbid obesity, uncontrolled diabetes , Hypertension).	0.000	2.65
13	…	TPN[b]	Hemolysis	Deceased.	0.000	**3.63**
14	…	TPN[b]	Hemolysis	Deceased. Skeletal Dysplasia, Clotting Disorder, Renal Failure	0.002	5.54
15	Normal	Breast Milk	Severe Jaundice.	Structural Cardiac Defect	0.002	5.69
16	Normal	Breast Milk	Asymptomatic	PAC abnormal but not c/w GA-II. No furtherwork-up. At age 6 years had speech delays. Moved out-of-state (Current Age 9 yrs)	**0.429**	**12.69**
17	Abnormal	Breast Milk & Formula	Asymptomatic	Clinically well at age 8 years. No documented hypoglycemia	**0.018**	**8.51**
18	Normal	Breast Milk	Asymptomatic	Incomplete Work-up. Currently Well (Age 4 years)	0.001	4.68
19	Normal	Breast Milk & Formula	Asymptomatic	Speech Delay; Frequent Falls (Age 2 years)	0.000	2.94
20	Normal	Breast Milk & Formula	Asymptomatic	No confirmatory testing, Currently Well (Age < 1 year)	0.000	3.67
21	Normal	Breast Milk & Formula	Asymptomatic	No confirmatory testing, Currently Well (Age < 1 year)	0.003	**6.11**

[a] Calculated using log normalized population
[b] Total parenteral nutrition with lipids

converted to 3-hydroxisoyvaleryl-CoA and thereby results in increased concentrations of its carnitine conjugates (C5OH) in 3-methylcrotonyl-CoA carboxylase deficiency (Van Hove et al. 1995), a reverse situation is also feasible; that is, the impaired conversion of isovaleryl-CoA to 3-methylcrotonyl-CoA due to the isovaleryl-CoA dehydrogenase deficiency in isovaleric acidemia (and GA-II) results in lower concentrations of 3-methylcrotonyl-CoA and consequently lower concentrations of 3-hydroxisoyvaleryl-CoA and its carnitine conjugates (C5OH). Based on these observations, the NENSP utilizes an index [C4xC5 x C8 x C14]/ [C0xC3] as a quantitative measure to reflect a GA-II profile; a higher value suggests a higher probability of the disorder.

The fact that three out of six of the cases highlighted in Table 3 who had not had complete diagnostic work-up had Index z-scores > 6 opens the possibility that some of these individuals are mild cases, carriers, or that the OOR screen was due to a maternal riboflavin deficiency. Sixty-one specimens with a "GA-II profile" were from VLBW infants, but one VLBW infant was confirmed to have GA-II, thus positive screens from VLBW infants cannot be ignored. Our data suggests that quantitative indexes (similar to our GA-II index) could predict risk even in this complex subset.

We propose categorizing screening results with elevations of multiple acylcarnitine species into those at "High Risk" and those at a lower ""Risk" for GA-II based on a GA-II Index in conjunction with the magnitude of the acylcarnitine concentrations. In neonates with a "High Risk" NBS, enzymatic or molecular studies need to be pursued if a diagnosis cannot be conclusively established by the initial biochemical investigations (organic acids and acylcarnitines). The algorithms available through ACMG considers elevations of C4 and C5 (+/− other acylcarnitines), a profile commonly seen in neonates on TPN, as at risk for GA-II and recommends biochemical testing, and if initial biochemical testing is normal, molecular or enzymatic testing is considered optional. The GA-II indexes and categorizations shown help refine the GA-II profile and provide better risk assessment to direct urgency of intervention and need for enzymatic molecular studies when faced with normal initial biochemical investigations in positive screens.

Acknowledgments The authors wish to acknowledge the Massachusetts Department of Health, the Maine Department of Health and Human Services, the New Hampshire Department of Health and Human Services, the Rhode Island Department of Health, and the Vermont Department of Health for their partnership and cooperation. Further, the efforts of the treating physicians cannot be underscored. This study was supported in part by Priority Focus I and Priority Focus II funding bound to HRSA Grant U22MC03959.

Synopsis

We report the experience of the New England Newborn Screening Program in identifying individuals at risk for GA-II, the characteristics and outcomes of all specimens and neonates with a positive screen, and long-term outcomes of confirmed cases.

Conflict of Interest

All authors (I Sahai, CL Garganta, J Bailey, P James, HL Levy M Martin, E Neilan, C Phornphutkul, DA Sweetser, TH Zytkovicz and RB Eaton) declare that they have no conflict of interest.

Informed Consent/Human or Animal Studies

This report summarizes the experience of the New England Newborn Screening Program. This chapter does not contain any studies with human or animal subjects performed by any of the authors.

Authors Attestations

- The authors have not submitted similar publications previously or simultaneously.
- All authors have inspected the manuscript.
- All authors are in agreement for the submission.
- All authors have been involved in (a) conception and design, or analysis and interpretation of data, and (b) drafting the article or revising it critically for important intellectual content.

References

al-Essa MA, Rashed MS, Bakheet SM et al (2000) Glutaric aciduria type II: observations in seven patients with neonatal- and late-onset disease. J Perinatol 20:120–128

Bohm N, Uy J, Kiessling M, Lehnert W (1982 Sep) Multiple acyl-CoA dehydrogenation deficiency (glutaric aciduria type II), congenital polycystic kidneys, and symmetric warty dysplasia of the cerebral cortex in two newborn brothers. II. Morphology and pathogenesis. Eur J Pediatr 139(1):60–65

Browning MF, Larson C, Strauss A et al (2005) Normal acylcarnitine levels during confirmation of abnormal newborn screening in long-chain fatty acid oxidation defects. J Inherit Metab Dis 28(4):545–550

Chiong MA, Sim KG, Carpenter K et al (2007 Sep–Oct) Transient multiple acyl-CoA dehydrogenation deficiency in a newborn female caused by maternal riboflavin deficiency. Mol Genet Metab 92(1–2):109–114

Curcoy A, Olsen RK, Ribes A, Trenchs V, Vilaseca MA, Campistol J, Osorio JH, Andresen BS, Gregersen N (2003 Apr) Late-onset form of beta-electron transfer flavoprotein deficiency. Mol Genet Metab 78(4):247–249

de Visser M, Scholte HR, Schutgens RB, Bolhuis PA, Luyt-Houwen IE, Vaandrager-Verduin MH, Veder HA, Oey PL (1986 Mar) Riboflavin-responsive lipid-storage myopathy and glutaric aciduria type II of early adult onset. Neurology 36(3):367–372

Di Donato S, Frerman FE, Rimoldi M et al (1986) Systemic carnitine deficiency due to lack of electron transfer flavoprotein:ubiquinone oxidoreductase. Neurology 36:957–963

Frerman FE, Goodman SI (1985) Deficiency of electron transfer flavoprotein or electron transfer flavoprotein ubiquinone oxidoreductase in glutaric acidemia type II fibroblasts. Proc Natl Acad Sci USA 82:4517–4520

Frerman FE, Goodman SI (2001) Defects of electron transfer flavoprotein and electron transfer flavoprotein-ubiquinone oxidoreductase: glutaric aciduria type 2. In: Charles R Scriver, Arthur L Beaudet, William S Sly, David Valle. The metabolic and molecular bases of inherited disease. Vol. 8. McGraw-Hill, New York. pp 2357–2365

Goodman SI, Binard RJ, Woontner MR, Frerman FE (2002 Sep–Oct). Glutaric acidemia type II: gene structure and mutations of the electron transfer flavoprotein:ubiquinone oxidoreductase (ETF: QO) gene. Mol Genet Metab 77(1–2):86–90

Loehr JP, Goodman SI, Frerman FE (1990) Glutaric acidemia type II: heterogeneity of clinical and biochemical phenotypes. Pediatr Res 27:311–315

Millington DS, Kodo N, Norwood D et al (1990) Tandem mass spectrometry: a new method for acylcarnitine profiling with potential for neonatal screening for inborn errors of metabolism. J Inherit Metab Dis 13(3):321–324

Olsen RK, Andresen BS, Christensen E et al (2003) Clear relationship between ETF/ETFDH genotype and phenotype in patients with multiple acyl-CoA dehydrogenation deficiency. Hum Mutat 22:12–23

Olsen RK, Olpin SE, Andresen BS et al (2007) ETFDH mutations as a major cause of riboflavin-responsive multiple acyl-CoA dehydrogenation deficiency. Brain 130:2045–2054

Online Mendelian Inheritance in Man (OMIM) (2012). Johns Hopkins University, Baltimore, Maryland. MIM Number: 231680

Rhead WJ, Wolff JA, Lipson M et al (1987) Clinical and biochemical variation and family studies in the multiple acyl CoA dehydrogenase disorders. Pediatr Res 21:371–376

Sahai I (2011) Multicenter validation of algorithms to improve communication of positive newborn screening results. Newborn screening and genetic testing symposium (APHL), San Diego, CA

Van Hove JL, Rutledge SL, Nada MA et al (1995) 3-Hydroxyisovalerylcarnitine in 3-methylcrotonyl-CoA carboxylase deficiency. J Inherit Metab Dis 18(5):592–601

Zytkovicz TH, Fitzgerald EF, Marsden D et al (2001 Nov) Tandem mass spectrometric analysis for amino, organic, and fatty acid disorders in newborn dried blood spots: a two-year summary from the New England Newborn Screening Program. Clin Chem 47(11):1945–1955<

JIMD Reports
DOI 10.1007/8904_2013_266

INVITED ARTICLES

Systematic Data Collection to Inform Policy Decisions: Integration of the Region 4 Stork (R4S) Collaborative Newborn Screening Database to Improve MS/MS Newborn Screening in Washington State

Ashleigh Fleischman · John D. Thompson · Mike Glass

Received: 01 June 2013 / Revised: 10 September 2013 / Accepted: 13 September 2013 / Published online: 5 November 2013

Abstract In the past 50 years, newborn screening (NBS) has grown significantly in the breadth of screening programs and the number of conditions tested for each baby. The adaptation of tandem mass spectrometry (MS/MS) technology to detect inherited metabolic diseases is arguably one of the most impactful advancements in NBS testing. The addition of new conditions to the screening panel and the rarity of these conditions pose challenges for NBS program development, improvement, and evaluation. The Region 4 Stork (R4S) project is an international collaborative NBS database and a resource for programs across the world to overcome these challenges. By pooling true-positive case and laboratory testing data, the R4S database provides insight into complex MS/MS profiles for these rare conditions. The Washington State NBS Program is integrating aspects of the R4S web application and utilizing R4S resources to examine current protocols, identify improvements, implement changes, and review outcomes. Washington uses R4S resources to choose informative analytes and evaluate cutoffs. The program also examines the performance of R4S tools that are designed to aid in evaluating a baby's MS/MS screening results. This article documents these efforts in utilizing a subset of the R4S tools to improve their program, demonstrating the flexibility of the application. Other NBS programs can use the knowledge Washington has gained to strengthen their ability to correctly identify babies with metabolic disorders and mitigate the impact of screening on babies and their families.

Communicated by: Rodney Pollitt, PhD

Competing interests: None declared

A. Fleischman (✉) · J.D. Thompson · M. Glass
Washington State Department of Health, Office of Newborn Screening, 1610 NE 150th Street,
Shoreline, WA 98155, USA
e-mail: Ashleigh.Fleischman@doh.wa.gov

Introduction

The year 2013 marks the 50th anniversary of newborn screening (NBS), which began with the screening of phenylketonuria (PKU) in two US states. Since its inception, NBS has progressed and expanded, and is hailed as one of the greatest achievements in public health. Over the past 50 years, NBS has been implemented across most of the world and all babies born in the USA and in many other countries are now screened at birth for numerous dangerous or life threatening conditions. The adaptation of tandem mass spectrometry (MS/MS) to newborn screening during the 1990s allows NBS labs to screen for multiple amino acid, fatty acid, and organic acid metabolism disorders from one dried blood spot punch. Conditions on the MS/MS newborn screening panel are very rare, and for many of them, a NBS program may only see one true-positive case every few years. The rarity of true cases poses challenges for program development, improvement, and evaluation, particularly for smaller NBS programs. The Region 4 Stork (R4S) project was initiated in 2005 to pool information and generate data for NBS programs to improve MS/MS screening by (a) achieving uniformity of MS/MS testing panels, (b) improving analytical performance, and (c) reducing false-positive and false-negative screening results (McHugh et al. 2011). The project was initiated by the Region 4 Genetics Collaborative and funded through grants from the federal Health Resources and Services Administration (http://www.region4genetics.org/). In 2008 the R4S website was launched, allowing participant

NBS programs to upload information into the database and have live up-to-date access to a number of helpful screening tools developed by the R4S project utilizing the collaborative data. The R4S website was recently described in detail (McHugh et al. 2011). As of May 2013, the database contains NBS results for over 15,000 true-positive cases from 49 US states and 42 countries (https://www.nbstrn.org/research-tools/lab-performance-database). An average of five new cases are added to R4S every day; this is more true-positive cases than some NBS programs will find in a year. By compiling case data and laboratory results from across the world, the database provides insight into the complex MS/MS profiles for the rare conditions on the NBS panel. The comprehensive R4S website can be used by NBS programs to examine condition profiles, identify informative markers, examine site-specific cutoffs, and improve test sensitivity and specificity using the R4S-generated tools. R4S contains a multitude of tools that can be customized and applied in hundreds of ways to NBS programs. The Washington State (WA) NBS Program participated in the website training program and continues to actively contribute to the R4S database. This article highlights the specific ways by which WA NBS has employed R4S functions to strengthen screening operations.

Washington Newborn Screening

In the Washington State Newborn Screening Program, the laboratory and follow-up teams reside in the same building, in a single administrative unit and work together to develop screening methods for each condition on the required panel. It is the responsibility of the follow-up team to review and evaluate screening algorithms for continual program improvement. The team stays abreast of new techniques and advancements in the screening community and several staff members participated in the training program for R4S hosted by the Region 4 Genetics Collaborative. The weeklong course reviewed the R4S database and taught users how to use the R4S website and tools. The WA NBS program has taken the knowledge gained in this course and applied many of the site functions in program evaluation and improvement efforts.

Across the world, NBS programs differ on screening procedures, cutoff algorithms, and condition panels. In Washington State, the State Board of Health is the governing body which oversees the screening panel and determines which conditions are required for screening based on five criteria: (1) prevention potential and medical rationale, (2) treatment availability, (3) public health rationale, (4) available technology, and (5) cost-benefit/cost-effectiveness. In 2008, Washington underwent a rigorous NBS advisory committee review with the State Board of Health to expand the panel using MS/MS technology. Currently, Washington is screening for 27 of the conditions on the US federal government's Recommended Uniform Screening Panel (RUSP); 19 of these are tested using MS/MS technology. This is not an extensive panel of conditions detectable through MS/MS screening, and in order to limit incidental findings (conditions not approved by the State Board of Health), MS/MS testing is done using multiple reaction monitoring (MRM) which only measures specific analytes defined by the user. This differs from many NBS labs that use a full MS/MS scan which measures all analytes within a specified range, resulting in identification of many disorders that are not on Washington's panel. In 2008, the analytes selected for the MS/MS panel were determined using information available at the time from R4S and other laboratories. With the progression of the R4S database as a resource of true-positive cases and their associated laboratory findings, the profiles of these rare conditions are now better understood.

Analyte Selection and Review

With the limitations of MRM, it is critical that each analyte provide useful information. The tools within R4S provide a quick and easy way to identify informative markers (analytes and analyte ratios) for all the NBS conditions. The best screening markers are out of range in the affected population and normal in the unaffected population, with good separation between the two. Rarely does this happen for any screening test, and for most conditions, a combination of markers is used to help tease out the differences between these two populations. Using the R4S tools, the MS/MS panel in WA can be reviewed and modified as necessary to ensure its full potential to identify the required conditions. This can be done quickly and efficiently.

To optimize the MS/MS panel, WA NBS needed to identify the most informative markers for each condition on the panel. This was done using two of the R4S Project Tools, one which examines analytes by condition and one which examines conditions by analytes. The first tool, called Plots by Condition, generates box plots of the disease and normal ranges for markers associated with a specific condition. This can be done for all acylcarnitines, acylcarnitine ratios, amino acids, and amino acid ratios measured by MS/MS. Plots can be filtered to view only those analytes considered informative for a particular condition (categorized by the median of the affected population being outside the 90th percentile of the unaffected population). Markers where there is no overlap between the two populations are the most informative and likely have clinical utility for

interpretation of screening results. Individual plots can be produced for every condition in the R4S database. The Plots by Condition tool can quickly identify markers that should be included on the MS/MS MRM panel.

Conversely, a tool called Plot by Marker (available for every marker) generates box plots of the disease and normal ranges for conditions associated with a specific marker. A marker is considered informative for a condition if the median of the affected population is outside the normal range. Conditions where the marker is most informative have no overlap between the two populations. Once again, these plots quickly identify conditions in which the marker is out of range and users can easily identify the potential influence of each additional analyte or analyte ratio. The information from R4S can be used to identify the markers which will make the most impact and limit incidental findings for programs using MRM. Washington undertook a careful review, comparing the current MS/MS panel with the identified informative markers. The review resulted in the addition of nine new analytes and nine new ratios, impacting nine conditions on the screening panel. Twelve of the 18 new markers had no or very little overlap between the affected and unaffected populations.

Cutoff Determinations

The addition of new conditions to a screening panel can be a long and arduous process. Often there is only limited knowledge of the natural progression of the disease, and data for disease and normal ranges may be based on only a small nonrepresentative population. In the past, Washington has mainly used experiences from other programs when determining initial cutoff algorithms for new screening tests. When the expansion of MS/MS screening occurred in 2008, preliminary R4S data assisted in cutoff determinations. Now, R4S has a variety of tools that can be used to review, compare, and improve cutoffs. The Analyte Comparison tool visually displays the disease and normal ranges and cutoff values from all participants for individual analytes. The users can quickly compare their normal range and cutoffs to those of other programs. They can also see if their cutoff value is within a recommended target range and if it overlaps the normal range of their population. This tool has been helpful in evaluating the cutoffs historically used in Washington.

The Normal Percentiles Comparison tool can be used to compare program normal ranges to those in the database, identifying analytes in which they differ from the R4S population. Differences may be attributable to testing methods, population, or errors in data. If program-specific normal ranges differ vastly from the R4S population, recommended cutoff ranges may not be appropriate for that particular analyte. If the normal ranges are comparable, a Score Card provides recommended cutoff values, with percentiles for the normal population, participant cutoffs, and true-positive disease ranges. The user can then choose a cutoff value using the available percentile ranges. In Washington, cutoffs are reviewed periodically using these tools to evaluate their effectiveness. For the 18 new analytes and ratios where Washington-specific normal ranges were not available, initial cutoffs were chosen using the target range from the Score Card. After normal range data can be collected, temporary cutoffs will be reviewed to ensure they are appropriate for the Washington population. R4S provides a robust data set to support decisions made in program review of cutoffs and the addition of new analytes to a screening panel.

Post-Analytical Tools

It is well known in the screening community that using cutoffs is not a perfect method for detecting conditions; there is an art to the science of balancing false-positives and false-negatives. Programs try to mitigate errors by using multiple markers, demographics, and clinical information to make determinations on screening results. R4S has developed Post-Analytical (PA) tools to assist programs in making these decisions, and in the case of Minnesota's MS/MS panel, to eliminate cutoffs all together (Rinaldo 2013). A recent paper documents how the PA tools use multivariate pattern-recognition software to create case scores based on the MS/MS results uploaded into R4S, in particular the degree of overlap of informative analytes (Marquardt et al. 2012). As with many other programs, Washington is uneasy with eliminating cutoff algorithms, but is interested in finding ways to integrate the PA tools into the program as an additional resource in the evaluation of test results. A plan was developed to use the PA tools in parallel with the current cutoff scheme and regard them as a guide in decision-making processes. NBS programs may find the Tool Runner to be most effective because it can process batched NBS data directly from the MS/MS instruments, generating hundreds of scores instantly. Washington NBS is not routinely using this tool due to some logistical challenges but would like to increase its usage in the future.

Currently, WA NBS routinely uses the All Condition tool. Screening data is uploaded directly into the application and the All Condition tool runs every One Condition PA tool simultaneously. It then outputs an overview of each PA tool that has a summary of tools with informative results. Each One Condition tool contains useful information specific to that condition, including normal percentiles, disease ranges, and percent of overlap between the two.

The data is also provided in graphical form which is instantly helpful as the user can visually compare case analyte values against the normal and disease ranges. There is also a clear visual categorization of the informative markers. To assist in interpretation, each tool is programmed to generate a Case Score. These scores can be compared to other true-positive cases both in a Percentile Rank and in a graphical presentation. Interpretation Guidelines categorize the Case Scores into *not informative*, *possibly* disease, *likely* disease, and *very likely* disease using percentile distributions of true-positive cases. The Case Score interpretation is intended to provide guidance for follow-up programs. Some Case Score interpretations recommend further screening tests that are not available in most programs. These programs must decide how to proceed without the additional information provided by the recommended tests. For states with routine second screens, like Washington, the decision process may be even more complex. The question many programs ask is how do these Case Score interpretations translate into their population? What does *very likely* mean? Does every *very likely* translate into a true-positive case? Does every true-positive receive a score of *very likely*? Are some tools better than others at predicting the outcome? Washington NBS is collecting data to help answer these questions. Every abnormal specimen is run through the All Condition tool and the Case Score, Percentile Rank, and Interpretation are recorded for each one.

The PA tools have been run hundreds of times in Washington over the past few years, but the number of true-positive cases with MS/MS data available is relatively small for some conditions, inhibiting conclusive answers to the questions above. However, preliminary numbers are providing insight into the utility of some of the PA tools. In R4S, there are four One Condition tools where propionylcarnitine (C3) is considered the primary marker: (1) propionic acidemia (PROP), (2) methylmalonic acidemia-mutase or Cobalamin A and B deficiencies (MUT/Cbl A,B), (3) methylmalonic acidemia-Cobalamin C and D deficiencies (Cbl C,D), and (4) maternal Vitamin B12 deficiency (B12 Def (mat)). Table 1 depicts the distribution of Case Score interpretations for all specimens in Washington where the C3 was considered abnormal on the first screen and the baby was referred for diagnostic testing. Table 1 also includes the positive predictive value (PPV) of One Condition tool interpretations. The PPV of a *very likely* interpretation varied across the PA tools (28–100%), with the PROP tool having 100% PPV, but including only two cases. All true-positive C3 cases received an interpretation of *very likely*, with two exceptions. One received an interpretation of *possibly*; however, this was a case of maternal Vitamin B12 deficiency, which is considered an incidental finding of NBS. The other exception was an uncommon presentation of mild propionic acidemia: the baby was 6 months old when finally diagnosed, he was asymptomatic and only treated briefly. When combining *very likely*, *likely*, and *possibly* interpretations compared to a *not informative* interpretation, the PPV becomes more consistent across the different PA tools, ranging from 21% to 33%. If all four PA tools are combined, the sensitivity is 94% and the PPV is 25%. Determining the PPV for MS/MS analytes will allow NBS follow-up to provide this information at the time of referral and give the families a better idea of the likelihood that their baby is affected.

The Dual Scatter Plot PA tools can also be valuable assets to NBS programs. These tools compare two One Condition PA tools to determine if the profile is more consistent with one condition or the other. These can be used to separate serious conditions from heterozygotes (het) and milder forms of the condition. For example, the Dual Scatter Plot Guidelines for the VLCAD vs VLCAD(het) tool are: *VLCAD*, *VLCAD(het)*, *neither*, or *not informative* (meaning it could be either VLCAD deficiency or a VLCAD carrier). Data in Table 2 are for commonly used Dual Scatter Plots in Washington where specimens were abnormal on the first NBS and diagnostic testing was performed. The preliminary data for the Dual Scatter Plot tools show that when disease status was predicted (*VLCAD*, *MCAD*, or *PKU*) the tool was correct 100% of the time. However, not every true-positive case was as clear: some received scores in the uninformative category indicating the tool could not distinguish between the condition on the NBS panel and the heterozygous or mild state. Over the past few years, Washington has experienced some difficulty with C14:1 having a high false-positive rate for VLCAD deficiency: in the past year, there have been 51 babies with elevated C14:1 on the first screen. Forty-six of these had a C14:1 value under 1.0 (approximately 80% of babies with VLCAD have a C14:1 value greater than 1.0 on the NBS). Washington found that the vast majority of babies being referred were either VLCAD carriers or false-positive newborn screens (VLCAD and VCLAD carriers are diagnosed by DNA sequencing). In order to reduce the amount of unnecessary diagnostic testing, WA NBS has piloted a procedure using the VLCAD vs VLCAD(het) Dual Scatter Plot tool. When NBS results show an elevated C14:1 that is less than 1.0 with one or more secondary ratios in the normal range, specimens are run through the VLCAD vs VLCAD(het) Dual Scatter Plot tool. If the results are clearly in the *VLCAD(het)* range, the baby is not referred for diagnostic testing and a second NBS is requested. If the tool predicts either *VLCAD* or *not informative,* the baby is referred for diagnostic testing. There was only one true-positive mild VLCAD case where the Dual Scatter Plot indicated the results were *not informative*. Since the implementation of this protocol, 28

Table 1 Region 4 Stork (R4S) Case Score interpretations and positive predictive values (PPV) for babies in Washington State with elevated propionylcarnitine (C3) on the first newborn screen and diagnostic testing outcomes

Interpretation	Diagnostic outcome (*n*)		PPV (%)
PROP tool	**True-positive**	**Normal**	
Very likely	2	0	100
Possibly	0	4	0
Not informative	1	12	-
MUT/Cbl A,B tool			
Very likely	5	8	39
Likely	0	7	0
Possibly	0	1	0
Cbl C,D tool			
Very likely	3	5	38
Likely	0	5	0
Possibly	0	4	0
Not informative	0	2	-
B12 Def (mat) tool			
Very Likely	5	13	28
Likely	0	2	0
Possibly	1	1	50
All C3 PA tools	**True-positive**	**Normal**	
Very likely	15	26	37
Likely	0	14	0
Possibly	1	7	13
Not informative	1	14	-

PROP: propionic acidemia, *MUT/Cbl A,B*: methylmalonic acidemia (mutase or Cobalamin A and B deficiencies), *Cbl C,D*: methylmalonic acidemia (Cobalamin C and D deficiencies), *B12 Def (mat)*: maternal Vitamin B12 deficiency

Table 2 Region 4 Stork (R4S) Dual Scatter Plot interpretations for babies in Washington State with abnormal results on the first newborn screen and diagnostic testing outcomes

Interpretations	Diagnostic outcome (*n*)		
VLCAD vs VLCAD(het) tool	**VLCAD**	**VLCAD(het)**	**Normal**
VLCAD	1	0	0
VLCAD(het)	0	3	5
*Not informative**	1	10	1
Neither	0	0	2
MCAD vs MCAD(het) tool	**MCAD**	**MCAD(het)**	**Normal**
MCAD	3	0	0
MCAD(het)	0	0	1
PKU vs H-Phe tool	**PKU**	**H-Phe**	**Normal**
PKU	1	0	0
*Not informative***	3	4	0

very long-chain acyl-CoA dehydrogenase (VLCAD) deficiency vs very long-chain acyl-CoA dehydrogenase (VLCAD) heterozygote (het), medium-chain acyl-CoA dehydrogenase (MCAD) deficiency vs medium-chain acyl-CoA dehydrogenase (MCAD) heterozygote (het), pheylketonuria (PKU) vs hyperphenylalaninemia (H-Phe)

*Could be either VLCAD or VLCAD (het)

**Could be either PKU or H-Phe

babies and their families have avoided the fiscal and emotional expense of a diagnostic referral for VLCAD. These Dual Scatter Plot tools provide an opportunity for programs to adjust cutoffs to reduce false-positives, and to improve the PPV of their screens.

Limitations

While Washington has found many aspects of the R4S web application useful in program evaluation and improvement, there are some limitations to its utility. Currently there is no definition of a true-positive case: each participant uses different clinical measures to determine if a case is a true-positive newborn screen or not. Fortunately, every case that is uploaded into the system is reviewed by the curators for extreme values in an effort to reduce skewing of the results. With the pooling of data and the exclusion of outliers, misclassified results should have little effect on the tools and outcomes.

Some limitations only apply to a subset of the screening community. The MS/MS Portal is only validated for specimens less than 10 days of age at collection, indicating the tools may not be as useful for programs with routine second specimens collected outside the 10-day window, or for the NICU population (which generally receives three routine newborn screens in the USA). R4S has developed a second portal called MS/MS[2] in an effort to capture data specific to specimens collected at an older age. The R4S system was designed so that users can request portals, such as MS/MS[2], add conditions or ratios, and build their own PA tools. With only five participants and less than 400 true-positive cases, the MS/MS[2] Portal does not yet have the level of participation of the MS/MS Portal, but Washington plans to collaborate with other two-screen NBS programs to increase the utility of MS/MS[2].

Finally, there are limitations to the data available in Washington. The small number of true-positive cases is a barrier to complete validation of the PA tools available in R4S. Following the example set by R4S, collaboration with other NBS programs would increase the power of the validation study started in Washington, providing an opportunity to reach evidence-based conclusions on the utility of the Post-Analytical tools in a live NBS program.

Conclusion

Washington will continue to explore the integration of R4S into its screening program and is happy to serve as a resource for other programs who hope to do the same. When faced with the reality of screening for rare and deadly disorders in a climate where funding is scarce and public perception can be easily swayed, it is paramount for NBS programs to utilize available resources to ensure screening is performed quickly, efficiently, and reliably. R4S is a shining example of how teamwork within the screening community can provide improved outcomes for newborns across the globe. Not all of the R4S tools will be applicable to every NBS program; Washington State's experience using the tools to choose informative analytes, evaluate cutoffs, and collect longitudinal data on performance of the PA tools demonstrates that using a subset of individual R4S tools can strengthen a program's ability to correctly identify babies with metabolic disorders and mitigate the impact of screening on babies and their families.

Synopsis

Newborn screening programs can integrate tools from the Region 4 Stork (R4S) collaborative database to evaluate current protocols, identify improvements, and review outcomes of implemented changes. The power of a large pool of data for rare conditions makes R4S an excellent resource for newborn screening programs.

Compliance with Ethics Guidelines

Conflict of Interest

Ashleigh Fleischman, John D. Thompson, and Mike Glass declare that they have no conflicts of interest.

Animal Rights and Human Subjects

This article does not contain any studies with human or animal subjects performed by any of the authors.

Details of the Contributions of Individual Authors

Ashleigh Fleischman attended the Region 4 Stork MS/MS training and is assigned to follow-up for abnormal MS/MS conditions. She performed the review of the MS/MS panel, identified new markers to add to the panel, executed the cutoff review, proposed cutoff changes, conducted validation of the Post-Analytical tools including running specimens through the R4S tools, and recording results. Ashleigh was responsible for generating and reviewing the data and is the primary author of this article.

John D. Thompson is the supervisor for the follow-up group in Washington State's Newborn Screening program.

He attended the Region 4 Stork MS/MS training, collaborated and approved changes in the Washington MS/MS panel and cutoff algorithms, and oversaw the data collection and validation of the Post-Analytical tools. He served as an advisor for this article including planning, editing, and content review.

Mike Glass is the director of Washington's newborn screening program. He reviewed and approved all changes made in follow-up or lab protocols. He served as an advisor for this article including, planning, editing, and content review.

References

Marquardt G, Currier R, McHugh DMS et al (2012) Enhanced interpretation of newborn screening results without analyte cutoff values. Genet Med 14(7):648–655

McHugh DMS, Cameron CA, Abedenur JE et al (2011) Clinical validation of cutoff target ranges in newborn screening of metabolic disorders by tandem mass spectrometry: a worldwide collaborative project. Genet Med 3(3):230–254

Rinaldo P (2013) The C. Ronald Scott lecture series in biochemical genetics. The impact, products and future applications of the Region 4 Stork (R4S) collaborative project. May 23 [lecture]. Seattle Children's Hospital, Seattle

JIMD Reports
DOI 10.1007/8904_2013_275

CASE REPORT

Application of a Second-Tier Newborn Screening Assay for C5 Isoforms

T Cloppenborg • N Janzen • HJ Wagner • U Steuerwald • M Peter • AM Das

Received: 08 August 2013 / Revised: 24 September 2013 / Accepted: 07 October 2013 / Published online: 6 November 2013

Abstract We report a case of false-positive metabolic screening for isovaleric acidemia in a newborn due to treatment of the mother with pivalic acid containing antibiotics before delivery. By using a recently established second-tier test based on the tandem-MS technique, we could identify pivalic acid in a dried blood sample taken during routine neonatal screening. Before this second-tier test was initiated, diverse analytical procedures were performed in the baby to rule out isovaleric acidemia and carnitine supplementation was started. This caused additional psychological burden to the family. The direct use of the second-tier test would have avoided these negative consequences of a false-positive screening result.

Introduction

Electrospray ionization tandem mass spectrometry is used as a standard method for newborn mass screening of inborn errors of metabolism worldwide. Isovaleric acidemia (IVA) is a target disease of the current newborn screening program in Germany with an incidence of 1–1.5 per 100,000 screened newborns (own observation and Ensenauer et al. (2011); Smith and Matern (2010); McHugh et al. (2011)). IVA has a spectrum of biochemical and clinical phenotypes, including an attenuated form that makes clinical diagnosis difficult and may be associated with only mild elevation of isovalerylcarnitine in newborn screening.

A known cause of false-positive testing for IVA is the presence of the isomer pivalic acid in the dried blood spots. The established newborn mass screening method is not suited to separate isomers. Antibiotics given to the mother before delivery are a common source of the C5 isoform pivalic acid (Abdenur et al. 1998). Pivampicillin is hydrolyzed to pivalic acid after absorption (Melegh et al. 1987).

False-positive results have to be avoided whenever possible as they will cause a considerable psychological burden to the family. Furthermore, they give rise to unwarranted follow-up procedures that are invasive and sometimes even require hospital admission (Smith and Matern 2010; Hewlett and Waisbren 2006; Fyrö and Bodegård 1987; Lipstein et al. 2009).

We report a case of false-positive metabolic screening for IVA in a newborn due to treatment of the mother with antibiotics before delivery, which resulted in pivalic acid production. By using a recently established second-tier test based on the tandem-MS technique (Janzen et al. 2013), we could identify pivalic acid in a dried blood sample taken during routine neonatal screening. Second-tier tests are not uncommon in newborn screening to identify false-positive results, for example in tyrosinemia type I (Sander et al. 2006).

Communicated by: Bridget Wilcken

Competing interests: None declared

Authors Cloppenborg T and Janzen N contributed equally

T. Cloppenborg (✉) · A. Das (✉)
Department of Paediatric Kidney-, Liver- and Metabolic Diseases, Hannover Medical School, Carl-Neuberg Str. 1, D-30625, Hannover, Germany
e-mail: das.anibh@mh-hannover.de1

N. Janzen · U. Steuerwald · M. Peter
Screening Laboratory Hannover, Hannover, Germany

H. Wagner
Tostedt, Germany

Case Report

The patient is the first child of non-consanguineous healthy parents. After an uncomplicated pregnancy, the child was born via caesarean section at 36 weeks of gestation during a family holiday in Denmark. Because of early rupture of membranes, the mother received an antibiotic treatment with six doses of Pondocilline® (à 500 mg pivampicillin) and metronidazole (à 500 mg). The treatment was stopped immediately after delivery.

Delivery was uncomplicated, and cardiorespiratory adaptation of the child was fine. The child was breastfed, supplemented with formula milk. A first newborn screening for inborn errors of metabolism was carried out in Denmark at the age of 3 days with normal results. IVA is not included in the standard Danish neonatal screening program. A second screening test was performed by the local German pediatrician on day 5, as he wanted to offer the family the newborn screening panel available at the local program. This test showed an elevated level of isovalerylcarnitine at 2.6 μmol/l (reference <0.5 μmol/l). The isovalerylcarnitine/acetylcarnitine ratio was increased (0.1; reference <0.03). Values were similar in the recall sample.

Follow-up testing in dried blood spots showed a spontaneous decrease of isovalerylcarnitine to 1.0 μmol/l on day 9, while the isovalerylcarnitine/acetylcarnitine ratio dropped to 0.04 (within reference range). Organic acids in urine were negative for isovaleric acid and isovalerylglycine. As a variant form of IVA was suspected after the initial positive result, carnitine supplementation (50 mg/kg per day) was started. In the meantime, second-tier testing as described below revealed substantial amounts of pivaloylcarnitine in the blood, while isovalerylcarnitine was normal. After obtaining this result, carnitine supplementation was discontinued. Further controls showed a normalization of blood "isovalerylcarnitine," i.e., pivaloylcarnitine.

Initially, the mother was not aware that she had been given antibiotics. Subsequently she remembered that some medication was given to her before delivery. The clinical file was obtained from the Danish hospital where birth took place. It revealed treatment with Pondocilline® and metronidazole because of early rupture of membranes. Pondocilline® contains pivampicillin which is broken down to ampicillin and pivalic acid in vivo. The initial newborn screening sample from Denmark was sent to us for analysis and showed a high peak of pivaloylcarnitine.

Materials and Methods

A second-tier test for differentiation of C5 acylcarnitines using UPLC-MS/MS in dried blood was carried out using the method recently described (Janzen et al. 2013).

Results

The time course of acylcarnitine levels is summarized in Table 1. A chromatogram from the patient is shown in Fig. 1.

Discussion

IVA is a target disease of the newborn screening program in Germany and other countries. Pivalic acid as a constituent of some antibiotics is known to interfere with IVA-testing leading to false-positive results (Abdenur et al. 1998). This will lead to considerable psychosocial burden for the parents and other relatives and will give rise to further biochemical testing in the baby. We describe the use of a second-tier test that enables screening laboratories to identify pivaloylcarnitine as the cause of elevated C5 giving false-positive results for IVA (Janzen et al. 2013). Over a 2-year period we obtained a total of 350,837 German neonatal samples, 227 cases with elevated C5 were reported as positive (0.064 %). The samples received from abroad (22,084 cases) showed a higher percentage of positive samples (104 cases, 0.47 %). Thus, a significant number of positive samples are found during neonatal screening for IVA. These figures emphasize the need for rapid specification of C5 isomers. The second-tier test described allows rapid separation and quantification of various C5 acylcarnitines which may underlie elevated C5 levels in routine newborn screening in the original blood sample (Janzen et al. 2013).

Maeda et al. (2008, 2007) previously described the chromatographic separation of acylcarnitines from serum and urine. However, their method needs a second sample from the patients (urine or serum) and the sample preparation requires the use of solid phase extraction material (SPE).

Forni et al. (2010) used similar hardware equipment for the separation using plasma or dried blood spot material. Before quantification, they derivatized the acylcarnitines. During this chemical process some acylcarnitines can be fragmented to free acids and carnitine; therefore, we decided to measure the acylcarnitines without any chemical modification.

Ferrer et al. (2007) described a rapid method to separate C4 and C5 acylcarnitine isomers in plasma samples. The validation data agree well with our findings. The separation time was about twice as long, the sample volume was 50 μl. The most important advantage of our method is the option to use blood from the original screening card. By using a UPLC-technique the test is faster, more sensitive, and cheaper compared to the conventional HPLC method. Thus, false-positive results can be rapidly excluded without any burden to the newborn and his family.

Table 1 Acylcarnitine concentrations in dried blood spots from our patient. The cutoff for the routine screening method with butylation is 0.5 µmol/L. nd – not detected

Sample number	Day after birth	C5 carnitines (butylated) [µmol/l]	Pivaloylcarnitine [µmol/l]	2-Methylbutyrylcarnitine [µmol/l]	Isovalerylcarnitine [µmol/L]	Valerylcarnitine [µmol/L]
1	3	4.12	6.02	nd	0.05	nd
2	5	2.64	3.55	0.02	0.04	nd
3	5	-	3.69	nd	0.04	nd
4	5	-	3.74	0.02	0.04	nd
5	9	1.00	1.20	0.02	0.05	nd
6	19	0.32	0.29	0.04	0.08	nd
7	41	0.18	0.04	0.04	0.08	nd
8	55	0.13	0.02	0.05	0.08	nd
9	126	0.08	0.01	0.03	0.05	nd

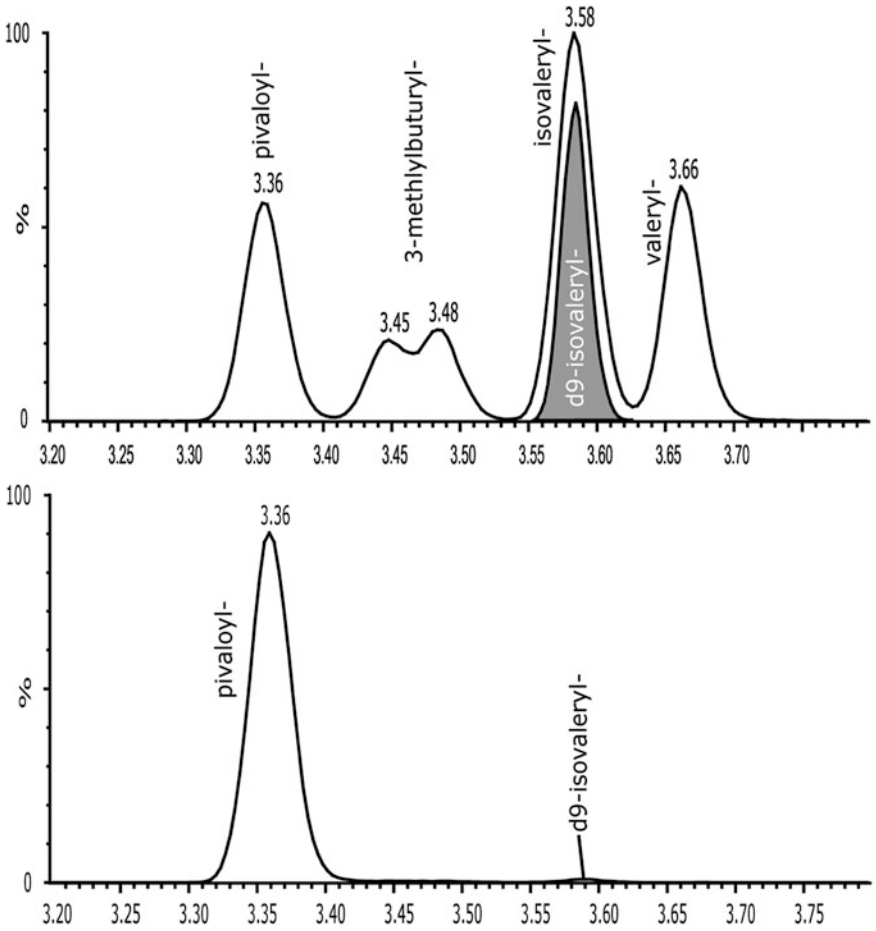

Fig. 1 Chromatographic separation of the C5 isoforms (solved in methanol/water). The deuterated d9 isovalerylcarnitine (internal standard) is shown in the bottom chromatogram. Sample of the patient (day 3) eluted from the dried blood spot (bottom chromatogram). The pivaloylcarnitine was the most prominent peak, all other C5 acylcarnitines were only detected in low concentrations

The newly established test is able to increase specificity without hampering sensitivity in IVA-testing and does not require additional instrumentation. The small sample volume of a 4.7 mm diameter blood spot equaling 5μl whole blood prolongs the lifetime of the column and the hardware equipment, the method therefore is fast and cost-efficient.

We advocate including this second-tier test in screening in every sample tested "positive" for IVA. It is generally possible to run the method on a conventional HPLC with a less powerful mass spectrometer. This is associated with a longer run time and a lower sensitivity with an increased consumption of flow agents. The advantage of the described method is the use of very little material and rapid separation with high sensitivity.

Further testing in a large newborn cohort is necessary to corroborate our promising results.

Acknowledgments We are grateful to M. Terhardt, Dr. S. Sander, and the other laboratory staff of the "Screening-Labor Hannover" for technical assistance and the staff from the screening laboratory in Copenhagen for providing the initial screening card from the patient.

Compliance with Ethics Guidelines

Thomas Cloppenborg, Nils Janzen, Hans-Joachim Wagner, Ulrike Steuerwald, Michael Peter, and Anibh Martin Das declare that they have no conflict of interest.

Details of the Contributions of Individual Authors

T. Cloppenborg treated the child at the metabolic clinic and drafted the manuscript, N. Janzen drafted the manuscript and supervised the technical analysis, H.J. Wagner initiated the second neonatal screening and is the community pediatrician of the patient, U. Steuerwald and M. Peter evaluated the results at the screening laboratory, A.M. Das treated the child at the metabolic clinic and finalized the manuscript.

References

Abdenur JE, Chamoles NA, Guinle AE, Schenone AB, Fuertes AN (1998) Diagnosis of isovaleric acidaemia by tandem mass spectrometry: false positive result due to pivaloylcarnitine in a newborn screening programme. J Inherit Metab Dis 21:624–630

Ensenauer R et al (2011) Newborn screening for isovaleric acidemia using tandem mass spectrometry: data from 1.6 million newborns. Clin Chem 57:623–626

Ferrer I et al (2007) Separation and identification of plasma short-chain acylcarnitine isomers by HPLC/MS/MS for the differential diagnosis of fatty acid oxidation defects and organic acidemias. J Chromatogr B Analyt Technol Biomed Life Sci 860:121–126

Forni S, Fu X, Palmer SE, Sweetman L (2010) Rapid determination of C4-acylcarnitine and C5-acylcarnitine isomers in plasma and dried blood spots by UPLC-MS/MS as a second tier test following flow-injection MS/MS acylcarnitine profile analysis. Mol Genet Metab 101:25–32

Fyrö K, Bodegård G (1987) Four-year follow-up of psychological reactions to false positive screening tests for congenital hypothyroidism. Acta Paediatr Scand 76:107–114

Hewlett J, Waisbren SE (2006) A review of the psychosocial effects of false-positive results on parents and current communication practices in newborn screening. J Inherit Metab Dis 29:677–682

Janzen N et al (2013) UPLC-MS/MS analysis of C5-acylcarnitines in dried blood spots. Clin Chim Acta 421:41–45

Lipstein EA, Perrin JM, Waisbren SE, Prosser LA (2009) Impact of false-positive newborn metabolic screening results on early health care utilization. Genet Med 11:716–721

Maeda Y et al (2007) Simultaneous quantification of acylcarnitine isomers containing dicarboxylic acylcarnitines in human serum and urine by high-performance liquid chromatography/electrospray ionization tandem mass spectrometry. Rapid Commun Mass Spectrom 21:799–806

Maeda Y et al (2008) Determination of 3-hydroxyisovalerylcarnitine and other acylcarnitine levels using liquid chromatography-tandem mass spectrometry in serum and urine of a patient with multiple carboxylase deficiency. J Chromatogr B Analyt Technol Biomed Life Sci 870:154–159

McHugh DMS et al (2011) Clinical validation of cutoff target ranges in newborn screening of metabolic disorders by tandem mass spectrometry: a worldwide collaborative project. Genet Med 13:230–254

Melegh B, Kerner J, Bieber LL (1987) Pivampicillin-promoted excretion of pivaloylcarnitine in humans. Biochem Pharmacol 36:3405–3409

Sander J et al (2006) Newborn screening for hepatorenal tyrosinemia: tandem mass spectrometric quantification of succinylacetone. Clin Chem 52:482–487

Smith EH, Matern D (2010) Acylcarnitine analysis by tandem mass spectrometry. Curr Protoc Hum Genet, Chapter 17, Unit 17.8.1–20<

JIMD Reports
DOI 10.1007/8904_2013_256

CASE REPORT

Cystinosis with Sclerotic Bone Lesions

S. Sirrs • P. Munk • P.I. Mallinson • H. Ouellette • G. Horvath • S. Cooper • G. Da Roza • D. Rosenbaum • M. O'Riley • G. Nussbaumer • L.N. Hoang • C.H. Lee

Received: 31 May 2013 / Revised: 15 July 2013 / Accepted: 30 July 2013 / Published online: 6 October 2013

Abstract A 26-year-old male with nephropathic cystinosis treated with cysteamine and renal transplantation presented for evaluation of multiple sclerotic bone lesions, which were an incidental finding on chest computerized tomography. These lesions were in a pattern consistent with osteoblastic metastases. He did not have a history of clinically significant hyperparathyroidism or cytopenias either preceding or following his transplant. Bone and tumor markers (including alkaline phosphatase and calcium) were all normal. A percutaneous bone biopsy of the lesions showed changes compatible with cystine deposition. Our case demonstrates that sclerotic bone lesions can be a feature of cystinosis in patients with normal parathyroid function and that significant bone marrow infiltration with cystine can be present even in the absence of cytopenias.

Communicated by: Eva Morava, MD PhD

Competing interests: None declared

S. Sirrs (✉) · G. Horvath · M. O'Riley
Adult Metabolic Diseases Clinic, Vancouver General Hospital, Level 4 – 2775 Laurel Street, Vancouver, BC, Canada V5Z 1M9
e-mail: Sandra.Sirrs@vch.ca2

P. Munk · P.I. Mallinson · H. Ouellette
Department of Radiology, Vancouver General Hospital, Vanvouver, BC, Canada

S. Cooper · G. Da Roza
Divisions of Nephrology, Fraser Health Authority, Vancouver, BC, Canada

D. Rosenbaum
Department of Medicine, Vancouver General Hospital, Vancouver, BC, Canada

G. Nussbaumer
Divisions of Nephrology, St. Paul's Hospital, Vancouver, BC, Canada

L.N. Hoang · C.H. Lee
Department of Pathology, Vancouver General Hospital, Vancouver, BC, Canada

Nephropathic cystinosis (OMIM 219800) is an autosomal recessive disorder caused by defects in the gene coding for the lysosomal cystine carrier cystinosis (CTNS). Cystinosis causes multiorgan manifestations, including renal insufficiency, eye disease, endocrinopathies, myopathy, and pulmonary involvement (Gahl et al. 2007). Many bone manifestations of cystinosis have been eported, including osteopenia and fractures (Zimakas et al. 2003), renal osteodystrophy, short stature, and hypophosphatemic rickets (Gahl et al. 2007). Bone marrow involvement with deposits of cystine crystals has also been reported in patients presenting with cytopenias (Busuttil and Liu Yin 2000; Quinn et al. 2004; Bigley et al. 2006). We present a case with bone marrow involvement from cystinosis presenting with multifocal osteosclerotic lesions mimicking osteoblastic bone metastases in a patient with normal parathyroid function and no cytopenias.

Case Report

The patient is a 26-year-old male who was diagnosed with cystinosis when he was evaluated at the age of 10 months for bowing of his legs, renal Fanconi syndrome, and corneal crystal deposition. He was placed on oral cysteamine therapy and WBC cystine levels were initially within the target of <1 nmol/mg protein. However, his compliance with therapy as an adult was limited. He went on to develop end-stage renal disease and received a related live donor renal allograft at the age of 14. He did not have significant parathyroid hormone abnormalities

Table 1 Biochemical parameters including tumor markers at the time of evaluation for osteosclerotic bone lesions and parathyroid hormone status pre- and post-transplant

Parameter	Patient values	Normal or target range
Parameters prior to the development of bone lesions		
PTH pre transplant[a] (mean; range)	31.5 pmol/L (14.2–63.3)	16.5–33 pmol/L[b]
PTH post-transplant[c] (mean; range)	5.7 pmol/L (2.1–8.3)	
WBC cystine levels (mean; range for 2 years prior to evaluation for osteosclerotic bone lesions)	1.34 (0.91–2.23) nmol/2Cys/mg pr	<1 (optimal) <2 (still beneficial)
Parameters at the time of evaluation for osteosclerotic bone lesions		
Serum creatinine	110 umol/L	45–110
eGFR	70 mL/min/1.73 m^2	>59
PTH	7.6 pmol/L	1.5–7.6
Total calcium	2.38 mmol/L	2.10–2.60
Alkaline phosphatase	104 U/L	40–145
LDH	179 U/L	90–240
Hemoglobin	143 g/L	135–170
WBC	5.0 giga/L	4.0–11
Platelet count	145 giga/L	150–400
Serum/urine protein electrophoresis	Normal pattern	–
Alpha fetoprotein	4.0 ug/L	<8
Human chorionic gonadotropin	<2.0 IU/L	<10
Prostate-specific antigen	0.37 ug/L	<2.5
Carcinoembryonic antigen	1.2 ug/L	<5

[a] Values are in the 15 months prior to live donor renal transplantation. In this time interval, his glomerular filtration rate declined from 21.7 to 7.8 ml/min/1.73m^2. He was on intermittent hemodialysis for 6 weeks prior to transplantation

[b] Target parathyroid hormone level for children with chronic kidney disease (National Kidney Foundation Kidney Disease Outcomes Quality Improvement Guidelines)

[c] Values are for the 12 years following live donor renal transplantation. In this time interval, his renal function was normal

prior to or after his transplant (Table 1). Chest X-rays done around the time of his transplant showed vertebral osteopenia but no compression fractures and no other abnormalities.

He underwent regular assessment of his pulmonary function as is recommended in patients with cystinosis (Anikster et al. 2001) and a progressive reduction in his diffusing capacity to 67% of the predicted value with preserved lung volumes was noted over serial pulmonary function tests done over 3 years. This pattern was not suggestive of myopathic pulmonary dysfunction (Anikster et al. 2001) but was more suggestive of possible interstitial lung disease, and he underwent computerized tomography as is recommended in the evaluation of patients with possible interstitial lung disease (Behr 2012) at the age of 26. Although the chest CT showed no evidence of involvement of his lung parenchyma, multiple sclerotic lesions were noted in his vertebral bodies (Fig.1a and b), which were confirmed by MRI (Fig. 1c). The low signal intensity on T1W and T2W MRI (Fig. 1c) and increased uptake on bone scan was suggestive of osteoblastic metastases (Fig. 1d).

The patient at this time was clinically well and had no symptoms of fevers, night sweats, or weight loss. Blood work, including calcium, alkaline phosphatase, tumor markers, and hematologic parameters, was all normal (Table 1). CT of his neck, abdomen, and pelvis did not show lymphadenopathy or organomegaly.

In this patient with a history of renal transplantation, the clinical index of suspicion for malignancy was high and so a percutaneous biopsy (Fig. 1a) of one of the sclerotic lesions in his right anterior superior iliac crest was performed. This biopsy (Fig. 2a–c) showed thickened benign trabecular bone with scattered aggregates of histiocytes and admixed hematopoietic elements in the marrow space. There was trilineage hematopoiesis present, but the overall cellularity was decreased. These aggregates of histiocytes were found to be CD68 positive and S100 negative immunohistochemically, which further confirms their nature as histiocytes. They contained abundant pale clear cytoplasm, which was filled with variably sized angular vacuolated spaces, in contrast to the small uniform

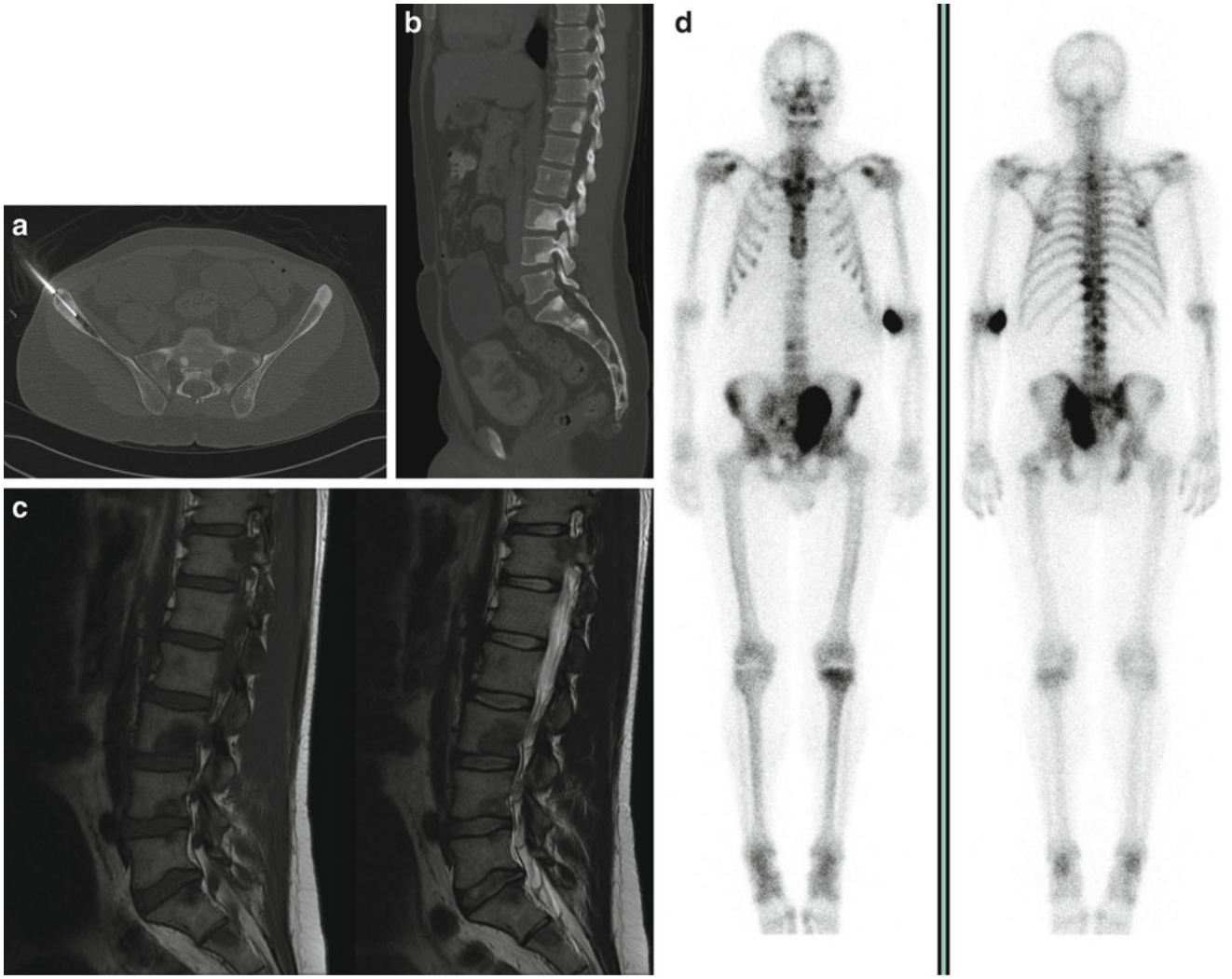

Fig. 1 Radiologic findings showing osteosclerotic bone lesions. (**a**) Sagittal CT scan of the lumbar spine demonstrating multiple well-defined sclerotic lesions in the vertebral bodies and pelvis. The biopsy needle can be seen entering a lesion at the anterior superior aspect of the right iliac blade. (**b**) Axial CT view of the pelvis showing the sclerotic lesions. (**c**) T1 and T2 weighted images MRI of the lumbar spine demonstrating lesions of low signal intensity on T1W and T2W imaging within the vertebral bodies and posterior elements. Appearances correlate with the sclerotic nature of the lesions on CT. (**d**) Technetium 99m-labeled bone scan showing multiple areas of uptake in the spine, pelvis, and proximal tibia corresponding to the lesions seen on CT and MRI

round vacuoles that are sometimes seen within the cytoplasm of histiocytes present in reactive processes like fat necrosis. The appearance of these vacuolated intracytoplasmic spaces within the histiocytes was unusual compared to typical foamy appearance previously documented in hereditary cystinosis (Gebrail et al. 2002). This was a highly unexpected finding as, given the sclerotic appearance on the imaging, crystalline deposits were not considered in the differential diagnosis prior to the biopsy, which was subjected to aqueous tissue processing as is standard in our institution. While no polarizable crystal material was identified, the aqueous tissue processing would have completely dissolved the putative cystine crystals, leaving behind only the "ghost" outline of these angulated clear intracytoplasmic spaces. This was therefore interpreted, in the present clinical context, as being consistent with cystine accumulation in the histiocytes.

Follow-up MR imaging of these lesions performed 6 months later was unchanged.

Discussion

This case is interesting for three reasons. Firstly, this patient demonstrated a marked osteosclerotic response without parathyroid hormone abnormality. It is unclear whether there is a relation between the cystine accumulation in marrow histiocytic aggregates and the osteoclerotic changes, as cystinosis presents more often with osteopenia (Zimakas et al. 2003). Sclerotic lesions in bone are most often related to metastatic disease (Leffler and Chew 1999).

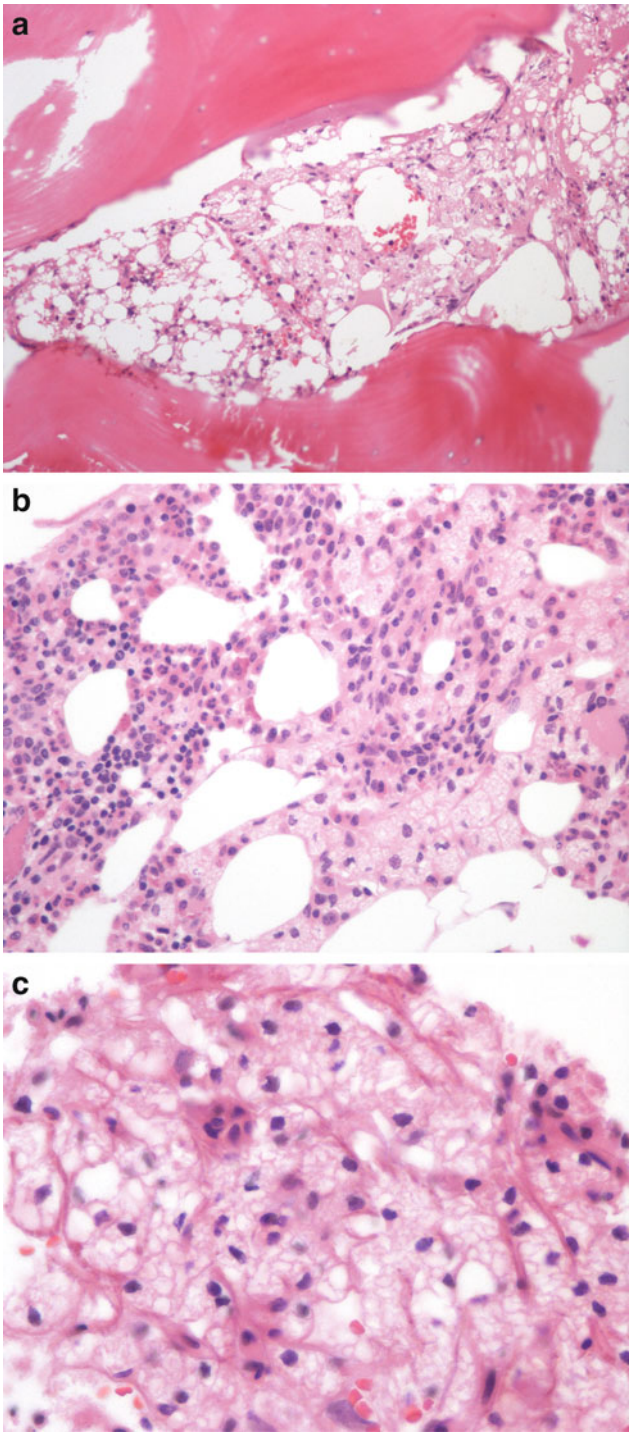

Fig. 2 Histological findings of right iliac core biopsy. (**a**) Low power magnification (4× objective) showing thickened trabecular bone and clusters of histiocytes in the marrow space. (**b**) Intermediate magnification (10× objective) showing clusters of histiocytes with clear/vacuolated cytoplasm intermixed with hematopoietic marrow. (**c**) High magnification (40× objective) shows aggregates of histiocytes that show clear vacuolated cytoplasm with angulated ghost outline of crystals dissolved by aqueous tissue processing

Hematologic disorders, including systemic mastocytosis (Fritz et al. 2012), Langerhans cell histiocytosis, and Erdheim-Chester disease (Wilejto and Abla 2012), can also present with sclerotic bone changes, although there are usually other features on history of imaging to suggest these and the negative S100 immunostaining of the histiocytes from the biopsy exclude Langerhans cell histiocytosis. Nonmalignant causes of sclerotic bone lesions include Paget's disease, osteopoikilosis (Woyciechowsky et al. 2012), and parathyroid-related bone disease. There is a single case (Quinn et al. 2004) where marrow involvement with cystine crystals was accompanied by changes suggestive of parathyroid-related bone disease in a patient with marked elevation (20-fold upper limit of normal) of parathyroid hormone levels. We do not believe that the sclerotic lesions we are seeing in our case are related to parathyroid bone disease for several reasons:

1. His parathyroid hormone levels (Table 1) were controlled within suggested targets (National Kidney Foundation 2003) for end-stage renal disease prior to transplantation.
2. Parathyroid hormone levels have been normal post-transplantation.
3. The bone lesions were clearly not present on imaging done prior to the transplant when his parathyroid hormone levels were highest.
4. The radiologic finding of multiple discrete sclerotic lesions (and reduced bone mineral density is not typical for parathyroid related bone disease in patients with renal disease where the sclerosis is more often diffuse (Burnstein et al. 1985).

This case is also unique because the patient did not have significant cytopenias. Bone marrow involvement with cystine crystals has been documented by other authors (Busuttil and Liu Yin 2000; Quinn et al. 2004; Bigley et al. 2006), but all patients presented with refractory anemia and, in some cases (Busuttil and Liu Yin 2000; Quinn et al. 2004), other cytopenias.

Conclusion

Our case shows that cystine accumulation in histiocytes can occur in cystinosis patients prior to the onset of cytopenia. It also documents multifocal osteoclerotic changes of the bone in a cystinosis patient without parathyroid hormone abnormalities.

Conflict of Interest

Sandra Sirrs, Peter Munk, Paul Mallinson, Hugue Ouellette, Gabriella Horvath, Susan Cooper, Gerald Da Roza, Debbie Rosenbaum, Margaret O'Riley, Gary Nussbaumer, Lien

Hoang, and Cheng Lee have no disclosures related to this manuscript.

Informed Consent

All procedures followed were in accordance with the ethical standards of the responsible committee on human experimentation (institutional and national) and with the Helsinki Declaration of 1975, as revised in 2000 (5). Informed consent was obtained from all patients for being included in the study.

Contributions of the Individual Authors

All authors contributing to the planning, conduct, and reporting of the work described in this article and all authors have approved the manuscript. Radiologic images were analyzed and provided by Drs. Munk, Mallinson, and Oulette. Histology images were analyzed and provided by Drs. Hoang and Lee. Clinical information about the patient (before and after his transplant) was provided by Drs. Sirrs, Rosenbaum, Cooper, Horvath, Da Roza, Nussbaumer, and Ms. O'Riley. Dr. Sirrs serves as guarantor of the work.

References

Anikster Y, Lacbawan F, Brantly M et al (2001) Pulmonary dysfunction in adults with neprhopathic cystinosis. Chest 119:394–401

Behr J (2012) Approach to the diagnosis of interstitial lung disease. Clin Chest Med 33:1–10

Bigley V, Bhartia S, Wood A (2006) Nephropathic cystinosis with bone marrow involvement. Br J Hemat 136:180

Burnstein MI, Kottamasu SR, Pettifor JM, Sochette E, Ellis BI, Frame B (1985) Metabolic bone disease in pseudohypoparathyroidism: radiologic features. Radiology 155:351–356

Busuttil DP, Liu Yin JA (2000) The bone marrow in hereditary cystinosis. Br J Hemat 111:385

Fritz J, Fishman EK, Carrino JA, Horger MS (2012) Advanced imaging of skeletal manifestations of systemic mastocytosis. Skelet Radiol 41:887–897

Gahl WA, Balog JZ, Kleta R (2007) Nephropathic cysinosis in adults: natural history and effects of oral cyteamine therapy. Ann Intern Med 147:242–250

Gebrail F, Knapp M, Perrotta G et al (2002) Crystalline histiocytosis in hereditary cystinosis. Arch Pathol Lab Med 126(9):1135

Leffler SG, Chew FS (1999) CT-guided percutaneous biopsy of sclerotic bone lesions: diagnostic yield and accuracy. Am J Radiol 172:1389–1392

National Kidney Foundation (2003) Kidney Disease Outcomes Quality Improvement clinical practice guidelines for bone metabolism and disease in chronic kidney disease. Am J Kidney Dis 42:S1–201

Quinn JP, Royston D, Murphy PT (2004) Bone marrow findings in hereditary cystinosis with renal failure. Am J Hemat 76:79

Wilejto M, Abla O (2012) Langerhans cell histiocytosis and Erdheim-Chest disease. Curr Opin Rheumatol 24:90–96

Woyciechowsky TG, Monticielo MR, Keiserman B, Monticielo OA (2012) Osteopoikilosis: what does the rheumatologist must know about it? Clin Rheumatol 31:745–748

Zimakas PJA, Sharma AK, Rodd CJ (2003) Osteopenia and fractures in cystinotic children post renal transplantation. Pediatr Nephrol 18:384–390

JIMD Reports
DOI 10.1007/8904_2013_259

CASE REPORT

Pregnancy and Lactation Outcomes in a Turkish Patient with Lysinuric Protein Intolerance

Özlem Ünal · Turgay Coşkun · Diclehan Orhan · Ayşegül Tokatl · Ali Dursun · Burcu Hişmi · Özgür Özyüncü · Serap Hatice Kalkanoğlu Sivri

Received: 20 July 2013 / Revised: 20 August 2013 / Accepted: 29 August 2013 / Published online: 20 October 2013

Abstract Maternal lysinuric protein intolerance (LPI) is associated with increased risk of anemia, toxemia, and retarded growth in fetus during pregnancy, and bleeding complications during delivery. There has been limited number of reports about pregnancy and outcomes of lactation in LPI. Here we present pregnancy and lactation outcomes in a Turkish patient with LPI. In the pregnancy and delivery period, her metabolic status was stable with protein-restricted diet and citrulline. Pathological examination of the placenta revealed multifocal placental infarcts. A successful outcome was achieved with well-controlled anemia, thrombocytopenia despite hemophagocytosis in bone marrow, and placental infarcts during pregnancy. The baby was exclusively breastfed for 6 months. His growth and development was normal. Mild proteinuria started at the fourth month of the delivery. Our case report showed the importance of follow-up of these patients in terms of placental pathologies during pregnancy and for other complications during lactation period.

Communicated by: Eva Morava, MD PhD

Competing interests: None declared

Ö. Ünal · T. Coşkun · A. Tokatl · A. Dursun · B. Hişmi · S.H.K. Sivri
Division of Metabolism, Department of Pediatrics, Hacettepe University, İhsan Doğramacı Children's Hospital, Ankara, Turkey

D. Orhan
Division of Pediatric Pathology, Department of Pediatrics, Hacettepe University, İhsan Doğramacı Children's Hospital, Ankara, Turkey

Ö. Özyüncü
Department of Obstetrics and Gynecology, Hacettepe University, Ankara, Turkey

Ö. Ünal (✉)
Eserköy Sitesi 3A-1 06530, Ümitköy/Ankara, Turkey
e-mail: unalozlem@gmail.com

Introduction

Lysinuric protein intolerance (LPI) is an autosomal recessively inherited, rare, multisystem disorder affecting cationic amino acid transport including ornithine, arginine, and lysine in the kidney and intestine. *SLC7A7* (MIM#603593) named solute carrier family 7A member 7 is the only gene which is known to cause LPI and it was identified in 1997 (Borsani et al. 1999; Torrents et al. 1999). The gene encodes the y(+)LAT−1 protein, the catalytic light chain subunit of a complex belonging to the heterodimeric amino acid transporter family (Sebastio et al. 2011). Main clinical findings are severe failure to thrive, aversion to protein-rich foods, periodic vomiting and diarrhea, hepatomegaly, and tendency to mild leukopenia. Episodes of hyperammonemia that is caused by impaired urea cycle accompany the disease. Interstitial changes, progressing into severe pulmonary alveolar proteinosis in the lung, glomerular and tubular involvement of the kidney, bone marrow anomalies resembling hemophagocytic lymphohistiocytosis/macrophage activation syndrome, lipid abnormalities including hypercholesterolemia and hypertriglyceridemia, autoimmunity and immunologic abnormalities, growth retardation and growth hormone deficiency, pancreatitis, and increased risk of pregnancy complications are the major complications of the disease (Sebastio and Nunes 2006; Sebastio et al. 2011).

Increasing number of patients with inborn errors of metabolism (IEMs) including LPI, are now reaching adulthood, and childbearing age. Therefore, pregnancy complications of IEMs are becoming more important. Maternal LPI is associated with increased risk of anemia, toxemia, and retarded growth in fetus during pregnancy and bleeding complications during delivery (Tanner et al. 2006). There has been limited number of reports about pregnancy

and outcomes of lactation in LPI. Here we present pregnancy and lactation outcomes in a Turkish patient with LPI.

Case Report

The patient was admitted to our center when she was15 years old with the complaints of aversion to protein-rich foods from the infancy, growth failure, and delayed puberty. Her parents were second cousins. On physical examination, her weight was 33.400 kg (<3rd percentile), height was 136 cm (<3rd percentile); she had hepatomegaly (6–7 cm) and muscle wasting. She was prepubertal according to Tanner staging. Serum amino acid analysis showed decreased levels of lysine (93 μmol/L N: 108–223) and arginine (30 μmol/L N: 44–130), and urine amino acid analysis showed highly elevated levels of lysine (6895 μmol/24 h N: 48–328), ornithine (137 μmol/24 h N: 0–53), and arginine (115 μmol/24 h N: <57). Ammonia level was elevated after protein loading (409 μg/dL N ≤120). Abdominal USG revealed hepatomegaly and nephrolithiasis. Molecular genetic analysis revealed c.283insTGG/-(p.Glu95_Thr96insTrp) in the SLC7A7 gene.

She was diagnosed with LPI and treated with citrulline and protein-restricted diet. Pulmonary function tests and HRCT were normal. Complete blood count revealed hemoglobin: 10.5 g/dL; leukocyte count: 3.8 × 10^9/L; and platelet: 313×10^9/L and it was consistent with mild bicytopenia. Serum biochemical investigations showed elevated levels of total cholesterol (250 mg/dL N: <200), triglyceride (1076 mg/dL N: <140 mg/dL), lactate dehydrogenase (699 U/L N: 240–480), and hypofibrinogenemia (107 mg/dL N: 144–430). She had no renal involvement and proteinuria. Liver enzymes were within normal limits. Light microscopic evaluation of bone marrow aspirate yielded increased histiocytes and prominent hemophagocytosis. Specific treatment for hemophagocytic syndrome was not given. Her bone mineral density Z score was −5.4 and calcium and 1,25-dihydroxyvitamin D3 were added to the treatment. Her menstrual cycle started at 19 years of age. In addition, she was treated with hormone replacement therapy for menstrual cycle irregularities.

When she was 25 years old, conception occurred after 10 weeks from ceasing of hormone replacement therapy. She continued to be treated with protein-restricted diet (1 g/kg/day) and citrulline 5 g/day. Hemoglobin, blood pressure, urinary protein, and serum ammonia levels were checked on every visit during pregnancy. Biochemical parameters, lipid profile, and thyroid testing was checked every 4 months. In the pregnancy and delivery period, her metabolic status was stable. Arterial blood pressure was normal. Serum transaminase levels and renal functions were

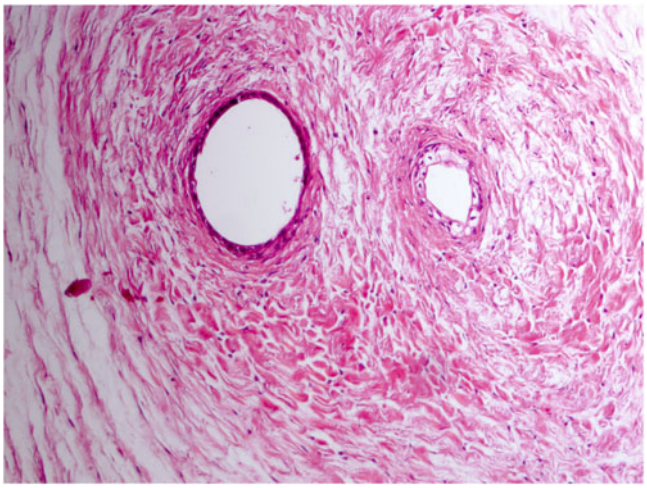

Fig. 1 Omphalomesenteric duct remnants in umblical cord section (Hematoxylin & Eosin, original magnification x100)

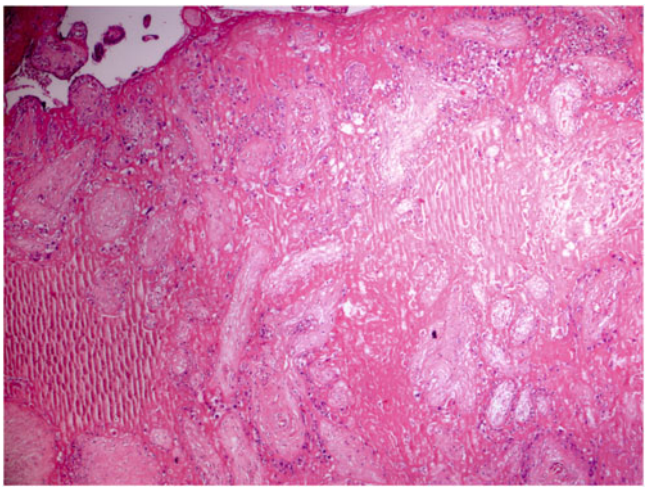

Fig. 2 Ischemic infarct area under the membrane (Hematoxylin & Eosin, original magnification x40)

normal. Total cholesterol and triglyceride levels did not increase when compared to prepregnancy levels. No complications occurred except for mild thrombocytopenia (73,000/mm^3) and severe anemia that fell to 6 g/dL, requiring erythrocyte suspension transfusion before delivery. Thrombocyte transfusion was given during delivery. Her serum ammonia levels were within normal levels both before and after delivery. The baby was born full-term and healthy with a birth weight of 3,200 g. Head circumference was 35.5 cm.

Pathological examination of the placenta revealed multifocal placental infarcts (Figs. 1 and 2). Prothrombotic risk factors other than metabolic disorder were searched for. Molecular genetic analysis for Factor V Leiden, prothrombin 20210A, methylenetetrahydrofolate reductase (MTHFR) A1298C mutations were normal. She was found heterozygous for

PAI-I 4G/5G and homozygous for MTHFR C677T. Serum homocystein and folic acid levels were normal [11.83 μmol/L (N: 4.44–13.56), 4.03 ng/mL (N: 3.1–19.9), respectively]. Anti-cardiolipin and antiphospholipid antibodies were negative. Complement 3 and 4 levels were normal. INR, activated prothrombin time, antithrombin activity, protein C activity, and activated protein C resistance were normal. Free protein S was 48% and mildly low (N: 60–130).

The baby was exclusively breastfed for 6 months. His growth and development was normal. Because lactating women have increased nutrient demands, dietary protein was increased. The mother received 1.3 g/kg/day protein in the lactation period. Metabolic status was stable also in the lactation period as in pregnancy. But mild proteinuria started at the fourth month of the delivery. Total urine protein and microprotein was 154 mg/gün (N: 0–80) and microprotein was 17.06 mg/dL (N<12), respectively.

Discussion

Lysinuric protein intolerance (LPI) is an autosomal recessively inherited disorder affecting the basolateral transporter for cationic amino acids including ornithine, arginine, and lysine in the kidney and intestine. Mutant form of *SLC7A7* gene causes lysinuric protein intolerance. Product of the gene, y^+ LAT–1 protein, is a light chain of the heterodimeric amino acid transporter. Highest prevalence of LPI was reported in Finland. Southern Italy and Japan have relatively high prevalence (Sperandeo et al. 2005; Koizumi et al. 2003). LPI cases were also reported from other countries. There are limited reports about pregnancy outcomes in the patients with LPI and no reports about lactation period in the literature. Here we presented pregnancy and lactation outcomes in a Turkish patient with LPI.

Although number of cases are a few, the most comprehensive study about pregnancy and delivery complications in LPI has been reported by Tanner et al. (2006) from Finland. In their study, outcomes of 18 pregnancies of 9 Finnish mothers with LPI and the follow-up of their 19 children showed that maternal LPI is truly associated with increased risk of anemia, toxemia, and intrauterine growth retardation during pregnancy and bleeding complications during delivery. But the children of the mothers with LPI generally had developed normally. They concluded that successful pregnancies and deliveries could be achieved with careful follow-up of blood pressure and laboratory parameters. Special care of maternal protein nutrition and control of blood ammonia levels, anemia, and toxemia during pregnancy are essential. In another case report from Japan, a successful outcome without serious complication of maternal LPI has been reported (Takayama et al. 1995).

In our patient, pregnancy occurred after severe pubertal delay and menstrual irregularity that was treated with hormone replacement therapy for 6 years. There was no severe complication related to pregnancy except for worsening anemia and thrombocytopenia, but multifocal placental infarcts were detected on placental pathological examination. Although etiological investigations showed heterozygosity for PAI-I 4G/5G and homozygosity for MTHFR C677T mutations that could contribute to thrombophilia and placental infarction, homocystein and folic acid levels were within normal limits, suggesting placental infarctions were more likely to be related to LPI. Placental bleeding after amniotic sac puncture, partial retention of the placenta, overweight of placenta for gestational age, altered fetal-placental ratio, and altered vascular development of the placenta that is considered the probable underlying cause for preeclampsia were reported placental abnormalities in patients with LPI in the study of Tanner et al. (2006), but no histological examination has previously been performed on the placentas of mothers with LPI in their study.

There has been no report on outcomes of lactation period in patients with LPI. Breast milk is made from nutrients in the mother's bloodstream and bodily stores. Although maternal nutritional status and amino acid levels may affect the quality of breastfeeding, composition and amount of the breastfeeding changes depending on how often and how effectively the infant sucks and, as well as on the age of the child. Even if the breastfeeding mother is undernourished, breastfeeding is recommended. The child of our patient was exclusively breastfed for 6 months. Normal growth and development of the baby showed that the breastfeeding was safe. But proteinuria started during lactation. Glomerular and tubular involvement is common in LPI. Isolated mild proteinuria is the initial sign of renal disease. The pathogenesis of the renal involvement is unknown. Pregnancy and lactation may have additional physiological stresses, and organs that are already damaged by the underlying metabolic illness may be compromised further. So, theoretically, it was thought that, pregnancy and lactation period might aggravate renal involvement in this patient. Blood pressure was normal during pregnancy and after delivery. Complete urine analysis was normal except for mild proteinuria. The patient was in lactation period, and treatment was not started for microproteinuria. But, follow-up for renal involvement is going on.

In our patient, a successful outcome was achieved with well-controlled anemia, thrombocytopenia despite hemophagocytosis in bone marrow, and placental infarcts during pregnancy. However, it is very important to follow up closely of patients with LPI for pregnancy complications. Our case report showed the importance of follow up of these patients in terms of placental pathologies during pregnancy and for other complications during lactation period.

Take-Home Message

Follow-up of the patients with lysinuric protein intolerance is important in terms of placental pathologies during pregnancy and for other known complications of the disease during lactation period.

Compliance with Ethical Guidelines

- The article has not been and will not be published elsewhere in the same form (Accepted as a poster presentation at ICIEM 2013).
- The submitting author has circulated the article and secured final approval of the version to be peer-reviewed from all coauthors prior to the publication of the article.
- Substantial contribution of coauthors to the work: The report was planned by first, second, and last authors; pathological investigations were performed by third author; obstetrical follow-up of the patient was performed by seventh author. All authors contributed to the conception and interpretation of data. First draft was written by the first author and revised by the second author.
- Özlem Ünal, Turgay Coşkun, Diclehan Orhan, Ayşegül Tokatl, Ali Dursun, Burcu Hişmi, Özgür Özyüncü, and Serap Hatice Kalkanoğlu Sivri declare that they have no conflict of interest.
- All procedures followed were in accordance with the ethical standards of the responsible committee on human experimentation (institutional and national) and with the Helsinki Declaration of 1975, as revised in 2000 (5).
- Informed consent was obtained from the patient for publication.
- This article does not contain any studies with human subjects performed by the any of the authors.

References

Borsani G, Bassi MT, Sperandeo MP et al (1999) SLC7A7, encoding a putative permease related protein, is mutated in patients with lysinuric protein intolerance. Nat Genet 21:297–301

Koizumi A, Matsuura N, Inoue S et al (2003) Mass Screening Group. Evaluation of a mass screening program for lysinuric protein intolerance in the northern part of Japan. Genet Test 7:29–35

Sebastio G, Nunes V (2006) [updated 2011] Lysinuric protein ntolerance. In: Pagon RA, Adam MP, Bird TD, Dolan CR, Fong CT, Stephens K (eds) GeneReviews™ [Internet]. University of Washington, Seattle. Available from http://www.ncbi.nlm.nih.gov/books/NBK1361

Sebastio G, Sperandeo MP, Andria G (2011) Lysinuric protein intolerance: reviewing concepts on a multisystem disease. Am J Med Genet C Semin Med Genet 157:54–62

Sperandeo MP, Annunziata P, Ammendola V et al (2005) Lysinuric protein intolerance: identification and functional analysis of mutations of the SLC7A7 gene. Hum Mutat 25:410–416

Takayama N, Hamada H, Kubo T (1995) Lysinuric protein intolerance in pregnancy: case report with successful outcome. Arch Gynecol Obstet 256:49–52

Tanner L, Näntö-Salonen K, Niinikoski H, Erkkola R, Huoponen K, Simell O (2006) Hazards associated with pregnancies and deliveries in lysinuric proteinintolerance. Metabolism 55:224–231

Torrents D, Mykkänen J, Pineda M et al (1999) Identification of SLC7A7, encoding y+LAT-1, as the lysinuric protein intolerance gene. Nat Genet 21:293–296<

JIMD Reports
DOI 10.1007/8904_2013_267

CASE REPORT

Adult-Onset Fatal Neurohepatopathy in a Woman Caused by *MPV17* Mutation

Bryce A. Mendelsohn • Neil Mehta • Bilal Hameed • Melike Pekmezci • Seymour Packman • Jeffrey Ralph

Received: 22 July 2013 / Revised: 18 September 2013 / Accepted: 23 September 2013 / Published online: 5 November 2013

Abstract Hepatocerebral mitochondrial DNA depletion syndromes are classically considered diseases of early childhood, typically affecting the liver, peripheral, and central nervous systems with a rapidly progressive course. Evidence is emerging that initial symptom onset can extend into adulthood, though few such cases have been reported. We describe a 25-year-old woman who presented initially with secondary amenorrhea, followed by a megaloblastic anemia, lactic acidosis, leukoencephalopathy, progressive peripheral neuropathy, and liver cirrhosis. An apparently homozygous P98L mutation was identified in *MPV17*, a gene associated with a lethal infantile neurohepatopathy. Homozygosity for the same allele was recently reported in a man with a similar hepatic and neurologic phenotype. This is the first clinical report of an adult female with this disorder, and the first to describe amenorrhea and megaloblastic anemia as likely associated symptoms.

Communicated by: Gregory Enns

Competing interests: None declared

B.A. Mendelsohn · S. Packman
Division of Medical Genetics, Department of Pediatrics, UCSF Benioff Children's Hospital, San Francisco, CA, USA

N. Mehta · B. Hameed
Division of Gastroenterology, Department of Internal Medicine, UCSF Medical Center, San Francisco, CA, USA

M. Pekmezci
Department of Pathology, UCSF Medical Center, San Francisco, CA, USA

J. Ralph
Department of Neurology, UCSF Medical Center, San Francisco, CA, USA

B.A. Mendelsohn (✉)
533 Parnassus Ave, Box 0748, San Francisco, CA 94143, USA
e-mail: mendelsohnb@peds.ucsf.edu

Mitochondrial DNA depletion syndromes are a heterogeneous group of diseases associated with reduced copy number of mitochondrial DNA due to defects in the replication or maintenance of the mitochondrial genome. Frequent manifestations include neuropathy, leukoencephalopathy, myopathy, and hepatic disease. Though depletion of the circular mitochondrial genome and subsequent mitochondrial dysfunction and energy failure are thought to underlie the pathophysiology of these disorders, they are caused by mutations in nuclear-encoded mitochondrial proteins; the inheritance pattern is usually autosomal recessive. These syndromes generally present in infancy, and death often occurs within the first year of life.

Located on chromosome 2, *MPV17* encodes an inner membrane-associated mitochondrial protein of unclear function (El-Hattab and Scaglia 2013). Mutations in *MPV17* are known to cause Navajo neurohepatopathy (OMIM #256810), a recessive, rapidly progressive mitochondrial DNA depletion syndrome of liver failure and neurologic deterioration with onset in the first year of life (Karadimas et al. 2006; El-Hattab et al. 2010; AlSaman et al. 2012). More recently, mutations in this gene have been identified in an older child (El-Hattab et al. 2010) and two adults (Blakely et al. 2012; Garone et al. 2012) with subacute onset of many of the same symptoms seen in the infantile form, including peripheral neuropathy, liver dysfunction or failure, progressive white matter disease, and lactic acidosis.

The *MPV17* mutation P98L was identified in the heterozygous state in a child who survived to 2.5 years without liver transplantation, and was hypothesized to be a milder allele (El-Hattab et al. 2010). This same mutation in the homozygous state was then reported in a man with onset of symptoms at age 14 who was still living at age 21 (Blakely et al. 2012). A second man was reported with

Table 1 Motor and sensory nerve conduction studies

	Normal		Patient	
	SNAP (μV)	NCV (m/s)	SNAP (μV)	NCV (m/s)
Sensory nerves				
Right sural	>5	>41	NR	NR
Left sural	>5	>41	NR	NR
Left median	>14	>44	12	57
	CMAP (mV)	NCV (m/s)	CMAP (mV)	NCV (m/s)
Motor nerves				
Left peroneal (TA)	>2	>41	0.6	30
Left tibial	>2	>41	NR	NR
Right tibial	>3	>41	NR	NR
Left median	>4	>49	7.6	51

SNAP sensory nerve action potential, *CMAP* compound muscle action potential, *NR* no response obtained

compound heterozygosity for the mutations KM88-89ML and L143X with initial symptoms at age 34 (Garone et al. 2012). These cases highlight that *MPV17*-mediated disorders – and likely mitochondrial DNA depletion syndromes in general – can present in adulthood with multisystem involvement, and the scarcity of such reports in the literature suggests that the range of adult phenotypes is yet to be fully appreciated. Here, we report the first known case of adult-onset *MPV17*-mediated neurohepatopathy in a female, who experienced secondary amenorrhea as the putative first symptom of the disorder.

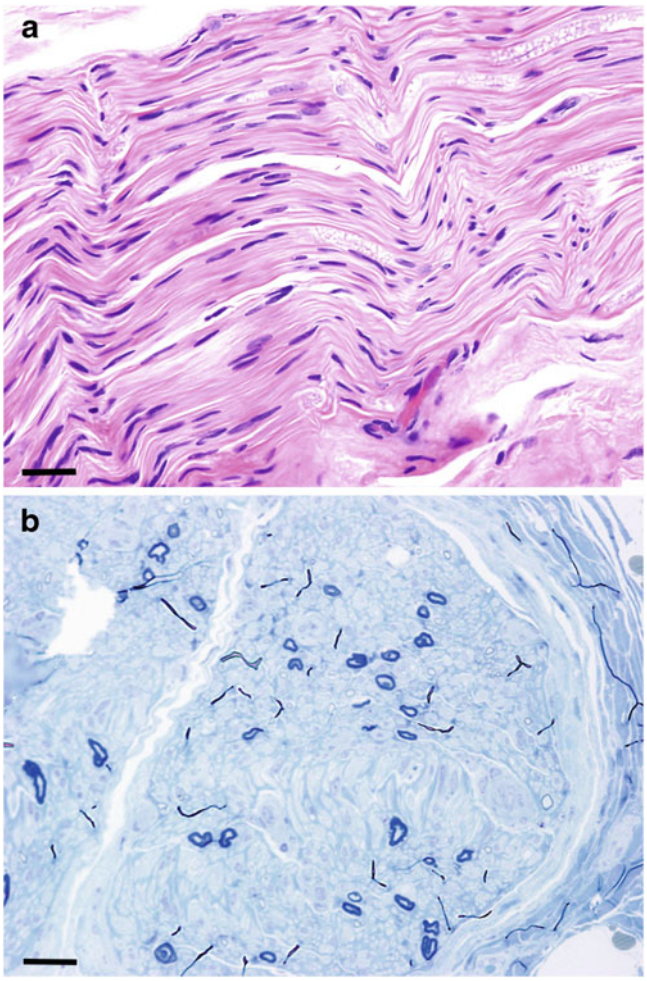

Fig. 1 (**a**) Hematoxylin and eosin stain, 400x magnification, calibration bar is 0.1 mm. Significantly decreased amount of myelinated fibers without evidence of digestion chambers or inflammation. (**b**) Toluidine blue stain, 400x magnification, calibration bar is 0.1 mm. Severe (>95 %) loss of myelinated axons without onion bulbs or regenerating clusters

Case Report

We report a 25-year-old woman of second-cousin Pakistani parents who, after normal cognitive and motor development and normal menarche, presented at age 18 years with secondary amenorrhea. Her only other health concern was a short stature of 4'11", while her adult siblings were 5'4" and 5'6".

Up to this time, she had been physically active without difficulties. Shortly after her periods ceased, she developed a steppage gait and weakness in her ankles that required orthotics. She also noticed mild numbness in her lower extremities. The numbness and weakness progressed slowly and eventually involved the upper extremities. Electromyography and nerve conduction studies showed a severe axonal peripheral neuropathy (Table 1). Nerve biopsy confirmed these findings (Fig. 1). A concomitantly performed muscle biopsy did not contain sufficient viable muscle tissue to quantify mitochondrial DNA. Difficulty with memory and word-finding developed, and a brain MRI at age 24 showed a leukodystrophy with diffuse and symmetrical white matter involvement (Fig. 2) concerning for a genetic syndrome.

Between the time of the onset of symptoms and her diagnosis, she was repeatedly hospitalized for worsening weakness, and during these admissions additional involved organ systems were noted. She developed a mild, permanent lactic acidosis, and the level of ammonia was intermittently elevated. Chronic thrombocytopenia and a macrocytic anemia also developed, with hemoglobin 9.5 g/dL and MCV 105 fL (upper limit of normal <100 fL), and normal serum levels of vitamin B12. Elevated blood glucose values developed and were treated with insulin and later with sitagliptin (Januvia). Hepatomegaly was noted and abdominal CT showed a nodular appearing liver,

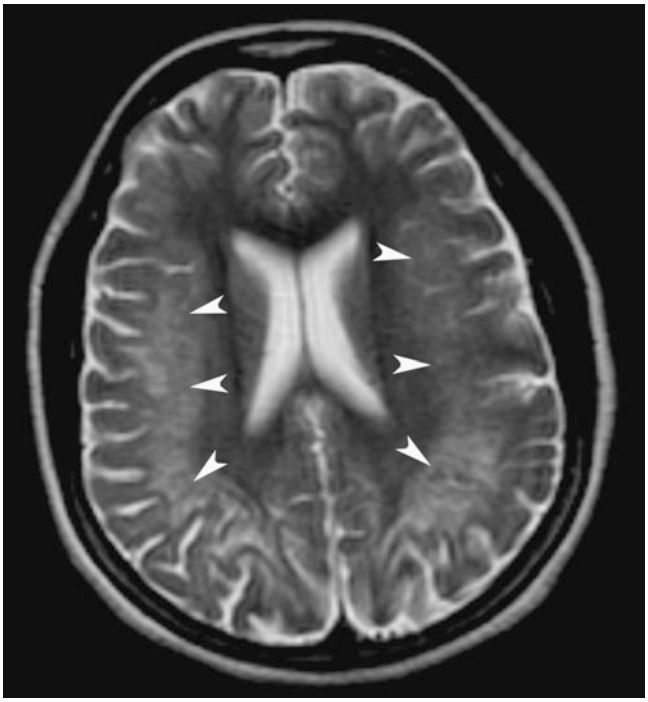

Fig. 2 T2-weighted axial MRI image shows confluent and symmetrical hyperintensities within the deep and subcortical white matter of the posterior frontal and parietal cerebral hemispheres (*arrowheads*) involving the subcortical U-fibers, with sparing of the prefrontal cortices. There is associated cortical thinning. These hyperintensities did not show enhancement after the administration of IV gadolinium

splenomegaly, and gastroesophageal varices consistent with cirrhosis. Portal hypertension was confirmed by both direct portal pressure measurement and upper endoscopy showing moderate esophageal varices. She also had evidence of synthetic liver dysfunction with an INR of 1.8 despite administration of vitamin K. A liver biopsy showed cirrhosis as well as steatosis and hepatocyte swelling suggestive of steatohepatitis despite her thin body habitus. Electron microscopy showed most hepatocytes to contain abundant mitochondria of varying sizes and shapes, some dilated and others with a nonuniform distribution of cristae. Quantification of mitochondrial DNA on the liver biopsy sample was not performed.

At age 25, her exam was notable for appropriate mental status, normal cranial nerve and fundal exam, striking atrophy of the muscles of the hands and lower legs with diminished strength in the finger extensors, abductor digiti minimi, and marked weakness of the tibialis anterior, gastrocnemius, and toe extensors and flexors. Deep tendon reflexes were absent in the triceps, patellae, and ankles. Pain sensation was intact in the fingertips but impaired in a stocking distribution to the mid-shin level bilaterally. Vibration sensation was intact at the fingertips. Vibration sensation was absent distal to the knees bilaterally. Joint position sensation was moderately impaired at the toes. She had a steppage gait and was too unsteady to attempt Romberg testing. The liver edge was palpable 3cm below the costal margin. The spleen could not be palpated.

Based on the clinical findings of brain and liver involvement, a hepatocerebral mitochondrial DNA sequencing panel was sent to Baylor College of Medicine, which revealed an apparently homozygous P98L mutation in *MPV17*. Given the known consanguinity of the parents it is most probable that this patient was indeed homozygous for this mutation, but because sequencing of the parents was not performed, we cannot formally exclude a deletion or sequencing failure affecting one allele. Additionally, a heterozygous mutation Q139X in *OPA3* was detected. Homozygous mutations in *OPA3* cause 3-methylglutaconic aciduria type 3, characterized by childhood onset of optic atrophy, a choreoathetoid movement disorder, and elevated urine 3-methylglutaconate. Our patient lacked these findings, indicating that the heterozygous *OPA3* mutation was an incidental finding. The patient succumbed to a respiratory infection shortly after diagnostic results were received.

This is the second report of a patient homozygous for the *MPV17* mutation P98L (Blakely et al. 2012) and the first in a female. Features such as amenorrhea, probably due to ovarian failure, and macrocytic anemia have not been previously reported for syndromes associated with *MPV17*.

Discussion

The connection between *MPV17* and a hepatocerebral mitochondrial DNA depletion syndrome has been known since 2006 (Spinazzola et al. 2006), when an integrative genomics strategy suggested a mitochondrial gene resided in a chromosomal region linked with hepatocerebral disease in infants. Previously, *MPV17* had been thought to be a peroxisomal protein, but studies indicated that it was in fact localized to the mitochondrial inner membrane (Spinazzola et al. 2006). Since this initial breakthrough, little additional insight has been gained into how mutations in this gene cause mitochondrial DNA depletion, or why the liver and nervous system are disproportionately affected. Other genes associated with hepatocerebral mitochondrial DNA depletion such as *POLG* and *DGUOK* have clear roles in mitochondrial DNA synthesis and maintenance. Deletion of the yeast ortholog of *MPV17* recapitulates the DNA depletion phenotype, and experiments in yeast have suggested that *MPV17* may be important for anaplerosis of TCA cycle intermediates and for maintaining mitochondrial integrity during stress conditions (Dallabona et al. 2010). It is important to note that P98, the residue mutated in this patient, is conserved across evolution in organisms including worms and yeast (Blakely et al. 2012). Further insight into the molecular function of *MPV17* may provide

better diagnostic or therapeutic approaches to patients with DNA depletion syndromes.

Adult-onset disease caused by mutations in *MPV17* was only recently recognized. As in other reported cases, our patient did not have any upper motor neuron findings or disabling cognitive deficits despite the abnormal imaging that showed a leukoencephalopathy (Blakely et al. 2012). She did report some memory and word-finding difficulties as discussed above. The polyneuropathy in these syndromes is axonal, with a dropout of both large- and small-diameter nerve fibers, consistent with the patient's weakness, gait abnormality, and loss of sensation.

Liver involvement in patients with *MPV17* mutations is quite common but typically manifests in neonates and in children under the age of 5 (Nogueira et al. 2012). Manifestations can include steatohepatitis, cholestasis, cirrhosis, and liver failure (Holve et al. 1999). The mechanism is thought to be from impaired mitochondrial oxidative phosphorylation and fatty acid oxidation, resulting in impaired bile flow and steatosis, cell death, and fibrogenesis (Lee and Sokol 2007). Interestingly, our patient's presentation included steatohepatitis and cirrhosis with portal hypertension that was not symptomatic until adulthood, but then progressed rapidly within a year as would be consistent with cases in much younger patients (Holve et al. 1999). We speculate that this course reflects a threshold of mitochondrial DNA depletion that is reached later in life in adult cases, but is then followed by rapid hepatic deterioration. Unfortunately, medical therapies for mitochondrial hepatopathies are largely ineffective (Lee and Sokol 2007). Liver transplantation was considered in this patient but not pursued due to concurrent neuromuscular disease, poor functional status, and her severe respiratory infection, which proved to be her ultimate cause of death.

To our knowledge, this is the third report of an adult, and the first female, with an *MPV17*-mediated mitochondrial neurohepatopathy. Even though a mitochondrial DNA depletion syndrome satisfactorily accounts for the majority of her symptoms, it must be noted, however, given the known consanguinity of the patient's parents, that the coexistence of another recessive disorder cannot be fully excluded. This patient's initial presentation was with amenorrhea after normal menarche. Because no other adult females with *MPV17* mutations have been reported, it is possible that *MPV17* has a critical but unappreciated function in the postpubertal ovary. The role of mitochondrial DNA depletion in ovarian function has not been extensively studied, but there are reports of reduced mitochondrial DNA content in the blood of women with premature ovarian failure (Kim et al. 2004), and mutations in *POLG* were associated with premature ovarian failure and mitochondrial DNA depletion (Luoma et al. 2004; Pagnamenta et al. 2006). Women with premature ovarian failure may represent milder forms of mitochondrial depletion syndromes that have not yet caused typical heptocerebral symptoms, and should be considered for evaluation for mitochondrial disorders if nervous system or hepatic disease are present or develop. Finally, mitochondrial DNA depletion syndromes ought to be considered when severe axonal polyneuropathies occur in young people with coexisting cryptogenic hepatic failure or leukoencephalopathy.

Acknowledgment The authors would like to thank Robert B. Layzer, MD, from the University of California, San Francisco, for his help in evaluating this patient.

Summary

Mitochondrial DNA depletion syndromes can present in adulthood with multisystem involvement, including amenorrhea and megaloblastic anemia as newly described in this report.

Compliance with Ethics Guidelines

Bryce Mendelsohn has received consulting fees from Counsyl.

Neil Mehta, Bilal Hameed, Melike Pekmezci, Seymour Packman, and Jeffrey Ralph declare that they have no conflicts of interest.

All procedures followed were in accordance with the ethical standards of the responsible committee on human experimentation (institutional and national) and with the Helsinki Declaration of 1975, as revised in 2000 (5). The studies described in this report are of a retrospective nature regarding clinical care and do not require informed consent. No identifying information is provided. No animals were used in this study.

Drs. Mendelsohn, Mehta, Hameed, Packman, and Ralph all clinically evaluated the patient and provided critical insight into medical and diagnostic management. Dr. Pekmezci reviewed and reported the pathology samples described herein. All authors contributed to and critically reviewed the manuscript.

References

AlSaman A, Tomoum H, Invernizzi F, Zeviani M (2012) Hepatocerebral form of mitochondrial DNA depletion syndrome due to mutation in MPV17 gene. Saudi J Gastroenterol 18 (4):285–289

Blakely EL, Butterworth A, Hadden RD et al (2012) MPV17 mutation causes neuropathy and leukoencephalopathy with multiple

mtDNA deletions in muscle. Neuromuscul Disord 22 (7):587–591

Dallabona C, Marsano RM, Arzuffi P et al (2010) Sym1, the yeast ortholog of the MPV17 human disease protein, is a stress-induced bioenergetic and morphogenetic mitochondrial modulator. Hum Mol Genet 19(6):1098–1107

El-Hattab AW, Scaglia F (2013) Mitochondrial DNA depletion syndromes: review and updates of genetic basis, manifestations, and therapeutic options. Neurotherapeutics 10(2):186–198

El-Hattab AW, Li FY, Schmitt E, Zhang S, Craigen WJ, Wong LJ (2010) MPV17-associated hepatocerebral mitochondrial DNA depletion syndrome: new patients and novel mutations. Mol Genet Metab 99(3):300–308

Garone C, Rubio JC, Calvo SE et al (2012) MPV17 mutations causing adult-onset multisystemic disorder with multiple mitochondrial DNA deletions. Arch Neurol 69(12):1648–1651

Holve S, Hu D, Shub M, Tyson RW, Sokol RJ (1999) Liver disease in Navajo neuropathy. J Pediatr 135(4):482–493

Karadimas CL, Vu TH, Holve SA et al (2006) Navajo neurohepatopathy is caused by a mutation in the MPV17 gene. Am J Hum Genet 79(3):544–548

Kim JH, Lee SH, Cho SW et al (2004) The quantitative analysis of mitochondrial DNA copy number in premature ovarian failure patients using the real-time polymerase chain reaction. Korean J Obstet Gynecol 47(1):16–24

Lee WS, Sokol RJ (2007) Liver disease in mitochondrial disorders. Semin Liver Dis 27(3):259–273

Luoma P, Melberg A, Rinne JO et al (2004) Parkinsonism, premature menopause, and mitochondrial DNA polymerase gamma mutations: clinical and molecular genetic study. Lancet 364 (9437):875–882

Nogueira C, de Souza CF, Husny A, Derks TG, Santorelli FM, Vilarinho L (2012) MPV17: fatal hepatocerebral presentation in a Brazilian infant. Mol Genet Metab 107(4):764

Pagnamenta AT, Taanman JW, Wilson CJ et al (2006) Dominant inheritance of premature ovarian failure associated with mutant mitochondrial DNA polymerase gamma. Hum Reprod 21 (10):2467–2473

Spinazzola A, Viscomi C, Fernandez-Vizarra E et al (2006) MPV17 encodes an inner mitochondrial membrane protein and is mutated in infantile hepatic mitochondrial DNA depletion. Nat Genet 38 (5):570–575

JIMD Reports
DOI 10.1007/8904_2013_268

CASE REPORT

Multiple Acyl-CoA Dehydrogenation Deficiency (Glutaric Aciduria Type II) with a Novel Mutation of Electron Transfer Flavoprotein-Dehydrogenase in a Cat

Shoichi Wakitani • Shidow Torisu • Taiki Yoshino • Kazuhisa Hattanda • Osamu Yamato • Ryuji Tasaki • Haruo Fujita • Koichiro Nishino

Received: 24 June 2013 / Revised: 23 September 2013 / Accepted: 24 September 2013 / Published online: 20 October 2013

Abstract Multiple acyl-CoA dehydrogenation deficiency (MADD; also known as glutaric aciduria type II) is a human autosomal recessive disease classified as one of the mitochondrial fatty-acid oxidation disorders. MADD is caused by a defect in the electron transfer flavoprotein (ETF) or ETF dehydrogenase (ETFDH) molecule, but as yet, inherited MADD has not been reported in animals. Here we present the first report of MADD in a cat. The affected animal presented with symptoms characteristic of MADD including hypoglycemia, hyperammonemia, vomiting, diagnostic organic aciduria, and accumulation of medium- and long-chain fatty acids in plasma. Treatment with riboflavin and L-carnitine ameliorated the symptoms. To detect the gene mutation responsible for MADD in this case, we determined the complete cDNA sequences of feline ETFα, ETFβ, and ETFDH. Finally, we identified the feline patient-specific mutation, c.692T>G (p.F231C) in ETFDH. The affected animal only carries mutant alleles of ETFDH. p.F231 in feline ETFDH is completely conserved in eukaryotes, and is located on the apical surface of ETFDH, receiving electrons from ETF. This study thus identified the mutation strongly suspected to have been the cause of MADD in this cat.

Communicated by: Jerry Vockley, M.D., Ph.D.

Competing interests: None declared

S. Wakitani · T. Yoshino · K. Nishino
Laboratory of Veterinary Biochemistry and Molecular Biology, Faculty of Agriculture, University of Miyazaki, Miyazaki, Japan

S. Torisu
Veterinary Teaching Hospital, Faculty of Agriculture, University of Miyazaki, Miyazaki, Japan

K. Hattanda
Otsuka Animal Clinic, Miyazaki, Japan

O. Yamato
Laboratory of Clinical Pathology, Joint Faculty of Veterinary Medicine, Kagoshima University, Kagoshima, Japan

R. Tasaki · H. Fujita
Kaketsuken, Kumamoto, Japan

K. Nishino (✉)
1-1 Gakuenkibanadai-nishi,
Miyazaki 889-2192, Japan
e-mail: aknishino@cc.miyazaki-u.ac.jpa

Introduction

Multiple acyl-CoA dehydrogenation deficiency (MADD, also known as glutaric aciduria type II, GAII, OMIM 231680) is a type of mitochondrial fatty-acid oxidation disorder (FAOD) characterized by hypoketotic hypoglycemia; metabolic acidosis; fatty infiltration of the liver, heart, and kidneys; and diagnostic organic aciduria (Frerman and Goodman 2001; Gordon 2006). In addition, MADD may be accompanied by various symptoms including vomiting, hypotonia, hyperammonemia, hepatomegaly, renal cysts, myopathy, an odor of sweaty feet, and congenital anomalies. Severe MADD appears in the neonatal period, and patients die within the first few weeks of life. However, MADD can also develop in later life. Treatment with riboflavin and L-carnitine is effective only for patients with mild symptoms (Gordon 2006; Olsen et al. 2007; Henriques et al. 2009; Law et al. 2009; Ishii et al. 2010; Lund et al. 2010).

MADD is an autosomal recessive disease, and most cases are caused by a defect of electron transfer flavoprotein (ETF) or ETF dehydrogenase (ETFDH, also

known as ETF-ubiquinone oxidoreductase, EC 1.5.5.1) (Frerman and Goodman 2001; Er et al. 2011). These proteins play a role in the metabolism of fatty acids. ETF forms a heterodimer composed of α- and β-subunits, and contains flavin adenine dinucleotide (FAD) as a redox cofactor. In the mitochondrial matrix, ETF receives electrons from acyl-CoA dehydrogenase (EC 1.3.99.3) in the process of fatty acid degradation. ETFDH is a monomer, and contains FAD and a 4Fe-4S cluster as redox prosthetic groups (Frerman and Goodman 2001; Watmough and Frerman 2010). ETFDH transfer electrons from ETF to ubiquinone, which exists in the inner mitochondrial membrane and participates in electron transport system to produce ATP. In this process, electrons enter through the flavin center of ETFDH and exit via the 4Fe-4S cluster for delivery to ubiquinone. Deficiency of ETF or ETFDH leads to dysfunction of acyl-CoA dehydrogenase, resulting in accumulation of long- and medium-chain fatty acids. As metabolites of the accumulated substances, the urine and plasma levels of specific organic acids increase; these include isovaleric, isobutyric, 2-methylbutyric, glutaric, ethylmalonic, 3-hydroxyisovaleric, 2-hydroxyglutaric, 5-hydroxyhexanic, adipic, suberic, sebacic, and dodecanedioic acid, as well as isovalerylglycine, isobutyrylglycine, and 2-methylbutyrylglycine.

According to the Genetics Home Reference serviced by the U.S. National Library of Medicine (http://ghr.nlm.nih.gov/), the precise incidence of MADD is still unknown in view of its rarity. Tamaoki et al. surveyed Japanese patients with FAODs identified between 1985 and 2000, and found 14 patients with MADD out of 64 such patients (Tamaoki et al. 2002). They estimated that the frequency of FAODs in Japan is at least 1/5,000 births, implying that the frequency of MADD is about 1/20,000. Some studies have investigated the epidemiology of MADD in southern China, where c.250G>A mutation in ETFDH is carried at high frequency in patients with riboflavin-responsive MADD (Law et al. 2009; Liang et al. 2009; Er et al. 2010; Lan et al. 2010; Wen et al. 2010; Wang et al. 2011).

In animals, outbreaks of fatal MADD have been recorded in horses with atypical myopathy in particular weather conditions (Finno et al. 2006; Cassart et al. 2007; Westermann et al. 2008; van der Kolk et al. 2010; Valberg et al. 2012). In these cases, an exogenous factor was predicted to cause MADD, and a genetic mutation of ETF and ETFDH has never been recognized. In any event, MADD associated with gene mutation in animals has never been reported. Here, we report a novel case of inherited MADD that developed in a cat, which we consider to be the first of its kind to have been reported in an animal.

Table 1 Diet loading test

	NH_3 (μg/dl)	SBA (μmol/l)
Fasting	227	3.7
Postprandial	71	18.2
Reference range	23–78	0–20

SBA serum bile acid

Materials and Methods

Subject

A 6-month-old castrated cat with a previous history of hypoglycemia and hyperammonemia was brought by its owner to the animal hospital with a chief complaint of collapse, loss of appetite, and vomiting. Blood biochemistry revealed elevated levels of ammonia and liver enzymes (NH_3, 227 μg/dl; ALT, 610 U/l; and AST, more than 1,000 U/l); reference values of NH_3, ALT, and AST are 23–78 μg/dl, 22–78 U/l, and 22–84 U/l, respectively, in cats. A generalized seizure also occurred during follow-up. We treated the cat for hyperammonemia with administration of lactulose and infusion of Ringer's solution. Although we suspected hepatic encephalopathy associated with a portosystemic shunt, measurement of fasting and postprandial blood ammonia and serum bile acid (SBA) concentrations revealed no evidence of hepatic dysfunction (Table 1). In addition, computed tomographic angiography revealed no congenital vascular anomaly or any enlargement of the liver. Symptoms were improved within 10 days after the first visit. Just a year later, this cat was brought again in worse condition than that at the first visit. As a countermeasure against hepatic lipidosis accompanied by lack of energy, the cat received nutritional care via a gastrostomy tube, in addition to the treatment for hyperammonemia.

Diet Loading Test

To exam hepatic function, blood ammonia and SBA concentrations were measured during fasting and postprandial periods at the first visit. Blood samples were collected after an overnight fast and at 2 hours after a meal.

GC-MS Analysis

To assay urine organic acids, GC-MS analysis was conducted in MILS INTERNATIONAL (Kanazawa, Japan) as published previously (Zhang et al. 2000). The first sample of urine was collected under the condition in loss of appetite at the second visit, when the present cat was 18 months old. At 6 days

Table 2 List of primers used in this study

Purpose	Sequence	
Target	Forward	Reverse
5'-RACE		
ETFα	*	CTTTCCAAAGGCAGATGCTC
ETFβ	*	GCATAGCGAGGTTCGTTGAG
ETFDH	*	GGGCACCATCCTTTTGTATC
3'-RACE		
ETFα	TACCATCACTGCAGCCAAAC	*
ETFβ	CCGCTGGATTTCTAGACTGG	*
ETFDH	CTCCCAGGTCTTCCAATGAA	*
Gene expression		
ETFα	TACCATCACTGCAGCCAAAC	CTTTCCAAAGGCAGATGCTC
ETFβ	CCGCTGGATTTCTAGACTGG	GCATAGCGAGGTTCGTTGAG
ETFDH	CTCCCAGGTCTTCCAATGAA	GGGCACCATCCTTTTGTATC
GAPDH	GTTTGTGATGGGCGTGAAC	CGTATTTGGCAGCTTTCTCC
ORF sequence		
ETFα	TGAGACTGACGGTGCTTCTAG	AAAGCATTCTGGCATCTGTGAG
ETFβ	ACTGACCCCGGCAGGTG	CGGGAGGGTCATAGTTTTATTGCTG
ETFDH	AACTTCAGCGGAGGTGTTGG	GGTAAGATAGTTTGACAACCTGTTGACTTC
PCR-RFLP		
ETFDH	GAGGGCACCTGTTGGGAT	TCCTTGAGTCCAATTCCATAGGTT

*Attached in GeneRacer kit

after the first sampling, we received the result suggesting MADD. The affected cat has received the oral administration of riboflavin (100–300 mg/day) and L-carnitine (100–150 mg/day) since then. At 16 days of treatment, posttreatment sample was collected after an overnight fast.

LC-MS/MS Analysis

To assay the blood levels of acylcarnitines, LC-MS/MS analysis was conducted as published previously (Chang et al. 2012). The first sample was collected under the condition in force-feeding via a gastrostomy tube at the age of 18 months, when we start the treatment with riboflavin and L-carnitine as described above. At 3 months of treatment, posttreatment sample was collected after an overnight fast. Physical value of the blood levels of acylcarnitines was obtained from 27 of healthy cats. For statistical analysis, the Smirnov-Grubbs test was used.

Cell Culture

From among cats brought to the Veterinary Teaching Hospital of Miyazaki University by their owners, small pieces of subcutaneous adipose tissues were collected by scraping from surgical specimens with the informed consent of their owners, then cultured on plastic dishes with Dulbecco's modified Eagle medium (D6429, Sigma-Aldrich, St. Louis, MO, USA) including 10 % fetal bovine serum (Lot no. ABL0106, Biofill, Victoria, Australia), 50 μM β-mercaptoethanol (Life Technologies, Carlsbad, CA, USA), 10 units/ml penicillin, 10 μg/ml streptomycin, and 250 ng/ml amphotericin B (Antibiotic-Antimycotic, 15240-062, Life Technologies). Tissue pieces were removed from the dishes four days later, and monolayer cells were allowed to proliferate on the dishes. After the first passage, amphotericin B was not included in the medium (Penicillin-Streptomycin, Life Technologies).

RT-PCR

Total RNA was isolated from cultured cells using a RNeasy Plus Mini Kit (Qiagen, Hilden, Germany) after the third passage. Complementary DNA was synthesized using Super-Script III Reverse Transcriptase (Life Technologies) with the oligo dT primer. For rapid amplification of cDNA ends (RACE) sequencing, a cDNA library was produced using a GeneRacer kit (Life Technologies). PCR was conducted using specific primers (Table 2) and BIOTAQ HS DNA Polymerase (Bioline, London, UK). The specificity of the reaction products was confirmed by agarose-gel electrophoresis. PCR products were also collected and sequenced. The protein conformation and cysteine bonding state were predicted using the fully automated protein structure homology-modeling server (SWISS-MODEL, http://swissmodel.expasy.org/) and

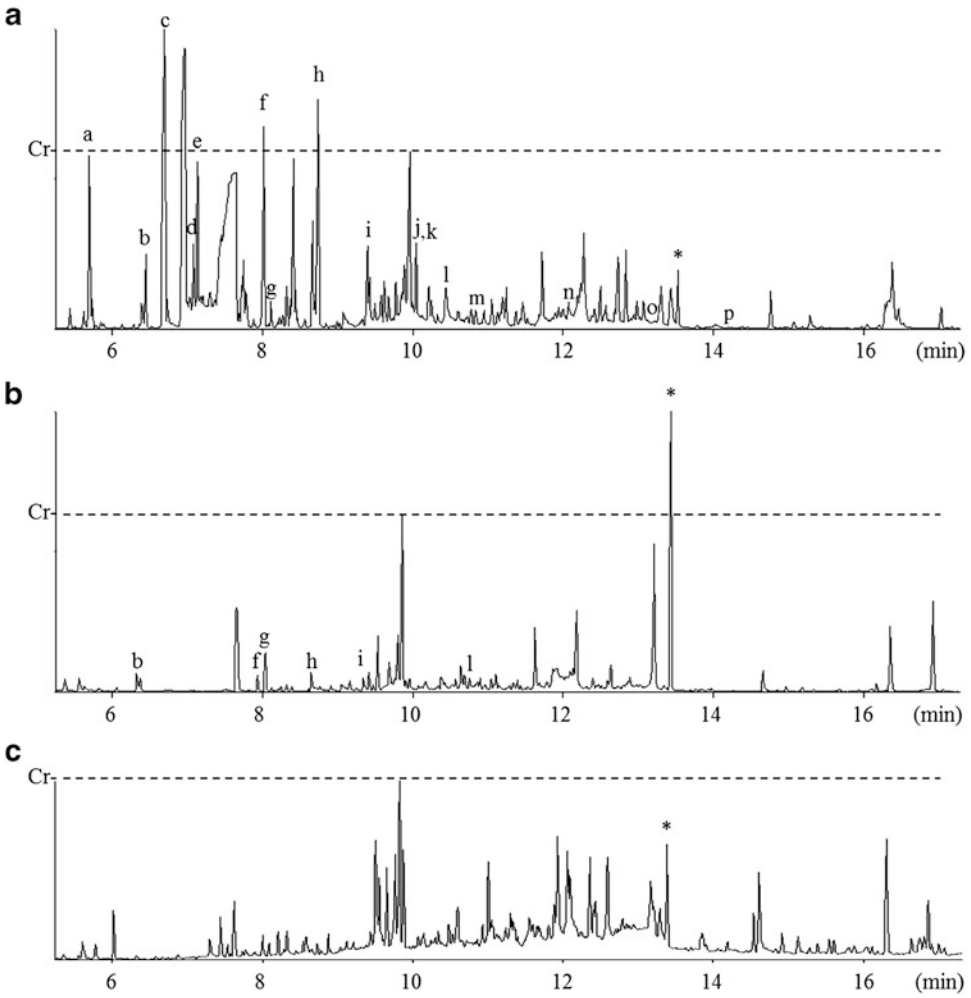

Fig. 1 GC-MS analysis of urine organic acids. Total ion chromatograms are obtained from the cat with MADD (**a**) before, and (**b**) after treatment with riboflavin and L-carnitine. (**c**) Reference chromatogram is obtained from urine of a normal cat. Horizontal and vertical axes are scales of retention time and signal intensity, respectively. Scale marks represented as Cr indicates a signal intensity of creatinine in each chromatogram. Various organic acids characteristic of MADD are increased in the present cat with MADD, and treatment with riboflavin and L-carnitine suppresses the elevated levels of organic acids. *a*: lactic acid, *b*: sarcosine, *c*: 3-hydroxybutyric acid, *d*: malonic acid, *e*: 3-hydroxyisovaleric acid, *f*: succinic acid, *g*: ethylmalonic acid, *h*: glutaric acid, *i*: isovalerylglycine, *j*: 2-hydroxyglutaric acid, *k*: 3-hydroxyglutaric acid, *l*: hexonylglycine, *m*: suberic acid, *n*: sebacic acid, *o*: 3-hydroxysebacic acid, *p*: suberylglycine, and *: heptadecanoic acid added as internal standard

the cysteine disulfide bonding state and connectivity predictor (DISULFIND, http://disulfind.dsi.unifi.it/), respectively.

PCR-Restriction Fragment Length Polymorphism (PCR-RFLP)

Genomic DNA was isolated from cultured cells after the third passage using a QIAamp DNA Mini kit (Qiagen). PCR was conducted using specific primers (Table 2) and BIOTAQ HS DNA Polymerase (Bioline). The amplified ETFDH was reacted with the restriction enzyme *PciI* (New England Biolabs, Ipswich, MA, USA). The specificity of the reaction products was confirmed by agarose-gel electrophoresis.

Results

Feline MADD

We assayed urine organic acids because we suspected a metabolic disorder such as dihydropyrimidinase deficiency (OMIM 222748), which has been reported in a cat exhibiting hyperammonemia (Chang et al. 2012). Surprisingly, the results indicated a MADD-like profile, with increased levels of lactic acid, sarcosine, 3-hydroxybutyric acid, malonic acid, 3-hydroxyisovaleric acid, succinic acid, ethylmalonic acid, glutaric acid, isoverylglycine, 2-hydroxyglutaric acid, 3-hydroxyglutaric acid, hexonylglycine, suberic acid, sebacic acid, 3-hydroxysebacic acid, and suberylglycine (Fig. 1a).

Table 3 Blood levels of acylcarnitine species

Numerical symbol	Normal feline reference value		Pretreatment	Posttreatment
	Mean (nmol/ml)	S.D.	Value (nmol/ml)	Value (nmol/ml)
C0	12.7	6.8	22.1	29.3
C2	7.27	2.38	7.42	4.98
C3	0.55	0.31	0.38	0.35
C4	0.14	0.06	9.36**	3.49
C5	0.15	0.09	7.5**	2.88
C5DC	0.01	0.01	0.2**	0.14
OH-C5	0.16	0.06	0.13	0.17
C5:1	0.02	0.01	0.02	0.02
C6	0.02	0.02	1.48**	1.12*
C8	0.02	0.01	0.72**	0.6**
C10	0.01	0.01	0.45**	0.57**
C12	0.02	0.01	0.46**	0.44**
C14	0.04	0.02	0.77**	0.44
C14:1	0.03	0.02	1.27**	0.93*
C16	0.26	0.15	2.27**	0.79
OH-C16	0.00	0.00	0.02**	0.01
C18	0.18	0.10	2.29**	0.87
OH-C18:1	0.01	0.01	0.06*	0.04
C18:1	0.26	0.23	1.96**	0.67

**$P < 0.01$

*$P < 0.05$

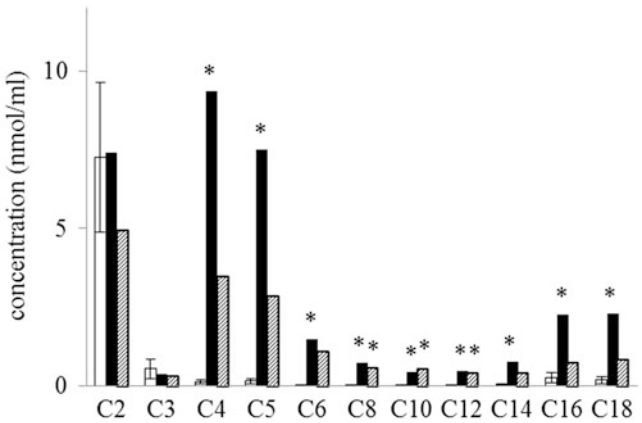

Fig. 2 LC-MS/MS analysis of acylcarnitine species. The present cat with MADD had high blood levels of carnitines conjugated with saturated fatty acids longer than C4 (*black columns*). Treatment with riboflavin and L-carnitine improved the blood levels of acylcarnitines as normal (*shaded columns*). White columns and their error bars indicate mean and standard deviation, respectively, of the blood levels of acylcarnitines in 27 of healthy cats. *: $P < 0.01$

For definitive diagnosis, we assayed the blood levels of acylcarnitines. The results supported our diagnosis of MADD; increases of C4, C5, C6, C8, C10, C12, C14, C16, and C18 were evident, but no increase of C0, C2, and C3 (Table 3 and Fig. 2). MADD was thus confirmed, and treatment with riboflavin and L-carnitine improved the symptoms, including the elevated levels of urine organic acids and blood levels of acylcarnitines (Table 3 and Fig. 1b and 2).

Sequencing of Feline ETFα, ETFβ, and ETFDH

To detect the gene mutation causing MADD, we tried to amplify the cDNA of feline ETFα, ETFβ, and ETFDH

Table 4 List of sequenced genes

Gene	GenBank ID
ETFα	KF682224
ETFβ	KF682225
ETFDH	KF682226

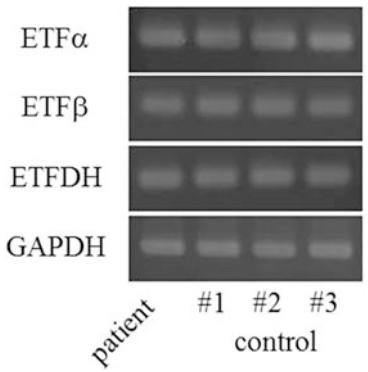

Fig. 3 RT-PCR analysis of MADD-related genes. All of the cats examined, including the one with MADD, expressed ETFα, ETFβ, and ETFDH

including the region of the open reading frame (ORF) based on the Ensembl genome browser (http://www.ensembl.org/). However, this was not successful for ETFα and ETFDH. The referenced sequence of ETFβ cDNA also seemed to lack the 5'- and 3'-untranslated regions. Therefore, we attempted to determine the complete cDNA sequences of ETFα, ETFβ, and ETFDH in normal cats. Using RACE sequencing, we identified the specific sequences (Table 4) for the feline ETFα, ETFβ, and ETFDH cDNAs, which were 1340, 841, and 2153 bp long, respectively, apparently encoding proteins of 333, 255, and 617 amino acids, respectively, and each showing 96 % similarity with their human homologs. No splicing variants were detected in any of the three genes. Based on this refined information, we succeeded in amplifying the complete ETFα, ETFβ, and ETFDH cDNAs including an ORF region from the present cat with MADD and three control cats. In cultured cells derived from adipose tissue, the cat with MADD expressed ETFα, ETFβ, and ETFDH at the same levels as those in control cats (Fig. 3).

Presence of a Novel Mutation in the Cat with MADD

We analyzed the sequence of amplified cDNA from all cats including that of the patient, and finally identified a specific mutation in the latter: c.692T>G in ETFDH (Fig. 4a). No other mutation was detected in ETFDH, ETFα, or ETFβ. PCR-RFLP analysis showed that the patient only carries mutant alleles of ETFDH (Fig. 4b). The c.692T>G mutation in ETFDH causes an amino acid substitution: p.F231C. To assess the importance of p.F231 for the function of ETFDH, we compared the amino acid sequences of various species using a database search, and this revealed that p.F231 in feline ETFDH is completely conserved in eukaryotes, including human (*Homo sapiens*), mouse (*Mus musculus*), amphibia (*Xenopus laevis*), fish (*Danio rerio*), insect (*Drosophila melanogaster*), nematode (*Caenorhabditis elegans*), plant (*Arabidopsis thaliana*), and fungus (*Saccharomyces cerevisiae*) (Fig. 5a). The disulfide bonding predictor, DISULFIND, showed that no abnormal disulfide bond is formed on the aberrant p.C231 in ETFDH. Analysis of the protein conformation showed that p.F231 is located on the surface of the FAD-binding domain opposite the ubiquinone domain in ETFDH (Fig. 5b).

Discussion

A surviving individual with MADD is rare because patients with neonatal-onset MADD die soon after birth. As an animal model of MADD has been never established, research on MADD has made little progress. The present case of inherited MADD in a cat is the first of its kind to have been reported other than in humans, indicating that inherited MADD is latent in animals.

The cat we studied presented with symptoms of hypoglycemia, hyperammonemia, vomiting, and increased levels of urine organic acids including 3-hydroxyisovaleric, ethylmalonic, glutaric, 2-hydroxyglutaric, suberic, and sebacic acids, as well as isovalerylglycine (Fig. 1a). The blood levels of medium- and long-chain acylcarnitine species were also elevated (Table 3 and Fig. 2). Therefore, the symptoms of MADD in this cat were consistent with those in humans (Frerman and Goodman 2001; Gordon 2006), suggesting that the present individual would be a valuable pathological model of human MADD.

Various mutations have been identified in ETFα, ETFβ, and ETFDH in human MADD patients. Most mutations causing riboflavin-responsive MADD have been located in ETFDH (Olsen et al. 2007; Law et al. 2009; Trakadis et al. 2012). The present cat, which responded to riboflavin treatment, also carried a mutation in ETFDH (Fig. 4), but not in ETFα or ETFβ. The mutations inherited in human patients with riboflavin-responsive MADD all cause a single amino acid substitution (Olsen et al. 2007; Law et al. 2009; Trakadis et al. 2012). The present cat expressed ETFDH mRNA at the same level as control cats (Fig. 3). The p.F231C substitution in ETFDH does not appear to lead to the formation of an abnormal disulfide bond. Therefore, cases of mild MADD responsive to riboflavin treatment may involve less severe dysfunction of ETFDH.

The mutation identified in this study has not been reported previously in human cases of MADD (Goodman et al. 2002; Olsen et al. 2003; Schiff et al. 2006; Yotsumoto

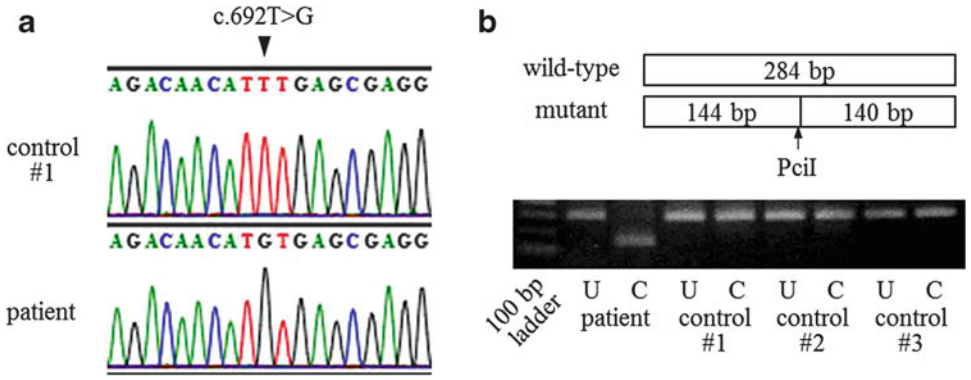

Fig. 4 The ETFDH mutation in the present cat with MADD. (**a**) The mutation c.692T>G (*arrow head*) was identified by sequencing analysis. (**b**) The allelic frequency of the mutation was determined by PCR-RFLP analysis. The *PciI* restriction site (*arrow*), ACATGT, was located on the fragment amplified from the mutant ETFDH, but not on that from wild-type ETFDH. The lanes labeled U and C show the electrophoretic profiles of the ETFDH fragments without and with *PciI* cleavage, respectively, after PCR amplification. The fragment derived from the cat with MADD was completely cleaved by *PciI*

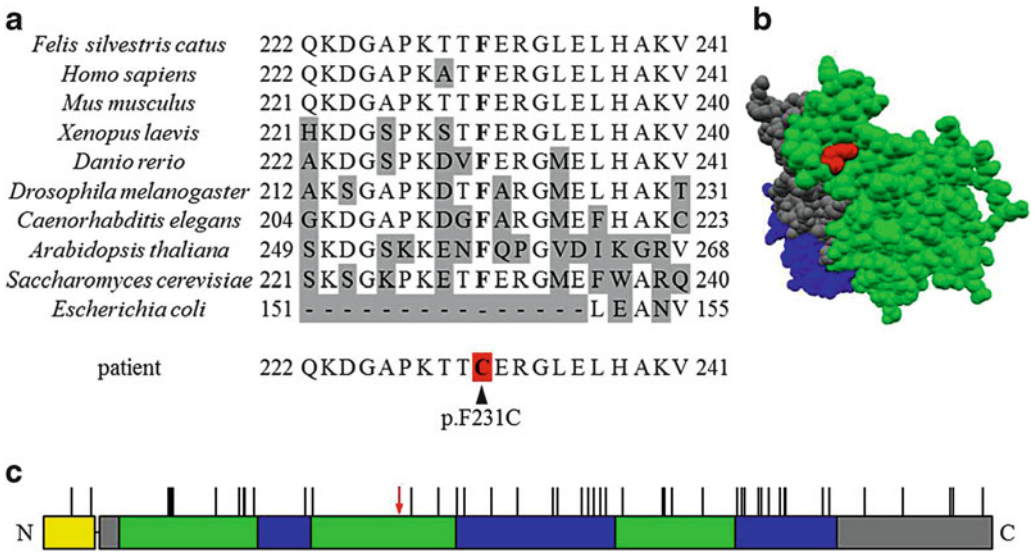

Fig. 5 Characterization of the p.F231C mutation. (**a**) The peptide sequence of feline ETFDH is compared with its homologs for the amino acids covering the region p.Q222 to p.V241. Phenylalanine encoded by c.692T in feline ETFDH is conserved in ETFDH from *Homo sapiens*, *Mus musculus*, *Xenopus laevis*, *Danio rerio*, *Drosophila melanogaster*, *Caenorhabditis elegans*, *Arabidopsis thaliana*, and *Saccharomyces cerevisiae*. *Escherichia coli* lacks the homologous region including p.F231. The gray background indicates amino acids that differ from the feline sequence. The *red* background indicates the mutation site. (**b**) The protein conformation of feline ETFDH represented in space-fill mode predicted by SWISS-MODEL. p.F231 (*red*) is located on the surface of the FAD-binding domain (*green*) opposite the ubiquinone domain (*blue*). (**c**) The primary structure of the ETFDH precursor with the mutation locus is shown. The colors indicate the domain of the signal peptide (*yellow*), the 4Fe-4S cluster (*gray*), the FAD-binding site (*green*), and ubiquinone (*blue*). *Vertical lines* on each domain indicate the locus of mutations reported previously in human cases of MADD (Trakadis et al. 2012). The present novel mutation (*red arrow*) does not overlap with any of these mutations

et al. 2008; Er et al. 2010; Wolfe et al. 2010; Er et al. 2011; Wang et al. 2011; Trakadis et al. 2012) (Fig. 5c). p.F231 in ETFDH has been completely conserved in eukaryotes across mammal to fungus (Fig. 5a), implying that p.F231 has an important role in the function of ETFDH. Phenylalanine has a role in electron transfer in Alzheimer's amyloid beta-peptide, methylamine dehydrogenase, sulfite oxidase, and triheme cytochrome PpcA (Davidson 2003; Pogocki 2004; Dantas et al. 2013; Davis et al. 2013). p.F231 is located on the FAD-binding domain, which is involved in the receipt of electrons from ETF, at the end opposite the ubiquinone domain, which is buried in the inner mitochondrial membrane (Fig. 5b) (Watmough and Frerman 2010). Thus, p.F231 is located on the apical surface of ETFDH, where it is exposed

to the mitochondrial matrix. Therefore, the p.F231C amino acid substitution in ETFDH might hinder the receipt of electrons from ETF, followed by accumulation of reduced ETF, and leading to a deficiency of acyl-CoA dehydrogenase. There is possibility that this p.F231C substitution in ETFDH causes MADD in humans.

Our analysis of allelic frequency showed that present cat only carries mutant alleles of ETFDH (Fig. 4b). In humans, most cases of MADD are attributable to a zygotic effect on different mutations in ETF or ETFDH (Olsen et al. 2003), although the majority of patients with late-onset MADD recorded in southern China carried a homozygous mutation of c.250G>A in ETFDH (Wang et al. 2011). According to the owner, the present cat is derived from a group of dozens of stray cats, which were fed by a particular person. They were likely to breed in a small colony. The present cat might have been produced by inbreeding of ancestors carrying the mutation c.692T>G in ETFDH, although there is the possibility of a hemizygous point mutation or uniparental disomy containing ETFDH gene. Unfortunately, all three littermates and parents already died, so we could not observe genetic information about this mutation. Accordingly, we recommend avoiding unnecessary inbreeding of companion animals to prevent the production of genetic abnormalities such as the present one.

In conclusion, we have described the first case of inherited MADD in an animal, and identified a novel mutation in ETFDH suspected to be the cause. The cat we examined is the only one currently known to be diagnosed as having MADD, and the knowledge gained from it is anticipated to be valuable for the development of an effective therapy for MADD. As gene therapy can be applied for patients carrying a single gene mutation, we are currently studying the possibility of gene therapy for this cat.

Acknowledgments The authors sincerely thank the owners of the studied cats for their participation. We are grateful to MILS INTERNATIONAL for GC-MS analysis of urine organic acids. This study was supported by a Grant-in-Aid from University of Miyazaki (3901020300: to KN) and a Grant-in-Aid from the Japan Society for the Promotion of Science (KAKENHI-B 25292187: to KN).

Synopsis

We discovered the first case of MADD in a cat.

Compliance with Ethics Guidelines

Shoichi Wakitani, Shidow Torisu, Taiki Yoshino, Kazuhisa Hattanda, Osamu Yamato, Ryuji Tasaki, Haruo Fujita, and Koichiro Nishino declare that they have no conflicts of interest. This article does not contain any studies with human subjects performed by the any of the authors. All institutional and national guidelines for the care and use of laboratory animals were followed. The work presented here was carried out in collaboration between all authors. SW and KN conceived and designed this experiment, analyzed a gene mutation, and wrote this article. ST and KH diagnosed the cat. TY conducted DNA sequencing; OY, RT, and HF conducted LC-MS/MS analysis.

References

Cassart D, Baise E, Cherel Y et al (2007) Morphological alterations in oxidative muscles and mitochondrial structure associated with equine atypical myopathy. Equine Vet J 39:26–32

Chang HS, Shibata T, Arai S et al (2012) Dihydropyrimidinase deficiency: the first feline case of dihydropyrimidinuria with clinical and molecular findings. JIMD Rep 6:21–26

Dantas J, Morgado L, Pokkuluri P et al (2013) Solution structure of a mutant of the triheme cytochrome PpcA from Geobacter sulfurreducens sheds light on the role of the conserved aromatic residue F15. Biochim Biophys Acta 1827:484–492

Davidson V (2003) Probing mechanisms of catalysis and electron transfer by methylamine dehydrogenase by site-directed mutagenesis of alpha Phe55. Biochim Biophys Acta 1647:230–233

Davis A, Cornelison M, Meyers K et al (2013) Effects of mutating aromatic surface residues of the heme domain of human sulfite oxidase on its heme midpoint potential, intramolecular electron transfer, and steady-state kinetics. Dalton Trans 42:3043–3049

Er TK, Liang WC, Chang JG, Jong YJ (2010) High resolution melting analysis facilitates mutation screening of ETFDH gene: applications in riboflavin-responsive multiple acyl-CoA dehydrogenase deficiency. Clin Chim Acta 411:690–699

Er TK, Chen CC, Liu YY et al (2011) Computational analysis of a novel mutation in ETFDH gene highlights its long-range effects on the FAD-binding motif. BMC Struct Biol. doi:10.1186/1472-6807-11-43

Finno C, Valberg S, Wünschmann A, Murphy M (2006) Seasonal pasture myopathy in horses in the midwestern United States: 14 cases (1998–2005). J Am Vet Med Assoc 229:1134–1141

Frerman FE, Goodman SI (2001) Defects of electron transfer flavoprotein and electron transfer flavoprotein-ubiquinone oxidoreductase: glutaric academia type II. In: Scriver CR, Beaudet AL, Sly WS et al (eds) The metabolic and moleculer bases of inherited disease, 8th edn. McGraw-Hill, New York, pp 2357–2365

Goodman S, Binard R, Woontner M, Frerman F (2002) Glutaric acidemia type II: gene structure and mutations of the electron transfer flavoprotein:ubiquinone oxidoreductase (ETF:QO) gene. Mol Genet Metab 77:86–90

Gordon N (2006) Glutaric aciduria types I and II. Brain Dev 28:136–140

Henriques B, Rodrigues J, Olsen R et al (2009) Role of flavinylation in a mild variant of multiple acyl-CoA dehydrogenation deficiency: a molecular rationale for the effects of riboflavin supplementation. J Biol Chem 284:4222–4229

Ishii K, Komaki H, Ohkuma A et al (2010) Central nervous system and muscle involvement in an adolescent patient with riboflavin-responsive multiple acyl-CoA dehydrogenase deficiency. Brain Dev 32:669–672

Lan MY, Fu MH, Liu YF et al (2010) High frequency of ETFDH c.250G > A mutation in Taiwanese patients with late-onset lipid storage myopathy. Clin Genet 78:565–569

Law LK, Tang N, Hui J et al (2009) Novel mutations in ETFDH gene in Chinese patients with riboflavin-responsive multiple acyl-CoA dehydrogenase deficiency. Clin Chim Acta 404:95–99

Liang WC, Ohkuma A, Hayashi Y et al (2009) ETFDH mutations, CoQ10 levels, and respiratory chain activities in patients with riboflavin-responsive multiple acyl-CoA dehydrogenase deficiency. Neuromuscul Disord 19:212–216

Lund A, Skovby F, Vestergaard H et al (2010) Clinical and biochemical monitoring of patients with fatty acid oxidation disorders. J Inherit Metab Dis 33:495–500

Olsen R, Andresen B, Christensen E et al (2003) Clear relationship between ETF/ETFDH genotype and phenotype in patients with multiple acyl-CoA dehydrogenation deficiency. Hum Mutat 22: 12–23

Olsen R, Olpin S, Andresen B et al (2007) ETFDH mutations as a major cause of riboflavin-responsive multiple acyl-CoA dehydrogenation deficiency. Brain 130:2045–2054

Pogocki D (2004) Mutation of the Phe20 residue in Alzheimer's amyloid beta-peptide might decrease its toxicity due to disruption of the Met35-cupric site electron transfer pathway. Chem Res Toxicol 17:325–329

Schiff M, Froissart R, Olsen R et al (2006) Electron transfer flavoprotein deficiency: functional and molecular aspects. Mol Genet Metab 88:153–158

Tamaoki Y, Kimura M, Hasegawa Y et al (2002) A survey of Japanese patients with mitochondrial fatty acid beta-oxidation and related disorders as detected from 1985 to 2000. Brain Dev 24:675–680

Trakadis Y, Kadlubowska D, Barnes R et al (2012) Pregnancy of a patient with multiple acyl-CoA dehydrogenation deficiency (MADD). Mol Genet Metab 106:491–494

Valberg S, Sponseller B, Hegeman A et al (2012) Seasonal pasture myopathy/atypical myopathy in North America associated with ingestion of hypoglycin A within seeds of the box elder tree. Equine Vet J. doi:10.1111/j.2042-3306.2012.00684.x

Van der Kolk JH, Wijnberg ID, Westermann CM et al (2010) Equine acquired multiple acyl-CoA dehydrogenase deficiency (MADD) in 14 horses associated with ingestion of Maple leaves (Acer pseudoplatanus) covered. Mol Genet Metab 101: 289–191

Wang ZQ, Chen XJ, Murong SX et al (2011) Molecular analysis of 51 unrelated pedigrees with late-onset multiple acyl-CoA dehydrogenation deficiency (MADD) in southern China confirmed the most common ETFDH mutation and high carrier frequency of c.250G > A. J Mol Med 89: 569–576

Watmough NJ, Frerman FE (2010) The electron transfer flavoprotein: ubiquinone oxidoreductases. Biochim Biophys Acta 1797: 1910–1916

Wen B, Dai T, Li W et al (2010) Riboflavin-responsive lipid-storage myopathy caused by ETFDH gene mutations. J Neurol Neurosurg Psychiatry 81:231–236

Westermann C, Dorland L, Votion D et al (2008) Acquired multiple Acyl-CoA dehydrogenase deficiency in 10 horses with atypical myopathy. Neuromuscul Disord 18:355–364

Wolfe L, He M, Vockley J et al (2010) Novel ETF dehydrogenase mutations in a patient with mild glutaric aciduria type II and complex II-III deficiency in liver and muscle. J Inherit Metab Dis. doi:10.1007/s10545-010-9246-8

Yotsumoto Y, Hasegawa Y, Fukuda S et al (2008) Clinical and molecular investigations of Japanese cases of glutaric acidemia type 2. Mol Genet Metab 94:61–67

Zhang C, Xu K, Dave U et al (2000) Inborn errors of metabolism discovered in Asian department of pediatrics and mental retardation research center. J Chromatogr B Biomed Sci Appl 746:41–49

JIMD Reports
DOI 10.1007/8904_2013_271

CASE REPORT

Biotin-Responsive Basal Ganglia Disease: A Treatable Differential Diagnosis of Leigh Syndrome

Felix Distelmaier • Peter Huppke • Peter Pieperhoff • Katrin Amunts • Jörg Schaper • Eva Morava • Ertan Mayatepek • Jürgen Kohlhase • Michael Karenfort

Received: 27 June 2013 / Revised: 23 September 2013 / Accepted: 26 September 2013 / Published online: 29 October 2013

Abstract Biotin-responsive basal ganglia disease (BBGD) is an autosomal recessive disorder, which is caused by mutations in the *SLC19A3* gene. BBGD typically causes (sub)acute episodes with encephalopathy and subsequent neurological deterioration. If untreated, the clinical course may be fatal. Our report on a 6-year-old child with BBGD highlights that the disease is a crucial differential diagnosis of Leigh syndrome. Therefore, biotin and thiamine treatment is recommended for any patient with symmetrical basal ganglia lesions and neurological symptoms until BBGD is excluded. In addition, we exemplify that deformation-field-based morphometry of brain magnetic resonance images constitutes a novel quantitative tool, which might be very useful to monitor disease course and therapeutic effects in neurometabolic disorders.

Communicated by: Wolfgang Sperl

Competing interests: None declared

Electronic supplementary material: The online version of this chapter (doi:10.1007/8904_2013_271) contains supplementary material, which is available to authorized users.

F. Distelmaier (✉) · E. Mayatepek · M. Karenfort
Department of General Pediatrics, Neonatology and Pediatric Cardiology, University Children's Hospital, Heinrich-Heine University, Moorenstr. 5, D-40225 Düsseldorf, Germany
e-mail: felix.distelmaier@med.uni-duesseldorf.de1

P. Huppke
Department of Pediatrics and Pediatric Neurology, Faculty of Medicine, Georg August University, Göttingen, Germany

P. Pieperhoff
Research Centre Jülich, Institute of Neuroscience and Medicine-INM-1, Jülich, Germany

K. Amunts
C. and O. Vogt Institute for Brain Research, Heinrich-Heine University, Düsseldorf, Germany

J. Schaper
Department of Diagnostic and Interventional Radiology, Heinrich-Heine University, Düsseldorf, Germany

E. Morava
Hayward Genetics Center, Tulane University Medical School, New Orleans, LA, USA

J. Kohlhase
Center for Human Genetics, Freiburg, Germany

Introduction

Biotin-responsive basal ganglia disease (BBGD; OMIM 607483) is a rare autosomal recessive disorder, which is caused by mutations in the *SLC19A3* gene, encoding a thiamine transporter (hTHTR2). The disease was first described in 1998 and later genetically characterized in 2005 (Ozand et al. 1998; Zeng et al. 2005). The first patients reported were of Saudi, Syrian, or Yemeni ancestry. However, in the following, also European and Japanese patients were identified, indicating that BBGD is a pan-ethnic disease (Debs et al. 2010; Tabarki et al. 2013). So far, the influence of *SLC19A3* mutations on hTHTR2 function (i.e., transporter functionality, protein stability, targeting, or transport activity) and their impact on cell biology are unresolved (Subramanian et al. 2006).

BBGD frequently manifests in childhood with (sub) acute episodes of encephalopathy, dystonia, dysarthria, and seizures. If untreated, the clinical course may be fatal (Tabarki et al. 2013; Alfadhel et al. 2013). Brain magnetic resonance imaging (MRI) typically demonstrates bilateral hyperintensity of caudate nucleus and putamen on T2-weighted sequences. In addition, especially during

acute neurometabolic crisis, diffuse cortical and subcortical changes are characteristic, which are thought to be caused by vasogenic edema (Tabarki et al. 2013).

Treatment of BBGD consists of high doses of biotin and additional thiamine. The efficacy of biotin treatment is still unclear because hTHTR2 is unable to transport biotin. However, it has been shown that biotin regulates gene expression of *SLC19A3* (Debs et al. 2010). Therefore, a biotin-induced upregulation of hTHTR2 levels in combination with increased thiamine supplementation are most likely the therapeutic mechanisms.

Case Report

Here, we report on a 6-year-old girl, born to consanguineous Moroccan parents. She was the third child of the family. Two older sisters suffered from a progressive neurodegenerative disorder, which was classified as Leigh syndrome because of symmetrical brain lesions in the basal ganglia.

Leigh syndrome is a devastating disease caused by direct or indirect impairment of mitochondrial oxidative phosphorylation. The disorder typically causes symmetrical lesions in basal ganglia and/or brain stem and leads to a clinical course with rapid deterioration of cognitive and motor functions (Baertling et al. 2013).

However, in these two girls, biochemical diagnostics did not reveal any clear disturbance of mitochondrial metabolism. Both girls died during the course of the disease.

The girl reported here developed normal until the age of 3½ years. At that time, she suffered from a first encephalopathic episode with somnolence, dystonia, and dysarthria. Metabolic work-up was normal (including organic acids in urine, amino acids in blood and cerebrospinal fluid, acylcarnitines, etc.). Initial brain MRI showed symmetric basal ganglia lesions. In view of family history, Leigh syndrome was diagnosed.

At the age of 6 years, the child was seen at our department during an acute metabolic crisis (including somnolence and seizures). Brain MRI showed the previously described basal ganglia lesions (Fig. 1 a–b). In addition, single voxel spectroscopy demonstrated an intense lactate peak within the affected areas (see Supplementary Fig. 1). However, MRI also showed diffuse cortical and subcortical changes in addition to basal ganglia lesions, which appeared rather atypical for classical Leigh syndrome (Fig. 1 a–b). This finding brought up the differential diagnosis BBGD. Accordingly, the girl was treated with high-dose biotin (10 mg/kg/day) and additional thiamine (100 mg/day). This medication improved her clinical status dramatically. The child recovered from somnolence within several hours and seizures subsided completely.

Molecular genetic studies confirmed BBGD, demonstrating a mutation in the *SLC19A3* gene (c.1264G>A, p.T422A, in exon 5; mutation previously described by Zeng et al. 2005). In addition, molecular genetic studies were also carried out in cultured skin fibroblasts of the oldest sister, which allowed a postmortem diagnosis also in this child.

The further clinical course of the girl was favorable. Follow-up brain MRI, 3 months after the acute metabolic crisis revealed a clear regression of lesions in basal ganglia and other cortical and subcortical regions (Fig. 1 c–d).

In order to enable a quantitative evaluation of the disease course with respect to different brain areas, we applied deformation-field-based morphometry of the MR scans and cytoarchitectonic probabilistic maps to localize volume changes (Fig. 2; Pieperhoff et al. 2008). The superimposition of the MRI scans obtained prior and after 3 months of therapy showed a widespread involvement of brain regions, extending those of the previously identified changes in the caudate nucleus and putamen. The caudate nucleus and putamen were among those regions with most pronounced volume decrease under therapy. Other regions with volume decrease were the fundus striati, the ventral globus pallidus, the pulvinar of the thalamus, the periaqueductal gray matter, but also cortical areas PG and PGa of the angular gyrus. Volume increases were found in the ventricles, but also in the thalamus (paratenial nucleus, mammillary body, ventral anterior nuclei, and habenula).

These findings are in accordance with current MRI studies on BBGD (Tabarki et al. 2013) and indicate that brain pathology of the disease is much more complex than previously thought. The volume changes observed most probably constitute a combination of recovery processes (e.g., disappearance of vasogenic edema and normalization of cell metabolism) and residual tissue damage/atrophy.

Discussion

In conclusion, our report highlights that BBGD is an important treatable differential diagnosis of Leigh syndrome. The clinical picture may completely mimic a mitochondrial disorder, including lactic acidemia (which was present in one of the girls during acute metabolic crisis) and detection of a lactate peak on magnetic resonance spectroscopy (as demonstrated in the index patient). Importantly, atypical brain imaging findings (i.e., cortical signal alterations; indications of vasogenic edema) should alert clinicians to the differential diagnosis BBGD. Generally, biotin and thiamine treatment is suggested in any patient with symmetrical basal ganglia lesions and neurological symptoms until BBGD is excluded or a mitochondrial dysfunction has been clearly identified. Moreover, our morphometry analysis exemplifies that this

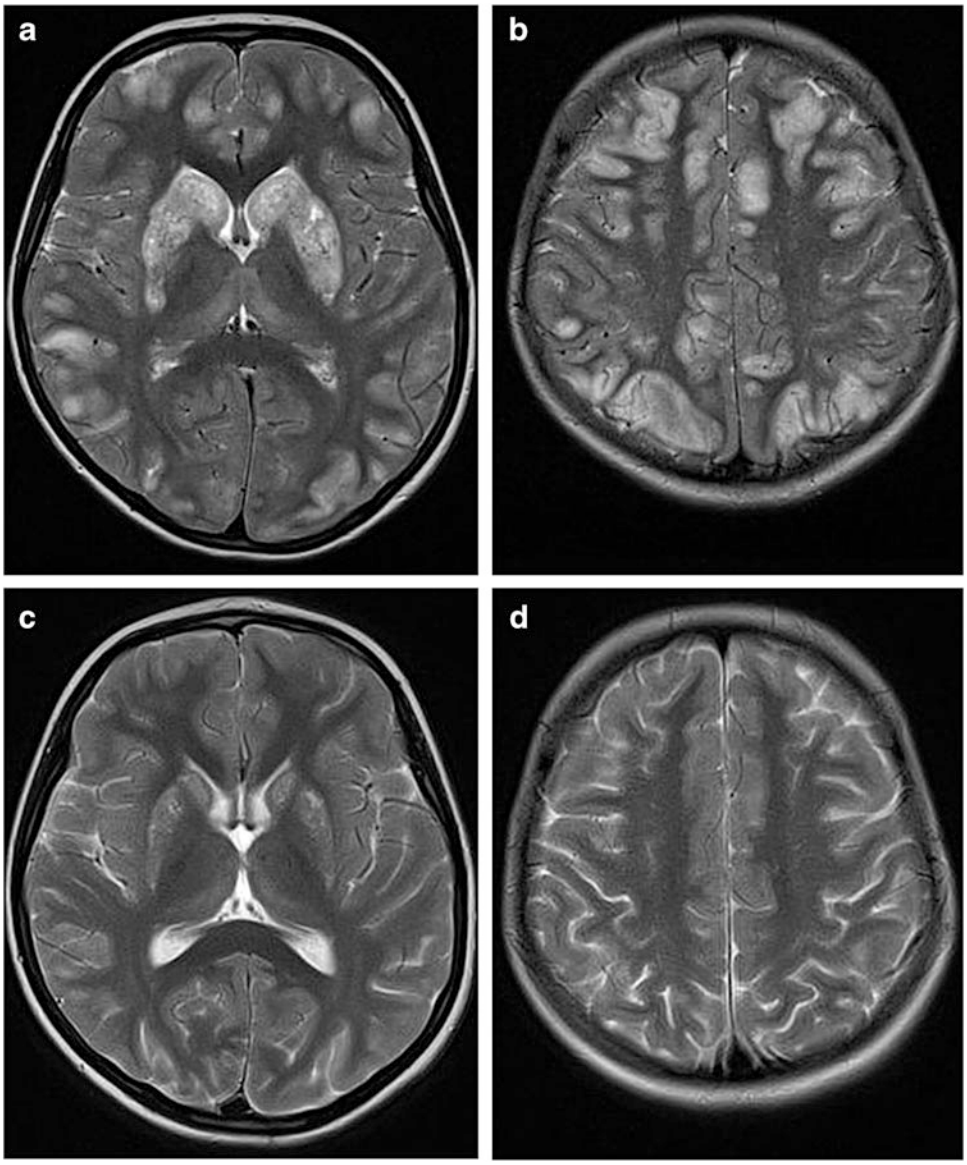

Fig. 1 MRI findings in biotin-responsive basal ganglia disease. (**a**–**b**), T2-weighted sequences during acute metabolic crisis demonstrating bilateral hyperintensity and swelling of caudate nucleus and putamen as well as abnormal signals in cortical-subcortical areas. (**c**–**d**) T2-weighted sequences 3 months after start of treatment with biotin and thiamine showing clear improvement of basal ganglia alterations and disappearance of cortical abnormalities

novel quantitative tool might be very useful to monitor disease course and therapeutic effects in neurometabolic disorders.

Synopsis

Biotin and thiamine treatment is lifesaving in patients with biotin-responsive basal ganglia disease.

Compliance with Ethics Guidelines

Conflict of Interest

Felix Distelmaier, Peter Huppke, Peter Pieperhoff, Katrin Amunts, Jörg Schaper, Eva Morava, Ertan Mayatepek, Jürgen Kohlhase, and Michael Karenfort declare that they have no conflict of interest.

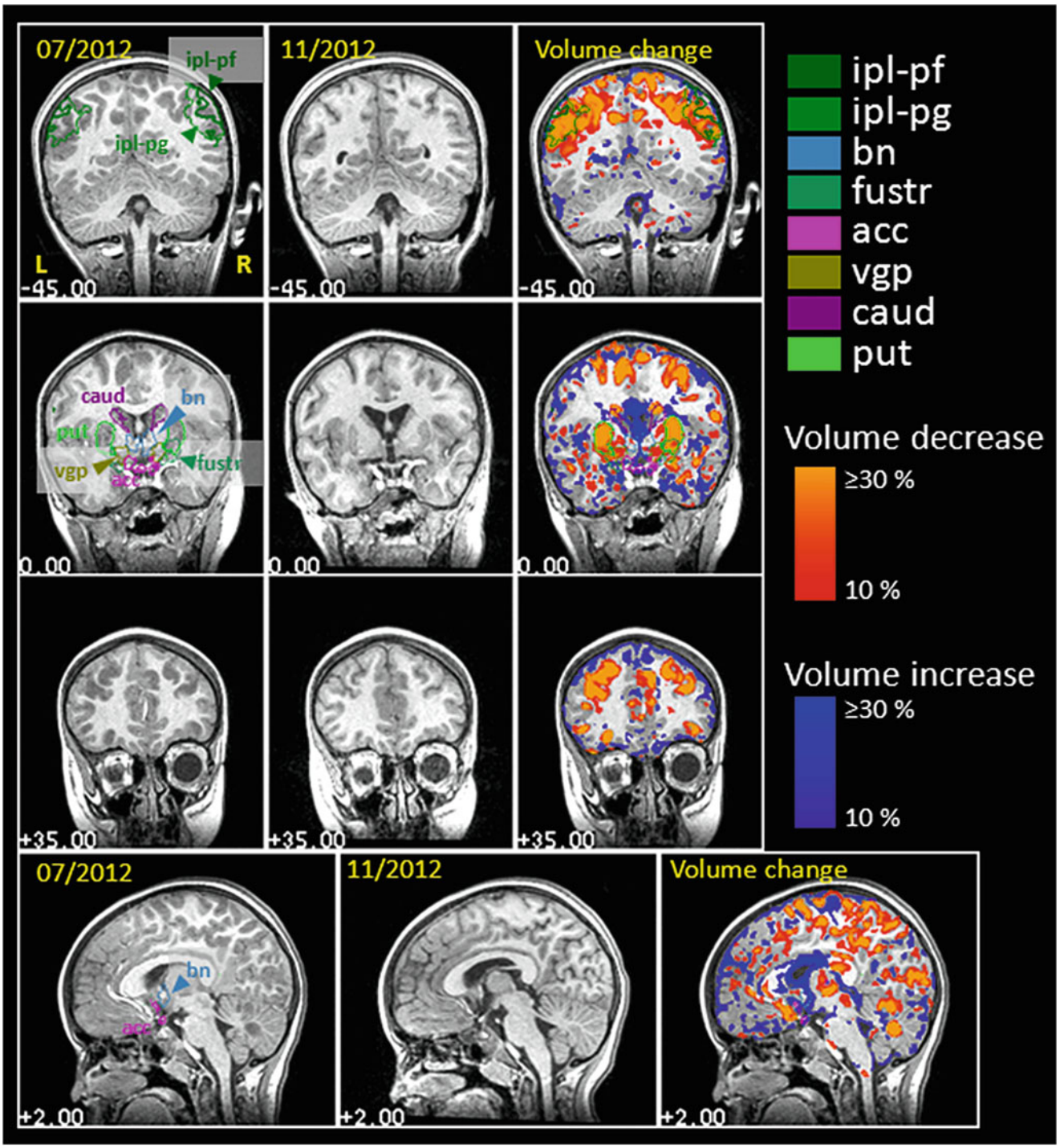

Fig. 2 Deformation-field-based morphometry of the MR scans. Volume changes in time as assed by means of deformation-field-based morphometry (DFM, Pieperhoff et al. 2008). The first and second pictures in each row show MR sections, which were acquired within an interval of ~3 months. The third picture in each row shows the difference in volume as compared to the first MR image, where the brain was imaged for the first time. Volume decreases and increases of more than 10 % are colored in red to yellow, and in blue, respectively. Contours of the following anatomical regions are labeled: ipl-pf, ipl-pg = areas PF and PG of the inferior parietal lobule (Caspers et al. 2008); *bn* bed nucleus, *fustr* fundus striati, *acc* ncl. accumbens, *vgp* ventral globus pallidus, *caud* ncl. caudatus, *put* putamen

Informed Consent

Additional informed consent was obtained from all patients, for which identifying information is included in this article.

Animal Rights

This article does not contain any studies with animal subjects performed by any of the authors.

References

Alfadhel M, Almuntashri M, Jadah RH et al (2013) Biotin-responsive basal ganglia disease should be renamed biotin-thiamine-responsive basal ganglia disease: a retrospective review of the clinical, radiological and molecular findings of 18 new cases. Orphanet J Rare Dis 8:83

Baertling F, Rodenburg RJ, Schaper J, et al (2013) A guide to diagnosis and treatment of Leigh syndrome. J Neurol Neurosurg Psychiatry Jun 14. [Epub ahead of print]. doi:10.1136/jnnp-2012-304426

Caspers S, Eickhoff SB, Geyer S et al (2008) The human inferior parietal lobule in stereotaxic space. Brain Struct Funct 212: 481–495

Debs R, Depienne C, Rastetter A et al (2010) Biotin-responsive basal ganglia disease in ethnic Europeans with novel SLC19A3 mutations. Arch Neurol 67:126–130

Ozand PT, Gascon GG, Al Essa M et al (1998) Biotin-responsive basal ganglia disease: a novel entity. Brain 121:1267–1279

Pieperhoff P, Südmeyer M, Hömke L, Zilles K, Schnitzler A, Amunts K (2008) Detection of structural changes of the human brain in longitudinally acquired MR images by deformation field morphometry: methodological analysis, validation and application. NeuroImage 43:269–287

Subramanian VS, Marchant JS, Said HM (2006) Biotin-responsive basal ganglia disease-linked mutations inhibit thiamine transport via hTHTR2: biotin is not a substrate for hTHTR2. Am J Physiol Cell Physiol 291:C851–C859

Tabarki B, Al-Shafi S, Al-Shahwan S et al (2013) Biotin-responsive basal ganglia disease revisited: clinical, radiologic, and genetic findings. Neurology 80:261–267

Zeng WQ, Al-Yamani E, Acierno JS Jr et al (2005) Biotin-responsive basal ganglia disease maps to 2q36.3 and is due to mutations in SLC19A3. Am J Hum Genet 77:16–26

JIMD Reports
DOI 10.1007/8904_2013_272

CASE REPORT

Severe Hypertriglyceridemia in a Newborn with Monogenic Lipoprotein Lipase Deficiency: An Unconventional Therapeutic Approach with Exchange Transfusion

Lorenza Pugni · Enrica Riva · Carlo Pietrasanta · Claudio Rabacchi · Stefano Bertolini · Cristina Pederiva · Fabio Mosca · Sebastiano Calandra

Received: 09 August 2013 / Revised: 17 September 2013 / Accepted: 26 September 2013 / Published online: 20 October 2013

Abstract Severe hypertriglyceridemia (sHTG) (plasma triglyceride level > 10 mmol/L) due to lipoprotein lipase (LPL) deficiency is a known risk factor for acute pancreatitis. A 23-day-old male with sHTG was admitted to the Neonatal Intensive Care Unit for plasmapheresis being at high risk for acute pancreatitis. Given the potential hazard of an extracorporeal technique in a very young infant, we decided to perform an exchange transfusion (ET), a procedure widely used by neonatologists and less invasive than plasmapheresis. ET led to a dramatic reduction in plasma triglyceride level, from 93.2 to 3.8 mmol/L at the end of the procedure, without adverse events. The subsequent administration of a special formula low in fat and high in medium-chain triglycerides was effective in keeping fasting plasma triglyceride level below 5.6 mmol/L during the first 5 months of life. The sequence of *LPL* gene revealed that the patient was apparently homozygous for a novel nucleotide deletion (c.840delG) in exon 6 leading to a premature termination codon (p.N281Mfs*23). However, family studies revealed that while the patient's mother was heterozygous for this mutation, the father was heterozygous for a novel deletion eliminating the whole *LPL* gene. The patient therefore turned out to be a compound heterozygous for two *LPL* gene mutations predicted to abolish LPL activity. This is the first case of sHTG treated with ET in a neonate reported in the literature. ET appears to be a safe procedure, alternative to plasmapheresis, to prevent acute pancreatitis in young infants with sHTG due to LPL deficiency.

Communicated by: Alberto B Burlina, MD

Competing interests: None declared

L. Pugni (✉) · C. Pietrasanta · F. Mosca
NICU, Department of Clinical Sciences and Community Health, Fondazione IRCCS Ca' Granda Ospedale Maggiore Policlinico, University of Milan, Via Commenda 12, 20122, Milan, Italy
e-mail: lorenza.pugni@mangiagalli.it

E. Riva · C. Pederiva
Department of Pediatrics, San Paolo Hospital, University of Milan, Milan, Italy

S. Bertolini
Department of Internal Medicine, University of Genova, Genoa, Italy

C. Rabacchi · S. Calandra
Department of Biomedical, Metabolic and Neural Sciences, University of Modena & Reggio Emilia, Modena, Italy

Introduction

Hypertriglyceridemia is conventionally defined as severe (sHTG) when the level of fasting plasma triglyceride (TG) is > 10 mmol/L. This condition is often referred to as chylomicronemia because of plasma accumulation of chylomicrons in the fasting state (Brahm and Hegele 2013). Familial chylomicronemia, also known as hyperlipoproteinemia (HLP) type 1, is a rare recessive disorder which often presents during early infancy and childhood (Brahm and Hegele 2013; Feoli-Fonseca et al. 1998). Fasting serum TG level is generally > 10 mmol/L and sometimes can exceed 100 mmol/L. The clinical features include failure to thrive, eruptive xanthomas, lipemia retinalis, hepatosplenomegaly, recurrent abdominal pain, and episodes of acute pancreatitis (Brahm and Hegele 2013; Feoli-Fonseca et al. 1998; Kavazarakis et al. 2004; Avis et al. 2010; Chen et al. 2012). Familial chylomicronemia is due to a defect in the lipolytic cascade of TG-rich lipoproteins that may result from mutations in at least five

different genes: *LPL* (encoding the lipoprotein lipase, LPL; OMIM #238600), *APOC2* (encoding apolipoprotein CII, the activator of LPL; OMIM #207750), *APOA5* (encoding apolipoprotein AV, also an activator of LPL; OMIM #144650), *GPIHBP1* (encoding the molecular platform which, on the endothelial surface of capillaries, allows the interactions of LPL with TG-rich lipoproteins, apolipoprotein CII, and apolipoprotein AV; OMIM #612757), and *LMF1* (encoding a tissue factor which allows the secretion of functional LPL and hepatic lipase, HL; OMIM #611761) (Johansen et al. 2011; Davies et al. 2012; Surendran et al. 2012). LPL deficiency due to mutations in the *LPL* gene is the most common disorder (95 % of cases) with an estimated prevalence of one per million individuals in most populations (Brahm and Hegele 2013).

Treatment of patients with familial chylomicronemia requires severe dietary fat restriction in order to maintain fasting TG levels below 4.5–5.6 mmol/L to reduce the risk of pancreatitis (Feoli-Fonseca et al. 1998; Leaf 2008). Plasmapheresis constitutes a therapeutic option in selected cases of sHTG for preventing this potentially life-threatening complication (Ewald and Kloer 2009; Stefanutti et al. 2009).

In this study, we report on a newborn with sHTG admitted to a Neonatal Intensive Care Unit (NICU) for therapeutic plasmapheresis by plasmafiltration, who was successfully treated with exchange transfusion (ET), a less invasive procedure than plasmapheresis. The patient was found to be a compound heterozygous for two novel *LPL* mutations, including the complete deletion of *LPL* gene.

Materials and Methods

Patient

The patient was a male neonate delivered by caesarean section after a full-term uneventful pregnancy. His birth weight was 3,305 g; he had a normal physical examination. Breastfeeding was started on day 1. He was discharged from hospital on day 6 of life in good clinical conditions with complementary feeding. His parents, apparently unrelated, were in good health as his two sisters.

On day 23 of life the capillary blood, collected for the second Guthrie screening routinely performed at the local hospital, was remarkably pink-creamy colored. Laboratory tests revealed extremely elevated plasma levels of TG (140 mmol/L) and total cholesterol (TC) (17.3 mmol/L); plasma lipase level was 209 IU/L (normal value 7–60 IU/L). Enteral feeding was suspended, an electrolyte solution was started, and the baby was transferred to our NICU after 12 h to undergo plasmafiltration.

At admission, the baby appeared in good health. Physical examination showed weight, height, and head circumference within the normal range (50th–75th percentile for his age), mild hepatomegaly, and some small yellowish papules on the face resembling eruptive xanthoma. Ophthalmoscopic examination revealed creamy-white retinal vessels, typical of lipemia retinalis. Blood chemistry confirmed the high plasma TG and TC levels (93.2 and 20.6 mmol/L, respectively); transaminase, alkaline phosphatase, total bilirubin, and serum electrolytes were within the normal range. No other biochemical data could be obtained because of the lipemic serum. Blood cell count was normal; hemoglobin level was 9.9 g/dL. Fasting was continued and the different therapeutic options were carefully evaluated. Conservative treatment only (i.e., dietary therapy) and plasmapheresis by plasmafiltration were excluded in favor of ET. A blood sample was collected from the patient and his family members for *LPL* gene analysis. A written informed consent was obtained from the parents before initiating the ET procedure and for DNA analysis.

Exchange Transfusion (ET) Procedure

ET is a procedure by which an infant's blood is replaced with donor blood by repeatedly removing and replacing small aliquots of blood over a short time period. We used fresh (collected <5 days before the procedure), filtered, irradiated 0 Rh-negative packed red blood cells suspended in AB plasma in a ratio to ensure a hematocrit of 40 %. Aliquots of 10 mL of donor blood were exchanged with infant blood till a cumulative volume of exchange of 200 mL/kg (twofold and half the estimated infant blood volume) was reached. ET was performed using a central venous catheter (double-lumen 5 French) placed in the right internal jugular vein by surgical cutdown, avoiding ligation of the vessel. The "pull-push technique" through special four-way stopcock was used. The procedure was completed within 120 min. No adverse events were observed except for mild thrombocytopenia which resolved spontaneously.

Analysis of *LPL* Gene

The exons and the promoter region of *LPL* gene (NG_008855.1, Chromosome 8p22) were amplified from genomic DNA by polymerase chain reaction (PCR) and sequenced using appropriate primers (Bertolini et al. 2000). Multiplex ligation-dependent probe amplification (MLPA) (SALSA MLPA P218-B1 LPL probe mix, MRC Holland, Amsterdam, the Netherlands) was used for the detection of major rearrangements of *LPL* gene. The PCR products were separated on an ABI PRISM 3100 sequencer and the data

analyzed by Peak Scanner™ software v1.0. The mutations were designated according to the Human Genome Variation Society, 2012 version (http://www.hgvs.org/mutnomen/recs-DNA.html). LPL protein sequence variants were designated according to http://www.hgvs.org/mutnomen/recs-prot.html.

Results

ET Procedure and Follow-Up

ET led to a dramatic reduction in plasma TG level: 3.84 mmol/L at the end of the procedure and 1.95 mmol/L 12 h later. Lipemia retinalis disappeared. Fasting and a lipid-free parenteral nutrition were continued. After 72 h from ET, laboratory tests were as follows: TG 1.03 mmol/L, TC 3.77 mmol/L, high-density lipoprotein cholesterol (HDL-C) 0.85 mmol/L, low-density lipoprotein cholesterol (LDL-C) 2.45 mmol/L; amylase, lipase, and the other biochemical parameters were within the normal range. Hemoglobin was 13.1 g/dL. After 3 days fasting, diet with a special formula low in fat and high in medium-chain triglycerides (MCTs) was started (Monogen®, 25 % of calories as fat, 90 % of fat as MCT). Plasma lipids slightly increased after starting the diet: TG 3.83 mmol/L, TC 4.13 mmol/L (HDL-C 0.54 mmol/L, LDL-C 2.25 mmol/L) after 4 days; TG 5.32 mmol/L, TC 4.13 mmol/L (HDL-C 0.62 mmol/L, LDL-C 2.09 mmol/L) after 8 days; TG 4.04 mmol/L, TC 3.20 mmol/L (HDL-C 0.57 mmol/L, LDL-C 1.47 mmol/L) after 14 days. Parenteral nutrition was discontinued and the catheter removed after 7 days from ET. The baby was discharged after 20 days in excellent clinical conditions with feeding with Monogen® milk. At the age of 5 months, the baby is still in good health and presents a normal growth (weight, height, and head circumference within the 75th percentile) and development. He is fed with the same milk and plasma lipid values are similar to those recorded at discharge: TG 4.18 mmol/L, TC 3.36 mmol/L, HDL-C 0.59 mmol/L, LDL-C 1.60 mmol/L.

Before the child was discharged, family members were evaluated for presence of dyslipidemia. In all subjects, fasting plasma lipids were found to be within the normal range for age and sex.

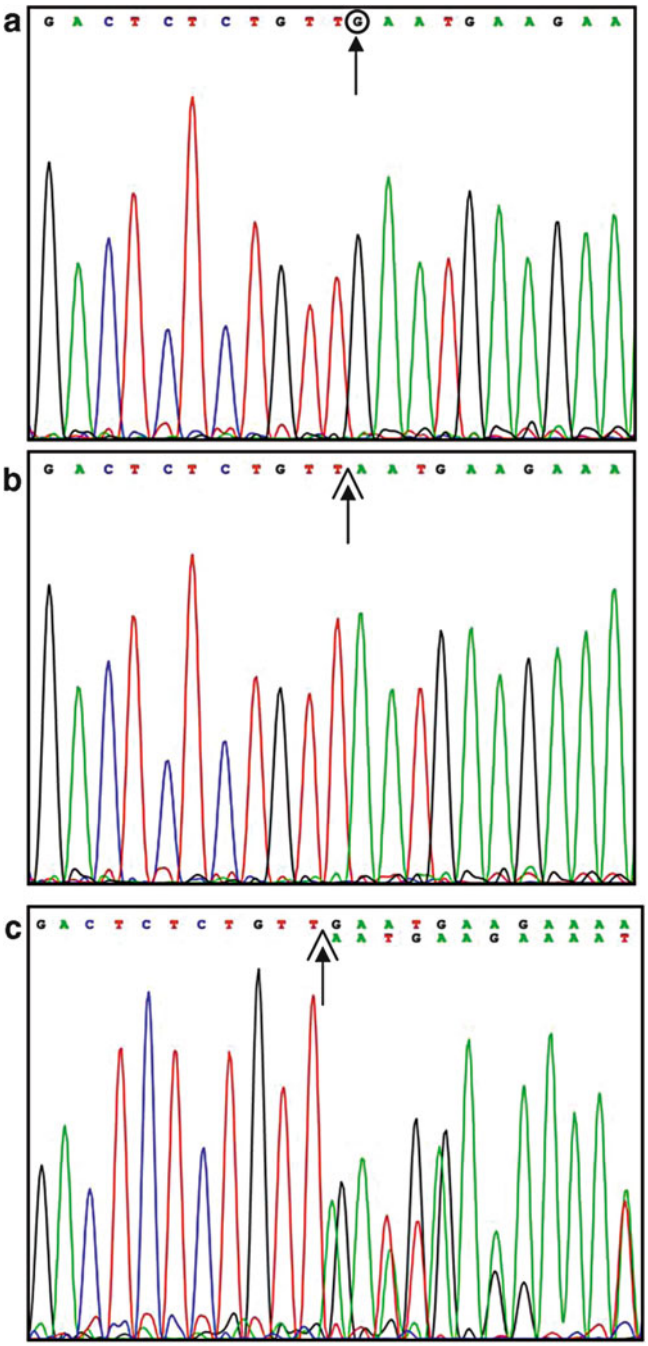

Fig. 1 Partial nucleotide sequence of exon 6 of *LPL* gene. The hypertriglyceridemic patient (panel **b**) appears to be homozygous for a single nucleotide deletion (c.840delG). This mutation was found in patient's mother (panel **c**) in heterozygous state, but not in patient's father (panel **a**) whose sequence was normal

Analysis of *LPL* Gene

The resequencing of *LPL* gene revealed that the patient was homozygous for a single nucleotide deletion in exon 6 (c.840delG) (Fig. 1). This mutation causes a shift in the reading frame leading to a truncated protein (p.N281Mfs*23) of 302 amino acids. Therefore, the sequence of exon 6 of *LPL* gene was performed in all family members (parents and two sisters) available for study. This screening revealed that the mother and one sister of the patient were heterozygous carriers of the mutation (Fig. 1). The absence of the mutation in the father (Fig. 1) was inconsistent with the genotype of the patient, suggesting either a condition of non-paternity or that the

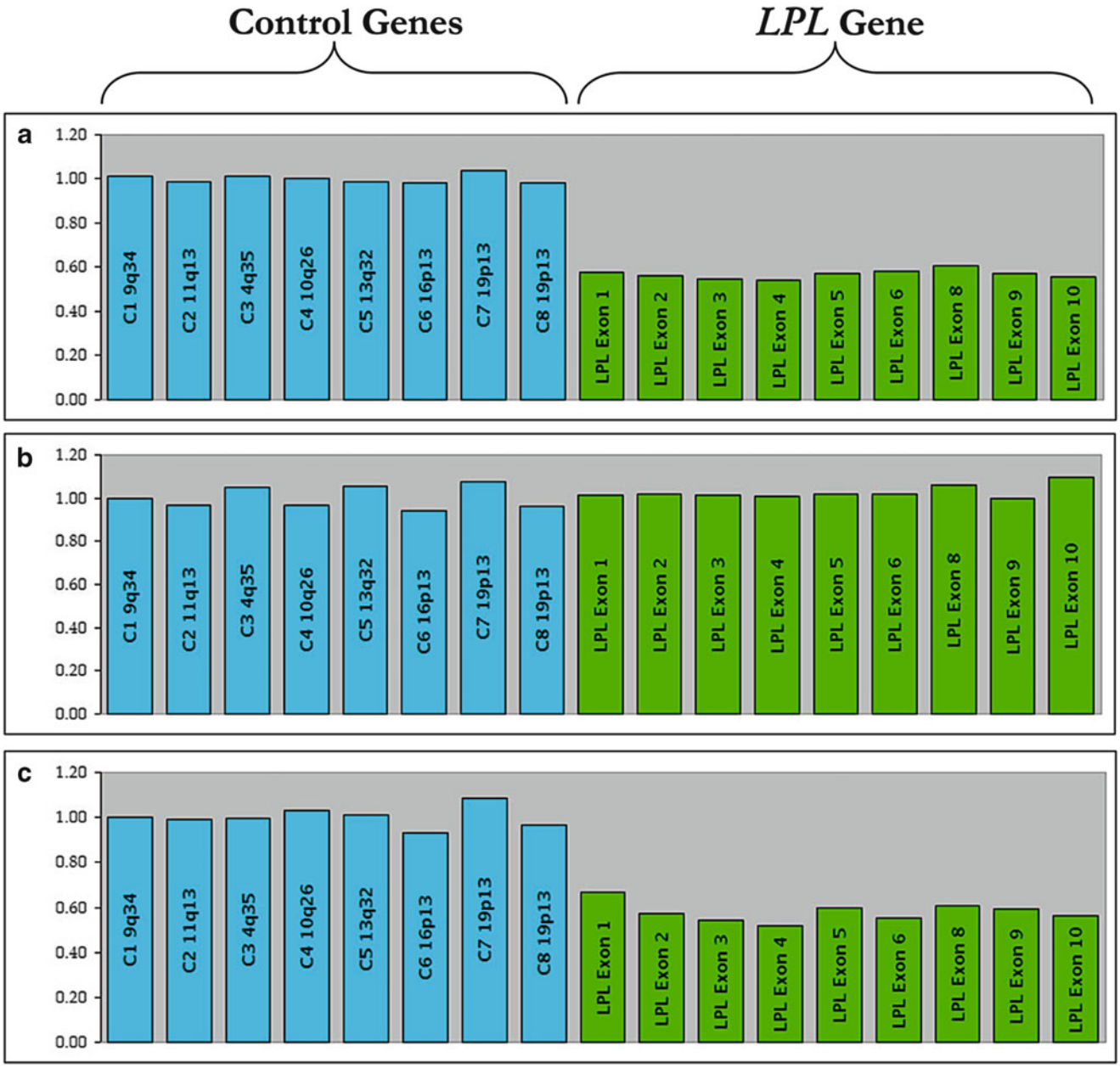

Fig. 2 Multiplex ligation-dependent probe amplification (MLPA) of *LPL* gene. The height of the histograms indicates that the patient is heterozygous for a large deletion which eliminates the entire *LPL* gene (panel **a**); this deletion is present also in the patient's father (panel **c**), but not in the patient's mother (panel **b**)

father might be heterozygous carrier of a partial deletion of *LPL* gene eliminating exon 6. To test this hypothesis, we analyzed the DNA of all family members by MLPA and found that the patient's father was, in fact, heterozygous for a complete deletion of *LPL* gene (Fig. 2) that had been transmitted to the patient. The latter therefore turned out to be a compound heterozygote with one allele harboring the c.840delG and the other harboring of deletion of the *LPL* gene. The *LPL* deletion was also found in the patient's sister previously found to be negative for the c.840delG mutation.

Discussion

Clinical Aspects

In this study, we describe the clinical features and the treatment of a 23-day-old male with sHTG who was admitted to our NICU for plasmapheresis, being at high risk for acute pancreatitis. Therapeutic plasmapheresis can be used to rapidly reduce TG levels as patients with sHTG are at high risk for acute pancreatitis (Ewald and Kloer 2009; Stefanutti et al. 2009).

Since 1978, different plasmapheresis techniques (plasmafiltration, plasma exchange) have been applied to the treatment of adult patients with sHTG. The use of plasmapheresis in newborn infants raises great concern, because of the potential risks related to the extracorporeal procedure, particularly the hemodynamic effects and hemorrhagic events. Plasmafiltration would be preferred in very young infants since it requires a lower volume of extracorporeal circulation than plasma exchange, but it seems to be less effective in sHTG, as chylomicrons remain trapped in the primary plasma filter because of their large size and high molecular weight (Ewald and Kloer 2009; Stefanutti et al. 2013). Stefanutti et al. (2004, 2013) reported two cases of sHTG in very young infants (a 25-day-old male and a 3-month-old female) treated successfully with plasma exchange without adverse events. These authors introduced modifications to the standard procedure to minimize the risks. Given the little chance of success with plasmafiltration we are familiar with and our limited experience in plasma exchange plasmapheresis, we decided to perform an ET. ET was introduced in the late 1940s to decrease the mortality of hemolytic disease of the newborn and to prevent kernicterus in the surviving infants. Since then, ET has been applied to many diseases (such as high levels of unconjugated hyperbilirubinemia in the newborn due to any cause, severe anemia, disseminated intravascular coagulation, neonatal sepsis), and has become one of the most common procedures performed by neonatologists (Steiner et al. 2007). The most common ET-related adverse effects include thrombocytopenia, hypocalcemia, hyperkalemia, apnea, bradycardia, hypotension, and catheter-related complications. A retrospective study by Steiner et al. (2007) reported ET-related morbidity and mortality over a 20-year period (1986–2006) at Yale New Haven Hospital. The majority of complications were transient and, when serious adverse events occurred, they were observed in infants who were preterm and/or very sick. No deaths were related to ET during the study period.

In our patient, ET led to a significant and immediate reduction in plasma TG level without adverse events. This effect is due to the ET procedure "per se" and, possibly, to the presence in transfused blood of LPL released from blood mononuclear cells (known to produce minute amounts of LPL) (Merkel et al. 2002; Stengel et al. 1998). Dietary therapy, started after the ET procedure, was effective in maintaining fasting plasma TG level below 5.6 mmol/L over time.

To the best of our knowledge, this is the first case of sHTG treated with ET in a newborn infant reported in the literature. Given the result we achieved, we believe that ET should be taken into account by neonatologists and pediatricians to treat sHTG in very young infants in order to rapidly decrease elevated TG levels and thus avoiding the potentially fatal risk of acute pancreatitis. This observation sets the stage for a future clinical trial of exchange transfusion in newborns with sHTG due to LPL deficiency or other genetic or acquired conditions.

Molecular Aspects

The hypothesis that the patient had familial chylomicronemia was confirmed by the analysis of *LPL* gene, which revealed at first that he was apparently homozygous for a single nucleotide deletion (c.840delG) predicted to result in a truncated protein. This truncated protein belongs to a group of functionally inactive LPL proteins, resulting from mutations that cause the elimination of the carboxyl-terminal domain of the protein (Bertolini et al. 2000; Merkel et al. 2002). This domain is involved in the intracellular processing and secretion of LPL, the formation of functionally active LPL homodimer, the interaction of LPL with TG-rich lipoproteins, and in the binding of LPL to the LDL receptor-related proteins (LRPs) and glycosaminoglycans of the endothelial cell surface (Murthy et al. 1996; Buscà et al. 1998; Wang and Eckel 2009).

The unexpected absence of the mutation c.840delG in the patient's father prompted us to consider the hypothesis that the father had transmitted to his son a partial deletion of *LPL* gene involving exon 6 (the exon harboring the c.840delG). By applying the MLPA method, we found that the patient's father was heterozygous for a large deletion eliminating the whole *LPL* gene. This deletion was transmitted to the patient (who was in fact a compound heterozygote) and to one of his healthy sisters. As far as we know, this is the first report of a complete deletion of *LPL* gene in humans. At the moment, we do not know the size of this deletion and whether or not other nearby genes are involved. The two heterozygous carriers of this deletion (the father and the sister of the patient) appear to be in good health and to have a normal plasma lipid profile.

Acknowledgments The authors would like to thank the patient and his family for their participation, Dr. Paolo Ernesto Villani (NICU, Department Mother and Children, Hospital "C. Poma", Mantua, Italy) for getting the patient transferred to our NICU, Dr. Gianluigi Ardissino (Unit of Pediatric Nephrology, Fondazione IRCCS Ca' Granda Ospedale Maggiore Policlinico, University of Milan, Milan, Italy) for helping us in evaluating different therapeutic options.

Synopsis

Exchange transfusion appears to be a safe procedure, alternative to plasmapheresis, to prevent acute pancreatitis in young infants with severe hypertriglyceridemia due to lipoprotein lipase deficiency.

Compliance with Ethics Guidelines

Conflict of Interest

Lorenza Pugni, Enrica Riva, Carlo Pietrasanta, Claudio Rabacchi, Stefano Bertolini, Cristina Pederiva, Fabio Mosca, and Sebastiano Calandra declare that they have no conflict of interest.

Informed Consent

All procedures followed were in accordance with the Helsinki Declaration of 1975, as revised in 2000. Informed consent was obtained from patient's parents for being included in the study. This manuscript is a case report containing no identifying patient information, and examinations and treatment of the patient fall in clinical practice.

Authors' Contributions

Lorenza Pugni, Carlo Pietrasanta, and Fabio Mosca designed the study, performed the blood exchange transfusion and collected the data. Enrica Riva and Cristina Pederiva followed up the patient after the discharge. Sebastiano Calandra, Claudio Rabacchi, and Stefano Bertolini performed the molecular investigation and analyzed the molecular data. Lorenza Pugni and Sebastiano Calandra wrote the manuscript.

Funding Support

Genetic analysis was supported in part by a grant from Emilia-Romagna Region: RARER – Area1 (E35E09000880002) project to Sebastiano Calandra.

References

Avis HJ, Scheffer HJ, Kastelein JJP, Dallinga-Thie GM, Wijburg FA (2010) Pink-creamy whole blood in a 3-month-old infant with a homozygous deletion in the lipoprotein lipase gene. Clin Genet 77:430–433

Bertolini S, Simone ML, Pes GM et al (2000) Pseudodominance of lipoprotein lipase (LPL) deficiency due to a nonsense mutation (Tyr302>Term) in exon 6 of LPL gene in an Italian family from Sardinia (LPL_{Olbia}). Clin Genet 57:140–147

Brahm A, Hegele RA (2013) Hypertriglyceridemia. Nutrients 5:981–1001

Buscà R, Martinez M, Vilella E et al (1998) The carboxy-terminal region of human lipoprotein lipase is necessary for its exit from the endoplasmic reticulum. J Lipid Res 39:821–833

Chen YH, Ke ZL, Wang YX, Wang Y, Zheng YZ (2012) Two case reports of familial chylomicronemia syndrome. Case Rep Pediatr 2012:384719

Davies BS, Beigneux AP, Fong LG, Young SG (2012) New wrinkles in lipoprotein lipase biology. Curr Opin Lipidol 23:35–42

Ewald N, Kloer HU (2009) Severe hypertriglyceridemia: an indication for apheresis? Atheroscler Suppl 10:49–52

Feoli-Fonseca JC, Lévy E, Godard M, Lambert M (1998) Familial lipoprotein lipase deficiency in infancy: clinical, biochemical and molecular study. J Pediatr 133:417–423

Johansen CT, Kathiresan S, Hegele RA (2011) Genetic determinants of plasma triglycerides. J Lipid Res 52:189–206

Kavazarakis E, Stabouli S, Gourgiotis D et al (2004) Severe hypertriglyceridemia in a Greek infant: a clinical, biochemical and genetic study. Eur J Pediatr 163:462–466

Leaf DA (2008) Chylomicronemia and the chylomicronemia syndrome: a practical approach to management. Am J Med 121:10–12

Merkel M, Eckel RH, Goldberg IJ (2002) Lipoprotein lipase: genetics, lipid uptake, and regulation. J Lipid Res 43:1997–2006

Murthy V, Julien P, Gagne C (1996) Molecular pathobiology of human lipoprotein lipase gene. Pharmacol Ther 70:101–135

Stefanutti C, Lanti A, Di Giacomo S et al (2004) Therapeutic apheresis in low weight patients: technical feasibility, tolerance, compliance, and risks. Transfus Apher Sci 31:3–10

Stefanutti C, Di Giacomo S, Vivenzio A et al (2009) Therapeutic plasma exchange in patients with severe hypertriglyceridemia: a multicenter study. Artif Organs 33:1096–1102

Stefanutti C, Gozzer M, Pisciotta L et al (2013) A three month-old infant with severe hyperchylomicronemia: molecular diagnosis and extracorporeal treatment. Atheroscler Suppl 14:73–76

Steiner LA, Bizzarro MJ, Ehrenkranz RA, Gallagher PG (2007) A decline in the frequency of neonatal exchange transfusions and its effect on exchange-related morbidity and mortality. Pediatrics 120:27–32

Stengel D, Antonucci M, Gaoua W et al (1998) Inhibition of LPL expression in human monocyte-derived macrophages is dependent on LDL oxidation state: a key role for lysophosphatidylcholine. Arterioscler Thromb Vasc Biol 18:1172–1180

Surendran RP, Visser ME, Heemelaar S et al (2012) Mutations in LPL, APOC2, APOA5, GPIHBP1 and LMF1 in patients with severe hypertriglyceridaemia. J Intern Med 272:185–196

Wang H, Eckel RH (2009) Lipoprotein lipase: from gene to obesity. Am J Physiol Endocrinol Metab 297:E271–E288<

JIMD Reports
DOI 10.1007/8904_2013_257

RESEARCH REPORT

Liver Engraftment and Repopulation by In Vitro Expanded Adult Derived Human Liver Stem Cells in a Child with Ornithine Carbamoyltransferase Deficiency

Etienne M Sokal · Xavier Stéphenne · Chris Ottolenghi · Nawal Jazouli · Philippe Clapuyt · Florence Lacaille · Mustapha Najimi · Pascale de Lonlay · Françoise Smets

Received: 15 June 2013 / Revised: 28 July 2013 / Accepted: 01 August 2013 / Published online: 20 October 2013

Abstract A 3-year-old girl suffering from ornithine carbamoyltransferase (OTC) deficiency was poorly equilibrated under conventional diet and scavenger treatment. Following unsuccessful cryopreserved hepatocyte transplantation, she received two infusions of Adult Derived Human Liver Stem/Progenitor Cells (ADHLSCs) expanded in vitro under GMP settings, the quantity being equivalent to 0.75% of her calculated liver mass. Using FISH immunostaining for the Y chromosome, the initial biopsy did not detect any male nuclei in the recipient liver. Two liver biopsies taken 100 days after ADHLSC transplantation showed 3% and 5% of male donor cells in the recipient liver, thus suggesting repopulation by donor cells. Although limited follow-up did not allow us to draw conclusions on long-term improvement, these results provide a promising proof of concept that this therapy is feasible in an OTC patient.

Communicated by: Daniela Karall

Competing interests: None declared

E.M. Sokal · X. Stéphenne · C. Ottolenghi · N. Jazouli · F. Lacaille · M. Najimi · P. de Lonlay · F. Smets
Université Catholique de Louvain & Cliniques Universitaires Saint Luc, 10 av Hippocrate, B 1200, Bruxelles, Belgium

E.M. Sokal (✉) · X. Stéphenne · N. Jazouli · M. Najimi · F. Smets
Service de Gastroentérologie et Hépatologie Pédiatrique, Cliniques St Luc, 10 av Hippocrate, B 1200, Bruxelles, Belgium
e-mail: Etienne.sokal@uclouvain.be

P. Clapuyt
Service de radiologie, Gastroentérologie et Hépatologie pédiatrique, 10 av Hippocrate, B 1200, Bruxelles, Belgium

E.M. Sokal · X. Stéphenne · N. Jazouli · M. Najimi · F. Smets
Centre de Thérapie Cellulaire et Institut de Recherche Expérimentale et Clinique, 10 av Hippocrate, B 1200, Bruxelles, Belgium

C. Ottolenghi · F. Lacaille · P. de Lonlay
Hôpital Necker Enfants Malades, Centre de Référence des Maladies Héréditaires du Métabolisme, service de biochimie spécialisée et hépato-gastroentérologie, Université Paris Descartes, Institut Imagine, Paris, France

Introduction

The urea cycle is the pathway responsible for the metabolism of wasted nitrogen in humans. This pathway is dependent of the functional integrity of the liver ornithine transcarbamylase (OTC). OTC deficiency is the most common urea cycle enzyme defect. Ammonia incorporation is impaired leading to recurrent high blood values, causing severe neurological damage and long-term cognitive defects (Nassogne et al. 2005; Leonard 2001; Ensenauer et al. 2005). OTC deficiency is an x-chromosomal transmitted disorder. Current treatment encompasses a low natural protein diet, use of ammonium scavengers, and supplements in arginine and citrulline (Enns et al. 2007). Patients can still present episodes of decompensation, and most of them develop secondary anorexia requiring gastric tubing. Their total protein intake remains often below the WHO recommendation. Orthotopic liver transplantation (OLT) applies to the sickest patients, while some other patients are perfectly equilibrated. There is a wide range of clinical presentations, with recurrent episodes of moderate hyperammonemia, and in less severe cases, parents and physicians are balanced between conventional therapy or liver transplantation, the procedure in which access remains highly limited by donor shortage and because of the inherent short- and long-term risks of the procedure. Less invasive, innovative therapies are expected

to improve the phenotype and the quality of life of these children and their families.

Liver regenerative medicine aims to repair a deficient liver with cells. In the context of inborn errors of liver metabolism, allogeneic cells are used to correct a liver-based enzyme defect. The proof of concept has been established with hepatocyte transplantation. After infusion in the recipient's portal system, transplanted hepatocytes have been documented to provide the missing enzyme for urea cycle defects and other metabolic diseases (Sokal et al. 2003; Stéphenne et al. 2005, 2006). However, hepatocyte transplantation faces several limitations, including organ shortage, poor quality of livers offered for cell isolation, poor resistance of mature hepatocytes to cryopreservation and culture conditions, as well as risk of disease transmission with a transplant product (Meyburg and Hoffmann 2010; Jorns et al. 2012; Smets et al., 2008). Therefore, stem/progenitor cells are upcoming as the next generation of cells for regenerative medicine, being developed for their capacity to overcome the limitations of mature hepatocytes, and to be expanded industrially under GMP conditions. This technology brings regenerative medicine of the liver widely available to any patient suffering from this disorder and other inborn metabolic diseases of the liver (Nussler et al. 2006; Sancho-Bru et al. 2009; Khuu et al. 2010; Najimi et al. 2007).

Here we report the first human stem/progenitor cell transplantation, with engraftment and repopulation of recipient liver, using Adult Derived Human Liver Stem Cells (ADHLSCs) intraportal infusion in a 3-year-old girl with OTC deficiency.

Patient and Methods

Patient's History

A 3-year-old girl suffered severe OTC deficiency with neonatal onset. The diagnosis had been established after a neonatal coma occurring 38 h after birth (NH3 380 μmol/L, TP 10%) and was confirmed by DNA analysis, indicating a de novo deletion of exons 6–8 on the paternal allele of OTC gene. She was under protein restriction diet (1 g/kg/day by amino acid mixture and natural proteins) and received Na-Benzoate (200 mg/kg/day), Na-phenylbutyrate (150 mg/kg/day), citrulline (150 mg/kg/day), and arginine (150 mg/kg/day). Anorexia and impossibility to provide oral feeding led to enteral feeding by gastrostomy tube starting at age 9 months. The child's growth was normal with good psychomotor development, but despite intensive treatment she displayed recurrent episodes of hyperammonemia (NH3 $>$ 300 μmol/L) and frequent (monthly) hospital admissions. Glutamine levels were persistently elevated ($>$1,400 μmol/L – normal range: 250–850 μmol/L).

In an attempt to improve her metabolic control, and decrease the risk related to recurrent hyperammoniemia, she was proposed to receive hepatocyte transplantation, according to a protocol used in previously reported patients (Sokal et al. 2003). The project and procedure was approved by the institution ethical committee. Hepatocytes were procured from a ministry of health accredited tissue bank.

She received two infusions of 1.25 and 2.3 billions cryopreserved/thawed female hepatocytes over two days (viability post thawing 72% and 84%, respectively, using trypan blue exclusion assay). Four months later, she received a second series of infusions with 2.45 billions of cryopreserved/thawed male hepatocytes (viability post thawing 91%). The cells were infused through a percutaneous portal catheter, at a concentration of 10–15 $\times$ 10^6cells/mL, at a rate of 1 mL/min. Immunosuppression included Tacrolimus (Prograf, Astellas, Belgium). The tolerance was good without complications, but there was however no evidence of benefit from these hepatocyte transplantation courses.

During the 6-month follow-up treatment, she continued to have monthly episodes of metabolic decompensation with hyperammonemia up to 300 μmol/L and she was proposed to receive a new cell therapy course using ADHLSC. This protocol was approved by the ethical committee of the institution and informed consent was given to and received from the parents by an independent physician.

Large-Scale Production of ADHLSC

ADHLSCs were obtained after primary culture of cryopreserved/thawed liver cells previously isolated from the right lobe of a healthy cadaveric liver donor, an 11-year-old male. Emerging ADHLSCs become predominant after the second passage according to our previous documented observations (Najimi et al. 2007; Scheers et al. 2012). ADHLSCs were expanded in cell-stack 10 chambers to reach 15 cumulative population doublings after 6 passages.

The purity of the ADHLSC culture was investigated at the morphology, the hepato-mesenchymal phenotype (Albumin$^+$, alpha smooth muscle actin (α-SMA$^+$) and the absence of epithelial markers such as cytokeratins (CK) 7, 8, 18, and 19 as well as CD133 using immunocytochemistry, RT-PCR, and flow cytometry.

The hepatogenic differentiation potential was also evaluated as described elsewhere (Khuu et al. 2010; Khuu et al. 2012). The differentiated cells were analyzed at the morphological, genetic, and functional levels (Khuu et al.

2010; Najimi et al. 2007). The quality of cell suspensions recovered was also checked at the safety level. Cell cultures were analyzed at all passages and no bacterial or virus (EBV, CMV, HBV, and HCV) contamination was detected. In addition, no cytogenetic abnormalities were detected in ADHLSC cultures at passage 7 (end of large-scale production). No tumor formation was observed 24 weeks after subcutaneous injection to nude mice (Scheers et al. 2012).

Cryopreservation

Cells were resuspended in solution of 90% fetal bovine serum and 10% DMSO. Cell suspension concentration was adjusted to 2.4 million cells/mL. Cell suspension was cryopreserved using a programmed freezer equipment (Cryoson) using a stepwise decrease in temperature (1°C/min until −40°C and then 2°C/min until −90°C). While reaching −90°C, cells were transferred into liquid nitrogen tank.

Thawing and Formulation Before Infusion

Cells were thawed at 37°C for a few minutes and washed with thawing solution (human albumin 5%, glucose 5 g/100 mL, bicarbonate 84 mg/mL, and heparin 10 UI/mL) at a dilution of 1/10. Cells were washed and centrifuged twice before counting and viability evaluation. Cells were resuspended in infusion solution (thawing solution with N-AcetylCystein 10 mM), at a concentration of 10 millions of cells/mL in 50 mL syringe. Viability of cells after thawing was always above 85% using trypan blue exclusion assay.

Adult Derived Human Liver Stem Cells Infusion

ADHLSCs were obtained and expanded in 2009 from liver cell batches previously isolated and cryopreserved in 2007 (e.g., 11-year-old male donor). ADHLSCs were infused through a percutaneous intraportal catheter for a total of 0.9 billion cells (this corresponds to 60 million ADHLSCs per kg body weight, i.e., 0. 75% of the theoretical liver hepatocyte mass) (14).

In May 2009, two first infusions of respectively 262 millions (viability 89%) and 230 millions (viability 90%) of cryopreserved ADHLSCs were performed under general anesthesia (concentration 10×10^6/mL, infusion rate 1 mL/min). A transcutaneous catheter was placed in the main portal vein under fluoroscopy and ultrasound guidance as previously described (5).

Immunosuppression regimen remained identical, using tacrolimus monotherapy to reach trough levels of 6–8 ng/mL. Prophylactic antibiotherapy with cefazolin (40 mg/kg) was given immediately prior, 8, and 16 h post infusion. The infusion and post-infusion course were unremarkable and the child was discharged from hospital on day three post infusion.

The second infusion occurred 2 weeks later (June 2009) with freshly trypsinized ADHLSC (430 millions of cells, viability 98%) at same concentration and infusion rate as for the first session. Liver Doppler ultrasounds were performed before and after each cell infusion.

Biochemical Monitoring

The ammonia level in plasma was measured by using ammonia reagent by a timed endpoint method (Synchron LX system, Fullerton, CA) (nl < 125 μg/dL).

The glutamine measurement was performed by ion exchange chromatography and ninhydrin detection (Jeol Aminotac analyzer).

Liver Biopsies: Fluorescence In Situ Hybridization

Liver biopsies were performed before ADHLSC infusion and three and half months after the infusions. FISH immunostaining was performed for the Y chromosome on liver-biopsy fingerprints mounted on slides. Transplanted male cells were detected by using a probe specific to the SRY gene labeled with a SpectrumOrange, with a CEP X SpectrumGreen control probe. Hybridized slides were examined using either a DMRB microscope or an axioplan 2 microscope equipped with a single-by-pass filter for excitation of DAPI, FITC, and rhodamine; double-by-pass filters for excitation of FITC/rhodamine and triple-by-pass filters for excitation of DAPI/FITC/rhodamine. Images were captured by using a Photometrics camera and processed by Isis software. For each hybridization, 200 cells in interphase were analyzed.

Statistical Analyses

Three different 6-month treatment phases have been defined:

- Baseline (BSL): within 6 months before start of hepatocytes infusion
- Post-hepatocytes (Post-Hep): over 6 months after end of hepatocytes infusion
- Post-cells: over 6 months after infusion with progenitor cells

Within each of these treatment phases, two different periods of interest have been considered: from 0 to 3 months and from 3 to 6 months.

Only data collected during these treatment phases have been included in the statistical analysis. To account for their lognormal distribution, glutamine, ammonia, and orotic acid concentrations have been log-transformed (Ln) prior statistical analysis. The Ln-transformed levels have been statistically analyzed using a two-way analysis of variance, with the phase, the period, and the interaction between the phase and the period included as fixed factors in the model.

Specific contrasts have been used to derive estimates (with 95% confidence interval) for each treatment period of interest and for the following comparisons:

- Post-Hep vs. Baseline
- Post-Cells vs. Baseline
- Post-Cells vs. Post-Hep (0–6 months)
- Post-Cells vs. Post-Hep (0–3 months)
- Post-Cells vs. Post-Hep (3–6 months)

Results

ADHLSC Engraftment and Clinical Outcome

Prior to the first infusion of ADHLSC, (9 months after the last hepatocyte infusion), a biopsy was performed to evaluate the engraftment of previously received male hepatocytes using Fluorescent in situ hybridization (FISH) technique for the Y chromosome (male donor and female receiver). No Y-chromosome-positive cells were detected in the recovered biopsy. Three and half months after both infusions of ADHLSCs, two percutaneous biopsies were performed in two separate areas of the right liver lobe to evaluate cell engraftment. Demonstration was made of the presence of 3% of male donor cells in the first biopsy and 5% in the second biopsy, while no Y positive cells were found in the basal biopsy. Taking into account the quantity of infused cells (0.9×10^9), the average 4% chimerism, the theoretical liver cell mass of the patient ($15\ kg \times 5 \times 10^9/kg = 75 \times 10^9$) (Fox et al. 1998), and the homogeneous liver distribution as shown in other patients (data not shown), this would mean an absolute quantity of donor cells reaching 3×10^9 cells, i.e., 3.3 times the quantity of cells infused. This theoretical calculation suggests a proliferation and liver repopulation capacity of ADHLSC.

The serum transaminases and bilirubin levels during the immediate post infusion period and in the long-term follow-up stayed within normal laboratory values.

The 8-month follow-up period was characterized by temporary recovery from disease related anorexia and improvement of the child's overall condition as evaluated by the parents, with less frequent hospital admissions (see below). The psychomotor evolution was however not evaluated by behavioral or intellectual score assessments.

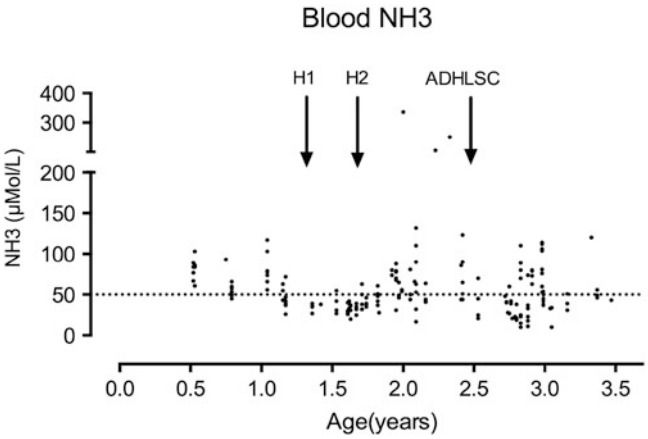

Fig. 1 Ammonium blood levels at different points of the evolution. Normal value < 50 µMol/L (*dotted horizontal line*). H1 and H2 represent the hepatocyte infusions and ADHLSC the ADHLSC infusion

Metabolic Control After Infusion

The data obtained for each treatment phase and for each period of interest are presented in Figs. 1, 2, 3, and 4 and are summarized in Table 1.

Glutamine levels were not significantly influenced by hepatocytes or ADHLSC infusion.

Ammonia levels were significantly increased after hepatocyte infusion. After ADHLSC infusion, ammonia levels decreased to levels close to baseline, with a significant decrease compared to levels observed after hepatocyte transfusion (Figs. 1 and 4).

Compared to baseline, orotic acid levels were significantly lower after hepatocyte and ADHLSC infusions, without significant differences between both interventional procedures (Figs. 3 and 4).

The number of decompensations was multiple before ADHLSC infusions with four admissions in the 6-month period preceding hepatocyte infusions and three additional severe decompensations between hepatocyte transfusion and ADHLSC infusion (6 months, 12 and 16 months after hepatocytes transfusion, NH3 > 300 µmol/L). After ADHLSC infusions, one mild decompensation occurred at 6 months of the procedure (NH3 100 µmol/L) and a second mild to moderate decompensation at 8 months (NH3 120 µmol/L). The protein content of the diet remained at 1 g/Kg/day (mostly aminoacid mixture). Urea cycle disorder (UCD)-medications were unchanged. In addition, the patient was under tacrolimus therapy at a dosage adapted to reach a level of 5–6 ng/mL.

The follow-up was limited in time, as immunosuppression was stopped 6 months after the ADHLSC infusion, by fear

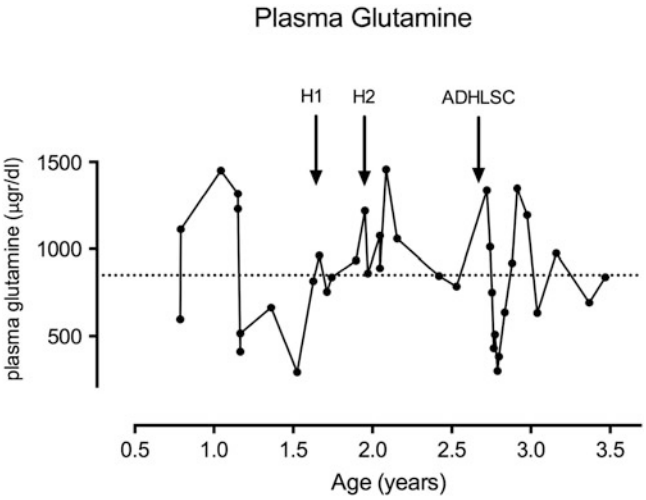

Fig. 2 Plasma glutamine levels at different time points of the evolution. Normal values: 250–850 µg/dL (*dotted horizontal line* = maximal value). H1 and H2 represent the hepatocyte infusions and ADHLSC the ADHLSC infusion

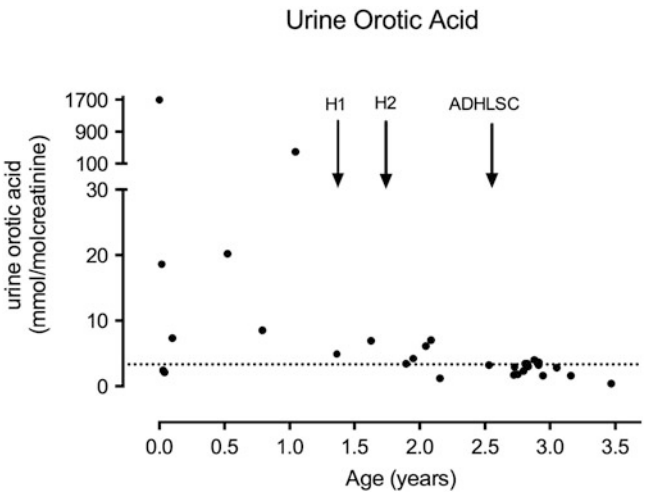

Fig. 3 Urine orotic acid excretion at different time points of the evolution. Normal value: <3.3 mmol/mol creatinine (*dotted horizontal line*). H1 and H2 represent the hepatocyte infusions and ADHLSC the ADHLSC infusion

of viral infection during the H1N1 flu epidemic. There was no more evidence of cell effect, and a liver transplantation was proposed 3 months later. The child unfortunately died from the procedure.

Pro-coagulant Effects of ADHLSC

At the end of the second infusion of ADHLSC, sudden increase of portal vein pressure occurred and partial thrombosis of the left intrahepatic portal vein branch was observed by Doppler ultrasound, leading to arrest of infusion. This adverse event was treated by low molecular weight heparin (Fraxiparin^{R}, Glaxo Smith Kline, Genval, Belgium) and coumarinic anticoagulant (Sintrom^{R}, Novartis, Vilvoorde, Belgium), 5 mg/day for 30 days. D-Dimers were markedly elevated after both cell infusion courses, confirming the procoagulant effect of the cell preparation. This adverse event did not lead to any consequence for the patient but encouraged our team to investigate further the procoagulant effect of the progenitor cells and adapt the anticoagulation protocol accordingly.

Discussion

This is the first report demonstrating engraftment of an advanced therapy medicinal product after intraportal transplantation in human. The theoretical calculation tended to show that cells had repopulated the recipient liver, as the percentage of donor cells in two liver biopsies taken 3 months after the infusion, extrapolated to the entire liver, would correspond to a threefold increase of the original transplanted cell number. Such interpretation must be taken cautiously, as sampling error may play a role.

The first attempt to treat the child using cryopreserved hepatocyte has not been clinically successful in improving the child condition, and there was even a trend toward higher ammonium values following hepatocyte infusions.

Following ADHLSC infusion, there was some indication of clinical improvement (parental reporting, decompensation episodes with milder level of NH3). However, we were not able to follow the further metabolic data as immunosuppression was stopped after 6 months; the child was thereafter liver transplanted and died from complications of this procedure.

Thus, we are unable to conclude on the long-term clinical efficacy of the therapy, but overall, the data suggest that cells had engrafted and started to expand and/or to differentiate to a more protective extent. Indeed, patients with neonatal onset OTC are well known to be extremely prone to sudden fatal decompensations, and in the absence of successful liver transplantation, their survival is less than 10% beyond age 5 years (Kido et al. 2012; Uchino et al. 1998). Thus, it is possible that, if immunosuppression had been maintained and in absence of liver transplantation, ADHLSC infusion would have helped to prolong the life of this patient long enough to allow for greater repopulation by the engrafted cells, perhaps as early as during the so-called early “honeymoon” period of the disease (Leonard 2001; Ensenauer et al. 2005).

Markers, such as NH3 and glutamine which represents the gold standard of diagnostic and follow-up studies on UCD disorders, may be unsuitable to detect early limited improvements of potential clinical relevance. We stress the need for longer follow-up and of composite end points to explore more finely any behavioral, dietary, and biochemical

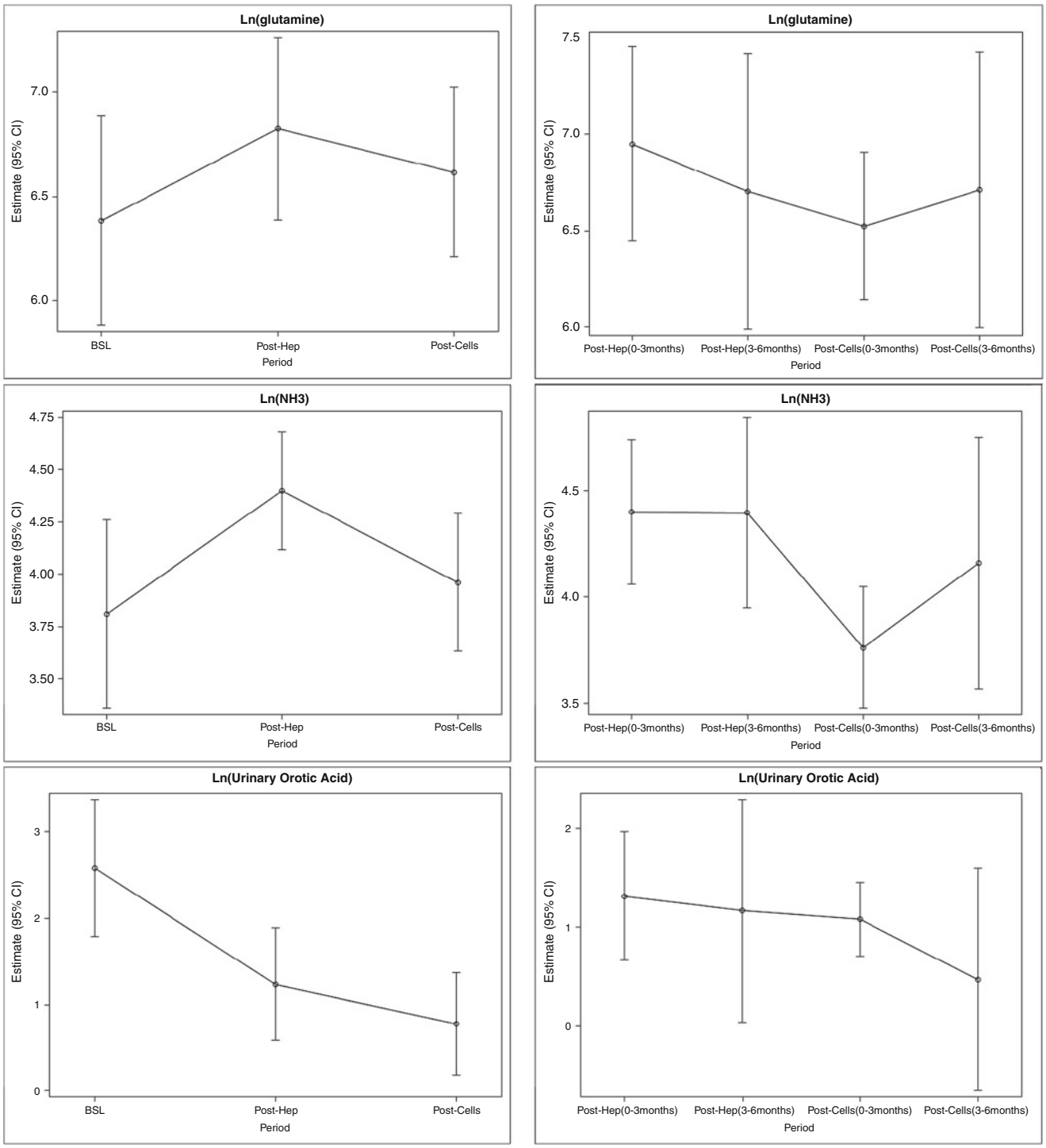

Fig. 4 Estimates of Ln(glutamine), Ln(ammoniac), and Ln(orotic acid) levels at each treatment period. Symbols are the mean estimates, errors bars represent the 95% confidence interval *Left*: 6-month period; *Right*: over 0–3 and 3–6-month period. *Top*: Ln(glutamine); *Middle*: Ln(ammoniac); *Bottom*: Ln(orotic acid)

effects. The improvement of urea cycle function in vivo could be explored in the future by measurement of C13 incorporated into urea, following C13 Na acetate administration (Yudkoff et al. 2010).

As hepatocyte, islets, and other mesenchymal stromal cells (MSCs) do, the ADHLSCs express tissue factor and induce the coagulation cascade. This was most probably responsible for the partial left portal vein thrombosis observed during the

Table 1 Statistical analysis and comparisons of Ln(glutamine), Ln(ammoniac), and Ln(orotic acid) at each treatment period

Treatment period	Ln(glutamine)	Ln(ammoniac)		Ln(orotic acid)	
0–6 months					
BSL	6.38 (5.88–6.89)	3.81 (3.36–4.26)		2.59 (1.79–3.38)	
Post-Hep	6.83 (6.39–7.26)	4.40 (4.12–4.68)	#	1.24 (0.59–1.89)	#
Post-Cells	6.62 (6.21–7.02)	3.96 (3.63–4.29)	§	0.77 (0.18–1.37)	##
0–3 months					
Post-Hep	6.95 (6.44–7.46)	4.40 (4.06–4.74)		1.31 (0.66–1.96)	
Post-Cells	6.52 (6.14–6.91)	3.76 (3.48–4.05)	§§	1.08 (0.7–1.45)	
3–6 months					
Post-Hep	6.70 (5.99–7.42)	4.40 (3.95–4.85)		1.16 (0.04–2.29)	
Post-Cells	6.71 (6.00–7.43)	4.16 (3.57–4.75)		0.47 (−0.65–1.59)	

Values are mean estimates (95% CI) #/##: significantly different from baseline (#: $p < 0.05$, ##: $p < 0.01$) §/§§: significantly different from Post-Hep (§: $p < 0.05$, §§: $p < 0.01$)

second infusion. This led our group to conduct studies on the procoagulant properties of the ADHLSC and to identify the specific combination of anticoagulant that could prevent thrombosis. In vitro investigation using clotting factor analysis and thromboelastography confirmed the procoagulant effect of both hepatocytes and progenitor cells. However, hepatocyte procoagulant effect can be inhibited by heparin and only partly for the progenitor cells. The mechanisms of procoagulant effect were identified and a specific anticoagulant cocktail containing heparin (10 UI/mL) and bivalirudin (0.75 mg/kg) was developed and submitted for patent application. The use of this anticoagulant combination in successive patients confirmed safety and inhibition of the procoagulant effect of the cells (Stephenne et al. 2012).

In metabolic diseases, cell therapy requires the use of allogeneic cells and hence immunosuppression. ADHLSCs are of mesenchymal phenotype, and like MSCs of other origins, exhibit immunotolerogenic properties (Le Blanc et al. 2008). Trials are being conducted in various autoimmune diseases, with the aim to modulate the patient immune system. We detected similar features in vitro for the liver-derived MSCs, which can block an ongoing mixed lymphocyte reaction (Sana et al. 2013). However, it is not clear whether any such immune suppressive features would persist once the cells engraft and differentiate. For this reason, immunosuppression must be given to the patient, and in our case, we choose to use the same immunosuppression protocol that is widely used in pediatric liver transplantation.

We conclude that liver-based regenerative medicine using AHDLSC is feasible, and that it can lead to a significant engraftment and parenchymal repopulation at medium term after portal infusion. Although the limited follow-up of the patient did not enable us to draw any firm conclusion on the clinical evolution, the histological data provide a very promising proof of concept that ADHLSC therapy is a potential treatment. Urea cycle disease is one of the most desired targets, but composite end points must be further developed to better assess the efficacy and benefits for the patients. Ongoing research is about to bring new tools to improve the level of engraftment.

Our first-in-man study is another example that stem cell–based regenerative medicine is now coming to clinical application, and EMA approved phase I/II clinical trials are currently being conducted using this technology (clinicaltrial.gov identifier NCT01765283), which will allow to evaluate both safety and efficacy of this treatment.

Take-Home Message

Liver stem cells infused in the portal vein engraft and repopulate the liver in an OTC patient.

Compliance with Guidelines

This cell transplantation protocol was approved by the ethical committee of the institution and informed consent was given to and received from the parents by an independent physician.

Conflict of Interest

Etienne Sokal declares to own patent rights on ADHLSC, currently in clinical development plan (clinicaltrial.gov identifier NCT01765283) by Promethera Biosciences, spinoff of the laboratory of pediatric hepatology and cell therapy. ES Sokal is consultant CSO for Promethera Biosciences.

Xavier Stephenne declares that he has no conflict of interest.

Chris Ottolenghi declares no conflict of interest.

Nawal Jazouli declares no conflict of interest.

Florence Lacaille declares no conflict of interest.

Mustapha Najimi declares to own patent rights on ADHLSC, currently in clinical development (clinicaltrial.gov identifier NCT01765283). MN is consultant for Promethera Biosciences.

Pascale de Lonlay declares no conflict of interest.

Françoise Smets declares that she is currently principal investigator of a clinical trial (clinicaltrial.gov identifier NCT01765283).

Animal Rights: All preclinical animal studies done prior to the reported work were approved by the Institution Animal Ethical Committee.

Informed consent of the patient was obtained from her legal representative, and the protocol and informed consent was approved by the Université Catholique de Louvain & Cliniques St Luc Ethical committee. An ethical committee independent delegate explained the study to the patient and her legal representative.

References

Enns GM, Berry SA, Berry GT, Rhead WJ, Brusilow SW, Hamosh A (2007) Survival after treatment with phenylacetate and benzoate for urea-cycle disorders. N Engl J Med 356:2282–2292

Ensenauer R, Tuchman M, El-Youssef M, Kotagal S, Ishitani MB, Matern D, Babovic-Vuksanovic D (2005) Management and outcome of neonatal-onset ornithine transcarbamylase deficiency following liver transplantation at 60 days of life. Mol Genet Metab 84:363–366

Fox IJ, Chowdhury JR, Kaufman SS et al (1998) Treatment of the Crigler-Najjar syndrome type I with hepatocyte transplantation. N Engl J Med 338:1422–1426

Jorns C, Ellis EC, Nowak G, Fischler B, Nemeth A, Strom SC, Ericzon BG (2012) Hepatocyte transplantation for inherited metabolic diseases of the liver. J Intern Med 272:201–223

Khuu DN, Scheers I, Ehnert S et al (2010) In vitro differentiated adult human liver progenitor cells display mature hepatic metabolic functions: a potential tool for in vitro pharmacotoxicological testing. Cell Transplant 20(2):287–302

Khuu DN, Nyabi O, Maerckx C, Sokal E, Najimi M (2012) Adult human liver mesenchymal stem/progenitor cells participate to mouse liver regeneration after hepatectomy. Cell Transplant 22(8):1369–1380

Kido J, Nakamura K, Mitsubuchi H et al (2012) Long-term outcome and intervention of urea cycle disorders in Japan. J Inherit Metab Dis 35:777–785

Le Blanc K, Frassoni F, Ball L et al (2008) Mesenchymal stem cells for treatment of steroid-resistant, severe, acute graft-versus-host disease: a phase II study. Lancet 371:1579–1586

Leonard JV (2001) The nutritional management of urea cycle disorders. J Pediatr 138:S40–S44, discussion S44–S45

Meyburg J, Hoffmann GF (2010) Liver, liver cell and stem cell transplantation for the treatment of urea cycle defects. Mol Genet Metab 100(Suppl 1):S77–S83

Najimi M, Khuu DN, Lysy PA, Jazouli N, Abarca J, Sempoux C, Sokal EM (2007) Adult-derived human liver mesenchymal-like cells as a potential progenitor reservoir of hepatocytes? Cell Transplant 16:717–728

Nassogne MC, Héron B, Touati G, Rabier D, Saudubray JM (2005) Urea cycle defects: management and outcome. J Inherit Metab Dis 28:407–414

Nussler A, Konig S, Ott M et al (2006) Present status and perspectives of cell-based therapies for liver diseases. J Hepatol 45:144–159

Sana G, Lombard C, Vosters et al (2013) Adult human hepatocytes promote CD4+ T cell hyporesponsiveness via interleukin-10 producing allogeneic dendritic cells. Cell Transplant

Sancho-Bru P, Najimi M, Caruso M et al (2009) Stem and progenitor cells for liver repopulation: can we standardise the process from bench to bedside? Gut 58:594–603

Scheers I, Maerckx C, Khuu DN, Marcelle S, Decottignies A, Najimi M, Sokal E (2012) Adult derived human liver progenitor cells in long term culture maintain appropriate gatekeeper mechanisms against transformation. Cell Transplant 21(10):2241–2255

Smets F, Najimi M, Sokal EM (2008) Cell transplantation in the treatment of liver diseases. Pediatr Transplant 12:6–13

Sokal EM, Smets F, Bourgois A et al (2003) Hepatocyte transplantation in a 4-year-old girl with peroxisomal biogenesis disease: technique, safety, and metabolic follow-up. Transplantation 76:735–738

Stéphenne X, Najimi M, Smets F, Reding R, de Ville de Goyet J, Sokal EM (2005) Cryopreserved liver cell transplantation controls ornithine transcarbamylase deficient patient while awaiting liver transplantation. Am J Transplant 5:2058–2061

Stéphenne X, Najimi M, Sibille C, Nassogne MC, Smets F, Sokal EM (2006) Sustained engraftment and tissue enzyme activity after liver cell transplantation for argininosuccinate lyase deficiency. Gastroenterology 130:1317–1323

Stephenne X, Nicastro E, Eeckhoudt S et al (2012) Bivalirudin in combination with heparin to control mesenchymal cell procoagulant activity. PLoS One 7:e42819

Uchino T, Endo F, Matsuda I (1998) Neurodevelopmental outcome of long-term therapy of urea cycle disorders in Japan. J Inherit Metab Dis 21(Suppl 1):151–159

Yudkoff M, Ah Mew N, Daikhin Y et al (2010) Measuring in vivo ureagenesis with stable isotopes. Mol Genet Metab 100(Suppl 1): S37–S41<

JIMD Reports
DOI 10.1007/8904_2013_258

RESEARCH REPORT

Distribution and Severity of Neuropathology in β-Mannosidase-Deficient Mice is Strain Dependent

Kathryn L. Lovell · Mei Zhu · Meghan C. Drummond · Robert C. Switzer III · Karen H. Friderici

Received: 10 May 2013 / Revised: 17 July 2013 / Accepted: 12 August 2013 / Published online: 20 October 2013

Abstract Neurological dysfunction is common in humans and animals with lysosomal storage diseases. β-Mannosidosis, an autosomal recessive inherited disorder of glycoprotein catabolism caused by deficiency of the lysosomal enzyme β-mannosidase, is characterized by intracellular accumulation of small oligosaccharides in selected cell types. In ruminants, clinical manifestation is severe, and neuropathology includes extensive intracellular vacuolation and dysmyelination. In human cases of β-mannosidosis, the clinical symptoms, including intellectual disability, are variable and can be relatively mild. A β-mannosidosis knockout mouse was previously characterized and showed normal growth, appearance, and lifespan. Neuropathology between 1 and 9 months of age included selective, variable neuronal vacuolation with no hypomyelination. This study characterized distribution of brain pathology in older mutant mice, investigating the effects of two strain backgrounds. Morphological analysis indicated a severe consistent pattern of neuronal vacuolation and disintegrative degeneration in all five 129X1/SvJ mice. However, the mice with a mixed genetic background showed substantial variability in the severity of pathology. In the severely affected animals, neuronal vacuolation was prominent in specific layers of piriform area, retrosplenial area, anterior cingulate area, selected regions of isocortex, and in hippocampus CA3. Silver degeneration reaction product was prominent in regions including specific cortical layers and cerebellar molecular layer. The very consistent pattern of neuropathology suggests metabolic differences among neuronal populations that are not yet understood and will serve as a basis for future comparison with human neuropathological analysis. The variation in severity of pathology in different mouse strains implicates genetic modifiers in the variable phenotypic expression in humans.

Communicated by: Ashok Vellodi

Competing interests: None declared

K.L. Lovell (✉)
Department of Neurology and Ophthalmology, Michigan State University, 965 Fee Road, A502D East Fee Hall, East Lansing, MI 48824, USA
e-mail: lovell@msu.edu1

M. Zhu · M.C. Drummond · K.H. Friderici
Department of Microbiology and Molecular Genetics, Michigan State University, East Lansing, MI, USA

R.C. Switzer III
NeuroScience Associates, Knoxville, TN, USA

Introduction

β-Mannosidosis (OMIM 248510) is a rare lysosomal storage disease that was first identified in Nubian goats (Jones and Dawson 1981; Jones and Laine 1981; Jones et al. 1983) and later in Salers cattle (Abbitt et al. 1991; Bryan et al. 1993; Patterson et al. 1991) and humans (Alkhayat et al. 1998; Cooper et al. 1986; Wenger et al. 1986). This autosomal recessive inherited disorder of glycoprotein catabolism is caused by a deficiency of the lysosomal enzyme β-mannosidase (*MANBA*; EC 3.2.1.25, 609489). MANBA acts exclusively at the last step of oligosaccharide catabolism in glycoprotein degradation and functions to cleave the β-linked mannose sugar found in N-linked oligosaccharides of glycoproteins (Neufeld 1991; Winchester et al. 2000). β-Mannosidosis is characterized by the intracellular accumulation of small oligosaccharides (mainly disaccharides and trisaccharides) in selected cell types (Jones and Laine 1981). In human cases of β-mannosidosis, the clinical symptoms, including intellectual disability, are relatively mild and are variable,

even in patients with null mutations (Bedilu et al. 2002); however, little is known about the pathology of the disease. In contrast, the two ruminant animal models (goats and cows) have a severe clinical presentation at birth (Jones et al. 1983; Abbitt et al. 1991) and pathology includes extensive regionally variable myelin deficits as well as widespread cytoplasmic vacuolation (Patterson et al. 1991; Lovell and Jones 1983,1985).

A mouse model of β-mannosidosis was created by targeted disruption of the β-mannosidase gene by homologous recombination in 129X1/SvJ ES cells (Zhu et al. 2006). Homozygous mutant animals had the expected enzyme deficiency and had accumulation of disaccharide in brain tissue, but showed normal growth, appearance, and lifespan. Previous examination of mutant animals between 1 and 9 months of age showed selective, variable neuronal vacuolation with no hypomyelination, closer to what would be expected in the human β-mannosidosis phenotype given the human clinical presentation. Cell populations identified with variable vacuolation included pyramidal cells (layer V) in dorsolateral cortex, choroid plexus, specific segments of Ammon's horn, striatum, amygdala, deep cerebellar nuclei, and spinal cord (Zhu et al. 2006).

This study was designed to define the distribution and severity of central nervous system (CNS) pathology in the isocortex and allocortex of older mice, and to determine if there are phenotypic or pathologic differences based on the clone or background of the animals. This study characterized the distribution of brain pathology in mutant mice between the ages of 15 and 20 months, investigating the effects of two different embryonic stem cell (ES) clones and two strain backgrounds: 129X1/SvJ congenic and mixed C57BL/6J x 129X1/SvJ.

Methods

Animals

A β-mannosidosis knockout mouse was produced by targeted disruption of the β-mannosidosis gene (Zhu et al. 2006). The congenic line, labeled "sv129" in Table 1, was generated by backcrossing the chimeras from the transgenic 129X1/SvJ ES cells (clone A2) to 129X1/SvJ mice. The line labeled "mixed" in Table 1 was generated by backcrossing the chimeras from the transgenic 129X1/SvJ ES cells (clones A2 and B2) to C57BL/6J mice, leading to F1 animals with mixed strain background. The resulting F1 mice of a mixed 129X1/SvJ:C57Bl/6J background were intercrossed to generate homozygotes in the F2 generation. All of the homozygous knockout mice (of both clones and both strains) lacked β-mannosidase enzyme activity and showed similar patterns of storage material (Zhu et al. 2006). This study utilized 21 homozygous mutant mice and 4 wild-type (WT) mice between the ages of 15 and 20 months. See Table 1 under Results for the age and strain for each mouse.

All animal experiments were approved by the Institutional Animal Care and Use Committee at Michigan State University and were in accordance with the NIH Guide to the Humane Care of Laboratory Animals.

Embedding, Sectioning, and Staining

Animals were perfused transcardially with 4% paraformaldehyde. Following removal from the skull, brains were placed in 4% paraformaldehyde for 24 h, and then transferred to cacodylate storage buffer. Brains were embedded in a 5×5 array in a gelatin matrix using MultiBrain Technology (NeuroScience Associates, Knoxville, TN) as reported in previous studies (Fix et al. 1996; Ong et al. 2001). The block of embedded brains was frozen and sectioned coronally at 30 μm beginning at the olfactory bulb and proceeding to the medulla. A serial set of every sixth section was selected for staining with hematoxylin and eosin (H&E), with Weil myelin stain, and with amino cupric silver stain to reveal disintegrative degeneration (Ong et al. 2001). A few selected sections were subjected to Nissl staining, GFAP staining for astrocytes, or Iba1 staining for microglia.

Since each of the large sections cut from the block was a composite section holding individual sections from each of the brains embedded in each block, uniformity of staining was achieved across normal and mutant mice. Sections at each level were analyzed for the distribution and extent of pathology as seen in each type of stain.

Morphological Analysis

Sections from all animals at all levels were analyzed to determine the overall characteristics and severity of pathology. Charts using a 5×5 grid were developed to record observations on each section at each level without regard to status of strain or clone. The type and extent of the pathology in each structure was recorded. Severity was classified as mild, mild/variable, and severe by characterizing the extent of vacuolation or degeneration staining in specific regions. For those regions where pathology was observed in any of the animals, "severe" indicated that vacuoles or degeneration staining were prominent in all of the affected regions. "Mild" indicated less prominent pathology in those regions. "Mild/variable" indicated that mild pathology was present in some regions, but in some regions, no pathology was apparent. After the variation in severity was determined, selected sections were analyzed in greater detail to record the precise location of vacuolation and degeneration staining in each severely affected mouse.

Table 1 Summary of characteristics and outcomes (severity of pathology)

ID number	Age (mo)	Sex	Status	Strain	Clone	Vacuolation	Degeneration stain
127	20	M	WT	Mixed	A2	None	None
365	15	M	WT	Mixed	A2	None	None
272	18	F	WT	sv129	A2	None	None
352	16	F	WT	sv129	A2	None	None
104	20	F	Mutant	Mixed	A2	Mild/variable	None
106	20	F	Mutant	Mixed	A2	Mild/variable	None
131	20	F	Mutant	Mixed	A2	Mild	None
149	19	F	Mutant	Mixed	A2	Mild	None
150	19	F	Mutant	Mixed	A2	Mild	Mild
209	19	F	Mutant	Mixed	A2	None	None
154	19	F	Mutant	Mixed	B2	Mild	None
155	19	F	Mutant	Mixed	B2	Mild	Mild
160	19	F	Mutant	Mixed	B2	Mild/variable	Mild
169	19	M	Mutant	Mixed	B2	Mild	Mild
177	19	M	Mutant	Mixed	B2	Mild	Mild
361	15	F	Mutant	Mixed	A2	Mild/variable	Mild/variable
366	15	F	Mutant	Mixed	A2	Mild/variable	None
371	15	F	Mutant	Mixed	A2	Severe	Severe
376	15	F	Mutant	Mixed	A2	Mild/variable	None
386	15	F	Mutant	Mixed	A2	None	None
262	18	F	Mutant	sv129	A2	Severe	Severe
264	18	F	Mutant	sv129	A2	Severe	Severe
342	16	F	Mutant	sv129	A2	Severe	Severe
348	16	M	Mutant	sv129	A2	Severe	Severe
349	16	F	Mutant	sv129	A2	Severe	Severe

See Methods for description of mild, mild/variable, and severe classifications

Results

Overall Severity of Pathology Analyzed by Strain and Clone

Table 1 provides a summary of the age and strain for each mouse, indicating the overall severity of vacuolation and degeneration staining. Analysis indicated a severe consistent pattern of neuronal vacuolation and disintegrative degeneration in all five 129X1/SvJ mice (clone A2). However, the mixed background mice (A2 and B2 clones) showed substantial variability in the severity of pathology (Table 1). There was no discernible difference related to the ES clone. In the severely affected animals (all 129X1/SvJ mutant mice, one mixed background mouse), neuronal vacuolation was prominent in a consistent pattern. Thus, the background strain was an important factor in determining the phenotype of the CNS pathology.

Distribution of Vacuolation

The vacuole distribution at four selected levels is shown diagrammatically in Fig. 1. In general, vacuolation consistently occurred in specific layers of piriform cortex, retrosplenial cortex, anterior cingulate cortex, some dorsal and lateral cortical regions, and in hippocampus. The structures involved are illustrated and will be discussed as labeled in the Allen Mouse Brain Atlas (http://mouse.brain-map.org/). In the dorsal hippocampus, the only neurons showing vacuolation were pyramidal cells in the dorsal aspect of CA3 (Fig. 1c), in a narrow region at the junction of CA3 and CA2. An example of the specificity of the vacuolation is demonstrated in Fig. 2b,g in HE-stained and Weil-myelin-stained sections. In the medial isocortex, vacuolation was prominent in neurons of the anterior cingulate cortex (rostrally) and the retrosplenial cortex (caudally) (Fig. 2b,e,f). In the retrosplenial cortex, the

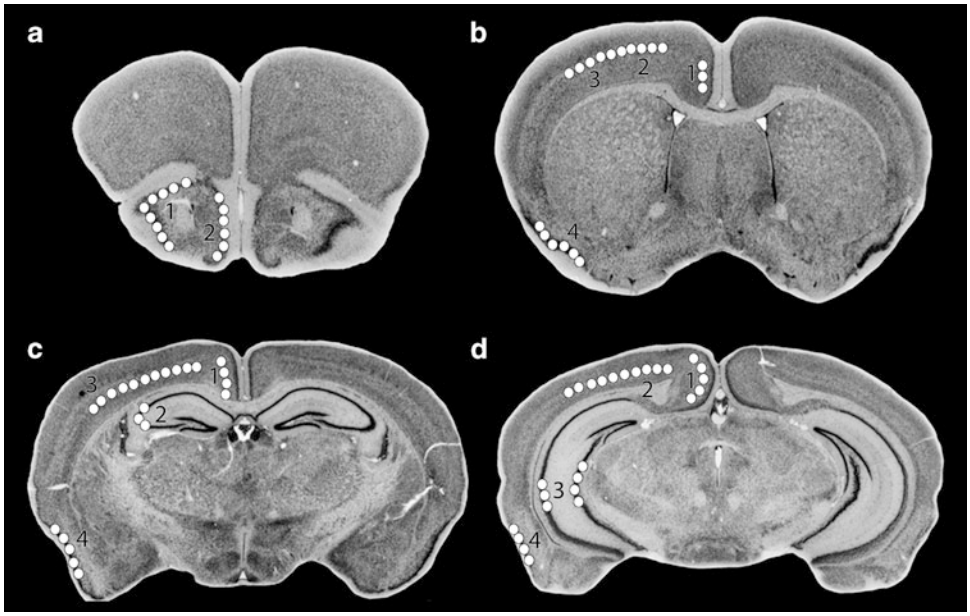

Fig. 1 Structures showing prominent vacuolation at four levels of coronal sections. Diagrams are from The Mouse Brain Library DBA2J atlas (www.mbl.org). Regions with consistent vacuolation are shown by white circles on one side of the brain; all lesions are bilaterally symmetric. Regions involved include: *1* – molecular layer of piriform area, *2* – layer 2 of taenia tecta (**a**); *1* – anterior cingulate cortex, *2* – layer 5 of primary motor area, *3* – layer 5 of primary somatosensory area, 4 – molecular layer of piriform area (**b**); *1* – retrosplenial cortex, *2* – hippocampus CA3, *3* – layer 5 of primary motor, somatosensory, visual cortex, *4* – piriform area (**c**); *1* – retrosplenial cortex, *2* – layer 5 of visual cortex, *3* – parts of hippocampus including part of CA3, *4* – piriform area (**d**)

vacuolation appeared more dense in the ventral retrosplenial cortex compared to the dorsal retrosplenial cortex and lateral agranular part, resulting in an apparent gap (Fig. 1c,d; Fig. 2b,f) between the vacuolation in medial cortex and in dorsal cortex. A similar gap is seen more rostrally (Fig. 1b), with vacuolation more prominent in the ventral anterior cingulate cortex than in the dorsal anterior cingulate cortex. In Fig. 1b,c,d and Fig. 2b,e,f, the prominent vacuolation in regions of dorsal and lateral cortex is illustrated. With respect to layers showing vacuolation, it appeared that in the medial cortex, neurons in layers 4–5 contained vacuoles, while vacuolation was prominent in layer 5 of dorsal and lateral cortex. The vacuoles were intraneuronal, as illustrated in Fig. 2d, and previously demonstrated with 1μ thick toluidine-blue-stained plastic sections and electron microscopy (Zhu et al. 2006).

Distribution of Degeneration Staining

A consistent pattern of silver reaction product was observed only in the same β-mannosidosis mutants that showed substantial vacuolation. In the cerebellar molecular layer, large numbers of silver-stained puncta consistent with degenerating nerve terminals were observed, with variation among folia in the intensity of staining (Fig. 2i,j). No neuronal abnormalities were observed in inferior olivary nuclei (source of projection of climbing fibers to the cerebellar cortex). In the region dorsal to the hippocampus, silver-stained puncta over a linear area were observed (Fig. 2k); the most intense staining of puncta occurred in deep layers of cortex adjacent to the corpus callosum/external capsule. Mild linear wisps were present in the corpus callosum, but these were also present to some extent in the control sections.

Discussion

Lysosomal storage diseases involve dysfunction of one of the more than 50 enzymes in the lysosome, resulting in the accumulation of the associated uncatabolized substrate (Neufeld 1991; Winchester et al. 2000) or toxic intermediates (Suzuki et al. 2003). A majority of lysosomal storage diseases affect the CNS and disease presentation can range from severe and consistent to mild and variable depending on the enzyme involved, the severity of the mutation, and the species concerned. In addition, the genetic mutations may trigger complex pathogenic cascades (Walkley 2009; Lieberman et al. 2012). For example, interference with signaling events and salvage processing normally controlled by the endosomal/lysosomal system and/or effects on autophagy may represent key mechanisms accounting for the inherent complexity of lysosomal disorders.

Goats and cattle affected with β-mannosidosis have very similar severe clinical features, and affected animals die in

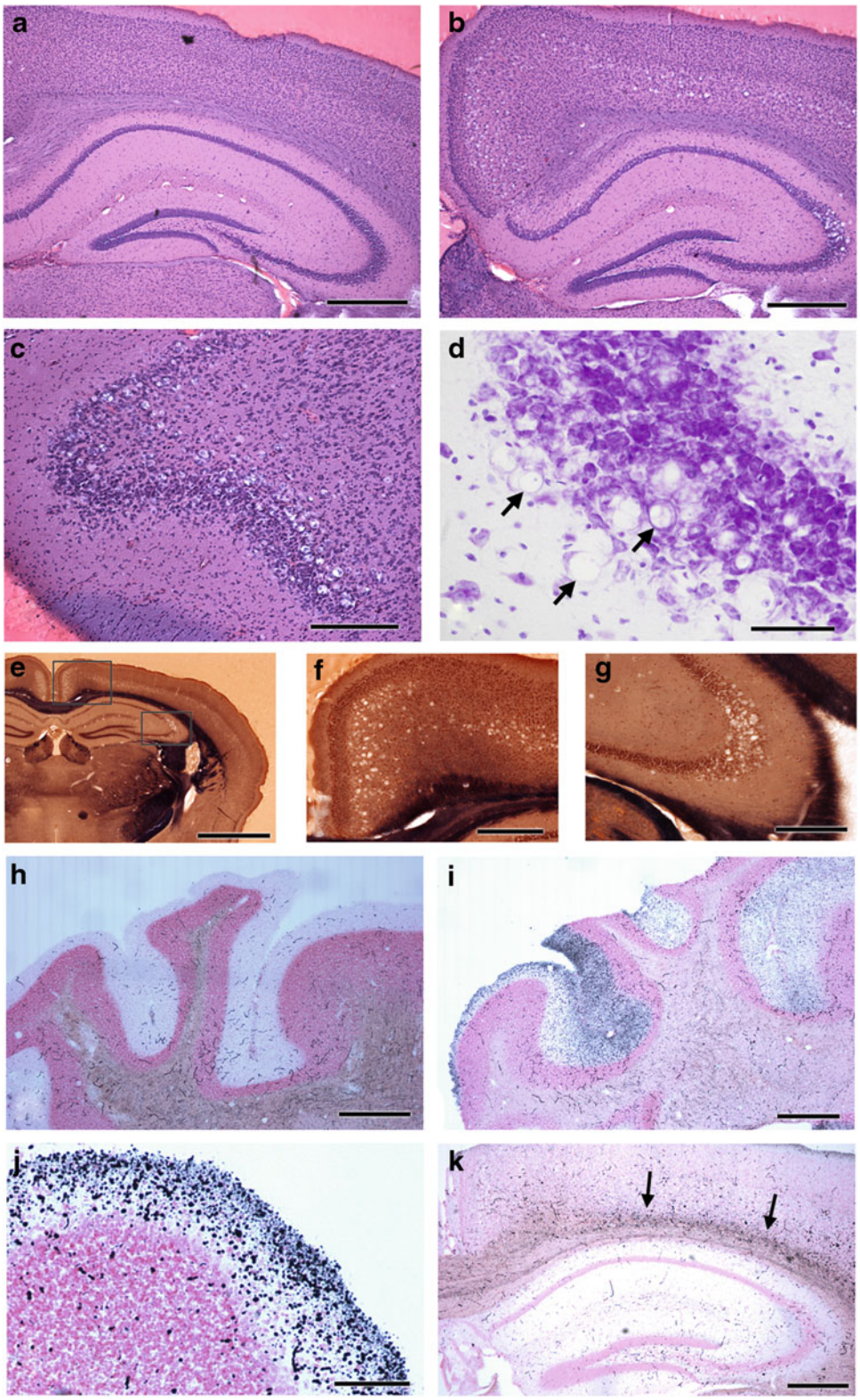

Fig. 2 Examples of pathology in selected locations in HE-stained sections (**a**–**d**), Weil-myelin-stained sections (**e**–**g**), and amino cupric silver–stained sections (h-k). Extensive vacuolation is present in hippocampus CA3, retrosplenial cortex, and cerebral cortex layer 5 in an affected mouse (**b**) compared to a control mouse (**a**). Vacuolation is prominent in piriform area in frontal lobe (**c**). Enlargement of vacuoles in part of hippocampus CA3 in Nissl stain reveals intracytoplasmic vacuoles; arrows indicate cells where a flattened nucleus is visible adjacent to a vacuole (**d**). Low-magnification view of one hemisphere (**e**) demonstrates restricted locations of vacuoles in cortex and hippocampus, with higher magnification views, indicated by rectangles, showing vacuolation in retrosplenial cortex and cerebral cortex layer 5

the neonatal period if intensive care is not provided (Jones et al. 1983; Abbitt et al. 1991). Microscopic examination reveals extensive cytoplasmic vacuolation in specific cell types of the nervous system and visceral organs. The storage material does not stain with PAS and appears clear in electron microscopic examination. Regionally specific myelin deficiency is present in the CNS but not in peripheral nerves (Jones et al. 1983; Lovell and Jones 1983; Boyer et al. 1990). In contrast with ruminant β-mannosidosis, human cases have a milder and heterogeneous clinical expression, even when caused by functionally null mutations (Alkhayat et al. 1998; Bedilu et al. 2002; Cooper et al. 1990). The most severe cases are associated with intellectual disability, developmental delay, dysmorphology, frequent infections, and hearing loss. None of the human cases showed clinical signs that would indicate CNS hypomyelination. Little is known about the distribution of storage material or the severity of tissue vacuolation. Mutant β-mannosidase-deficient mice (Zhu et al. 2006) had normal growth, appearance, and lifespan, and no hypomyelination, closer to the human β-mannosidosis phenotype than the ruminant phenotype.

Reasons for the phenotypic differences among mouse, human, and ruminant β-mannosidosis are unknown, but speculation has centered on differences in the size and nature of the storage product and on the different developmental programs of the species (Cooper et al. 1990). In the lysosome, *N*-linked glycoproteins are degraded sequentially from the nonreducing end of the molecule. The β-mannoside linkage is unique to *N*-linked glycoproteins; therefore, unlike most other lysosomal enzymes, β-mannosidase has only a single substrate in the cell. In humans and rodents, the nonsequential cleavage of the terminal GlcNAc(β1-4)GlcNAc bond of the carbohydrate moiety of glycoprotein can be accomplished by chitobiase (ctbs), resulting in storage of disaccharide, Man(β1-4)GlcNAc (vanPelt et al. 1990; Winchester 2005). In ruminants, there is very low expression of chitobiase (Zhu et al. 2006; Aronson and Kuranda 1989) and storage of the trisaccharide Man(β1-4)GlcNAc(β1-4)GlcNAc predominates; novel complex oligosaccharides also accumulate (Jones and Laine 1981; Matsuura and Jones 1985). Cloning of the chitobiase gene (Balducci et al. 2008) permits the construction of a double β-mannosidase and chitobiase knockout mouse, to determine if the storage product is the trisaccharide, as in ruminants, and assess the clinical phenotype. There may also be other factors involved in the neuropathology mechanisms in different species.

In the β-mannosidase-deficient mice, there was considerable variation among two strains of mice in the severity of neuropathology as illustrated in Table 1. There was a consistent pattern of neuronal vacuolation and disintegrative degeneration in all five 129X1/SvJ mice. However, the mixed background mice showed substantial variability in the severity of pathology. The variability in severity for C57BL/6J mice is greater than in the examination of 9-month-old mice (Zhu et al. 2006); in that study, the majority of C57BL/6J mice had moderate to severe vacuolation. The influence of genetic background on knockout mouse phenotypes is well documented and can present itself as completely different phenotypes, as variations in penetrance of phenotype, or as variable expressivity of phenotype (Sanford et al. 2001). Modifier genes (Sanford et al. 2001) and/or biological robustness (Barbaric et al. 2007) may play a role in these effects, and such modifying factors may be epistatic, epigenetic, or of other origins. In β-mannosidosis, the variation in the pathology depending on genetic background indicates modifier factors are involved. One hypothesis is that protective factor(s) in the mixed strain mice, variable among animals, modifies the disease expression and determines differential susceptibility to phenotypic features such as neuronal vacuolation. Similar factors may be involved in the tremendous clinical heterogeneity among the small number of patients with β-mannosidosis, including intrafamilial variation and variation among patients with null mutations (Alkhayat et al. 1998). Thus, for future studies of this animal model, it will be important to use the congenic 129X1/SvJ strain (or characterize the phenotype in a different uniform genetic background). Identification of factors that modify the disease expression may help clarify the pathogenetic mechanisms involved in this or other lysosomal storage diseases.

In those mutant mice showing vacuolation, the locations of neuronal vacuoles were very consistent, including piriform area, taenia tecta, part of hippocampus CA3 (consistent in dorsal hippocampus but not ventral hippocampus), retrosplenial area, parts of anterior cingulate area and entorhinal cortex, and layer V in primary motor cortex, primary somatosensory cortex, primary visual cortex, and posterior parietal association cortex.

(**f**) and part of hippocampus CA3 (**g**). The absence of cupric silver reaction product in control cerebellum molecular layer, except for red blood cells in vessels (**h**) contrasts with reaction product in a section of cerebellum from an affected mouse showing degeneration staining in the molecular layer, variable among folia (**i**). Large numbers of silver-stained puncta consistent with degenerating nerve terminals were observed in some folia (**j**). Localized degeneration staining was consistently observed in deep layers of cerebral cortex of affected mice (**k**). Scale bars and mouse ID numbers for each image: a-300 μm, #352; b-300 μm, #262; c-250 μm, #264; d-20 μm, #349; e- 900 μm, #348; f – 275 μm, #348; g-200 μm, #349; h-520 μm, #352; i-520 μm, #348; j-250 μm, #349; k-420 μm, #262

The variation in vacuolation in the hippocampus may be related to multiple divisions identified by genetic and metabolic characteristics (Fanselow and Dong 2010; Thompson et al. 2008). The piriform area and taenia tecta are part of the olfactory system. The retrosplenial area is part of a network of brain regions that participates in a range of cognitive functions, including episodic memory and navigation. The entorhinal cortex mainly projects to the hippocampus, including both CA3 and CA1. The anterior cingulate area plays a role in emotional and attentive responses to internal and external stimulation. The pyramidal neurons in layer V of cerebral cortex integrate input and project to many other parts of the CNS. It is possible that the pattern of vacuolation seen in mouse β-mannosidosis would contribute to the intellectual disability and emotional changes reported in human cases. However, it is not clear why only these specific neuronal populations show vacuolation. In other lysosomal storage disorders, different, but disease-specific, patterns of neuropathology are characteristic. For example, α-mannosidosis (OMIM 248500), caused by mutations in the α-mannosidase (MAN2B1, EC 3.2.1.24, 609458) gene, has been described in cats, cattle, guinea pigs, humans, and knockout mice (Auclair and Hopwood 2007; Blanz et al. 2008; Crawley and Walkley 2007; Damme et al. 2011; Stinchi et al. 1999; Vite et al. 2001) and has somewhat different neurological manifestations and neuropathological characteristics depending on the species. Aspartylglucosaminuria (AGU, OMIM 208400) (Dunder et al. 2010; Jalanko et al. 1998; Kaartinen et al. 1996) is caused by mutations in the gene for glycosylasparaginase (AGA, EC 3.5.1.26, 613228), the enzyme necessary for hydrolysis of the protein-oligosaccharide linkage in N-linked glycoproteins. Glycosylasparaginase deficiency results in accumulation of glycoasparagines, such as aspartylglucosamine (GlcNAc-Asn), a small molecule that may be analogous to Man(β1-4)GlcNAc. In the AGU mouse model (Jalanko et al. 1998; Kaartinen et al. 1996), CNS vacuolation is prominent in neurons and astrocytes of cortical and subcortical gray matter. Further understanding of the different patterns of pathology may lead to delineation of specific metabolic characteristics of subsets of neurons that are not currently understood. Cognitive or behavioral deficits have been identified in α-mannosidosis and AGU knockout mice, and correlate with CNS pathology. Both animal models have been used successfully to explore therapeutic strategies to improve brain function (Blanz et al. 2008; Damme et al. 2011; Dunder et al. 2010).

In order to investigate a potential correlation between vacuolation and level of enzyme activity in β-mannosidosis, the distribution of lesions was compared with the distribution of mouse brain lysosomal β-mannosidase in situ hybridization and expression analysis as shown in the Allen Brain Atlas (Lein et al. 2007). There was no consistent correlation, although CA3 showed higher expression than other hippocampal regions. Some areas that were vacuolated did not show increased expression, and some regions with higher expression (e.g., Purkinje cells in cerebellum) did not show vacuolation. In general, β-mannosidase has very low expression throughout the CNS in mice (Lein et al. 2007) and in goats (Boyer et al. 1990; Lovell et al. 1994) compared to that of other glycoprotein catabolic enzymes. There is no apparent consistent correlation among gene expression, enzyme activity, and severity of vacuolation. There could be differences in levels of substrate, leading to vacuolation in cells with higher levels of substrate or other metabolic variations among brain regions. Production of antibodies to the enzyme and/or substrate would allow investigations of metabolic differences between neuronal and glial populations.

In β-mannosidosis mice, silver reaction product indicating neuronal degeneration was prominent only in the mutant mice that had severe vacuolation, suggesting that it is a consistent part of the neuropathology expression in this disease. The pattern of degeneration staining was very consistent among animals, and occurred mainly in cerebellar molecular layer and in cortical regions dorsal to the hippocampal formation (Fig. 2). Degeneration staining did not occur in areas of vacuolation or adjacent regions, suggesting that vacuolation does not lead to substantial cell body or axon loss. Further studies will be necessary to elucidate the mechanisms that lead to the degeneration staining in specific regions; results will provide new information about specific types of cellular pathophysiology. Preliminary staining of selected sections with GFAP for astrocytes and Iba1 for microglia showed some degree of reactivity in regions with vacuolation, but did not provide any additional information related to pathophysiology (data not shown).

In summary, a β-mannosidase knockout mouse model was utilized to characterize CNS pathology in mice with different strain backgrounds. The consistency of distribution of lesions in a congenic strain 129X1/SvJ reinforces the potential of this model for investigating treatment strategies important for brain function. The variation in pathology depending on genetic background indicates the complex nature of interactions that may determine the extent of cellular abnormalities and phenotypic expression. Animal models are important in the clarification of the pathophysiology/pathogenetic mechanism of disease (Suzuki et al. 2003) as well as giving insight into normal physiology and metabolism. Further investigation of the specific patterns of vacuolation and other pathology in this and related lysosomal storage diseases will lead to better understanding of specific metabolic characteristics among populations of neurons.

Acknowledgments Processing and staining of mouse brains was generously provided by NeuroScience Associates. This work was supported by NIDDK grant DK49782 from the National Institutes of Health to KHF, and by Michigan State University Foundation grant to KHF and KLL.

Synopsis

In β-mannosidosis, the neuronal pathology observed in mice is consistent with the intellectual disability displayed in human cases, and the variation among different strains implicates genetic modifiers in variable phenotypic expression.

Author Who Serves as Guarantor

Kathryn L. Lovell, Ph.D.

Details of Funding

Processing and staining of mouse brains was generously provided by NeuroScience Associates. This work was supported by NIDDK grant DK49782 from the National Institutes of Health to KF, and by Michigan State University Foundation grant to KF and KL.

Compliance with Ethics Guidelines

Conflict of Interest

Kathryn Lovell, Mei Zhu, Meghan Drummond, Robert Switzer, and Karen Friderici declare that they have no conflict of interest. The authors confirm independence from the sponsors; the content of the article has not been influenced by the sponsors.

Informed Consent

Informed consent: not required. This article does not contain any studies with human subjects performed by any of the authors.

Use of Vertebrate Animals

All institutional and national guidelines for the care and use of laboratory animals were followed.

Details of the Contributions of Individual Authors

KLL: designed the study, participated in perfusion and brain removal, analyzed results to generate distribution of pathology, took a lead role in writing the manuscript.

MZ: produced the mutant mice, bred them for the current experiments, responsible for perfusion and brain removal, participated in writing the manuscript.

MCD: assisted with breeding mice, assisted with analysis of data, participated in writing the manuscript.

RCS: processed the brains for sectioning and staining, participated in photography and analysis of results, participated in writing the manuscript.

KHF: supervised production of the mutant mice and breeding, participated in writing the manuscript.

References

Abbitt B, Jones MZ, Kasari TR et al (1991) Beta-mannosidosis in twelve Salers calves. J Am Vet Med Assoc 198:109–113

Alkhayat AH, Kraemer SA, Leipprandt JR, Macek M, Kleijer WJ, Friderici KH (1998) Human beta-mannosidase cDNA characterization and first identification of a mutation associated with human beta-mannosidosis. Hum Mol Genet 7:75–83

Aronson NN Jr, Kuranda MJ (1989) Lysosomal degradation of Asn-linked glycoproteins. FASEB J 3:2615–2622

Auclair D, Hopwood JJ (2007) Morphopathological features in tissues of alpha-mannosidosis guinea pigs at different gestational ages. Neuropathol Appl Neurobiol 33:572–85

Balducci C, Bibi L, Berg T et al (2008) Molecular cloning and structural organization of the gene encoding the mouse lysosomal di-N-acetylchitobiase (ctbs). Gene 416:85–91

Barbaric I, Miller G, Dear TN (2007) Appearances can be deceiving: phenotypes of knockout mice. Brief Funct Genomic Proteomic 6:91–103

Bedilu R, Nummy KA, Cooper A et al (2002) Variable clinical presentation of lysosomal beta-mannosidosis in patients with null mutations. Mol Genet Metab 77:282–290

Blanz J, Stroobants S, Lüllmann-Rauch R et al (2008) Reversal of peripheral and central nervous storage and ataxia after recombinant enzyme replacement therapy in alpha-mannosidosis mice. Hum Mol Genet 17:3437–3445

Boyer PJ, Jones MZ, Rathke EJS, Truscott NK, Lovell KL (1990) Regional central nervous system oligosaccharide storage in caprine beta-mannosidosis. J Neurochem 55:660–664

Bryan L, Schmutz S, Hodges SD, Snyder FF (1993) Bovine beta-mannosidosis: pathologic and genetic findings in Salers calves. Vet Pathol 30:130–139

Cooper A, Sardharwalla IB, Roberts MM (1986) Human beta-mannosidase deficiency. N Engl J Med 315:1231

Cooper A, Hatton CE, Thornley M, Sardharwalla IB (1990) Alpha- and beta-mannosidoses. J Inherit Metab Dis 13:538–548

Crawley AC, Walkley SU (2007) Developmental analysis of CNS pathology in the lysosomal storage disease alpha-mannosidosis. J Neuropathol Exp Neurol 66:687–697

Damme M, Stroobants S, Walkley SU et al (2011) Cerebellar alterations and gait defects as therapeutic outcome measures for enzyme replacement therapy in alpha-mannosidosis. J Neuropathol Exp Neurol 70:83–94

Dunder U, Valtonen P, Kelo E, Mononen I (2010) Early initiation of enzyme replacement therapy improves metabolic correction in

the brain tissue of aspartylglycosaminuria mice. J Inherit Metab Dis 33:611–617
Fanselow MS, Dong H-W (2010) Are the dorsal and ventral hippocampus functionally distinct structures? Neuron 65:7. doi:10.1016/j.neuron.2009.11.031
Fix AS, Ross JF, Stitzel SR, Switzer RC (1996) Integrated evaluation of central nervous system lesions: stains for neurons, astrocytes, and microglia reveal the spatial and temporal features of MK-801-induced neuronal necrosis in the rat cerebral cortex. Toxicol Pathol 24:291–304
Jalanko A, Tenhunen K, McKinney CE et al (1998) Mice with an aspartylglucosaminuria mutation similar to humans replicate the pathophysiology in patients. Human Molec Genet 7:265–272
Jones MZ, Dawson G (1981) Caprine beta-mannosidosis: inherited deficiency of beta-D-mannosidase. J Biol Chem 256:5185–5188
Jones MZ, Laine RA (1981) Caprine oligosaccharide storage disease accumulation of beta-mannosyl (1–4) beta-N-acetylglucosaminyl (1–4) beta-N-acetylglucosamine in brain. J Biol Chem 256:5181–5184
Jones MZ, Cunningham JG, Dade AW et al (1983) Caprine beta-mannosidosis: clinical and pathological features. J Neuropathol Exp Neurol 42:268–285
Kaartinen V, Mononen I, Voncken JW (1996) A mouse model for the human lysosomal disease aspartylglycosaminuria. Nat Med 2:1375–1378
Lein ES, Hawrylycz MJ, Ao N et al (2007) Genome-wide atlas of gene expression in the adult mouse brain. Nature 445:168–176
Lieberman AP, Puertollano R, Raben N, Slaugenhaupt S, Walkley SU, Ballabio A (2012) Autophagy in lysosomal storage disorders. Autophagy 8:719–730
Lovell KL, Jones MZ (1983) Distribution of central nervous system lesions in beta-mannosidosis. Acta Neuropathol 62:121–126
Lovell KL, Jones MZ (1985) Axonal and myelin lesions in beta-mannosidosis: ultrastructural characteristics. Acta Neuropathol 65:293–299
Lovell KL, Kranich RJ, Cavanagh KT (1994) Biochemical and histochemical analysis of lysosomal enzyme activities in caprine beta-mannosidosis. Molec Chem Neuropath 21:61–74
Matsuura F, Jones MZ (1985) Structural characterization of novel complex oligosaccharides accumulated in the caprine beta-mannosidosis kidney: Occurrence of tetra- and pentasaccharides containing a beta-linked mannose residue at the nonreducing terminus. J Biol Chem 260:15239–1524
Neufeld EF (1991) Lysosomal storage diseases. Annu Rev Biochem 60:257–280
Ong WY, Kumar U, Switzer RC et al (2001) Neurodegeneration in Niemann-Pick type C disease mice. Exp Brain Res 141:218–231
Patterson JS, Jones MZ, Lovell KL, Abbitt B (1991) Neuropathology of bovine beta-mannosidosis. J Neuropathol Exp Neurol 50:538–546
Sanford LP, Kallapur S, Ormsby M, Doetschman T (2001) Influence of genetic background on knockout mouse phenotypes. Gene Knockout Protocols, Methods in Molec Biol 158:217–225
Stinchi S, Lullmann-Rauch R, Hartmann D et al (1999) Targeted disruption of the lysosomal alpha-mannosidase gene results in mice resembling a mild form of human alpha-mannosidosis. Hum Mol Genet 8:1365–1372
Suzuki K, Ezoe T, Tohyama J, Matsuda J, Vanier MT, Suzuki K (2003) Are animal models useful for understanding the pathophysiology of lysosomal storage disease? Acta Paediatr Suppl 92:54–62
Thompson CL, Pathak SD, Jeromin A et al (2008) Genomic anatomy of the hippocampus. Neuron 60:1010–1021
vanPelt J, Hokke CH, Dorland L, Duran M, Kamerling JP, Vliegenthart JF (1990) Accumulation of mannosyl-beta(1–4)-N-acetylglucosamine in fibroblasts and leukocytes of patients with a deficiency of beta-mannosidase. Clin Chim Acta 187:55–60
Vite CH, McGowen JC, Braund KG et al (2001) Histopathology, electrodiagnostic testing, and magnetic resonance imaging show significant peripheral and central nervous system myelin abnormalities in the cat model of alpha-mannosidosis. J Neuropath Exp Neurol 60:817–828
Walkley SU (2009) Pathogenic cascades in lysosomal disease – Why so complex? J Inher Met Dis 32:181–189
Wenger DA, Sujansky E, Fennessey PV, Thompson JN (1986) Human beta-mannosidase deficiency. N Engl J Med 315:1201–1205
Winchester B (2005) Lysosomal metabolism of glycoproteins. Glycobiology 15:1R–15R
Winchester B, Vellodi A, Young E (2000) The molecular basis of lysosomal storage diseases and their treatment. Biochem Soc Trans 28:150–154
Zhu M, Lovell KL, Patterson JS, Saunders TL, Hughes ED, Friderici KH (2006) Beta-mannosidosis mice: a model for the human lysosomal storage disease. Human Molec Genetics 15:493–500

JIMD Reports
DOI 10.1007/8904_2013_260

RESEARCH REPORT

High Dietary Folic Acid and High Plasma Folate in Children and Adults with Phenylketonuria

Linn Helene Stølen · Rina Lilje · Jens Veilemand Jørgensen · Yngve Thomas Bliksrud · Runar Almaas

Received: 11 April 2013 / Revised: 21 August 2013 / Accepted: 29 August 2013 / Published online: 18 October 2013

Abstract **Background:** PKU patients on a strict low protein diet get most of their folic acid intake from protein substitute. Several protein substitutes contain high amounts of this vitamin. Concern has been raised about the safety of high levels of folic acid, especially in relation to cancer risk.

Methods: This cross-sectional study included 34 children and 22 adults with PKU. A dietary interview was performed and intake of folic acid and vitamin B12 from protein substitute was calculated for patients compliant with their protein substitute. Intakes of folic acid and vitamin B12 were compared with plasma levels of folate, vitamin B12, and homocysteine.

Results: Children aged 2–9 years had the highest intake of folic acid according to RDI (449 %), and children aged 7–10 years had the highest intake of folic acid according to UL (155 %). Median plasma folate level in PKU children was two times the upper reference level and in PKU adults well above. Children between 10 and 13 years had the highest level of plasma folate. Young children had both a high intake and high plasma levels of vitamin B12. Homocysteine levels were low or in the lower part of the normal reference range in most patients.

Conclusion: Children with PKU are at a particular risk of receiving folic acid high above RDI and many children with PKU receive doses above the UL. Many PKU patients have a very high level of plasma folate related to a very high content of folic acid in many of their protein substitutes.

Communicated by: Nenad Blau, PhD

Competing interests: None declared

L.H. Stølen (✉) · R. Lilje · J.V. Jørgensen · R. Almaas
Department of Paediatric Medicine, Women and Children's Division, Oslo University Hospital, Box 4950 Nydalen, 0424, Oslo, Norway
e-mail: lstolen@ous-hf.no1

Y.T. Bliksrud
Department of Medical Biochemistry, Division of Diagnostics and Intervention, Oslo University Hospital, Oslo, Norway

R. Almaas
Department of Pediatric Research, Women and Children's Division, Oslo University Hospital, Oslo, Norway

Introduction

Phenylketonuria (PKU) is a rare inborn error of metabolism resulting from deficient activity in the enzyme phenylalanine hydroxylase (PAH) that catalyzes the conversion of phenylalanine to tyrosine. Mainstay treatment of PKU is dietary restriction of phenylalanine and natural protein, to maintain blood phenylalanine in a nontoxic range. The diet is based on low phenylalanine foods, and natural protein is replaced by a phenylalanine-free protein substitute supplemented with tyrosine, vitamins, and other micronutrients. Supplementation of micronutrients thus seems necessary to prevent deficiencies. However, little is known about the optimal levels of micronutrients in the protein substitutes and their bioavailability.

We have observed that PKU patients, both children and adults, often have plasma folate levels above the reference range and also above cutoff levels for measurements. There are several commercial protein substitutes available containing different amounts of folic acid. For patients adhering with the low protein diet, the intake of folate from natural sources is minor compared to the amount obtained from protein substitutes (Wiig et al. 2013). The same is true for vitamin B12, as the diet allows very limited amounts of animal products (Wiig et al. 2013).

Folate is a cofactor for the synthesis of nucleic acids and required for cell division and growth. It is required for

DNA repair processes and increases DNA stability through methylation. Low folate status in pregnant women during the first trimester is associated with increased risk of neural tube defects (Smithells et al. 1976; Pitkin 2007). Concern about the need for folic acid supplementation in pregnancy is probably the reason why some protein substitutes are supplemented with higher amounts of folic acid. While a higher dietary intake of natural folate is linked with reduced cancer risk (Duthie 2011; Figueiredo et al. 2009), there are also reports that supplementation with synthetic folic acid actually increases cancer risk (Cole et al. 2007; Wien et al. 2012; Ebbing et al. 2009; Figueiredo et al. 2009), cancer mortality, and all-cause mortality (Ebbing et al. 2009).

Both high and low blood concentrations of folate and vitamin B12 have been reported in PKU patients compared to controls (Colome et al. 2003; Huemer et al. 2008; Schulpis et al. 2002). Colomé et al. found lower levels of homocysteine (hcy) concurrent with higher concentrations of folate and vitamin B12 (Colome et al. 2003), while Schulpis et al. found higher hcy levels and lower folate and vitamin B12 concentrations compared to controls (Huemer et al. 2008; Schulpis et al. 2002).

We wanted to compare intake of folic acid and vitamin B12 with plasma levels in children, adolescents, and adults with PKU using different types of protein substitutes to identify whether certain groups of PKU patients are at special risk of receiving either too much or too little folic acid. In particular, we wanted to address whether certain age groups are at special risk as vitamin requirements and intake levels of protein substitute are highly age dependent.

Subjects and Methods

The study protocol was approved by the institutional review board at Oslo University Hospital.

Subjects

Children below 18 years ($n = 34$) and adults ($n = 22$) with PKU coming for annual follow-up at Oslo University Hospital between June 2010 and June 2011 were included in this cross-sectional study.

This population includes 23 % of all patients diagnosed with PKU in Norway whereof seven were late-diagnosed patients. Patients on a phenylalanine-restricted diet compliant with their protein substitutes were included. Patients not on diet, on large neutral amino acid treatment, BH4-treatment, or taking supplements containing folic acid or vitamin B12 were excluded. Patients were classified as having classical PKU (Phe < 1,200 μmol/L), mild PKU (Phe 600–1,200 μmol/L), or mild hyperphenylalaninemia (MHPA) (Phe < 600 μmol/L) primarily based on pretreatment serum/blood phenylalanine concentrations. In Norway, MHPA patients with phenylalanine > 400 μmol/L are treated.

Calculation of Intake

Patients were interviewed about their habitual diet by a metabolic dietitian. Intake of folic acid, vitamin B12, and protein equivalents from protein substitute was calculated for all patients.

Patients used protein substitutes from SHS (XP Maxamaid, XP Maxamum, Lophlex/Lophlex LQ, PKMax, Anamix Junior), Vitaflo (PKU gel, PKU Express, PKU Cooler), and PreKUlab (Avonil). Protein substitutes were categorized into two groups: high folic acid (HighFA) protein substitutes with folic acid of 9.57–12.44 μg/g protein (XP Maxamaid, XP Maxamum, Lophlex/Lophlex LQ, PKMax) and lower folic acid (LowerFA) protein substitutes with folic acid of 3.1–6.7 μg/g protein (PKU gel, PKU Express, PKU Cooler, Anamix Junior, and Avonil).

Three to four days weighed dietary registrations were reviewed for a subgroup of children and adults. Folate intake from foods and intake of natural protein were calculated with "Mat på Data 5.1," a Norwegian food analysis program that uses data from the Norwegian Food Composition Database 2006 (The Norwegian Food Safety Authority and The Norwegian Directorate of Health & The University of Oslo 2006).

Blood Measurements

Blood samples were drawn fasting in the morning or at least 4 h fasting to measure plasma folate, vitamin B12, and total hcy at the time of the annual visit. Median serum phenylalanine levels from the last year were calculated.

Plasma folate was measured using the Roche Elecsys Folate III immunometric assay with a fully automated Roche Modular Analytics E170 immunoassay analyzer. Measuring range: 1.45–45.4 nmol/L. CV ≤ 10 % at 5 nmol/L, ≤ 7 % at 15.5 and 24 nmol/L. Samples with values above 45.4 nmol/L were diluted as described in the Roche manual 1:2 with Elecsys Diluent Universal. Plasma vitamin B12 was measured using the Roche Elecsys Vitamin B12 immunometric assay (Roche Modular Analytics E170). Measuring range: 22–1,476 pmol/L. CV ≤ 8 % at 146 pmo/L, ≤7 % at 428 pmol/L. Plasma total hcy was measured by an enzymatic assay using the Liquid Stable (LS) 2-Part Homocysteine Reagent with a fully automated Roche Modular P analyzer. Measuring range: 1–50 μmol/L. CV ≤ 5 % at 13.0 μmol/L, ≤4.5 % at 45.5μmol/L.

Serum phenylalanine was determined at the National Neonatal Screening Unit using tandem mass spectrometry.

Table 1 Artificial and natural protein intake according to recommendations in different age groups

	2–6 years	7–13 years	14–17 years	Adults
$N =$	10	15	13	22
Recommended total protein intake (g/kg/day)	2.0	1.5	1.0	1.0
Protein intake from substitute (g/day)	38.9 (33.6–52.5)	54 (31.5–80.6)	69.8 (59.8–90)	60 (41–81.4)
Protein intake from substitute (g/kg/day)	1.9 (1.4–2.4)	1.5 (0.8–2.6)	1.1 (0.7–1.4)	0.88 (0.47–1.6) *
Total protein intake (g/kg/day)**	2.2 (1.8–2.7)	1.8 (1.0–2.9)	1.2 (0.9–1.6)	NA

*$N = 21$. Protein intake is per actual weight, not corrected for overweight

Total protein intake is calculated from protein substitute and habitual daily phenylalanine exchanges. Total protein recommendations in PKU centers in Europe (g protein/kg/day) are **1–3 years: 2.5–3 g; **4–10 years:** 1.5–2 g; **11–16 years:** 1–1.5 g; > **16 years:** 1 g

Table 2 Plasma levels of folate, vitamin B12, and homocysteine according to reference levels

	Children	Adults	Reference level
$N =$	34	22	
Plasma folate (nmol/L)	63.5 (17–123)	45 (19–73.8)	11–30
Plasma B12 (pmol/L)	677 (376–2,280)	490 (246–838)	160–600
Plasma hcy (μmol/L)	4 (2–8)*	6 (4–10)	5–13 (♀), 6–16 (♂)

Hcy homocysteine

*$N = 32$

Statistical Analysis

Data are given as median (range). Mann–Whitney U test was used for comparison between groups and the Spearman test for correlations. Kruskal-Wallis test with Dunn's Multiple Comparison test was used for comparison between more than two groups. A two-tailed $p < 0.05$ was considered statistically significant. Statistical analyses were performed with the software PASW Statistics 18 and with GraphPad Instat version 03.10 for Windows (GraphPad Software Inc, San Diego, California).

Results

Patient Characteristics

A total of 34 children (18 males, 16 females) with a median (range) age of 9.9 (4.1–17.7) years and 22 adults (9 males, 13 females) with a median (range) age of 32 (18–57) years were included. Forty-six percent of the children had classical PKU, 37 % had mild PKU, and 17 % had MHPA. Among the adults, 59 % had classical PKU, 36 % had mild PKU, and 5 % had MHPA. All patients were treated with a phenylalanine-restricted diet and were compliant with a tyrosine-, vitamin-, and other micronutrient-enriched protein substitutes. Median (range) serum phenylalanine during the last year was 423 μmol/L (217–1,085) in children and 567 μmol/L (262–1,441) in adults. Table 1 shows protein intake from protein substitute according to recommendations.

Plasma Levels of Folate, Vitamin B12, and Homocysteine

Median plasma folate level in PKU children was more than two times the upper reference level and in PKU adults well above the upper reference level (Table 2). Ninety-one percent of children and 73 % of adults had plasma folate above the upper reference level. None had low plasma levels. Median plasma B12 level was slightly above the upper reference level in children and within range in adults. Fifty-three percent of children and 23 % of adults had plasma B12 levels above the upper reference level. Median plasma hcy was below the reference range in children and at the lower reference range in adults. Sixty-eight percent of children and 18 % of adults had plasma hcy below the reference range. None of the adults had plasma hcy above the reference range.

Intake of Folic Acid from Protein Substitute, Plasma Folate, and Homocysteine

Intake of folic acid from protein substitute was calculated for patients compliant with their protein substitute. Ninety-four percent of the children and 73 % of the adult patients had

Table 3 Intake of folic acid from protein substitute in relation to RDI, plasma folate, and homocysteine levels in different age groups

	2–5 years	6–9 years	10–13 years	14–17 years	Adults/men	Adults/women
$N =$	6	12	7	9	9	13
RDI*	80	130	200	300	300	400
Folic acid (μg/d)	359 (104–500)	571 (117–747)	700 (120–1,004)	747 (400–1,063)	750 (350–999)	525 (192–795)
Folic acid (% of RDI)	449 (130–625)	439 (100–575)	350 (60–502)	249 (133–354)	250 (117–333)	131 (48–199)
Plasma folate (nmol/L)	67 (28–73)	58 (38–67)	73 (17–123)	66 (30–78)	55 (29–66)	44 (19–74)
<ref level	0	0	0	0	0	0
>ref level	6	12	6	8	7	9
Plasma hcy (μmol/L)	4 (2–5)	4 (3–5)*	5 (3–6)**	5 (4–8)	7 (4–10)	6 (4–10)

RDI Recommended daily intake of folate in Nordic Nutrition Recommendations 2004, *Hcy* homocysteine

*$N = 11$

**$N = 6$

Table 4 Intake of folic acid from protein substitute in relation to Tolerable Upper Intake Level (UL) in different age groups

	4–6 years	7–10 years	11–14 years	15–17 years	Adults
$N =$	10	10	10	4	22
UL	300	400	600	800	1,000
Folic acid (μg/day)	300 (104–533)	618 (120–747)	774 (203–1,004)	484 (400–1,063)	660 (192–999)
Folic acid (% of UL)	100 (35–178)	155 (30–187)	129 (34–167)	60 (50–133)	66 (19–99.9)
% > UL	50	60	80	10	0

UL Tolerable Upper Intake Level of folic acid according to the European Commission's Scientific Committee on Food 2000, *% > UL* percent of patients with intake of folic acid from protein substitute above UL

intake of folic acid above the recommended daily intake (RDI) (Nordic Council of Ministers 2004a) (Table 3). One child (3 %) and three adults (14 %) had intakes of folic acid below the RDI. The three adults were using protein substitute tablets containing 4 μg folic acid/g protein. However, none of them had low plasma folate. Children aged 2–13 years had a median intake of folic acid 3.5–4.5 times higher than the RDI (Table 3). Fifty-nine percent of the children, but none of the adult patients, had intakes above the Tolerable Upper Intake Level (UL) (SCF 2000) (Table 4). Half of the children between 4 and 10 years and 80 % of children between 11 and 14 years had intakes of folic acid above the UL (Table 4).

All patients aged 2–13 years had plasma hcy below or at the lower reference range (Table 3). Adolescents between 14 and 17 years had plasma hcy below or in the lower reference range. Adults had plasma hcy slightly below or in the lower/middle reference range.

Folate Intake from Foods and Natural Protein Intake

Weighed dietary registrations in a subgroup of 7 children and 9 adults with a median (range) age of 14 (7–15) years and 31 (19–47) years showed a median (range) folate intake of 113 (94–202) μg folate/day among children and 177 (98–349) μg folate/day for adults. Natural protein intake was median (range) 12.8 (7.6–31.2) g/day for children and 34.8 (9.9–40.1) g/day for adults.

Plasma Levels of Folate According to Intake

High correlations between intake of folic acid from protein substitutes and plasma folate were found in both children ($rs = 0.643$, $p < 0.001$, $n = 34$) and adults ($rs = 0.77$, $p < 0.001$, $n = 26$).

Intake of Vitamin B12 from Protein Substitutes and Plasma Vitamin B12

Children 2–9 years of age had a median vitamin B12 intake of 358 % of the RDI (Table 5). Median intakes of vitamin B12 in children 10–17 years of age and adults were 283 and 270 % of the RDI (Nordic Council of Ministers 2004b). In the youngest age group, median plasma vitamin B12 was 25 % above the upper reference level, and 72 % had plasma vitamin B12 above the upper reference level. In older

Table 5 Intake of vitamin B12 from protein substitute in relation to RDI and plasma vitamin B12 in different age groups

	2–9 years	10–17 years	18 + years
$N =$	18	16	22
RDI	0.8–1.3	2	2
Vitamin B12 (μg/day)	4.5 (1.6–6.5)	5.7 (1.3–8.0)	5.4 (3.6–7.2)
Vitamin B12 (% of RDI)	358 (154–813)	283 (65–400)	270 (180–360)
Plasma vitamin B12 (pmol/L)*	823 (457–2,280)	596 (376–1,212)	490 (246–838)
< ref level	0	0	0

RDI Recommended daily intake of vitamin B12 in Nordic Nutrition Recommendations 2004

*Kruskal-Wallis test with Dunn's Multiple Comparison test showed significantly different plasma levels between children aged 2–9 years and adults ($p < 0.001$)

Table 6 Differences in intake of folic acid and vitamin B12 and plasma levels according to type of protein substitute used

	Children			Adults		
	HighFA protein substitute	LowerFA protein substitute	*p-value**	HighFA protein substitute	LowerFA protein substitute	*p-value**
$N =$	21	13		14	8	
Folic acid (μg/day)	700 (358–1,063)	203 (104–560)	<0.001	750 (500–999)	375 (192–450)	<0.001
Folic acid (% of RDI)	448 (249–625)	133 (60–303)	<0.001	194 (131–333)	100 (48–150)	<0.001
Plasma folate (nmol/L)	69 (44–123)	41 (17–73)	<0.001	57 (41–74)	29 (19–53)	<0.001
Vitamin B12 (μg/day)	5.4 (3.6–8.0)	2.6 (1.6–6.6)	<0.01	5.4 (3.6–7.2)	5.1 (4.2–6.8)	1.000
Plasma vitamin B12 (pmol/L)	750 (415–2,280)	611 (376–1,469)	0.193	552 (299–838)	419 (246–533)	<0.05
Plasma hcy (μmol/L)	4 (3–6)	5 (2–8)**	0.088	6 (4–10)	6.5 (4–10)	0.482
Serum phe last year (μmol/L)	423 (324–1,068)	433 (217–879)	0.753	572 (262–1,127)	532 (385–1,441)	0.868
Age (years)	9.8 (4.1–15.7)	10 (4.1–17.7)	0.944	31.5 (18–46)	34 (19–57)	0.525

RDI Recommended daily intake, *Hcy* homocysteine, *Phe* phenylalanine

*Mann–Whitney U test,

**$N = 11$

children and in adults, median plasma vitamin B12 was in the upper reference range. Thirty-one percent of older children and 23 % of adults had plasma vitamin B12 above the upper reference level. None had low plasma levels of vitamin B12. Plasma vitamin B12 levels were significantly higher among 2–9-year-old children than among adults ($p < 0.001$).

Plasma Levels of Vitamin B12 According to Intake

No correlations were found between intake of vitamin B12 from protein substitute and plasma B12 in children ($rs = -0.063$, $p = 0.723$, $n = 34$) or adults ($rs = 0.104$, $p = 0.647$, $n = 22$).

Differences According to Type of Protein Substitute Used

Both children and adults using HighFA protein substitutes had a significantly higher intake of folic acid (both in absolute levels and in percentage of recommendation) and plasma folate levels than children and adults using LowerFA protein substitutes (Table 6). Children using HighFA protein substitutes had a significantly higher intake of vitamin B12 than children using LowerFA protein substitutes ($p < 0.01$), but plasma levels of vitamin B12 did not differ between the groups. Plasma B12 was significantly higher in adults using HighFA protein substitutes ($p < 0.05$). There was a tendency to slightly higher plasma hcy in children using LowerFA substitutes

($p = 0.088$), but there was no difference among adults. Besides, there was no difference in median serum phenylalanine between the groups during the last year.

Discussion

The main finding of this study was that many patients with PKU have very high levels of plasma folate related to a very high content of folic acid in their protein substitutes. Children with PKU are at a particular risk of receiving too much folic acid and many patients receive doses above the UL. Young children had both high intake and high plasma levels of vitamin B12. Hcy levels were low or in the lower part of the reference range in most patients.

Our findings are in accordance with other studies reporting about twice as high folate levels in PKU children and young adults than in controls (Colome et al. 2003; Huemer et al. 2008). A recent report of 19 Norwegian late-treated adults found high intakes of folic acid and corresponding high blood folate concentrations (Wiig et al. 2013). Only one PKU center in Greece reported of lower folate levels in PKU children with good compliance compared to PKU children with less adherence to diet and to controls (Schulpis et al. 2002). Intake of folate among the patients with good compliance did not meet reference nutrient intakes for folate (Schulpis et al. 2002). Even though we tend to give some more total protein than our actual recommendations as shown in Table 1, the protein intake of our PKU children is within the range of other European PKU centers (Ahring et al. 2009; van Spronsen et al. 2009).

The folic acid content of different protein substitutes varies greatly. The protein substitutes used by our patients ranged from 3.1 to 9.6 μg folic acid/g protein for PKU children aged 6 months or 1 year up until 8–10 years. Protein substitutes suitable from 3 to 4 years or from 8 years of age ranged from 6.7 to 12.4 μg folic acid/g protein. Children often change to an adult protein substitute from age 8 to 10 years, some even from 3 to 4 years. Protein needs are still higher than in adults at this age, but with a HighFA substitute, it gives rise to very high intakes of folic acid.

A limitation of the study is that intake of folate from natural sources, folic acid from supplemented low protein flour and natural protein intake was available for only a subgroup of the patients. Natural protein intake was 270 % higher for adults than children, while folate was only 57 % higher. We also found high correlations between intake of folic acid from protein substitutes and plasma folate, indicating that protein substitute is the main source of folic acid. Another study of 19 Norwegian late-treated adults found that about 85 % of dietary folate equivalents (DFEs) originated from folic acid in the protein substitute. The remaining 15 % were from specially manufactured low protein foods, vegetables, fruits, and small amounts of dairy products (Wiig et al. 2013).

According to European recommendations, there is no evidence for risk associated with high intakes of folates from natural sources, but a high intake of folic acid from supplements may mask hematological symptoms caused by deficiency of vitamin B12 (SCF 2000). The risk of this is low in our patients compliant with protein substitute since they have good or high vitamin B12 status. However, little is known about the fate and effects of unmetabolized folic acid from high doses of folic acid supplements (Smith et al. 2008). A trial in which adults were supplemented with 800 μg folic acid daily showed that medium serum folate increased from 8.8 to 62.3 nmol/L. Hazard ratios for cancer incidence, cancer mortality, and all-cause mortality were significantly higher among subjects with serum folate > 62.7 nmol/L than among subjects with serum folate between 8.6 and 23.9 nmol/L (Ebbing et al. 2009). A recent systematic review and meta-analysis found a borderline significant increase in overall cancer frequency and increased risk of prostate cancer with folic acid supplementation (Wien et al. 2012). Folic acid suppresses tumor development and progression if supplementation is given before the establishment of neoplastic lesions. However, folic acid administration stimulates tumor progression and growth of already established preneoplastic lesions (Smith et al. 2008; Ulrich and Potter 2007). Whether high intakes of folic acid in PKU patients are beneficial or have adverse long-term effects is yet unknown, but the levels are well above the recommendations. Late-diagnosed PKU patients commencing dietary treatment at older age could have precancerous lesions with tumor progression affected by high intakes of folic acid.

Intakes of vitamin B12 were also high in our study. Children 2–9 years of age had the highest intake of vitamin B12, about 3.5 times higher than recommended. About 70% of patients in this group had plasma vitamin B12 levels above the upper reference range, while this was the case for only around 25% of older children and adults. There was no correlation between intake of vitamin B12 and plasma levels. A strict low protein diet contains little or no animal products and few sources of vitamin B12. PKU patients, following a more liberal diet, have more natural sources of vitamin B12 in the diet. Two studies both found significantly higher serum/plasma levels of vitamin B12 in PKU children and young adults than in controls (Colome et al. 2003; Huemer et al. 2008). On the other hand, Schulpis et al. found lower intakes and lower vitamin B12 levels in PKU children with good dietary compliance than in PKU patients with less compliance and controls (Schulpis et al. 2002), probably because of lower vitamin

B12 concentrations in the protein substitute. Functional vitamin B12 deficiency can exist despite levels within the reference range, and it is recommended to evaluate vitamin B12 levels against methylmalonic acid or hcy levels (Vugteveen et al. 2011). There is no reported danger related to high intake of vitamin B12, but the composition of the protein substitute should probably be adjusted to more age-appropriate levels.

Conclusion

A high content of folic acid in several protein substitutes for PKU patients results in high plasma folate levels and low plasma hcy levels. Children and adolescents with PKU are at a particular risk of receiving folic acid high above the RDI and many children with PKU receive doses above the UL. None of the patients had low plasma folate levels. The same protein substitutes are recommended for adults and children from 8 to 10 years, sometimes from 3 to 4 years. Folic acid content should be reduced in several protein substitutes available, and the supplemented levels of folic acid and vitamin B12 should have a more age-adjusted profile.

Acknowledgments The authors would like to thank the National Neonatal Screening Unit for the analysis of serum phenylalanine. We would also like to thank Cathrine Åkre Strandskogen for help with revising the manuscript.

Take-Home Message

Several protein substitutes for PKU contain high levels of folic acid giving rise to intakes above European Tolerable Upper Intake Levels and high plasma folate levels. Children are at a particular risk.

Contributions of Individual Authors

Linn Helene Stølen: conception and design of the study, collection of data, analysis of data and interpretation of data, drafting the article

Rina Lilje: conception and design of the study, collection and interpretation of data, revision of the manuscript

Jens Veilemand Jørgensen: contributed in discussion of design, acquisition of data, and revision of the manuscript

Yngve Thomas Bliksrud: contributed in discussion of design, responsible for biochemical analyses, participated in writing and revision of the manuscript

Runar Almaas: conception and design of the study, interpretation of data, participated in writing and revision of manuscript

Guarantor: Linn Helene Stølen

Compliance with Ethics Guidelines

Conflict of Interest

Linn Helene Stølen has received travel grants/accommodation/meeting expenses from Nutricia and Vitaflo.

Rina Lilje has received travel grants/accommodation/meeting expenses from Nutricia and Vitaflo.

Jens V. Jørgensen has received travel grants/accommodation/meeting expenses from Nutricia.

Yngve Thomas Bliksrud has received travel grants/accommodation/meeting expenses from Nutricia.

Runar Almaas has received travel grants/accommodation/meeting expenses from Nutricia.

The project has been initiated and performed by the authors. Nutricia and Vitaflo have not been involved in the project neither with respect to initiation, funding, organization of the study, interpretation of data, nor writing of the paper. Nutricia and Vitaflo have not read the submitted paper.

Informed Consent

All procedures followed were in accordance with the ethical standards of the responsible committee on human experimentation (institutional and national) and with the Helsinki Declaration of 1975, as revised in 2000. Informed consent was not required from the institutional review board at the time of the study, since the study included only routine data.

References

Ahring K, Belanger-Quintana A, Dokoupil K et al (2009) Dietary management practices in phenylketonuria across European centres. Clin Nutr 28:231–236

Cole BF, Baron JA, Sandler RS et al (2007) Folic acid for the prevention of colorectal adenomas: a randomized clinical trial. JAMA 297:2351–2359

Colome C, Artuch R, Sierra C et al (2003) Plasma thiols and their determinants in phenylketonuria. Eur J Clin Nutr 57:964–968

Duthie SJ (2011) Folate and cancer: how DNA damage, repair and methylation impact on colon carcinogenesis. J Inherit Metab Dis 34:101–109

Ebbing M, Bonaa KH, Nygard O et al (2009) Cancer incidence and mortality after treatment with folic acid and vitamin B12. JAMA 302:2119–2126

Figueiredo JC, Grau MV, Haile RW et al (2009) Folic acid and risk of prostate cancer: results from a randomized clinical trial. J Natl Cancer Inst 101:432–435

Huemer M, Fodinger M, Bodamer OA et al (2008) Total homocysteine, B-vitamins and genetic polymorphisms in patients with classical phenylketonuria. Mol Genet Metab 94:46–51

Nordic Council of Ministers (2004a) Folate. In Nordic Nutrition Recommendations 2004 – Integrating nutrition and physical activity. Norden, Copenhagen, pp 287–293

Nordic Council of Ministers (2004b) Vitamin B12. In Nordic Nutrition Recommendations 2004 – Integrationg nutrition and physical activity. Norden, Copenhagen, pp 297–300

Pitkin RM (2007) Folate and neural tube defects. Am J Clin Nutr 85:285S–288S

SCF (2000) Opinion of the Scientific Committee on Food on the tolerable upper intake level of folate. pp 1–13. 19-10-2000. European Commission. Ref Type: Report

Schulpis KH, Karikas GA, Papakonstantinou E (2002) Homocysteine and other vascular risk factors in patients with phenylketonuria on a diet. Acta Paediatr 91:905–909

Smith AD, Kim YI, Refsum H (2008) Is folic acid good for everyone? Am J Clin Nutr 87:517–533

Smithells RW, Sheppard S, Schorah CJ (1976) Vitamin deficiencies and neural tube defects. Arch Dis Child 51:944–950

The Norwegian Food Safety Authority and The Norwegian Directorate of Health & The University of Oslo (2006) Norwegian Food Composition Database 2006. http://www.matportalen.no/verktoy/Matvaretabellen/article9866.ece/BINARY/Matvaretabellen+%282006%29+–+hele+tabellen . Ref Type: Electronic Citation

Ulrich CM, Potter JD (2007) Folate and cancer–timing is everything. JAMA 297:2408–2409

van Spronsen FJ, Ahring KK, Gizewska M (2009) PKU-what is daily practice in various centres in Europe? Data from a questionnaire by the scientific advisory committee of the European Society of Phenylketonuria and Allied Disorders. J Inherit Metab Dis 32:58–64

Vugteveen I, Hoeksma M, Monsen AL et al (2011) Serum vitamin B12 concentrations within reference values do not exclude functional vitamin B12 deficiency in PKU patients of various ages. Mol Genet Metab 102:13–17

Wien TN, Pike E, Wisloff T, Staff A, Smeland S, Klemp M (2012) Cancer risk with folic acid supplements: a systematic review and meta-analysis. BMJ Open 2:e000653

Wiig I, Motzfeldt K, Bjørge Løken E, Kase BE (2013) Nutritional consequences of adhering to a low phenylalanine diet for late-treated adults with PKU. JIMD Reports 7:109–116<

JIMD Reports
DOI 10.1007/8904_2013_261

RESEARCH REPORT

A Novel *SLC6A8* Mutation in a Large Family with X-Linked Intellectual Disability: Clinical and Proton Magnetic Resonance Spectroscopy Data of Both Hemizygous Males and Heterozygous Females

S. Dreha-Kulaczewski · V. Kalscheuer · A. Tzschach · H. Hu · G. Helms · K. Brockmann · A. Weddige · P. Dechent · G. Schlüter · R. Krätzner · H.-H. Ropers · J. Gärtner · B. Zirn

Received: 19 June 2013 / Revised: 14 August 2013 / Accepted: 02 September 2013 / Published online: 5 November 2013

Abstract X-linked creatine transport (CRTR) deficiency, caused by mutations in the *SLC6A8* gene, leads to intellectual disability, speech delay, epilepsy, and autistic behavior in hemizygous males. Additional diagnostic features are depleted brain creatine levels and increased creatine/creatinine ratio (cr/crn) in urine. In heterozygous females the phenotype is highly variable and diagnostic hallmarks might be inconclusive. This survey aims to explore the intrafamilial variability of clinical and brain proton Magnetic Resonance Spectroscopy (MRS) findings in males and females with CRTR deficiency. X-chromosome exome sequencing identified a novel missense mutation in the *SLC6A8* gene (p.G351R) in a large family with X-linked intellectual disability. Detailed clinical investigations including neuropsychological assessment, measurement of *in vivo* brain creatine concentrations using quantitative MRS, and analyses of creatine metabolites in urine were performed in five clinically affected family members including three heterozygous females and one hemizygous male confirming the diagnosis of CRTR deficiency. The severe phenotype of the hemizygous male was accompanied by most distinct aberrations of brain creatine concentrations (−83% in gray and −79% in white matter of age-matched normal controls) and urinary creatine/creatinine ratio. In contrast, the heterozygous females showed varying albeit generally milder phenotypes with less severe brain creatine (−50% to −33% in gray and −45% to none in white matter) and biochemical urine abnormalities. An intrafamilial correlation between female phenotype, brain creatine depletion, and urinary creatine abnormalities was observed. The combination of powerful new technologies like exome-next-generation sequencing with thorough systematic evaluation of patients will further expand the clinical spectrum of neurometabolic diseases.

Communicated by: Nicole Wolf, MD PhD

Competing interests: None declared

S. Dreha-Kulaczewski · K. Brockmann · A. Weddige · R. Krätzner · J. Gärtner · B. Zirn
Department of Pediatrics and Pediatric Neurology, University Medicine Göttingen, Göttingen, Germany

V. Kalscheuer · A. Tzschach · H. Hu · H.-H. Ropers
Department of Human Molecular Genetics, Max-Planck Institute for Molecular Genetics, Berlin, Germany

A. Tzschach
Institute of Human Genetics, University of Tübingen, Tübingen, Germany

S. Dreha-Kulaczewski · G. Helms · P. Dechent
Department of Cognitive Neurology, MR-Research in Neurology and Psychiatry, University Medicine Göttingen, Göttingen, Germany

G. Schlüter
MVZ Prenatal Medicine and Human Genetics, Nürnberg, Germany

B. Zirn
genetikum, Human Genetics, Stuttgart, Germany

S. Dreha-Kulaczewski (✉)
Department of Pediatrics and Pediatric Neurology and Department of Cognitive Neurology, MR-Research in Neurology and Psychiatry, University Medicine Göttingen, Robert-Koch-Strasse 40, D-37075 Göttingen, Germany
e-mail: sdreha@gwdg.de

Introduction

Creatine deficiency syndromes constitute a group of neurometabolic disorders which include two autosomal recessive conditions with impaired creatine synthesis (arginine glycine amidinotransferase (AGAT) deficiency, OMIM #612718, and guanidinoacetate methyltransferase (GAMT) deficiency, OMIM #612736) as well as one X-linked defect of creatine transport (creatine transport (CRTR) deficiency, OMIM #300036). The latter is caused by mutations in the *SLC6A8* gene, located on chromosome Xq28 (Longo et al. 2011). Prevalent clinical symptoms of CRTR deficiency are intellectual disability (ID), expressive speech and language delay, epilepsy, and autistic behavior (van de Kamp et al. 2013).

CRTR deficiency is a quite common cause of X-linked ID (XLID) in males with an estimated frequency of 0.3–3.5% (Arias et al. 2007; Clark et al. 2006). The majority of affected males with CRTR deficiency present with non-syndromic ID. However, in some cases mild dysmorphic features such as mid-facial hypoplasia and short stature have been described (van de Kamp et al. 2013). Diagnostic hallmarks in males with CRTR deficiency are a markedly reduced or absent brain creatine (tCr) signal measured by proton magnetic resonance spectroscopy (MRS) and an increased creatine/creatinine (cr/crn) ratio in urine. In contrast to GAMT deficiency, guanidinoacetate (GAA) levels in plasma and urine remain within normal range.

To date, numerous mutations in the *SLC6A8* gene have been described (compare Leiden Open Variation Database, www.lovdnl/slc6a8). According to the X-chromosomal inheritance, females with heterozygous mutations in the *SLC6A8* gene can be mildly affected or may even be asymptomatic. The variable phenotype has been ascribed to the different X-inactivation patterns (van de Kamp et al. 2011). The female phenotypes that have been reported so far comprise developmental delay as well as mild to moderate ID. In addition, some affected females show subtle cerebellar symptoms, behavioral or gastrointestinal problems, and in one case severe epilepsy (Hahn et al. 2002; Kleefstra et al. 2005; Mancardi et al. 2007; Mercimek-Mahmutoglu et al. 2010). In females, MRS has failed to demonstrate an unambiguously reduced tCr signal (Bizzi et al. 2002; Salomons et al. 2001). Moreover, elevated cr/crn ratio in urine and impaired creatine uptake in fibroblasts, the biochemical markers in affected males, seem unreliable parameters in heterozygous females (van de Kamp et al. 2011).

Here, we report a large German family with non-syndromic ID caused by a novel *SLC6A8* gene mutation, which has been detected via thorough sequencing of all X-chromosome-specific exons. The survey of clinical and MRS data demonstrates the intrafamilial spectrum of clinical phenotypes in affected males and females and correlates the degree of ID with laboratory and MRS findings.

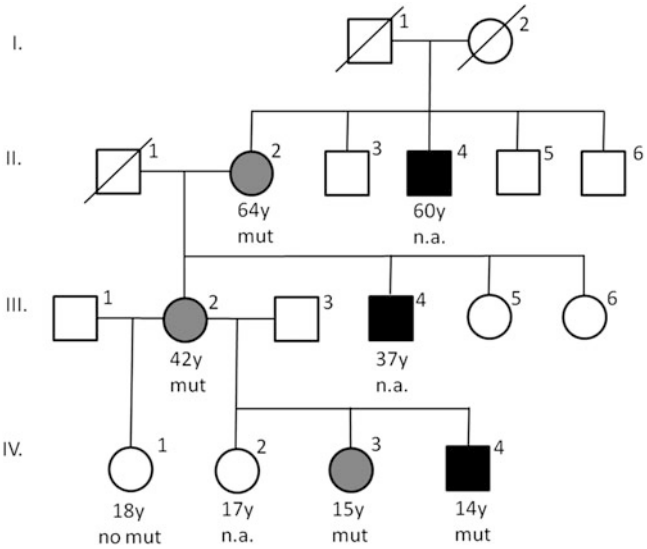

Fig. 1 Family tree. Family members of three generations were affected. *Gray symbols* represent affected heterozygous females, *black symbols* indicate affected males. *mut* genetic analysis revealed the mutation p.G351R in the *SLC6A8* gene, *no mut* the familial *SLC6A8* mutation was excluded by genetic analysis, *n.a.* not analyzed, genetic analysis has not been performed. Subjects II.4 and III.4 are not included in Table 1. Subject II.4 (age 60 years) is known to suffer from epilepsy, severe intellectual disability, and to live in a residential home for disabled people. Subject III.4 (age 37years) is known to have a severe intellectual disability and lives in a residential home

Subjects and Methods

Subjects

A large German family (D150) with intellectually disabled members in three generations was analyzed (compare family tree, Fig. 1). One affected male (II.4) with severe ID also had epilepsy. Two affected males with severe ID lived in sheltered homes (II.4 and III.4). Craniofacial dysmorphism was not present in this family. Five family members (four females: II.2, III.2, IV.1, IV.3 and one male: IV.4) were studied in detail. The healthy girl (IV.2) with normal intelligence was excluded from further investigations.

Neuropsychological Assessment

To evaluate intellectual abilities in this family, the Wechsler Adult Intelligence Test-Third Edition was used for subjects II.2, III.2, and IV.1. To study subjects IV.3 and IV.4, the Wechsler Intelligence Scale for Children-Forth Edition was applied. Mild ID was defined as an IQ score of 50–69 and moderate ID as an IQ score of 35–49.

Sequencing of X-Chromosome-Specific Exons

Genomic DNA (3 μg) from the index patient (IV.4 in Fig. 1) was used for constructing a single-end Illumina sequencing library using the Illumina Genomic DNA Single End Sample Prep kit, according to the instructions of the manufacturer. For X-chromosome exome enrichment, we used the Agilent SureSelect Human X Chromosome Kit, which contains 47,657 RNA baits for 7,591 exons of the human X chromosome. Single-end deep sequencing was performed on the Illumina Genome Analyzer GAIIx. Read length was 76 nt. Sequences were analyzed with in-house-developed tools. Confirmation of the *SLC6A8* mutation and segregation analysis in the family was done by PCR and conventional Sanger sequencing using the gene-specific primer pair 2769_10SLC6A8f TCCCGGCCTCCTACTACTTCC, 2769_10SLC6A8r CATACAGGCAATGTCGTCCA.

Proton MR-Spectroscopy

Combined MRS/MR-imaging (MRI) examinations were performed on a 3T clinical whole-body MR system (Magnetom Tim Trio, Siemens Healthcare, Erlangen, Germany) with an 8-channel receive array (Invivo, Gainesville, FL, USA). The study was approved by the institutional ethics committee.

For single voxel, MRS volumes of interest (VOI) were selected from T1- and T2-weighted images and positioned in posterior paramedian cortical gray matter (GM) (12.5 ml), in frontal (F) as well as parieto-occipital (PO) white matter (WM) (4.1 ml) (see Fig. 2). Fully relaxed spectra were obtained in each VOI by applying the short-echo time stimulated echo acquisition mode (STEAM) sequence (repetition time/echo time/mixing time: 6000/20/10 ms, 64 accumulations) (Frahm et al. 1989; Natt et al. 2005). Metabolites considered in this study include creatine and phosphocreatine (tCr) as ubiquitous compounds linked to energy metabolism, the neuroaxonal marker *N*-acetylaspartate and *N*-acetylaspartylglutamate (tNAA), choline-containing compounds (Cho) involved in membrane turnover, and the glial marker *myo*-inositol (Ins) (Dreha-Kulaczewski et al. 2009; Pouwels and Frahm 1998). Additionally, GAA, involved in creatine metabolism, was assessed. The absolute concentrations of these metabolites were calculated using LCModel and expressed in mmol/l (Provencher 1993).

Metabolite concentrations were compared to healthy age- and region-matched control groups from our local database. Deviations of >2 standard deviations (SD) from control values were considered significant.

Biochemical Analysis

GAA and cr were measured in urine by gas chromatography–mass spectrometry with deuterated internal standards as previously described (Almeida et al. 2004; Arias et al. 2004). Values were compared to healthy age-matched controls obtained from a local database.

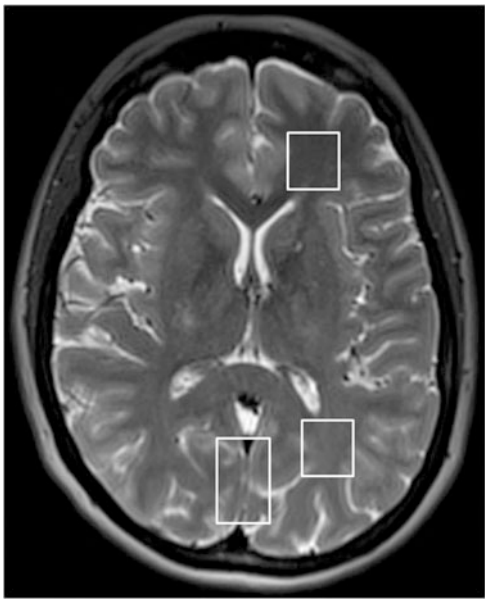

Fig. 2 Axial T2-weighted MRI of heterozygous female subject III.2. MRI demonstrates the placement of VOI in posterior paramedian cortical gray matter and in frontal as well as parieto-occipital white matter. No signal abnormalities could be detected. Mild cerebellar atrophy is not shown

Results

Clinical and developmental details of six family members are summarized in Table 1. Two female subjects (IV.1, IV.3 in Fig. 1) had a history of motor and speech delay. No developmental data were available for the two females II.2 and III.2. Female IV.1 had epilepsy from her 6th to 16th year of life which was well controlled by valproic acid. Three females (III.2, IV.1, and IV.3) required special education due to ID. In addition, aggressive and hyperactive behavior was evident in female subject IV.3. All four females (II.2, III.2, IV.1, and IV.3) had IQ scores in the mild ID range (IQ 50–69). The lowest score was reached by subject III.2.

The affected male (IV.4) presented a delay in motor and speech development as well as aggressive behavioral problems. The boy requires special education. Notably, his IQ score was the lowest of all family members and fell within the moderate ID range (IQ 35–49).

Genetic Studies

In an effort to identify the pathogenic mutations in families with XLID collected by the EUROMRX consortium and

Table 1 Clinical features, urine analysis and MRS data of individual family members

Subject	G	Age (yrs)	Developmental and neurological details	Education	IQ	*SLC6A8* mutation p.G351R	MRS (mmol/l)					Urine analysis	
							VOI	tCr	tNAA	Cho	Ins	cr/crn	GAA (μMol/mMol crn)
II.2	f	64	Developmental details n.k., mild ID	n.k.	62[e]	Heterozygous	n.p.					0.173	45.0
III.2	f	43	Developmental details n.k., mild ID	Special school, no profession	50[e]	Heterozygous	GM WM F	3.3* 3.5	6.2 6.9	1.1 1.6	3.4 4.6	0.235	31.6
IV.1	f	17	MD[a]/SD[b]; Epilepsy, mild ID	Special school, sheltered workplace	62[e]	None	GM WM F	5.2 5.0	7.0 7.8*	1.1 1.7	3.6 3.8*	0.047	37.7
IV.2	f	16	Normal development, normal intelligence	High school	n.t.	n.d.	n.d.					n.d.	n.d.
IV.3	f	14	SD[c], aggressive behavior, hyperactive, mild ID	Special school	57[f]	Heterozygous	GM WM PO	2.6* 2.3*	7.7 8.2	0.8 1.0	3.7 2.5	0.338[g]	33.4
IV.4	m	13	MD[a]/SD[d], aggressive behavior, moderate ID	Special school	40[f]	Hemizygous	GM WM PO	0.9* 0.9*	7.5 8.4*	0.9 1.2	4.8 2.7	2.094[g]	78.4

G gender, *f* female, *m* male, *yrs* years, *n.k.* not known, *n.t.* not tested, *n.d.* not done, *MD* motor delay, *SD* speech delay, *IQ* intelligence quotient, *cr* creatine, *crn* creatinine, *GAA* guanidinoacetate, *ID* intellectual disability, *mild ID* IQ score of <70, *moderate ID* IQ score of <50, *MRS* magnetic resonance spectroscopy, *VOI* volume of interest, *tCr* creatine and phosphocreatine; *tNAA* *N*-acetylaspartate and *N*-acetylaspartylglutamate, *Cho* choline-containing compounds, *Ins myo*-inositol, *GM* gray matter, *WM F* white matter frontal, *WM PO* white matter parieto-occipital

[a] Walking at ~2.5 years

[b] Single words at ~2.5 years

[c] Single words at ~2 years, short sentences at ~5 years

[d] Single words at 2.7 years

[e] Wechsler Adult Intelligence Test-Third Edition

[f] Wechsler Intelligence Scale for Children-Forth Edition

[g] Above normal range

* >2SD from control

associated groups, we sequenced all X-chromosome specific exons in the index patient (IV.4 in Fig. 1) of this large family (D150). After filtering of all identified variants against publicly available data, including the 1000 Genomes project database, dbSNP135 and the Exome Variant Server, the only mutation that was predicted to be deleterious was a missense mutation in *SLC6A8* (g.G>A, chrX:152959802–152959802, UCSC, hg19, p.Gly351Arg, NP_001136278; p.Gly456Arg, NP_001136277, p.Gly466Arg, NP_005620). Moreover, this change was absent in >450 X-chromosome exomes from males with XLID (data not shown). Subsequently, the presence of this *SLC6A8* mutation was confirmed by PCR using a gene-specific primer set and Sanger sequencing, and it was also present in additional affected family members (Table 1).

Proton MR-Spectroscopy

Spectra from GM and WM of four subjects are shown in Fig. 3. No distinct tCr peaks could be detected in GM and WM of the hemizygous male IV.4 (Fig. 3, row A). In the heterozygous girl IV.3 (Fig. 3, row B) tCr resonances were evident but decreased when compared to controls (Fig. 3, row E). The tCr peak heights of the adult heterozygote III.2 (Fig. 3, row C) approximated those of normal controls. By contrast, the spectra obtained from the female without *SLC6A8* mutation IV.1 (Fig. 3, row D) were unremarkable.

Quantitative analysis of tCr concentrations confirmed the most distinct reduction (GM −83%, WM −79% of normal control values in Table 2) in the affected boy (IV.4) (see Table 1). The tCr levels in the affected heterozygous sister (IV.3) were also significantly reduced compared to controls, albeit to a smaller degree (GM −50%, WM −45%). The heterozygous mother (III.2) showed a significant tCr decrease (−33%) only in GM. The tCr concentrations of the female (IV.1) without *SLC6A8* mutation were within normal range. The other major metabolites showed no significant differences in GM compared to controls. In WM, high levels of tNAA in subjects IV.1 and IV.4 as well as of Ins in subject IV.1 were found.

No signal clearly arising from GAA (at a chemical shift of 3.8 ppm) could be detected in any of the subjects' spectra. With GAA included into the LCModel analysis, low concentrations of GAA may be fitted in GM only, but these were comparable to normal controls and thus regarded an artifact.

The MRI of the hemizygous boy showed an unspecific small, hyperintense lesion on T2-weighted images within the left basal ganglia. Mild cerebellar vermis atrophy was detectable on the MRI of the heterozygous female subject III.2 and slightly more pronounced on the MR images of her daughter (IV.1) without *SLC6A8* mutation.

Biochemical Analysis

Notably, the most pronounced increase of cr/crn urinary level was measured in the hemizygous boy (IV.4). The comparatively much lower ratio of his heterozygous sister (IV.3) (Table 1) was still elevated with respect to her age-matched control group (Table 2). Their heterozygous mother (III.2) as well as the half-sister without *SLC6A8* mutation (IV.1) had normal cr/crn ratios. Urinary excretion of GAA was within normal ranges in all subjects.

Discussion

In a large family with non-syndromic XLID, X-chromosome exome screening revealed a novel mutation in the *SLC6A8* gene (p.G351R, NP_001136278) leading to CRTR deficiency syndrome. The diagnosis of CRTR deficiency was subsequently confirmed by MRS of the brain as well as urinary creatine/creatinine measurement in three affected females and one affected male. The phenotypic variability within this family is in line with numerous reports about the broad range of clinical presentations in this neurometabolic disease (deGrauw et al. 2003; van de Kamp et al. 2013). Profound ID was evident in all male members. The hemizygous male index patient presented with the characteristic severe phenotype comprising ID as well as severe speech delay and behavioral disturbances. All heterozygous females showed milder symptoms. Their IQs ranged from 50–62 (Table 1). However, the familial *SLC6A8* mutation was excluded in one half-sister (IV.1) of the index patient, who presented with mild ID and epilepsy. This half-sister has a different and also intellectually disabled father than subjects IV.2-IV.4 and therefore may be affected with ID of another origin. Cerebellar signs or gastrointestinal problems like chronic constipation, ileus, or megacolon, which had previously been reported in affected males and females (Kleefstra et al. 2005; van de Kamp et al. 2011), were not present in our family. Moreover, no affected family member had obvious craniofacial dysmorphism.

In the clinical setting, CRTR deficiency is usually diagnosed via a screening test in urine, which shows a strong elevation of the cr/crn ratio in affected males. In our index patient, cr/crn ratio screening in urine was problematic since he rejected urine sampling several times and wore diapers. The missense mutation in the *SLC6A8* gene was detected via X-chromosome exome sequencing. Subsequently, the cr/crn ratios were evaluated in all affected heterozygous females. Interestingly, only one of the three heterozygous females had a mild increase of the urinary cr/crn ratio. Remarkably, this female patient also presented with the lowest brain tCr levels and had a more severe

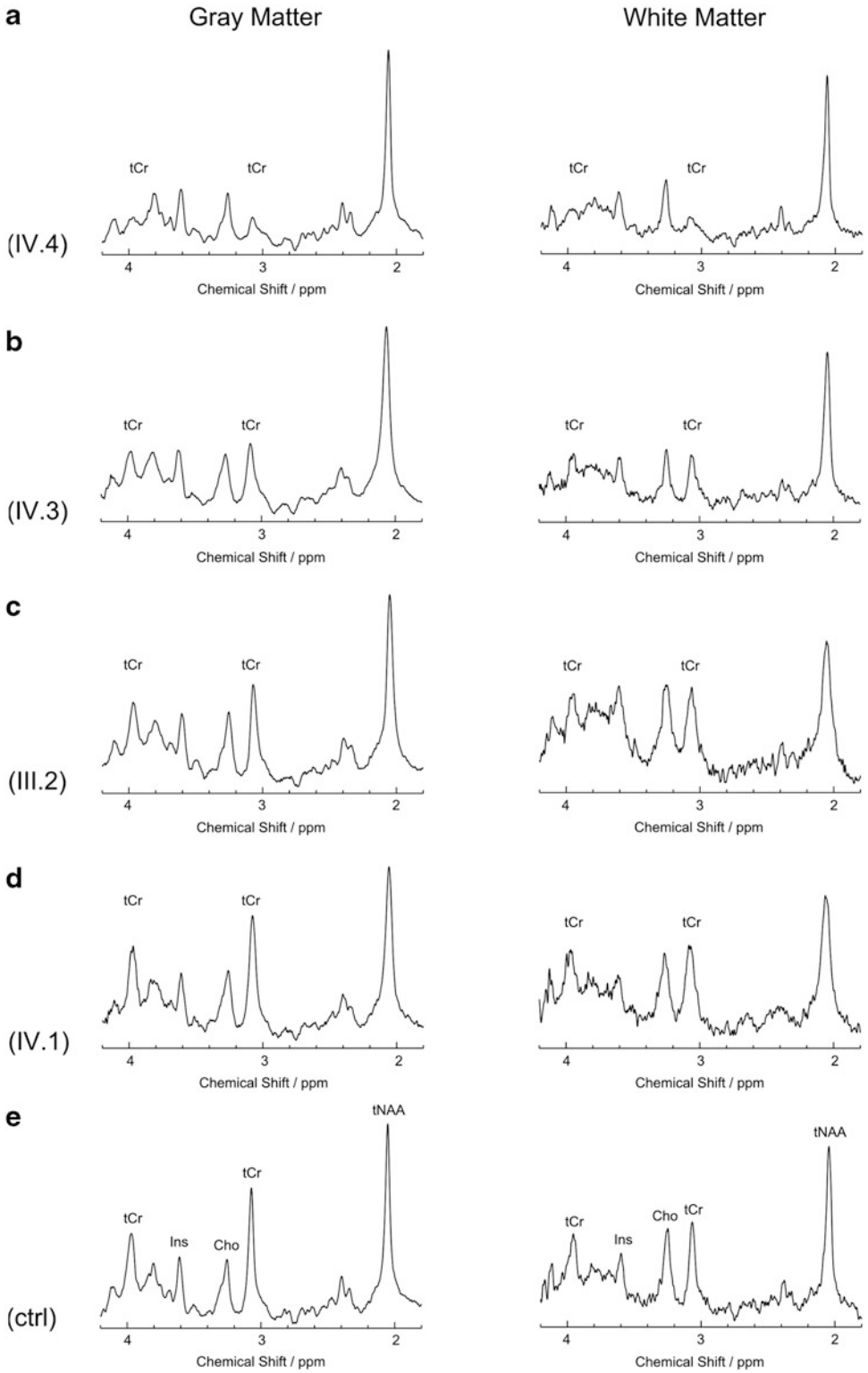

Fig. 3 Single voxel proton MR spectra from gray and white matter of affected family members with CRTR deficiency. (Row **A**) male subject IV.4 hemizygous for *SLC6A8* mutation. (row **B**) female subject IV.3 heterozygous for *SLC6A8* mutation. (Row **C**) female subject III.2 heterozygous for *SLC6A8* mutation. (Row **D**) female subject IV.1 without mutation. (Row **E**) healthy control subject (female, age 13 years). Note the variability of tCr (sum of creatine and phosphocreatine) peaks at 3.2 and 3.9 ppm between subjects. In row A no defined tCr peaks can be detected, whereas in row B they are clearly visible but reduced compared to controls (**row E**). In row C and D the tCr peaks are of normal heights compared to controls. Assignments of main peaks of the proton MR spectrum are added to the control spectra (**row E**). Note that scale of spectra varies to facilitate qualitative assessment of differences of tCr peak heights. *tNAA* sum of *N*-acetylaspartate and *N*-acetylaspartylglutamate, *Cho* choline-containing compounds, *Ins myo*-inositol

Table 2 Control values for MRS and urine analysis

MRS (mmol/l)					Urine analysis	
VOI	tCr	tNAA	Cho	Ins	cr/crn	GAA (μmol/Mmol crn)
GM	5.2 ± 0.9	7.2 ± 1.0	1.0 ± 0.3	3.4 ± 0.7	*n = 169*	*n = 169*
n = 22 (13.5 ± 2.6 yrs)					0.011–0.25	4–220
GM	4.9 ± 0.2	7.0 ± 0.6	1.0 ± 0.1	3.1 ± 0.2	*(>12 yrs)*	*(<15 yrs)*
n = 4 (40.6 ± 4.1 yrs)						10–160
WM F	3.9 ± 0.6	5.9 ± 0.9	1.4 ± 0.3	2.4 ± 0.6		*(>15 yrs)*
n = 18 (13.6 ± 2.6 yrs)						
WM F	3.9 ± 0.5	6.1 ± 0.4	1.7 ± 0.4	3.4 ± 1.2		
n = 4 (40.6 ± 4.1 yrs)						
WM PO	4.2 ± 0.5	7.3 ± 0.5	1.5 ± 0.3	2.7 ± 0.4		
n = 21 (13.5 ± 2.3 yrs)						
WM PO	3.9 ± 0.7	7.1 ± 0.6	1.6 ± 0.3	2.8 ± 0.3		
n = 4 (40.6 ± 4.1 yrs)						

n number of subjects, *yrs* years, *cr* creatine, *crn* creatinine, *GAA* guanidinoacetate, *VOI* volume of interest, *MRS* magnetic resonance spectroscopy, *tCr* creatine and phosphocreatine, *tNAA N*-acetylaspartate and *N*-acetylaspartylglutamate, *Cho* choline-containing compounds, *Ins myo*-inositol, *GM* gray matter, *WM* white matter, *F* frontal, *PO* parieto-occipital

phenotype comprising behavioral disturbances. This observation is in line with a correlation between clinical phenotype, cerebral tCr depletion and elevation of urinary cr/crn ratio postulated by van de Kamp et al (van de Kamp et al. 2011). However, a strict correlation between brain MRS or biochemical data and IQ scores, as suggested, has not been found in the heterozygous females with CRTR deficiency described here. Yet, an inverse correlation between cerebral tCr concentrations and urinary cr/crn ratios could be seen. The small sample size precluded further statistical analysis.

CRTR deficiency syndromes are increasingly detected among patients with non-syndromic unexplained ID (Clark et al. 2006; Lion-Francois et al. 2006; Rosenberg et al. 2004). In contrast, defects in creatine synthesis seem to be much less frequent. In affected females, it is difficult to diagnose CRTR deficiency via urine analysis. In our study, a significant elevation of cr/crn ratio in urine analysis was only found in one affected female.

We performed a quantitative brain MRS study in this family on both affected genders of two generations, which revealed significant reduction of brain tCr concentration in the GM of all family members with the *SLC6A8* gene mutation. In WM of the adult heterozygous female the concentration of tCr remained within normal ranges (see Table 1). The hemizygous male index patient IV.4 (Fig. 2, row A) showed almost complete absence of the tCr peaks in both GM and WM, which corresponds to previous reports (van de Kamp et al. 2013). The disparity of the tCr reduction among the heterozygous females within the same family, however, is a remarkable finding. The youngest girl with *SLC6A8* mutation showed a distinct tCr decrease, which was already qualitatively appreciable in the spectra (Fig. 2, row B) and subsequently confirmed by quantification. In contrast, the slighter tCr reduction in GM of the heterozygous mother has not been evident in the spectral pattern but was disclosed only as a result of the quantification (Fig. 2, row C). The tCr concentrations in one half-sister of the index patient, in whom the familial *SLC6A8* mutation was excluded, were within normal limits (Fig. 2, row D) as expected.

To date, quantitative brain MRS data of heterozygous females with CRTR deficiency have only been included in a minority of reports. Most publications are restricted to the qualitative description of a reduced peak of total creatine (tCr) in the spectrum (Cecil et al. 2003; deGrauw et al. 2003; Salomons et al. 2001). Dezertova et al. (2008) verified a decreased tCr concentration in an affected female only after quantification, thus emphasizing the importance of quantitative MRS. On the other hand, another quantitative MRS study of a cohort of eight female heterozygotes revealed a significant tCr reduction only on the group level (van de Kamp et al. 2011). Individual brain

creatine concentrations were within normal ranges regardless of the region, a finding that is consistent with our results. The observation of a GAA signal as described by Sijens et al. (2005) could not be confirmed in our study.

The small unspecific hyperintense lesion in the basal ganglia seen on T2-weighted MR images of the boy is consistent with a hamartoma. The atrophy of cerebellar vermis has been detected in female family members with as well as without *SLC6A8* mutation and thus is considered as unspecific.

Several therapeutic trials using creatine monohydrate, L-arginine, and glycine have so far failed to reliably improve cerebral tCr levels and/or clinical symptoms in patients with CRTR deficiency (van de Kamp et al. 2012). However, brain-specific *Slc6a8* knockout mice, an animal model of human CRTR deficiency, were treated with the creatine analog cyclocreatine and did indeed show improved cognition as recently reported by Kurosawa et al. (2012). The authors were also able to demonstrate that the cyclocreatine entered the mouse brain and was successfully funneled into its metabolism. Thus, further studies using this promising therapy approach are warranted to assess its implications for humans.

Conclusion

In a large family with X-linked intellectual disability of unknown cause, the novel *SLC6A8* mutation p.G351R was detected via X-chromosome exome sequencing. The diagnosis of CRTR deficiency was confirmed by MRS of the brain as well as urinary creatine/creatinine measurement, thus underlining the pathogenicity of this novel *SLC6A8* mutation. Female phenotypes heterozygous for the mutation varied significantly even within one family. However, a correlation between severity of clinical symptoms, brain creatine depletion and urinary creatine abnormalities could be observed.

The combination of powerful new technologies like exome-next-generation sequencing with thorough systematic evaluation of patients as in this study will work synergistically to further expand our knowledge of the clinical spectrum of neurometabolic diseases.

Acknowledgment This work has been supported by grants of the German Ministry of Education and Research through the German Leukonet (Grants 01GM0642 and 01GM0836; KB, SDK, JG); the MRNET (Grant 01GS08161; HHR); by the Project GENCODYS (241995), which is funded by the European Union Framework Program 7 (FP7); and the Volkswagen Stiftung (PD, GH). SDK has received funding from the Dorothea-Schloezer-Program of the Georg August University Goettingen, Germany. We thank Melanie Bienek and Ute Fischer for excellent technical assistance.

Synopsis

The combination of the powerful technology exome-next-generation sequencing with thorough systematic clinical evaluation of patients, as in this study of a family with X-linked creatine transport deficiency, will work synergistically to further expand the clinical spectrum of neurometabolic diseases.

Compliance with Ethics Guidelines

Conflict of Interest

Steffi Dreha-Kulaczewski, Vera Kalscheuer, Andreas Tzschach, HaoCougar Hu, Gunther Helms, Knut Brockmann, Almut Weddige, Peter Dechent, Gregor Schlüter, Ralf Krätzner, Hans-Hilger Ropers, Jutta Gärtner, and Birgit Zirn declare that they have no conflict of interest.

Informed Consent

All procedures followed were in accordance with the ethical standards of the responsible committee on human experimentation (institutional and national) and with the Helsinki Declaration of 1975, as revised in 2000 (5). Informed consent was obtained for all patients being included in the study.

Details of the Contributions of Individual Authors

SDK: designed and conducted the MR studies, interpreted the MR data, wrote the manuscript

VMK, HHR: designed the genetic studies, interpreted the data, substantially revised the manuscript

AT, HH, GS: conducted the genetic studies, analyzed and interpreted the data

AW: conducted the neuropsychological investigations

RK: designed and conducted the biochemical studies, interpreted the data, revised the manuscript

GH, PD: designed the MR studies, interpreted the data, revised the manuscript

KB, JG, BZ: designed and conducted the clinical study, substantially revised the manuscript

References

Almeida LS, Verhoeven NM, Roos B et al (2004) Creatine and guanidinoacetate: diagnostic markers for inborn errors in creatine biosynthesis and transport. Mol Genet Metab 82:214–219

Arias A, Garcia-Villoria J, Ribes A (2004) Guanidinoacetate and creatine/creatinine levels in controls and patients with urea cycle defects. Mol Genet Metab 82:220–223

Arias A, Corbella M, Fons C et al (2007) Creatine transporter deficiency: prevalence among patients with mental retardation and pitfalls in metabolite screening. Clin Biochem 40:1328–1331

Bizzi A, Bugiani M, Salomons GS et al (2002) X-linked creatine deficiency syndrome: a novel mutation in creatine transporter gene SLC6A8. Ann Neurol 52:227–231

Cecil KM, DeGrauw TJ, Salomons GS, Jakobs C, Egelhoff JC, Clark JF (2003) Magnetic resonance spectroscopy in a 9-day-old heterozygous female child with creatine transporter deficiency. J Comput Assist Tomogr 27:44–47

Clark AJ, Rosenberg EH, Almeida LS et al (2006) X-linked creatine transporter (SLC6A8) mutations in about 1% of males with mental retardation of unknown etiology. Hum Genet 119:604–610

deGrauw TJ, Cecil KM, Byars AW, Salomons GS, Ball WS, Jakobs C (2003) The clinical syndrome of creatine transporter deficiency. Mol Cell Biochem 244:45–48

Dezortova M, Jiru F, Petrasek J et al (2008) 1H MR spectroscopy as a diagnostic tool for cerebral creatine deficiency. Magma 21:327–332

Dreha-Kulaczewski SF, Helms G, Dechent P, Hofer S, Gartner J, Frahm J (2009) Serial proton MR spectroscopy and diffusion tensor imaging in infantile Balo's concentric sclerosis. Neuroradiology 51:113–121

Frahm J, Bruhn H, Gyngell ML, Merboldt KD, Hanicke W, Sauter R (1989) Localized high-resolution proton NMR spectroscopy using stimulated echoes: initial applications to human brain in vivo. Magn Reson Med 9:79–93

Hahn KA, Salomons GS, Tackels-Horne D et al (2002) X-linked mental retardation with seizures and carrier manifestations is caused by a mutation in the creatine-transporter gene (SLC6A8) located in Xq28. Am J Hum Genet 70:1349–1356

Kleefstra T, Rosenberg EH, Salomons GS et al (2005) Progressive intestinal, neurological and psychiatric problems in two adult males with cerebral creatine deficiency caused by an SLC6A8 mutation. Clin Genet 68:379–381

Kurosawa Y, Degrauw TJ, Lindquist DM et al (2012) Cyclocreatine treatment improves cognition in mice with creatine transporter deficiency. J Clin Invest 122:2837–2846

Lion-Francois L, Cheillan D, Pitelet G et al (2006) High frequency of creatine deficiency syndromes in patients with unexplained mental retardation. Neurology 67:1713–1714

Longo N, Ardon O, Vanzo R, Schwartz E, Pasquali M (2011) Disorders of creatine transport and metabolism. Am J Med Genet C Semin Med Genet 157:72–78

Mancardi MM, Caruso U, Schiaffino MC et al (2007) Severe epilepsy in X-linked creatine transporter defect (CRTR-D). Epilepsia 48:1211–1213

Mercimek-Mahmutoglu S, Connolly MB, Poskitt KJ et al (2010) Treatment of intractable epilepsy in a female with SLC6A8 deficiency. Mol Genet Metab 101:409–412

Natt O, Bezkorovaynyy V, Michaelis T, Frahm J (2005) Use of phased array coils for a determination of absolute metabolite concentrations. Magn Reson Med 53:3–8

Pouwels PJ, Frahm J (1998) Regional metabolite concentrations in human brain as determined by quantitative localized proton MRS. Magn Reson Med 39:53–60

Provencher SW (1993) Estimation of metabolite concentrations from localized in vivo proton NMR spectra. Magn Reson Med 30:672–679

Rosenberg EH, Almeida LS, Kleefstra T et al (2004) High prevalence of SLC6A8 deficiency in X-linked mental retardation. Am J Hum Genet 75:97–105

Salomons GS, van Dooren SJ, Verhoeven NM et al (2001) X-linked creatine-transporter gene (SLC6A8) defect: a new creatine-deficiency syndrome. Am J Hum Genet 68:1497–1500

Sijens PE, Verbruggen KT, Oudkerk M, van Spronsen FJ, Soorani-Lunsing RJ (2005) 1H MR spectroscopy of the brain in Cr transporter defect. Mol Genet Metab 86:421–422

van de Kamp JM, Mancini GM, Pouwels PJ et al (2011) Clinical features and X-inactivation in females heterozygous for creatine transporter defect. Clin Genet 79:264–272

van de Kamp JM, Pouwels PJ, Aarsen FK et al (2012) Long-term follow-up and treatment in nine boys with X-linked creatine transporter defect. J Inherit Metab Dis 35:141–149

van de Kamp JM, Betsalel OT, Mercimek-Mahmutoglu S et al (2013) Phenotype and genotype in 101 males with X-linked creatine transporter deficiency. J Med Genet 50:463–472

JIMD Reports
DOI 10.1007/8904_2013_263

RESEARCH REPORT

Influence of *PAH* Genotype on Sapropterin Response in PKU: Results of a Single-Center Cohort Study

Sarah Leuders • Eva Wolfgart • Torsten Ott • Marcel du Moulin • Agnes van Teeffelen-Heithoff • Lydia Vogelpohl • Ulrike Och • Thorsten Marquardt • Josef Weglage • Reinhold Feldmann • Frank Rutsch

Received: 18 June 2013 / Revised: 02 September 2013 / Accepted: 09 September 2013 / Published online: 5 November 2013

Abstract Objective: Identifying phenylalanine hydroxylase (*PAH*) mutations associated with sapropterin response in phenylketonuria (PKU) would be an advantageous means to determine clinical benefit to sapropterin therapy.

Methods: Sapropterin response, defined as a ≥30 % reduction in phenylalanine (Phe) levels after a dose of 10 mg/kg/day sapropterin for week one and 20 mg/kg/day for week two in 112 PKU patients aged 4–45 years, was assessed in an outpatient setting. *PAH* was sequenced in all patients. Mutations were correlated with sapropterin response. Dietary Phe intake was increased over a 6-week period in responsive patients.

Results: Forty-six of 112 patients were sapropterin responsive. Genotypes p.[L48S];[L48S] and p.[Y414C];[Y414C] were always associated with response at a low dose. The mutation Y414C (present on 16 alleles) was most frequently associated with response. Patients with presence of the mutation L48S on at least one allele (12 alleles in 7 patients) always showed response to sapropterin. Responsive patients had a mean Phe tolerance increase of 189 % (range 11–742 %). In the 66 nonresponders, mutations R408W (38 alleles) and IVS12+1G>A (18 alleles) were detected most frequently. Genotypes [IVS12+1G>A];[IVS12+1G>A], p.[L348V];[R408W], p.[P281L];[P281L], p.[R158Q];[R408W], and p.[R261Q];[R408W] were always associated with nonresponse.

Conclusion: Data from the study contributes to growing evidence of the relationship between *PAH* genotype and PKU phenotype. In most cases, response to sapropterin therapy cannot be predicted based on the presence of a single mutation on one allele alone, although the complete *PAH* genotype may help to predict sapropterin responsiveness in PKU patients.

Background

Phenylketonuria (PKU) is an autosomal recessive metabolic disorder resulting from mutations in the gene encoding phenylalanine hydroxylase (PAH) (Scriver and Kaufman 2001). More than 800 mutations have been identified (BIOPKU database, http://www.biopku.org/home/pah.asp, accessed Sep 2013), which lead to PAH deficiency and a wide range of clinical phenotypes. The deficient PAH activity results in a decreased ability to convert phenylalanine (Phe) to tyrosine (Tyr) and leads to toxic accumulation of Phe in the brain (Scriver et al. 2008). In developed countries, patients are identified at birth through newborn screening programs and classified by clinical phenotype. Minimum pretreatment Phe levels, requiring initiation of a Phe-restricted diet, vary between different countries. In

Communicated by: Nenad Blau, PhD

Sarah Leuders and Eva Wolfgart contributed equally to this study

Competing interests: None declared

S. Leuders · E. Wolfgart · T. Ott · A. van Teeffelen-Heithoff · L. Vogelpohl · U. Och · T. Marquardt · J. Weglage · R. Feldmann · F. Rutsch
Department of General Pediatrics, Münster University Children's Hospital, Albert-Schweitzer Campus 1, Gbd. A1, D-48149 Münster, Germany

M. du Moulin
Department of Paediatrics, University Medical Center Hamburg-Eppendorf, Martinistrasse 52, D-20246 Hamburg, Germany

F. Rutsch (✉)
Allgemeine Pädiatrie, Klinik und Poliklinik für Kinder- und Jugendmedizin, Universitätsklinikum Münster, Albert-Schweitzer-Campus 1, Gebäude A1, D-48149 Muenster, Germany
e-mail: rutschf@ukmuenster.de

Germany, patients with Phe levels >600 μmol/L (Weglage et al. 1996; Burgard et al. 1999) are treated with such a diet.

Although the Phe-restricted diet prevents the severe intellectual dysfunction associated with untreated PKU (National Institutes of Health Consensus Development Panel 2001), subtle neurocognitive deficits are still reported in individuals with PKU treated early and continuously with the Phe-restricted diet (Enns et al. 2010). As well, severely restricted diets, such as the Phe-restricted diet, are associated with a risk of nutritional deficiencies and present a substantial psychosocial burden and challenges with adherence, especially for adolescents who often fail to comply with the strict recommendations (Walter et al. 2002).

In 1999, Kure et al. published results of a study that identified a subgroup of PKU patients, who responded to exogenous BH4 with reduced blood Phe levels independent of the Phe-restricted diet (Kure et al. 1999). Initially thought to be primarily due to higher levels of available BH4, it was later determined to be caused in part by stabilization of PAH protein conformation and by preventing inactivation of the enzyme (Thöny et al. 2004; Gersting et al. 2010). Sapropterin dihydrochloride (sapropterin, Kuvan®) received marketing approval in Germany in April 2009 for individuals with PKU who are sapropterin responsive to reduce Phe levels and allows responders to modify their strict dietary regimen (Levy et al. 2007; Lee et al. 2008; Trefz et al. 2009a).

Most patients in the European Union (EU) must undergo a sapropterin response test as described in the EU summary of products characteristics (SmPC). Many protocols exist to determine sapropterin responsiveness in patients with PKU, varying significantly between continents and even between countries and clinics within a country (Blau et al. 2009). EU recommendations may include a 48-h sapropterin response test (Blau et al. 2009) under hospital supervision. An oral Phe loading of 100 mg/kg of body weight prior to the first dose of sapropterin (Muntau et al. 2002), which allows a more significant response to sapropterin for patients whose Phe levels are within recommended range by the Phe-restricted diet, was suggested as well (Staudigl et al. 2011). However, not all sapropterin response test protocols require a Phe loading test (Blau et al. 2009). For example, the United States (US) Food and Drug Administration (FDA) does not recommend the Phe loading component for sapropterin response testing, and does not require the patient to be hospitalized at any point of the response testing period (Kuvan® US Prescribing Information).

Both protocols first determine the patient's baseline blood Phe level. In the United States, the FDA-approved initial sapropterin dose is 10 mg/kg for 1 week and if a reduction in Phe level is not achieved, the dose is increased to 20 mg/kg and monitored for a maximum of 1 month (Kuvan® US Prescribing Information). In the EU, if the Phe level is well controlled, sapropterin treatment is initiated at 20 mg/kg/day. The Phe level is assessed at the 24-h mark. If it has not been reduced by ≥30 %, a second dose of sapropterin 20 mg/kg/day is given. The blood Phe level is reassessed at 24 h. In case of a decrease in Phe level <30 % after the 48 h of testing, the patient is classified as nonresponsive and sapropterin treatment is discontinued (Blau et al. 2009).

Existing protocols for sapropterin response testing pose challenges and have limitations. The strict dietary control and increased frequency of blood Phe monitoring required during the response test period may impact patients' compliance.

The use of *PAH* mutational analysis rather than sapropterin response testing protocols could potentially eliminate these challenges and reduce false-negative responses due to noncompliance and false-positive results due to natural fluctuations in Phe levels. The ability to predict long-term response to sapropterin therapy in individual patients through alternative means could positively impact patient outcomes. The *PAH* genotype could be an important factor for predicting response to sapropterin with mutations associated with BH4 response dispersed throughout the gene. However, although the nature and position of the mutations determines their effect on the activity of the PAH enzyme and the clinical phenotype of the patient, to date, no conclusive data exists to allow prediction of sapropterin responsiveness solely based on genotype.

Our primary objective in this Phase IV open-label study was to evaluate alternative methods for identifying individuals with PKU as responsive to sapropterin therapy including impact of genotype, individual mutation, and location of mutation in the *PAH* gene. We aimed to identify the influence of individual *PAH* mutations on response based on Phe levels and dietary Phe intake.

Methods

Patient Enrollment

This study was approved by the local ethical committee Ethikkommission der Ärztekammer Westfalen-Lippe. All PKU patients >4 years of age with plasma Phe levels ≥600 μmol/L at diagnosis currently being followed at our metabolic center at Münster University Children's Hospital were contacted by mail to request participation in the trial. Exclusion criteria were age of <4 years, proven BH4 deficiency, and pregnancy. All patients gave informed consent to participate.

Sapropterin Response Testing

Before receiving treatment, patients had to have a minimum blood Phe level of 360 μmol/L and maintain stable blood

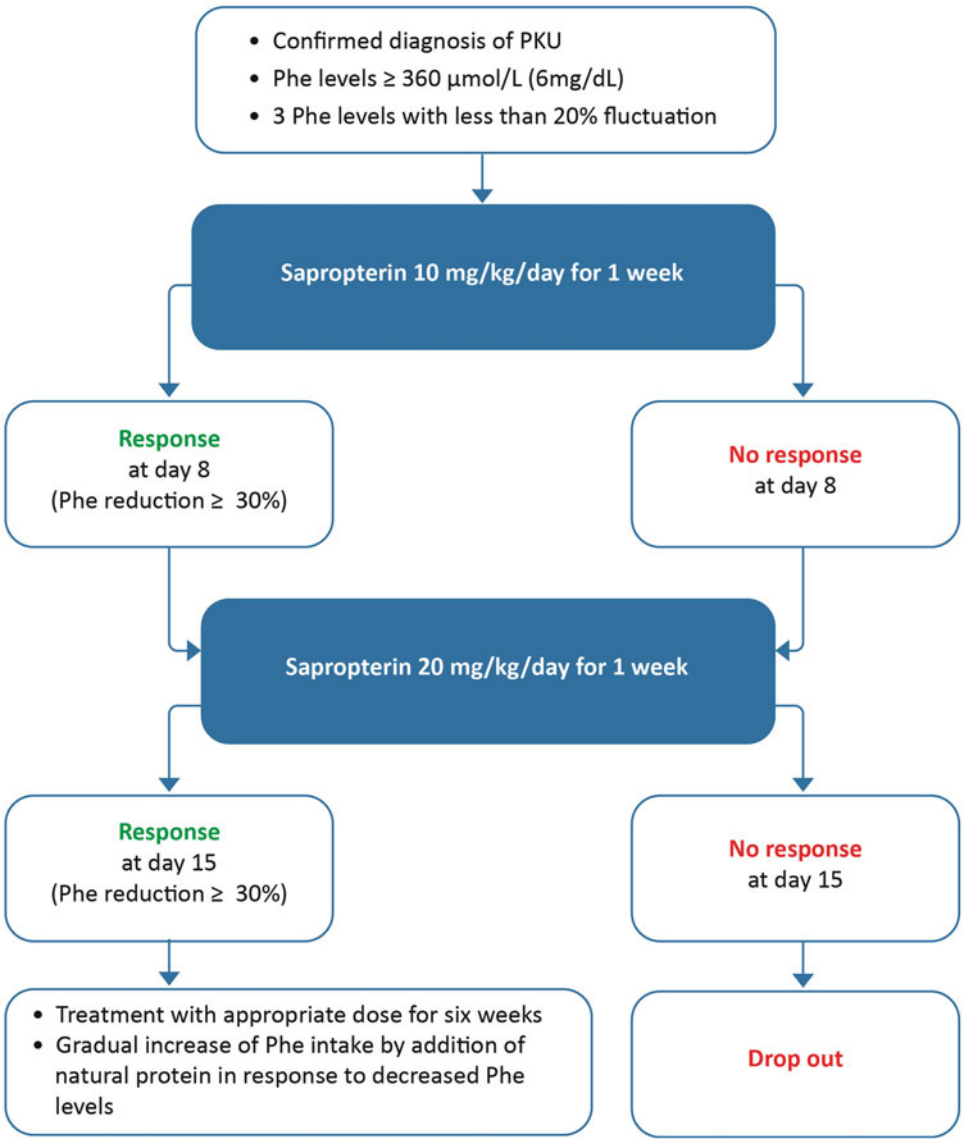

Fig. 1 Study design

Phe levels with <20 % fluctuation from baseline at three consecutive blood Phe draws (Fig. 1). To achieve this, plasma Phe levels were evaluated weekly by capillary blood draws. Patients' dietary regimens were assessed regularly by dieticians. If Phe levels were <360 µmol/L, patients were asked to increase dietary Phe intake slightly, but unlike in the protocol from Blau et al. (2009), a 100 mg/kg Phe challenge was not systematically performed. After having achieved three stable Phe levels, the patients were seen in the outpatient clinic for blood sampling for *PAH* mutation analysis and to obtain an additional blood Phe level prior to the first dose of sapropterin.

Sapropterin was dissolved in water or apple juice and was applied orally together with some food (Kuvan® US Prescribing Information). Sapropterin was initially administered at a dose of 10 mg/kg/day at the time of the outpatient visit. This dose was repeated at home every 24 h for another 6 days. At day 8 and regardless of the patient's response to sapropterin, the sapropterin dose was increased to 20 mg/kg per day for another 7 days to test the individual response to the higher dose to determine, if the higher dose has an additional effect on lowering Phe levels. The dietary regimen of the patients remained unchanged throughout the 2 weeks of the response test. Plasma Phe levels were measured at 24 h and 7 days after the first dose of sapropterin and 24 h and 7 days after the increased dose. All blood samples were taken in fasted state prior to the daily sapropterin intake.

Table 1 Demographic and baseline data for patients who completed the trial by December 2011

Demographic	
Completed trial N (% of those contacted)	112 (31.7 %)
Nationality N (%)	
German	84 (75 %)
Turkish	14 (13 %)
Russian	9 (8 %)
Other	5 (4 %)
Gender – male N (%)	59 (53 %)
Age mean (median; min, max) years	18 (15.7; 4, 45)
Baseline Phe levels mean (median; min, max) μmol/L	795.3 (754.5; 340.8, 1884)
Baseline Phe tolerance mean (median; min, max) mg/kg	14.88 (12.4; 2.84, 51.19)
Sapropterin responsive patients N (%)	46 (41.1 %)
Responsive at 10 mg/kg/day	22 (19.6 %)
Responsive only at 20 mg/kg/day	24 (21.4 %)

Extension Period After Sapropterin Response Resting

Sapropterin was discontinued for patients who did not show a ≥30 % decrease in Phe levels after 14 days. Those with ≥30 % decrease in Phe levels continued to be administered with sapropterin at a dose of 20 mg/kg/day regardless of whether response occurred at 10 mg/kg/day or 20 mg/kg/day. To determine the patients' individual increase in Phe tolerance due to sapropterin treatment in responsive patients, dietary Phe content was gradually increased over the subsequent 6 weeks through the addition of natural protein in the diet, potentially in form of natural bread or pasta products. The amount of Phe-free amino acid supplements required was reduced as appropriate. Phe levels were monitored weekly and were maintained within the age-appropriate target levels. It should be noted that these levels are currently under debate. We applied the target levels recommended for Germany: 0–9 years: 40–240 μmol/L; >9–15 years: 40–900 μmol/L; >15 years: 40–1200 μmol/L) (Schweitzer-Krantz and Burgard 2000). After the 8 weeks of the study period, the patients were seen on a regular basis in our outpatient metabolic clinic for dietary assessment and physical examination. Phe levels were monitored every 2 weeks.

Determination of Phenylalanine Plasma Levels

Phe levels were determined in plasma samples from capillary EDTA blood draws (100 μl EDTA blood) performed by the patients or their caregivers at home. Plasma samples were analyzed by ion exchange chromatography in an Eppendorf-Biotronik LC 3000 Amino Acid Analyzer® (Eppendorf GmbH, Wesseling-Berzdorf, Germany).

Mutation Analysis

Genomic DNA from each individual patient was isolated from EDTA blood samples according to a standard protocol using the EZ1DNA Blood Kit® (Qiagen GmbH, Hilden, Germany). PCR products were directly sequenced bidirectionally using the BigDye Terminator v3.1 Cycle Sequencing Kit on an ABI 3730 Genetic Analyzer according to the manufacturer's protocol (Applied Biosystems, Foster City, California, USA). All 13 exons of the *PAH* gene plus their exon–intron boundaries were analyzed. Primer sequences are available on request.

Reference accession number for normal alleles was ENSG00000171759.2 for *PAH*. Mutation designation was according to the official mutation nomenclature (http://www.hgvs.org/mutnomen/). To validate nomenclature of mutations, we used the program Mutalyzer 2.0 β-2 (http://www.mutalyzer.nl/2.0/). Mutations were confirmed by carrier analysis of parents.

Results

Patient Enrollment and Response Testing

The first patient was enrolled in the study in January 2010 and the last patient in October 2011. Three hundred and fifty-three patients were contacted by mail. Of these, we did not receive a response from 153 patients (43.3 %). Seventy patients (19.8 %) refused to take part in the study for a variety of reasons, including time constraints, effort required to comply with the strict regimen, safety concerns, satisfaction with current dietary regimen, aversion to tablets, and doubt about being sapropterin responsive.

Table 2 Baseline Phe levels and baseline Phe tolerance in all responders and corresponding changes in Phe levels and dietary Phe intake in all patients with continued treatment

Dosage for response	
10 mg/kg/day N	22
Patients with continuing treatment and increase in Phe tolerance N (%)	15 (68.2 %)[a]
Baseline Phe levels μmol/L mean (median; min, max)	607.3 (562.5; 403.8, 942)
Percentage decrease in Phe levels (median; min, max)	49.8 (44.9; 30, 84)
Baseline Phe tolerance mean (median; min, max) mg/kg	15.6 (15.3; 6.4, 36.9)
Mean percentage increase in Phe tolerance (median; min, max)	220.7 (150; 25, 742)
20 mg/kg/day excluding patients who responded at 10 mg/kg/day N	24
Patients with continuing treatment and increase in Phe tolerance N (%)	15 (62.5 %)[b]
Baseline Phe levels μmol/L mean (median; min, max)	673.1 (516.8;. 360, 1366.8)
Percentage decrease in Phe levels (median; min, max)	47.5 (42; 30, 77)
Baseline Phe tolerance mean (median; min, max) mg/kg	13.42 (11.9; 4.3, 42.4)
Mean percentage increase in Phe tolerance (median; min, max)	157.7 (122.2; 11, 450)

[a] 5 patients withdrew from follow-up due to noncompliance, 1 patient withdrew consent and 1 showed an unexplained increase of Phe levels after testing period despite constant Phe intake

[b] 5 patients did not show increased Phe tolerance despite response, 1 responsive patient showed an unexplained increase in Phe levels after testing period despite constant Phe intake, 3 patients withdrew consent

One hundred and thirty (36.8 %) patients contacted by mail consented and underwent sapropterin response testing. However, 16 patients were excluded, because they were not able to maintain stable Phe levels with less than 20 % fluctuation from baseline. One patient refused to have mutation analysis performed, and one was excluded due to noncompliance to the response test protocol. The remaining 112 (31.7 %) patients completed the response test by December 2011 (Table 1): 46 (41.1 %) patients were identified as responders (Table 2), while 66 (58.9 %) of patients who completed the response test did not show a reduction of $\geq$30 % in their serum Phe levels and were classified as nonresponsive to sapropterin therapy (Table 3). The median Phe levels in responders versus nonresponders during the test period are shown in Fig. 2.

Modification of Dietary Phe Intake Within the Six-Week Extension Period

Sapropterin treatment was stopped in 5 of the 46 patients identified as sapropterin responsive after the response test period due to noncompliance to the protocol and in 4 patients due to patient withdrawal of consent. Two patients showed an unexplained increase in Phe levels despite constant Phe intake and treatment was subsequently stopped in these patients as well. In the remaining 35 responders, dietary Phe was gradually increased with natural proteins in the daily diet. Sapropterin treatment was stopped in 5 further patients, who were initially classified as responders, because these patients showed elevated Phe levels while increasing the dietary Phe intake in the 6-week period.

In the 30 sapropterin-responsive patients, dietary Phe intake could be increased by a mean value of 189 % (median 128 %, range 11–742 %) compared to baseline while maintaining blood Phe levels in the age-appropriate range according to the German national guidelines (Schweitzer-Krantz and Burgard 2000) with a dose of 20 mg/kg/day. In these patients, average Phe tolerance increased from 13.8 mg/kg/day before sapropterin treatment to 35.2 mg/kg/day after 6 weeks of sapropterin therapy.

Conversely, the amount of amino acid supplements could be reduced on average of 41.5 % from 0.76 g/kg/day before sapropterin therapy to 0.46 g/kg/day for these patients after 6 weeks of sapropterin therapy (Table 2).

PAH Mutations in PKU Patients Associated with Response and with Nonresponse to Sapropterin Treatment

Mutation analysis of *PAH* was performed in all the 112 patients, who completed the observational trial for sapropterin response. The bi-allelic underlying *PAH* mutations were detected in 108 (96.4 %) patients. In 4 (3.6 %) patients, only one pathogenic mutation on one allele could be detected. The failure to detect the mutation on the other allele was likely based on our sequencing approach, which did not cover intronic mutations or large deletions within the *PAH* gene.

Several genotypes were consistently associated with nonresponse and low dose response to sapropterin treatment (Supplementary Table 1). Genotypes always associ-

Table 3 Baseline Phe levels and baseline Phe tolerance in all non-responders

Non-responders	
N	66
Baseline Phe levels µmol/L mean (median; min, max)	916.8 (900.6; 340.8, 1884)
Baseline Phe tolerance mean (median; min, max) mg/kg	15.16 (11.64; 2.84, 51.19)

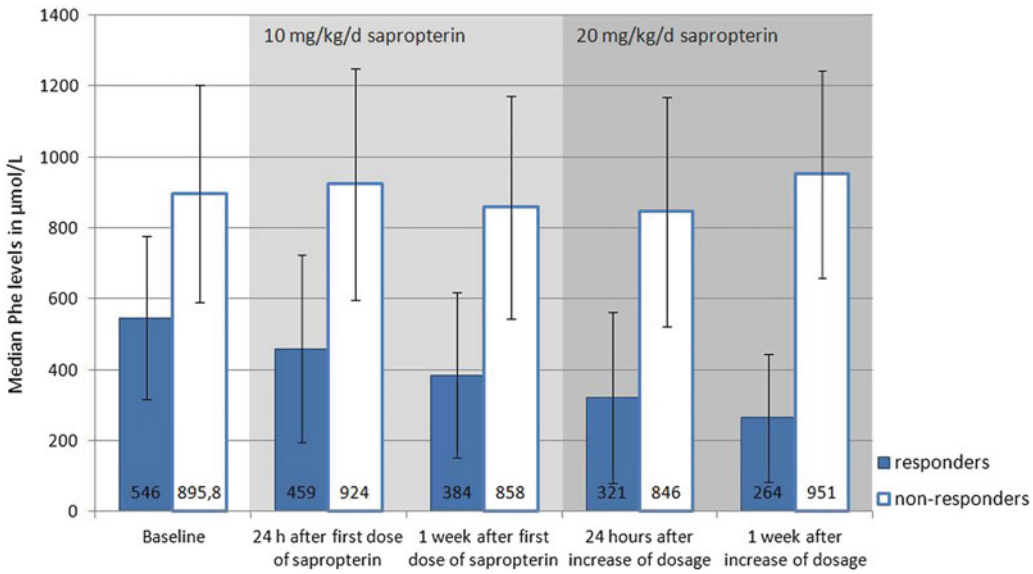

Fig. 2 Progress of median Phe levels during test period. Median Phe levels of 46 responders and 66 nonresponders are shown

ated with nonresponse to sapropterin at any dose were [IVS12+1G>A];[IVS12+1G>A], p.[L348V];[R408W], p.[P281L];[P281L], p.[R158Q];[R408W], and p.[R261Q];[R408W]. Genotypes always associated with low dose response were p.[L48S];[L48S] and p.[Y414C];[Y414C]. Thus, there were more genotypes that consistently predicted nonresponse than response to sapropterin therapy, and no genotype consistently predicted high dose response (Supplementary Table 1).

Mutations associated with response were dispersed throughout the *PAH* gene. In our study, we observed a high frequency of discriminative *N*-terminal mutations (regulatory domain, amino acid position 1-142) in the group of responders. Several mutations in the regulatory domain of PAH, for example I65T or R68S, were only present in responders and not detected in any of the 66 nonresponders. Mutations in the catalytic domain of the *PAH* protein (amino acid position 143-410) did not consistently predict response or nonresponse to sapropterin therapy.

Frequency of mutations found in our cohort varied, with the most common being the R408W mutation, present on 48 alleles of 42 patients. Several mutations were predictive of response or nonresponse. Y414C, L48S, I65T, F331S and R68S were always associated with response, while R158Q was consistently associated with nonresponse.

Discussion

In our cohort of 112 patients who participated in the study, 46 patients (41.1 %) showed a significant response on sapropterin therapy, consistent with the estimated response rate among PKU patients reported by Fiege and Blau (2007). Patients who responded at 10 mg/kg had higher baseline Phe tolerance and seemed to also have higher increase in Phe tolerance, suggesting mild/moderate PKU (Table 2). Of those "low dose responders," two probands were homozygous carriers of Y414C and five probands homozygous for L48S (Supplementary Table 1). Most of all responders show a clear increase in Phe tolerance (Table 2), with 7 of the 30 responders, treated continuously with sapropterin, being able to stop their Phe-restricted diet altogether while continuing a vegetarian diet.

Based on our cohort, *PAH* genotypes are helpful for predicting low dose response and nonresponse to sapropterin (Supplementary Table 1). However, no genotypes in our study were found to consistently predict high dose response. The genotype p.[P281L];[R408W] was found in six patients in our cohort (Supplementary Table 1). Of these, 5 were nonresponsive to sapropterin, yet one patient had a 31 % decrease in Phe levels at 20 mg/kg/day of sapropterin and was deemed responsive. While one might suspect change in dietary intake resulted in the decrease in Phe concentrations, this individual also had an 11 % increase in Phe tolerance, proving clinical benefit of treatment and thereby suggesting that this particular genotype cannot reliably discriminate between nonresponders and high dose response to treatment, consistent with the results of other studies (Trefz et al. 2009b). There are several other genotypes (Supplementary Table 1), which were found both, in nonresponders and in responders, underlying the difficulties in predicting sapropterin response only based on patients' genotype.

Interestingly, one individual of six found with homozygous R408W, the mutation most frequently found in our cohort and most commonly found throughout Europe associated with classical PKU (Eisensmith et al. 1995; Zschocke 2003; Zurflüh et al. 2008; Karacic et al. 2009; Dobrowolski et al. 2009) and generally nonresponse to sapropterin treatment (Dobrowolski et al. 2009), responded to sapropterin already at a low dose while the remaining five individuals were classified as nonresponsive. However, the responsive individual had increasing Phe levels with treatment despite consistent Phe intake, resulting in cessation of sapropterin treatment and the individual being classified as a false-positive responder. As a result, all individuals with homozygous R408W may be considered nonresponsive to sapropterin, consistent with findings in other studies (Dobrowolski et al. 2009). Also consistent with other findings, IVS12+1G>A was always associated with nonresponse when on both alleles (Polak et al. 2013; Utz et al. 2012) or when associated with the mutation R408W (Utz et al. 2012).

Genotypes with homozygous mutations are more likely to predict sapropterin response than compound heterozygous mutations (Supplementary Table 1). Homozygous Y414C, located in the tetramerization domain, is associated with response even at the low dose of sapropterin. In other studies, Y414C has been associated with response even when combined with other mutations strongly associated with nonresponse, such as R408W (Trefz et al. 2009b; Utz et al. 2012). Interestingly, in our study when Y414C was present on only one allele, it was found in patients with both an increased Phe tolerance of <100 % and in those with an increase >300 % after sapropterin therapy, suggesting that the mutation on the allele in trans of this particular mutation is important for predicting the full clinical benefit.

Homozygous L48S, also frequently found in Southern Europe (Zurflüh et al. 2008), was always associated with sapropterin response even at the 10 mg/kg/day dose and with a high increase of Phe tolerance on BH4 therapy in our cohort (Supplementary Table 1), consistent with other studies (Zurflüh et al. 2008). One patient carrying this mutation was able to tolerate >300 % more natural protein than before sapropterin therapy. L48S, previously detected on 24 alleles of sapropterin responders (*BIOPKU database,* http://www.biopku.org/BioPKU_DatabasesBIOPKU.asp), was associated with response even when present on only one allele.

In our study, a high frequency of mutations in the regulatory domain was found in the group of responders. However, in the literature mutations in the regulatory domain have been inconsistent in predicting response between studies, with some revealing sapropterin responsiveness even in classic PKU patients (Wang et al. 2007) and other studies have shown inconsistent responses with identical mutations having significantly differing response rates (Trefz et al. 2009b). Mutations in the predicted catalytic domain were associated with both response and nonresponse to sapropterin treatment. The F331S mutation was always associated with sapropterin response when present on both alleles in two patients of our cohort, while R158Q on at least one allele was always associated with nonresponse to sapropterin. While p.[R261Q];[R408W], found in five individuals, was always associated with nonresponse, individually the mutations R261Q (Staudigl et al. 2011) and R408W (Utz et al. 2012) failed to discriminate between responders and nonresponders in our study, consistent with what is reported in the literature.

Although it may be expected that patients receive increased support in our clinical trial in comparison to that available in a regular outpatient setting, almost 20 % of patients still refused to take part, some citing time constraints and effort required to comply with the strict regimen. Of those who participated, 18 withdrew before completion due to noncompliance or difficulties in reaching the required stability of pretest blood Phe values. These results reinforce the need for alternative, less rigorous means to determine clinical benefit to sapropterin treatment.

The most significant risk identified in our study and relevant to all response test protocols was illustrated by seven patients who were initially classified as sapropterin responsive whose blood Phe levels rose significantly either despite unchanged Phe intake or when challenged with an increase in dietary Phe intake. In these patients, we stopped sapropterin during the 6-week diet modification period. We hypothesize that the response test was not correctly performed in these patients and that the observed decrease

of Phe levels within the 2-week response test period merely reflected random fluctuations of their serum Phe levels or potential changes in diet during the response test protocol. As well, this limited control of the patient's diet may be the main argument against outpatient sapropterin response testing. However, combining the response test with a second phase of gradual increase of dietary Phe intake as done with our protocol allows efficient detection of false-positive responders, as seen with our patients. As well, the extended test time and the risk of false-positive results are outweighed by the increased comfort for patients being tested at home and a more cost-effective process than hospitalization.

Conclusions

Individual genotype influences response to sapropterin therapy in PKU patients. Based on our study, we can conclude that *PAH* genotypes can help predicting low dose and nonresponse to sapropterin. However, it still needs to be shown to what extent genotype information can be used to predict in vivo BH4 responsiveness, and as stated by Staudigl et al. the evaluation of sapropterin treatment should involve "personalized procedures to safely identify and treat patients with BH4-responsive PAH deficiency" (Staudigl et al. 2011).

Based on the limited number of patients included in our study and inconsistent results in the literature, it does not seem appropriate to preclude a particular mutation as not associated with sapropterin responsiveness due to the absence of this particular mutation in our group of responders or conclude that a group of patients will be responsive based on being classified as responder in this group. Still, the results of our study contribute to the growing body of literature on *PAH* genotypes associated with sapropterin response, and support performing sapropterin response testing in an outpatient setting as a feasible and reliable option to assess sapropterin responsiveness.

Acknowledgements This study and medical writing support was supported by an unrestricted grant from Merck Serono S.A. Medical writing support was provided by Judy Wiles of Facet Communications Incorporated.

References

Blau N, Bélanger-Quintana A, Demirkol M et al (2009) Optimizing the use of sapropterin (BH4) in the management of phenylketonuria. Mol Genet Metab 96:158–163

Burgard P, Bremer HJ, Bührdel P et al (1999) Rationale for the German recommendations for phenylalanine level control in phenylketonuria 1997. Eur J Pediatr 158:46–54

Dobrowolski SF, Borski K, Ellingson CC, Koch R, Levy HL, Naylor EW (2009) A limited spectrum of phenylalanine hydroxylase mutations is observed in phenylketonuria patients in western Poland and implications for treatment with 6R tetrahydrobiopterin. J Hum Genet 54:335–339

Eisensmith RC, Goltsov AA, O'Neill C et al (1995) Recurrence of the R408W mutation in the phenylalanine hydroxylase locus in Europeans. Am J Hum Genet 56:278–286

Enns GM, Koch R, Brumm V et al (2010) Suboptimal outcomes in patients with PKU treated early with diet alone: revisiting the evidence. Mol Genet Metab 101:99–109

Fiege B, Blau N (2007) Assessment of tetrahydrobiopterin (BH4) responsiveness in phenylketonuria. J Pediatr 150(6):627–630

Gersting SW, Lagler FB, Eichinger A et al (2010) *Pah*^{enu1} is a mouse model for tetrahydrobiopterin-responsive phenylalanine hydroxylase deficiency and promotes analysis of the pharmacological chaperone mechanism in vivo. Hum Mol Genet 19:2039–2049

Karacic I, Meili D, Saravka V et al (2009) Genotype-predicted tetrahydrobiopterin (BH4)-responsiveness and molecular genetics in Croatian patients with phenylalanine hydroxylase (PAH) deficiency. Mol Genet Metab 97:165–171

Kure S, Hou DC, Ohura T et al (1999) Tetrahydrobiopterin-responsive phenylalanine hydroxylase deficiency. J Pediatr 135:375–378

Kuvan® US Prescribing Information. http://www.kuvan.com/hcp/kuvan-full-prescribing-information.html, Accessed Sep 2013

Lee P, Treacy EP, Crombez E et al (2008) Safety and efficacy of 22 weeks of treatment with sapropterin dihydrochloride in patients with phenylketonuria. Am J Med Genet A 146A:2851–2859

Levy H, Milanowski A, Chakrapami A et al (2007) Efficacy of sapropterin dihydrochloride (tetrahydrobiopterin, 6R-BH4) for reduction of phenylalanine concentration in patients with phenylketonuria: a phase II randomised placebo-controlled study. Lancet 370:504–510

Muntau AC, Röschinger W, Habich M et al (2002) Tetrahydrobiopterin as an alternative treatment for mild phenalketonuria. N Engl J Med 347:2122–2132

National Institutes of Health Consensus Development Panel (2001) National Institutes of Health Consensus Development Conference Statement: Phenylketonuria: screening and management, October 16-18, 2000. Pediatrics 108:972–982

Polak E, Ficek A, Radvanszky J et al (2013) Phenylalanine hydroxylase deficiency in the Slovak population: genotype-phenotype correlations and genptype-based predictions of BH4-responsiveness. Gene 526(2):347–355

Schweitzer-Krantz S, Burgard P (2000) Survey of national guidelines for the treatment of phenylketonuria. Eur J Pediatr 159(Suppl 2):70–73

Scriver CR, Kaufman S (2001) Hyperphenylalaninemia: phenylalanine hydroxylase deficiency. In: Scriver CR, Beaudet AL, Sly WS, Valle D (eds) Metabolic and molecular basis of inherited disease. McGraw-Hill, New York, pp 1667–1724

Scriver CR, Levy H, Donlon J (2008) Hyperphenylalaninemia: phenylalanine hydroxylase deficiency. In: Valle D, Beaudet AL, Vogelstein B, Kinzler KW, Antonarakis SE, Ballabio A (eds) The online metabolic and molecular bases of inherited disease. http://www.ommbid.com. chapter 77

Staudigl M, Gersting SW, Danecka MK (2011) The interplay between genotype, metabolic state and cofactor treatment governs phenylalanine hydroxylase function and drug response. Hum Mol Genet 20:2628–2641

Thöny B, Ding Z, Martinez A (2004) Tetrahydrobioterin protects phenylalanine hydroxylase activity in vivo: implications for tetrahydrobiopterin-responsive hyperphenylalaninemia. FEBS Lett 577:507–511

Trefz FK, Burton BK, Longo N et al (2009a) Efficacy of sapropterin dihydrochloride in increasing phenylalanine tolerance in children

with phenylketonuria: a Phase III, randomized, double-blind, placebo controlled study. Pediatrics 154:700–707

Trefz FK, Scheible D, Götz H, Frauendienst-Egger G (2009b) Significance of genotype in tetrahydrobiopterin-responsive phenylketonuria. J Inherit Metab Dis 32:22–26

Utz JRJ, Lorentz CP, Markowitz D et al (2012) START, a double blind, placebo-controlled pharmacogenetic test of responsiveness to sapropterin dihydrochloride in phenylketonuria patients. Mol Genet Metab 105:193–197

Walter JH, White FJ, Hall SK et al (2002) How practical are recommendations for dietary control in phenylketonuria? Lancet 360:55–57

Wang L, Surendran S, Michals-Matalon K et al (2007) Mutations in the regulatory domain of phenylalanine hydroxylase and response to tetrahydrobiopterin. Genet Test 11:174–178

Weglage J, Ullrich K, Pietsch M et al (1996) Untreated non-phenylketonuric-hyperphenylalaninaemia: intellectual and neurological outcome. Eur J Pediatr 155(Suppl 1):S26–S28

Zschocke J (2003) Phenylketonuria mutations in Europe. Hum Mutat 21:345–356

Zurflüh MR, Zschocke J, Lindner M et al (2008) Molecular genetics of tetrahydrobiopterin responsive phenylalanine hydroxylase deficiency. Hum Mutat 29:167–175

JIMD Reports
DOI 10.1007/8904_2013_264

RESEARCH REPORT

Vestibular and Saccadic Abnormalities in Gaucher's Disease

Luke Chen • G. Michael Halmagyi • Michael J. Todd • Swee T. Aw

Received: 12 May 2013 / Revised: 28 August 2013 / Accepted: 09 September 2013 / Published online: 20 October 2013

Abstract Gaucher's disease (GD) is a hereditary lysosomal storage disease characterized by abnormal deposition of glucocerebroside due to the enzyme glucocerebrosidase deficiency, resulting in multi-organ pathology. GD type III has a progressive neurological involvement. We studied the vestibular and saccadic abnormalities in GD type III to determine if these parameters may be useful for assessing neurological involvement. We evaluated the vestibular and saccadic responses of two siblings with genetically identified GD type III on enzyme replacement therapy. Vestibular functions were assessed with the head impulse test (HIT), vestibular evoked myogenic potentials (VEMPs), and electrical vestibular stimulation (EVS). Saccadic functions were investigated with volitional horizontal and vertical saccades to ±20°. Three-dimensional head and eye movements were recorded with dual-search coils and VEMP with surface electrodes. HIT showed impaired individual semicircular canal function with halved angular vestibulo-ocular reflex (VOR) gains and absent horizontal refixation saccade. Ocular and cervical VEMPs to air-conducted clicks were absent in the older sibling, and only cervical VEMP was present in the younger sibling indicating otolithic dysfunction. EVS showed prolonged onset latency and attenuated tonic and phasic responses suggesting impaired neural conduction and vestibular function. Horizontal saccadic velocity was miniscule (<30°/s) and multiple back-to-back saccades with saccade-vergence interaction were utilized to minimize eye position error in the older sibling. Vertical saccades were slightly abnormal, but vergence and smooth pursuit were normal in both siblings. Our findings suggest that GD affected the vestibular nuclei in addition to the paramedian pontine reticular formation. These vestibular and saccadic abnormalities may be useful biomarkers to monitor neurological deterioration.

Communicated by: Ashok Vellodi

Competing interests: None declared

G.M. Halmagyi · S.T. Aw
Central Clinical School, University of Sydney, Sydney, Australia

L. Chen · G.M. Halmagyi · M.J. Todd · S.T. Aw (✉)
Institute of Clinical Neuroscience, Royal Prince Alfred Hospital, Camperdown, Sydney, NSW 2050, Australia
e-mail: sweea@icn.usyd.edu.au

Introduction

Gaucher's disease has three major subtypes: Type I is a non-neuropathic form; type II is an acute infantile neuropathic form; and type III is a subacute, juvenile neuropathic form (Winkelman et al. 1983). Slow horizontal saccade also termed as "ocular motor apraxia" a hallmark of types II and III has been reported as clinical observations (Harris et al. 1999), but never studied as three-dimensional eye movements. Previously, vestibular testing of the lateral semicircular canal function showed reduced caloric response (Winkelman et al. 1983) and absent vestibular response to yaw-axis rotation (Harris et al. 1999). Measurements of vestibular and saccadic functions in GD may provide quantitative parameters that may be used to evaluate enzyme replacement therapy's efficacy in preventing further neurological degeneration.

Our study aimed to determine the vestibular and saccadic abnormalities in GD type III. We characterized the vestibular function and its conduction pathways with mechanically and electrically evoked vestibular stimuli. We used the HIT to assess individual semicircular canal function (Aw et al. 2001); air-conducted click evoked ocular and cervical VEMPs to assess the otolith functions (Taylor et al. 2011) and EVS to examine the vestibular conduction pathway

latency, and low and high frequency response of the vestibular system (Aw et al. 2008). Ocular motor abnormalities were investigated with volitional horizontal and vertical saccades, vergence, and smooth pursuit (Fahey et al. 2008).

Methods

Subjects. Two siblings (male, age: 19, 17 years) with GD type III, treated with enzyme replacement therapy (Imiglucerase, Genzyme Therapeutics, USA) were studied. The older patient (P1) and his brother (P2) were diagnosed at age 4 and 2 by genetic identification. Hearing and brainstem auditory evoked responses were normal in both patients. The protocols were approved by our Ethics committee Sydney Local Health District Approval No: X10-0085, University of Sydney, Database No. 13076, in accordance with Helsinki II Declaration and written informed patient consents to perform this study were obtained.

Head and Eye Movement Recordings and Analysis

Three-dimensional head and binocular eye positions in response to vestibular and ocular motor tests were recorded with pre-calibrated dual-search coils (Universal, USA) in three-axes, horizontal, vertical, and torsional, while viewing a 2 mm fixation target. The search coil, target, and current stimulus signals were sampled at 1 kHz for the HIT and at 5 kHz for EVS using Labview (National Instruments, USA). Recording system resolution: horizontal/vertical = 0.1 arcminute; torsional = 0.3 arcminute. Maximum errors were <2%. The search coil signals were computed in three dimensions in rotation vectors and Euler angles as position and velocity in space/head fixed coordinates (Aw et al. 2001, 2008; Fahey et al. 2008; Weber et al. 2008).

Vestibular and Ocular Motor Tests

Head Impulse Test. HIT used high-acceleration passive head rotations at ~3,000°/s^2 along the six individual semicircular canal planes to test their angular VOR. VOR gains, onset latencies, and the saccadic refixation strategies were analyzed (Aw et al. 2001; Fahey et al. 2008; Weber et al. 2008).

Ocular and Cervical Vestibular Evoked Myogenic Potentials. VEMPs were tested using Nicolet EDX (CareFusion, UK) with air-conducted clicks (0.1 ms, 135 dB peak SPL) delivered via TDH49 headphone (Taylor et al. 2011). Ocular and cervical EMGs were sampled at 10 kHz and averaged. The first negative (n1) and positive (p1) peaks after stimulus onset, baseline to n1, and peak-to-peak amplitudes were measured. To judge an absent cervical VEMP, an average minimum level of baseline-rectified EMG of 100 μV must be present.

Electrical Vestibular Stimulation. EVS was a bilateral, bipolar 100 ms current-step at [0.9, 2.5, 5.0, 7.5] mA generated by a DS5 stimulator (Digitimer, UK) and delivered at 1/s via electrodes (Neutralect, USA) (Aw et al. 2008). Electrically evoked vestibulo-ocular reflex (eVOR) and onset latency were measured while tonic and phasic eVORs were determined with automated software (Aw et al. 2008).

Ocular Motor Test. Eye positions were recorded with dual-search coils for: (a) Saccades: subjects tracked target-steps at center and ±20° eccentric horizontally or vertically; (b) Vergence: subjects alternately viewed the target presented 15 cm or 60 cm away; (c) Smooth pursuit: subjects tracked a sinusoidal target that moved ±10° at (0.33 and 0.50) Hz (Fahey et al. 2008).

Results

The results of both patients' vestibular and ocular motor tests are summarized in Table 1.

Impaired Individual Semicircular Canal Function

The VOR gains from the HIT in all individual semicircular canals in both GD patients were reduced to a mean of 0.49 (Fig. 1a, b and Table 1), half of close to unity gain in normal subjects (Aw et al. 2001; Fahey et al. 2008; Weber et al. 2008). Head impulse latencies from all the semicircular canals were prolonged to a mean of 18 ms. Horizontal refixation saccades were absent in both patients to horizontal canal impulses, but overt and covert refixation saccades were present to anterior and posterior canal impulses (Weber et al. 2008).

Absent or Reduced Ocular and Cervical VEMP

Ocular and cervical VEMPs, which tested the otolith functions, were impaired in GD (Fig. 1c, Table 1). Ocular VEMPs were absent in both patients. Cervical VEMPs were absent in P1 in the presence average baseline-rectified EMG >100 μV. In P2, the cervical VEMP p13-n23 latencies were normal, and peak-to-peak amplitudes were at the lower limits of normal on both sides (Taylor et al. 2011).

Impaired Tonic and Phasic Responses to EVS

The eVOR latency measured with the torsional component was prolonged to 12 ms compared to normal of 9 ms (Aw et al. 2008). However, horizontal eVOR latency, which is

Table 1 Results from both Gaucher's Disease (GD) type III patients (P1, P2) to the head impulse test (HIT), ocular and cervical vestibular evoked myogenic potentials (VEMP), and electrical vestibular stimulation (EVS). The symbol (−) indicates absent response

		Head impulse test			
			VOR gain		
Patient	Side	Latency H/A/P (ms)	Horizontal	Anterior	Posterior
P1	L	21/18/19	0.38 ± 0.01	0.36 ± 0.01	0.58 ± 0.01
	R	20/16/19	0.53 ± 0.01	0.38 ± 0.01	0.57 ± 0.03
P2	L	16/18/20	0.71 ± 0.01	0.39 ± 0.01	0.35 ± 0.03
	R	14/19/20	0.81 ± 0.01	0.57 ± 0.02	0.27 ± 0.01
		Ocular VEMP			
		p13 (ms)	n23 (ms)	p-p (μV)	
P1	L	–	–	–	
	R	–	–	–	
P2	L	–	–	–	
	R	–	–	–	
		Cervical VEMP			
		p13 (ms)	n23 (ms)	p-p (μV)	
P1	L	–	–	–	
	R	–	–	–	
P2	L	10.8	19.0	71.7	
	R	10.7	18.9	63.3	
		Electrical vestibular stimulation			
		Onset latency at 7.5 mA	Tonic eVOR (°/s)	Phasic eVOR initiation (°/s^2)	Phasic eVOR cessation (°/s^2)
		(ms)	0.9/2.5/5.0/7.5 mA	0.9/2.5/5.0/7.5 mA	0.9/2.5/5.0/7.5 mA
P1	L	11.4	0.49/1.53/3.74/5.38	0/187/398/702	0/232/414/448
	R	11.4	0.58/1.39/2.92/4.17	0/193/381/439	0/196/341/537
P2	L	12.2	0.28/0.63/1.74/2.73	0/119/294/424	0/158/227/329
	R	12.2	0.51/0.70/1.76/2.59	0/0/187/322	0/0/230/349

normally the same as torsional latency, was prolonged to 16 ms. Tonic eVOR was symmetrically reduced in both GD patients (typified by P1 in Fig. 1d, Table 1) while phasic eVOR initiation and cessation were attenuated to about half normal response in both patients.

Slowed Horizontal Saccades and Impaired Vertical Saccades

Visually guided volitional horizontal saccades to ±20° were severely slowed when compared to vertical saccades in both patients (Fig. 2). The horizontal saccades in P1 consisted of multiple (≥5) tiny back-to-back saccadic steps of (1–2°) and peak horizontal eye velocities of between 5 and 30°/s (Fig. 2a). P1 achieved 75% of his desired eye position with multiple saccades assisted by vergence eye movements with resulting horizontal saccadic hypometria. Small vertical and torsional saccadic eye movements present during horizontal saccades were normal. Similar multiple (≥5) saccades in P2 with higher peak horizontal eye velocities of between 5 and 60°/s. P2 was able to achieve the target without saccadic hypometria and without requiring vergence because of higher peak horizontal eye velocity (Fig. 2b). Vertical saccades were also abnormal and impaired in P1 with the mean initial saccade amplitude of 12.6° with mean velocity of 211°/s, achieving 60% of target position typified by P1 in Fig. 2c. Downward saccade was more affected than upward saccade in P1. The mean latency in the P1 for horizontal saccade was 341 ms and vertical saccade was 211 ms which were similar to normal saccadic latencies. Horizontal smooth pursuit and vergence were normal in both patients (typified by P1 in Fig. 2d, e). The age-matched normal subject during either horizontal or vertical saccades to ±20° showed a large initial saccade amplitude of about 19° with peak velocity of 300–400°/s to achieve about 95% of the desired eye position followed by a smaller saccade to acquire the target (Fig. 2f, g). The mean latency in the normal subject for horizontal saccade was 380 ms and vertical saccade was 302 ms.

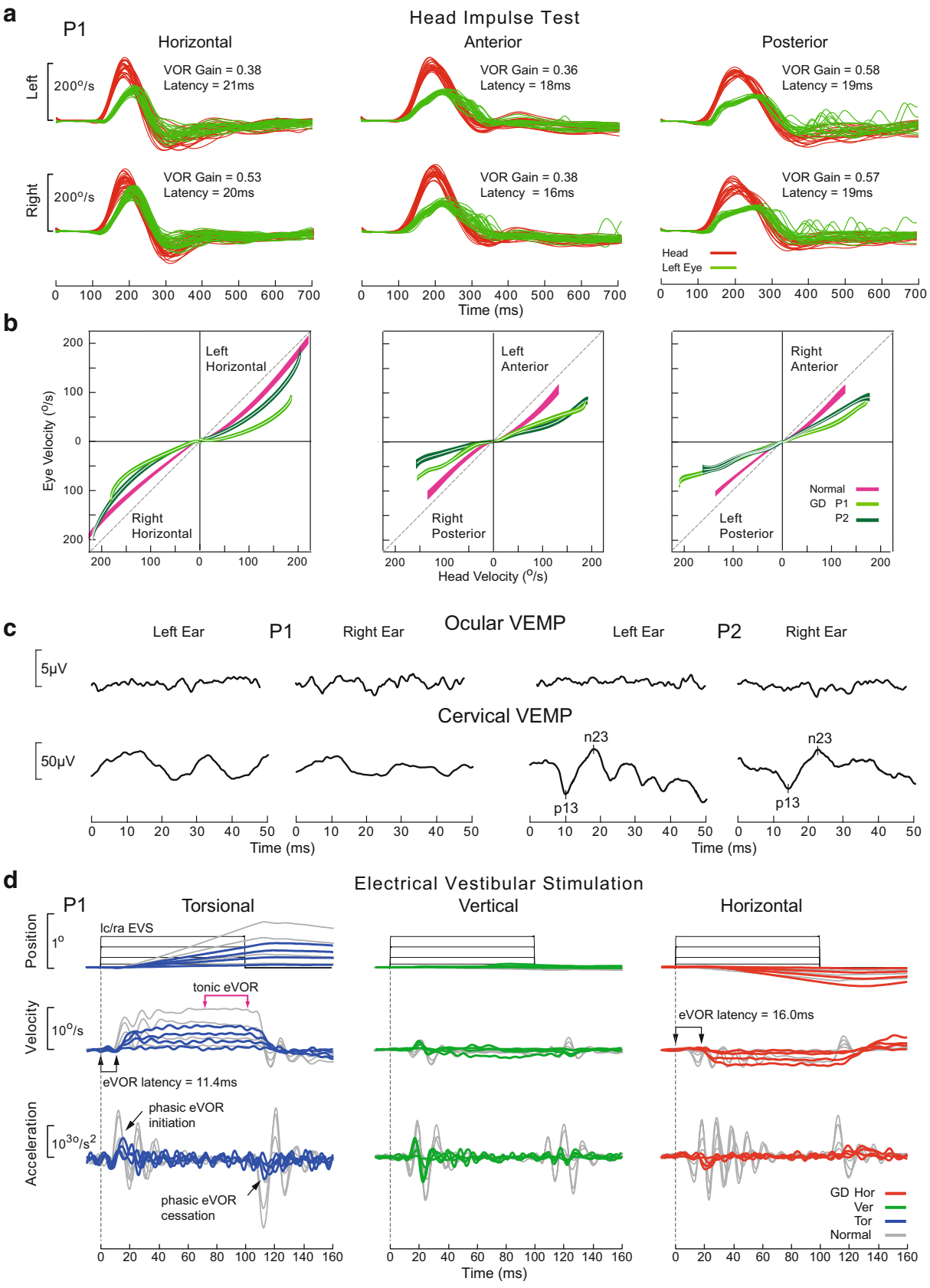

Fig. 1 (**a**) Time series of head impulse test of horizontal, anterior, and posterior semicircular canals in Gaucher's disease (GD) type III typified by patient P1 (*older sibling*). The angular vestibulo-ocular reflex (VOR) gains were reduced about half of normal close to unity gain. Latency of the angular VOR was prolonged to a mean of about 18 ms, twice normal latency. Despite the decline in horizontal angular

Discussion

The newer vestibular tests in this study provide quantitative measurements of the vestibular function. Vestibular abnormalities in the two GD type III patients from mechanically and electrically evoked vestibular stimuli suggest that GD also universally affects the brainstem vestibular nuclei which have been shown to suffer neuronal loss in infantile GD type II (Lacey and Terplan 1984).

Horizontal, anterior, and posterior semicircular canal functions measured with the HIT were impaired as the angular VOR gains were about half of the close to unity gain in normal subjects (Aw et al. 2001; Fahey et al. 2008; Weber et al. 2008). Onset latencies of HIT were prolonged from (7–10) ms (Aw et al. 1996) to ~18 ms. Horizontal saccadic initiation failure (Harris et al. 1999) caused the absence of horizontal refixation saccades in response to the reduced horizontal VOR gain. This precludes clinical observation of the horizontal refixation saccade in presence of deficient horizontal VOR gain (Halmagyi and Curthoys 1988). However, monitoring the head impulse test can now be done clinically using video-oculography (MacDougall et al. 2009).

Ocular VEMPs were absent in both patients and cervical VEMPs were absent in P1 and at the lower limit of normal in P2 suggesting that otolithic functions were also compromised (Taylor et al. 2011). Ocular VEMPs, which mostly screens utricular function, were more susceptible to damage than cervical VEMPs which assess saccular function (Rosengren and Kingma 2013).

EVS provides both low and high frequency stimuli to both semicircular canal and otolith pathways (Aw et al. 2008). Both tonic eVOR and phasic eVOR initiation and cessation were reduced and attenuated. The prolonged eVOR latency of 12 ms for the torsional component and 16 ms for the horizontal component compared to normal latency of 9 ms suggests a neural conduction delay. Neuronal loss in vestibular nuclei may account for both impaired vestibular response as well as the conduction delay (Lacey and Terplan 1984).

Gaucher's disease is well known to cause slow horizontal saccades due to neuronal destruction of the paramedian pontine reticular formation (Winkelman et al. 1983; Harris et al. 1999). However, the slow horizontal saccade observed clinically has never been quantitatively measured. Our study again quantitatively measured and confirmed this horizontal saccadic slowing in GD type III (Harris et al. 1999; Benko et al. 2011). Detailed three-dimensional examination of the slowed horizontal saccades increases our understanding of deficits in the neural substrates that control saccades in GD type III (Ramat et al. 2007). When a saccade is initiated, omnipause neurons in raphe interpositus nucleus stop tonic inhibition of premotor burst neurons of horizontal saccades in paramedian pontine reticular formation and vertical saccades in the rostral interstitial nuclei of the medial longitudinal fasciculus. Synchronous bursts of horizontal, vertical, and torsional saccadic velocities in our data support the integrity of the omnipause neurons. However miniscule horizontal saccadic velocity suggests the loss of premotor burst neurons in paramedian pontine reticular formation, responsible for horizontal saccadic velocity initiation and amplitude. The neural integrator in the nucleus prepositus hypoglossi and medial vestibular nucleus may also be impaired because of the saccadic hypometria observed in P1. Multiple back-to-back saccades with saccade-vergence interaction were utilized and minimized to eye position error, which can be observed clinically as slow horizontal saccades. Disconjugate eye movements in the older sibling confirmed that the premotor commands that encoded monocular eye movement signals to lateral rectus and medial rectus separately in paramedian pontine reticular formation (Zhou and King 1998) can be affected to different extents in GD type III. Presently saccadic test used to follow-up patients on the disease progression can also be clinically measured using infrared oculography (Fahey et al. 2008). The patients also showed early vertical saccadic abnormalities evidenced by the smaller initial saccadic amplitude with lower peak velocity and only achieving about 60% of desired target position similar to responses previously reported (Benko et al. 2011). However, their horizontal and vertical saccadic latencies were normal and not prolonged.

These novel vestibular tests together with saccadic measurements might be useful as qualitative and quantitative biomarkers to monitor further central nervous system deterioration in GD patients on therapeutic enzyme replacement. The vestibular parameters such as HIT VOR gain, EVS onset latency, and VEMP peak-to peak amplitude may be useful clinical outcome measures for clinical trials that, for example, can be correlated with their modified Rankin

VOR gain, there was absence of horizontal refixation saccades. (**b**) Phase-plane plots of eye velocity versus head velocity to head impulse tests of both GD patients (*P1*, *P2*) compared to normal response showing the reduction in angular VOR gain. (**c**) Ocular and cervical vestibular evoked myogenic potentials (VEMPs) evoked by air-conducted clicks (0.1 ms, 135 dB peak SPL) used to assess otolith functions. *P1* showed absence of both ocular and cervical VEMPs bilaterally. *P2* (*younger sibling*) had preserved cervical VEMP at the lower limits of normal, but complete absence of ocular VEMP. (**d**) Tonic and phasic eVORs in response to electrical vestibular stimulation (EVS) were symmetrically reduced to about half of age-matched normal subject. Latency of eVOR was prolonged to ~12 ms for torsion (normal latency was ~9 ms), but to 16 ms for horizontal

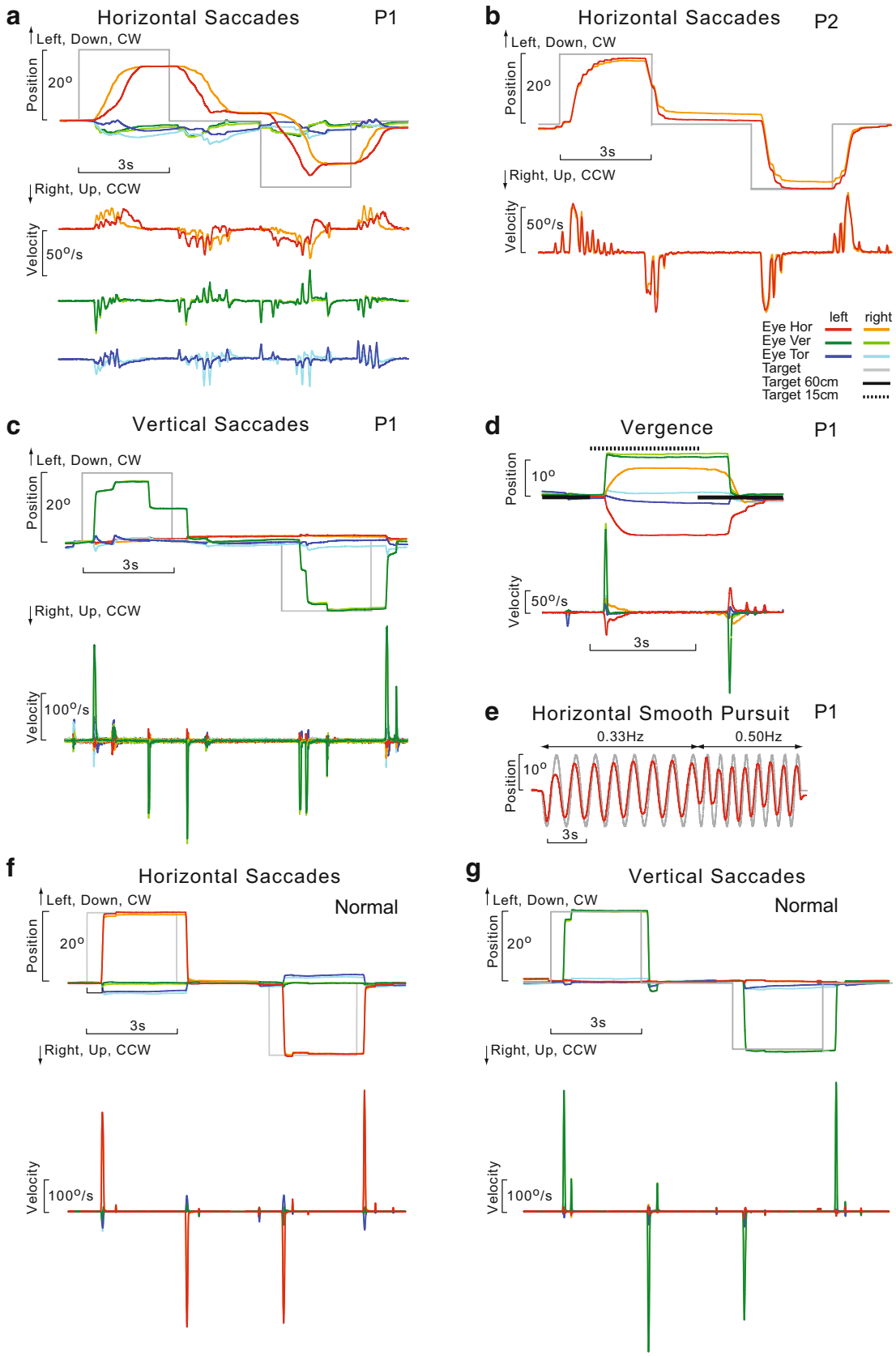
a
Horizontal Saccades
P1
Left, Down, CW
Position
20°
3s
Right, Up, CCW
Velocity
50°/s
b
Horizontal Saccades
P2
Left, Down, CW
Position
20°
3s
Right, Up, CCW
Velocity
50°/s
left
right
Eye Hor
Eye Ver
Eye Tor
Target
Target 60cm
Target 15cm
c
Vertical Saccades
P1
Left, Down, CW
Position
20°
3s
Right, Up, CCW
Velocity
100°/s
d
Vergence
P1
Position
10°
Velocity
50°/s
3s
e
Horizontal Smooth Pursuit
P1
0.33Hz
0.50Hz
Position
10°
3s
f
Horizontal Saccades
Normal
Left, Down, CW
Position
20°
3s
Right, Up, CCW
Velocity
100°/s
g
Vertical Saccades
Normal
Left, Down, CW
Position
20°
3s
Right, Up, CCW
Velocity
100°/s

Scale scores used for measuring the degree of disability and dependence (Patel et al. 2012). This information may then be used to manage the patient's activities of daily living such as driving a motor vehicle and occupational pursuits that require visual-vestibular interaction.

Acknowledgments This study was supported by National Health and Medical Research Council, Garnett Passe and Rodney Williams Memorial Foundation, The University of Sydney, Neurology Trustees Royal Prince Alfred Hospital.

Take-Home Message

Gaucher's disease has distinctive vestibular and eye movement abnormalities, which could be used as biomarkers of neurological involvement.

Compliance with Ethics Guidelines

Conflict of Interest

Luke Chen declares that he has no conflict of interest.

Michael J Todd declares that he has no conflict of interest.

G Michael Halmagyi is an unpaid consultant of GN Otometrics and received funding for travel related to GN Otometrics.

Swee T Aw declares that she has no conflict of interest.

Informed Consent

All procedures followed were in accordance with the ethical standards of the responsible committee on human experimentation: Sydney Local Health District, Approval No: X10-0085, University of Sydney, Database No. 13076, and with the Helsinki Declaration of 1975, as revised in 2000 (5). Informed consent was obtained from all patients for being included in the study.

No identifying information about patients is included in the article.

Contributions of Individual Authors

Luke Chen tested the patients, analyzed their data, assisted in interpreting the data, preparing and revising the manuscript for intellectual content.

Michael J Todd designed and implemented the hardware and software for data collection and data analysis and assisted in revising the manuscript for intellectual content.

G Michael Halmagyi recruited the patients from Royal Prince Alfred Hospital, Australia, and assisted in revising the manuscript for intellectual content.

Swee T Aw designed the study, prepared and interpreted all the research data and figures. She was in charge of drafting, revising for intellectual content, and submitting the manuscript.

Guarantor

Dr SweeT Aw serves as guarantor for the article, accepts full responsibility for the work and/or the conduct of the study, had access to the data, and controlled the decision to publish.

Research Funding

This study was funded by the National Health and Medical Research Council Australia, Garnett Passe and Rodney Williams Memorial Foundation, University of Sydney, and Royal Prince Alfred Hospital Neurology Trustees. The authors confirm independence from the sponsors; the content of the article has not been influenced by the sponsors.

References

Aw ST, Haslwanter T, Halmagyi GM, Curthoys IS, Yavor RA, Todd MJ (1996) Three-dimensional vector analysis of the human vestibuloocular reflex in response to high-acceleration head rotations. I. Responses in normal subjects. J Neurophysiol 76(6):4009–4020

Aw ST, Fetter M, Cremer PD, Karlberg M, Halmagyi GM (2001) Individual semicircular canal function in superior and inferior vestibular neuritis. Neurology 57(5):768–774

Fig. 2 (**a**) Horizontal saccades in Gaucher's Disease (GD) type III. *P1* had more severe abnormalities because he commenced enzyme replacement therapy at age 4, while *P2* had treatment at age 2 after genetic testing following his brother's diagnosis. In *P1* during horizontal saccades, horizontal eye velocities were between 5 and 30°/s (compared to an age-matched normal horizontal saccadic eye velocities 300–400°/s). There were multiple back-to-back horizontal saccades, and he achieved 75% of his desired eye position assisted by vergence eye movements resulting in saccadic hypometria. The small vertical and torsional saccadic eye movements were present during horizontal saccades were normal. (**b**) In *P2*, multiple saccades compensated for the slow horizontal saccadic eye velocity with any vergence eye movements. (**c**) Both patients' vertical saccadic eye movements (typified by *P1*) were slightly abnormal in position and velocity. (**d**) Vergence eye movements and (**e**) horizontal smooth pursuit were normal in both patients (typified by *P1*). (**f**) Age-matched normal horizontal saccades and (**g**) vertical saccades

Aw ST, Todd MJ, Aw GE, Weber KP, Halmagyi GM (2008) Gentamicin vestibulotoxicity impairs human electrically evoked vestibulo-ocular reflex. Neurology 71(22):1776–1782

Benko W, Ries M, Wiggs EA, Brady RO, Schiffmann R, Fitzgibbon EJ (2011) The saccadic and neurological deficits in type 3 Gaucher disease. PLoS One 6(7):e22410

Fahey MC, Cremer PD, Aw ST et al (2008) Vestibular, saccadic and fixation abnormalities in genetically confirmed Friedreich ataxia. Brain 131(Pt 4):1034–1045

Halmagyi GM, Curthoys IS (1988) A clinical sign of canal paresis. Arch Neurol 45(7):737–739

Harris CM, Taylor DS, Vellodi A (1999) Ocular motor abnormalities in Gaucher disease. Neuropediatrics 30(6):289–293

Lacey DJ, Terplan K (1984) Correlating auditory evoked and brainstem histologic abnormalities in infantile Gaucher's disease. Neurology 34(4):539–541

MacDougall HG, Weber KP, McGarvie LA, Halmagyi GM, Curthoys IS (2009) The video head impulse test: diagnostic accuracy in peripheral vestibulopathy. Neurology 73(14):1134–1141

Patel N, Rao VA, Heilman-Espinoza ER, Lai R, Quesada RA, Flint AC (2012) Simple and reliable determination of the modified ranking scale score in neurosurgical and neurological patients: the mRS-9Q. Neurosurgery 71:971–975

Ramat S, Leigh RJ, Zee DS, Optican LM (2007) What clinical disorders tell us about the neural control of saccadic eye movements. Brain 130(Pt 1):10–35

Rosengren SM, Kingma H (2013) New perspectives on vestibular evoked myogenic potentials. Curr Opin Neurol 26(1):74–80

Taylor RL, Wijewardene AA, Gibson WP, Black DA, Halmagyi GM, Welgampola MS (2011) The vestibular evoked-potential profile of Ménière's disease. Clin Neurophysiol 122(6): 1256–1263

Weber KP, Aw ST, Todd MJ, McGarvie LA, Curthoys IS, Halmagyi GM (2008) Head impulse test in unilateral vestibular loss: vestibulo-ocular reflex and catch-up saccades. Neurology 70(6): 454–463

Winkelman MD, Banker BQ, Victor M, Moser HW (1983) Non-infantile neuronopathic Gaucher's disease: a clinicopathologic study. Neurology 33(8):994–1008

Zhou W, King WM (1998) Premotor commands encode monocular eye movements. Nature 393(6686):692–695<

JIMD Reports
DOI 10.1007/8904_2013_265

RESEARCH REPORT

Evaluation of Physiological Amino Acids Profiling by Tandem Mass Spectrometry

Romain Filee • Roland Schoos • François Boemer

Received: 13 June 2013 / Revised: 30 August 2013 / Accepted: 09 September 2013 / Published online: 5 November 2013

Abstract Background: Nowadays, the most conventional method to quantify physiological amino acids consists in ion exchange chromatography (IEC) followed by post-column ninhydrin derivatization and UV detection at two wavelengths. Unfortunately, the technique presents some drawbacks such as long run time, large sample volume, and specific costs associated to the maintenance of a dedicated instrument. Therefore, we aimed to switch towards a mass spectrometry approach.

Methods: We have tested the aTRAQ kit for Amino Acid Analysis of Physiological Fluids (AB Sciex), affording the selective quantification of about 40 amino acids, and present here the results of our assessments.

Results: Outlined accuracy profiles for each amino acid demonstrated very reliable data. A good linearity was observed from 1 to 1,000 μmol/L. Results comparison with IEC showed a right concordance. Reference intervals established were very similar to those obtained by IEC and patients suffering from inborn error of metabolism have been readily identified.

Conclusions: The present approach offers a valid alternative to the IEC method, with several advantages: lower sample volume, run time reduction, and improved specificity. However, the aTRAQ method requires minute data reviewing, expending the overall time of procedure. Finally, financial and practical considerations of both techniques have to be counterbalanced before engaging any transition.

Communicated by: Bridget Wilcken

Competing interests: None declared

Electronic supplementary material: The online version of this chapter (doi:10.1007/8904_2013_265) contains supplementary material, which is available to authorized users.

R. Filee · R. Schoos · F. Boemer
Biochemical Genetics Laboratory, Human Genetics, CHU Liege, University of Liege, Liege, Belgium

F. Boemer (✉)
Biochemical Genetics Laboratory, CHU Sart-Tilman, University of Liege, 4000 Liege, Belgium
e-mail: F.Boemer@chu.ulg.ac.be

Abbreviations

1MHis	1-Methylhistidine
3MHis	3-Methylhistidine
Aad	Alpha-Aminoadipate
Abu	Alpha-Aminobutyrate
Ala	Alanine
Ans	Anserine
Arg	Arginine
Asa	Argininosuccinate
Asn	Asparagine
Asp	Aspartate
bAib	Beta-Aminoisobutyrate
bAla	Beta-Alanine
BSA	Bovine Serum Albumin
Car	Carnosine
Cit	Citrulline
Cth	Cystathionine
Cys	Cystine
ERNDIM	European Research Network for evaluation and improvement of screening Diagnosis and treatment of Inherited disorders of Metabolism
EtN	Ethanolamine
GABA	Gamma Aminobutyrate
Gln	Glutamine
Glu	Glutamate
Gly	Glycine

Hcit	Homocitrulline
Hcy	Homocystine
His	Histidine
HPLC	High Pressure Liquid Chromatography
Hyl	Hydroxylysine
Hyp	Hydroxyproline
IEC	Ion Exchange Chromatography
IEM	Inborn Error of Metabolism
Ile	Isoleucine
IS	Internal Standard
Leu	Leucine
Lys	Lysine
Met	Methionine
MRM	Multiple Reaction Monitoring
MS	Mass Spectrometry
Nle	Norleucine
Nva	Norvaline
Orn	Ornithine
PEtN	Phosphoethanolamine
Phe	Phenylalanine
Pro	Proline
PSer	Phosphoserine
Sar	Sarcosine
Ser	Serine
Tau	Taurine
Thr	Threonine
Trp	Tryptophane
Tyr	Tyrosine
Val	Valine

Introduction

Amino acid disorders represent an important field in the wide classification of inborn errors of metabolism (WHO 2010). Such conditions result from a defect in the metabolic pathways of amino acids, leading to the accumulation of the corresponding metabolite in plasma, urine, cerebrospinal, amniotic fluid, or other biological matrix.

Besides the conventional 20 proteinogenic amino acids, several nonstandard amino acids hold critical physiological functions. Some of them are the result of posttranslational protein modification (i.e., hydroxyproline), which is an essential process for the function or regulation of proteins, while others are intermediates of metabolic pathways (i.e., urea cycle intermediates) and they also act as neurotransmitters (i.e., GABA). Acknowledging the central role of amino acids in protein synthesis and metabolism homeostasis, profiling of these markers has became a noticeable tool in the identification and follow-up of primary disorders. The biochemical findings that may be present in amino acid disorders include metabolic acidosis, hyperammonemia, hypoglycemia with appropriate or increased ketosis, multi-system disorder, developmental delay, encephalopathy, coma, or death.

Amino acids are not only associated with inborn errors of metabolism, they are also sensitive markers of the nutritional state and of the function of various organs such as the liver, the kidneys, the intestine, or the muscles. These dysfunctions generate subtle alterations in amino acid concentrations; therefore, accuracy of the amino acid analysis is a crucial matter in order to interpret these changes.

In those contexts' workup, the most conventional method for amino acid quantification consists in ion exchange chromatography (IEC) followed by post-column ninhydrin derivatization and UV detection at two wavelengths. Actually, amino acid analyzers have been used since more than 50 years in biochemical laboratories and still are considered as a reference method (Dietzen et al. 2008; Duran 2008). Notwithstanding, the technology suffers some drawbacks; chromatographic separation lasts about 150 min and requires high sample volumes (>100 μL). In addition, running analysis on dedicated instruments, requiring expensive maintenance costs, depicts another leading concern.

Considering the disadvantages of IEC technique and owning a triple quadrupole mass spectrometer for the newborn screening of inborn errors of metabolism, we wanted to evaluate a mass spectrometry approach. Nowadays, identification and quantification of amino acids by mass spectrometry are rather uncommon in clinical laboratories. Only a few methods have already been developed and validated and are based either on native (Piraud et al. 2003, 2005; Waterval et al. 2009) or on derivatized (Dettmer et al. 2012; Dietzen et al. 2008; Harder et al. 2011; Held et al. 2011) metabolites identification.

Based on this perception, we have tested the aTRAQ kit for Amino Acid Analysis of Physiological Fluids (AB Sciex), affording the selective quantification of about 40 amino acids. We report here the results of our assessment, based on plasma, urine, and cerebrospinal fluid (CSF) samples.

Material and Methods

Chemicals

aTRAQ kit for Amino Acid Analysis of Physiological Fluids was provided by AB Sciex. Mixes of amino acid standards (reference numbers A6407 and A6282), glutamine and sodium chloride (NaCl) were obtained from Sigma. Bovine serum albumin (BSA) was purchased at Roche.

Samples

Five-point calibration curves were prepared by diluting amino acid standard mixes and glutamine in 75 g/L BSA, isotonized with 0.9 g/L NaCl. Final calibration concentrations were the following: 1,000, 250, 100, 50, and 10 μmol/L for all amino acids, except for cystine whose concentrations were 500, 125, 50, 25, and 5 μmol/L.

Validation samples were prepared in the same way with final concentrations at 1,000, 200, 75, 20, 5, and 1 μmol/L for all amino acids, except for cystine whose concentrations were 500, 100, 37.5, 10, 2.5, and 0.5 μmol/L. Samples from the ERNDIM Amino Acids Scheme have also been used for method validation; target concentrations used corresponded to the consensus mean concentrations of all participating laboratories.

Plasma, urine, and CSF samples were gathered from normal individuals.

Sample Derivatization

Conceptually, amino groups are labeled with tags of varying isotope patterns. The label consists of a reporter group (with the masses m/z 113 or 121), a neutral linker, and an amino-reactive group (N–hydroxysuccinimide ester). The 121-labeling reagent is used to derivatize the amino acids in the sample, whereas the 113-labeling reagent is employed to provide a 113-labeled standard mix containing 42 analytes for absolute quantification.

Briefly, sample (40 μL) proteins were precipitated with 10 % sulfosalicylic acid (10 μL) containing 400 μmol/L norleucine. After vortexing and centrifugation, the supernatant (10 μL) was mixed with 40 μL labeling buffer containing norvaline. At this moment, part of the mixture (20 μL) can be set aside if allo-isoleucine quantification is necessary. To 10 μL of this reaction mix, 5 μL of isopropanol diluted aTRAQ Δ8-reagent was added. After 30-min incubation at room temperature, 5 μL of hydroxylamine was added and homogenized mixture was incubated 15 min at room temperature. Then, 32 μL of reconstituted aTRAQ Internal Standard solution was added to the reaction mixture. If allo-isoleucine testing is mandated, 5 μL of underivatized mix, saved from the second step, is added. The specimen is then partly concentrated under nitrogen for 15 min. Finally, half-evaporated samples were diluted 10 times with milli-Q water before injection.

Allo-isoleucine coelutes with isoleucine when labeled with the aTRAQ Δ8-reagent. Therefore, for confirmation and follow-up of maple urine syrup disease (MSUD) patients, allo-isoleucine is quantified in its underivatized form, which is then chromatographically well separated from isoleucine.

Separation and Detection

Derivatized samples (1 μL) were introduced into a TQ5500 tandem mass spectrometer (AB Sciex) using a Prominence AR HPLC system (Shimadzu).

Tagged amino acids were chromatographically separated on the AB Sciex C18 column at 50 °C. The column dimension was 15 cm long, with a 4.6 mm inner diameter. A binary gradient of water (mobile phase A) and methanol (mobile phase B), both containing 0.1 % formic and 0.01 % heptafluorobutyric acids, was flowing through the system at 0.8 mL/min. The percentage of mobile phase B was gradually increased from 2 % to 90 % in 13 min, followed by a 5-min re-equilibration step.

Acquisition in the mass spectrometer was achieved by multiple reaction monitoring (MRM) using the scheduled MRM algorithm (See Supplemental Data Table 1). This latter functionality eliminates the requirement of multi-period experiments by monitoring each transition only across its expected elution time. MRM transitions are then organized automatically, optimizing dwell time, cycle time, and detection window.

Data recording and treatment were performed with the v.1.6 Analyst software (AB Sciex).

Quantification

As recommended by manufacturer, quantification was achieved dividing the analyte area by the IS area and then multiplying by the IS concentration. To evaluate the performance of such calibration protocol, we compared concentrations estimated by this internal quantification method with results calculated by a five-point external calibration curve.

Analytical Validation

The method was validated using accuracy profiles based on β-expectation tolerance intervals for the total error measurement and assessing the measurements' uncertainty (Gustavo Gonzales and Angeles Herrador 2006; Hubert et al. 2004; Hubert et al. 2007a, b; Rozet et al. 2006). For this purpose, five measurements of each validation samples have been analyzed in five independent series, and before each run, a calibration curve was tested twice. Computing of validation data was ensured using the v3.0 Enoval validation software (http://www.arlenda.com).

Method Comparison

Comparison was done between the MS method and the ion exchange chromatography (IEC) amino acid analyzer. Five independent measurements of 4 ERNDIM Amino Acids

Scheme samples, covering the main part of the physiological range, have been carried out. The ERNDIM "IEC with Ninhydrin and one Internal Standard" method has been considered for this purpose, and the IEC target result used for method comparison is therefore the consensus mean of more than 100 laboratories.

Slope and intercept were estimated by Passing and Bablok regression with Medcalc v12.1 software.

Reference Ranges

Normal population values have been set up for plasma, urine, and CSF on several age categories: 0–2 years, 2–12 years, and >12 years. Intervals, proceeding from about 20 to 30 samples in each age class, have been generated using nonparametric analysis and represent the central 90 % (5–95 %) of the populations evaluated.

Clinical Evaluation

Samples (urine and plasma) from patients with confirmed inborn error of metabolism have been tested. The assessment included urines from homozygote cystinuria, Non ketotic hyperglycinemia, tyrosinemia I, and cystathioninuria. Plasmas from treated phenylketonuria, maple syrup urine disease, and ornithinemia patients have also been tested.

Results

Internal Versus External Calibration

To compare the internal quantification versus the external five-point calibration curve, each back-calculated concentration was normalized, in percentage, against its expected value. These recovery results were then assayed with a one-sample *t*-test to evaluate whether the average of observations differs significantly from 100 %.

External calibration gave slightly better recovery results for most amino acids. This difference turns out to be very significant for the upper concentration (1,000 μmol/L). Therefore, all further results have been back calculated against this external calibration curve, which was reanalyzed twice before each run. Additionally, opting for this quantification way helps to decrease the batch-to-batch variability (Held et al. 2011).

Method Capacities

An approach using accuracy profiles based on tolerance intervals for the total error measurement, including both bias and standard deviation for intermediate precision, was applied to demonstrate the method capability. Method is considered as valid within the range for which the accuracy profile is fully included inside the accuracy acceptance limits, set at ±30 % for upper concentrations (>75 μmol/L) and at ±50 % for lower concentrations (≤75 μmol/L). The β-expectation tolerance interval, which describes a region where, on average, a proportion β of future measurements will fall, was fixed at 5 %. This proceeding gives the guarantee that each further measurement of unknown samples will be included within the tolerance limits at the fixed level and thus within the acceptance limits.

Accuracy profiles have been generated for all amino acids, and a profile example is provided in Fig. 1. Based on these profiles, the lower limit of quantitation (LLOQ) is defined as the smallest quantity of each amino acid that fits within acceptance range (Fig. 2 and Supplemental Data Table 2).

Accuracy profile can be used as a visual decision tool to assess the validity of an analytical method. However, as for every graphical representation, this visual interpretation is partly subjective. Therefore, different "desirability" indexes have been considered: dosing range index, precision index, and trueness index (Rozet et al. 2007). The dosing range index is defined as the ratio between the length of interval in which the method is considered as valid and the length of the interval between the highest and lowest concentration levels investigated during the validation. The precision index corresponds to the ratio between the area defined within the acceptance limits and the limits of β-expectation tolerance interval, and the area bounded by the upper and lower acceptance limits, for which the method is considered as valid. The trueness index is defined as 1 minus the ratio between the sum of the square of the observed bias at each concentration level and the sum of the square of the maximum tolerated bias at each concentration level, for which the method is considered as valid. All these three indexes vary from 0 to 1; the better is the method for a criteria, the closer to one is the corresponding index (See Supplemental Data Statistic) (Rozet et al. 2007).

A synthetic radar chart of each index has been built for each amino acid (Fig. 3). Dosing range of bAla, Pser, and Sar are narrower than for other amino acids. For Sar, this can be explained by the saturation of the instrument detector at higher concentrations (1,000 μmol/L). Nevertheless, clinical impact of such phenomenon is reduced; physiological concentrations of the analyte are far below. Additionally, intra- and inter-run coefficients of variation are presented under a usual way in Table 1. Finally, bAla, EtN, and PSer show the worst precision index with highest coefficient of variation.

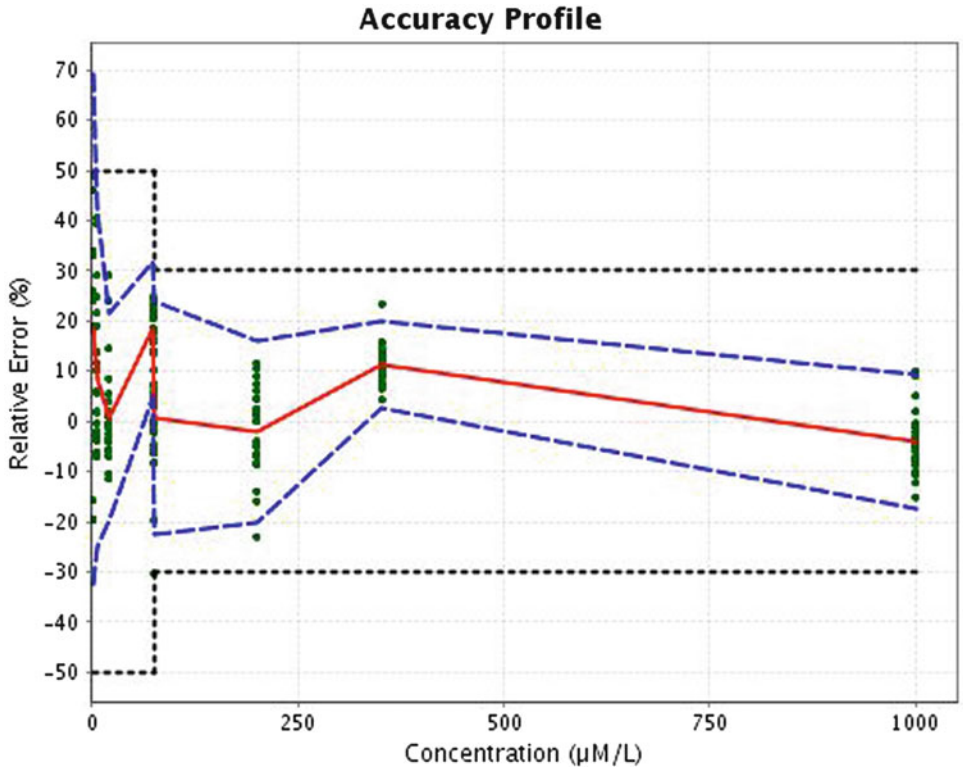

Fig. 1 Accuracy profile of phenylalanine. Plain *red line* is the relative bias, *dashed blue lines* are the β-expectation tolerance limit ($\beta = 5$ %), and dotted black curves represent the acceptance limit (±50 % for the concentration smaller than 75 µmol/L and ±30 % for concentration equal or greater than this value). The *dots* represent the relative back-calculated concentrations of the validation standards and are plotted according to their targeted concentration

MS Versus IEC

Results of method comparison are presented in Table 2. For all amino acids tested, slopes and intercepts are very close to 1 and 0, respectively.

Normal Population Values

Reference intervals have been established on plasma, urine, and CSF samples collected from normal controls (Table 3). For each, ranges were defined to cover the central 90 % of the measured values, and for plasma and urine matrices, three age classes have been considered.

In urine, the concentration of each amino acid was normalized against creatinine and then expressed in mmol/mol of creatinine. As previously described (Illsinger et al. 2010), large variations in amino acid concentrations are observed in urine of newborns, reflecting the variability of renal tubular function in the first months of life (Rossi et al. 1994).

Medical Valuation

Samples, collected from confirmed IEM patients, revealed positive results, according to their respective pathology (Table 4).

Discussion

We present here an exhaustive assessment of the aTRAQ kit for Amino Acid Analysis of Physiological Fluids, using a total error approach. To our knowledge, this is the first validation report of amino acid profiling through the use of accuracy profile.

Based on the most recent manufacturer's recommendations, a few modifications have been appended to the original protocol for sample preparation. These improvements are the consequence of some troubles reported by customers in methionine quantification with the native procedure.

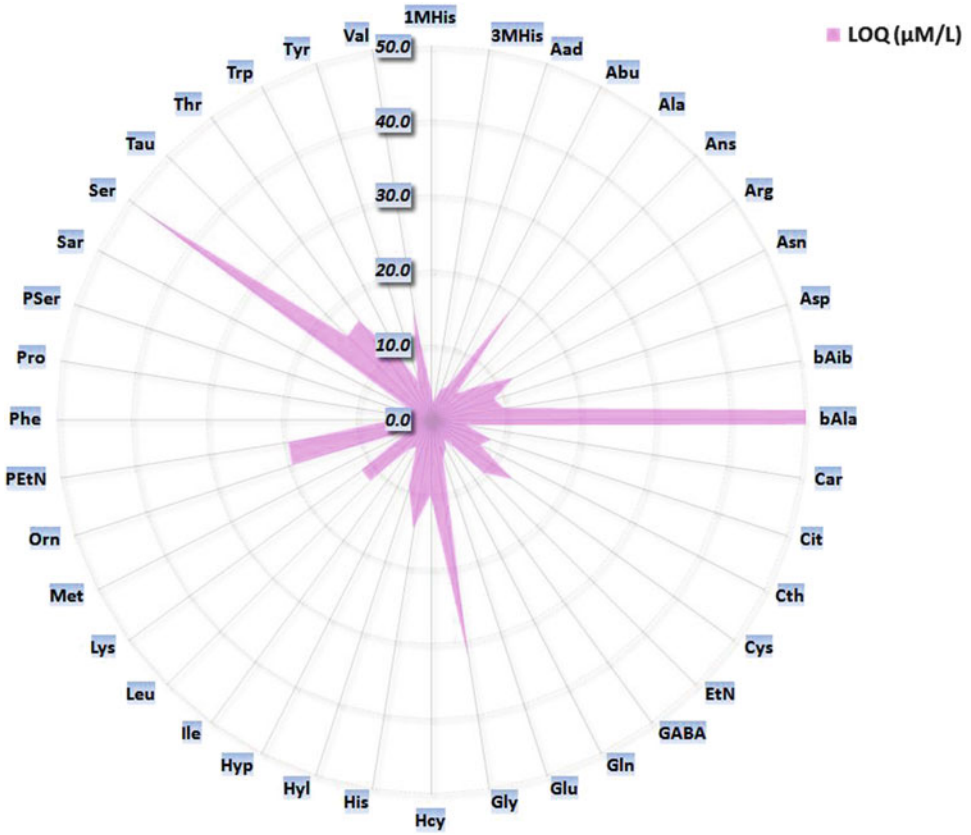

Fig. 2 Radar chart of calculated LLOQ, based on the accuracy profile approach

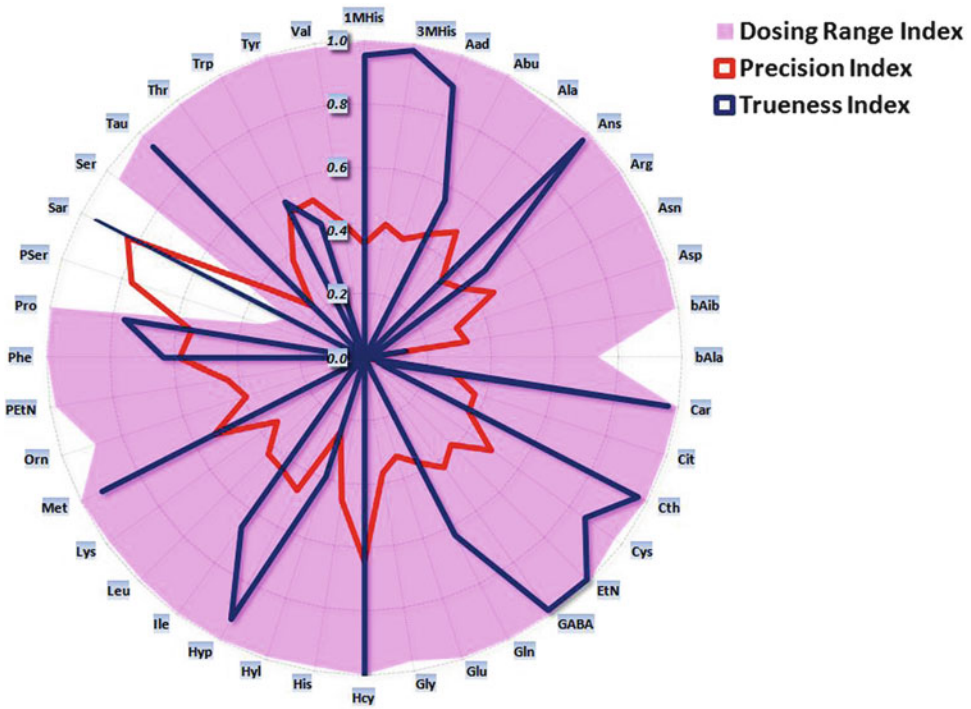

Fig. 3 Radar chart of each amino acid indexes. Indexes vary from 0 to 1; the better is the method for a criteria, the closer to one is the corresponding index. Compared to the other analytes, dosing range for Asp, Glu, Pser, and Sar are reduced, the instrument detector saturating at higher concentrations

Table 1 Intra- and inter-run variation for two levels of concentration

	Concentration level – 20 µmol/L		Concentration level – 200 µmol/L	
	Cystine – 10 µmol/L		Cystine – 100 µmol/L	
	Intra-run coefficient of variation (%)	Inter-run coefficient of variation (%)	Intra-run coefficient of variation (%)	Inter-run coefficient of variation (%)
1MHis	10.55	11.43	7.88	7.99
3MHis	9.11	9.36	8.54	8.54
Aad	10.93	11.17	8.16	8.16
Abu	8.85	11.48	8.41	9.30
Ala	10.66	11.84	9.42	9.42
Ans	10.78	11.47	7.70	8.31
Arg	11.45	13.11	9.05	9.40
Asn	10.01	10.01	7.27	7.43
Asp	18.72	18.72	6.96	6.96
bAib	11.46	12.19	7.84	7.99
bAla	26.84	41.24	8.38	9.02
Car	12.31	12.31	8.70	8.70
Cit	9.78	10.26	9.14	9.64
Cth	14.54	15.55	8.91	9.44
Cys	11.81	12.94	6.71	9.00
EtN	7.99	15.81	16.21	16.21
GABA	9.82	11.32	7.19	7.19
Gln	10.83	10.85	7.42	7.42
Glu	12.49	13.06	7.15	7.68
Gly	9.85	18.13	10.31	10.31
Hcy	5.02	38.29	17.16	17.16
His	9.61	9.61	10.92	10.92
Hyl	14.30	14.30	10.07	10.36
Hyp	12.14	13.05	3.93	4.39
Ile	12.55	12.55	8.67	8.72
Leu	15.02	15.02	7.79	7.85
Lys	10.73	11.99	9.00	9.00
Met	9.49	10.67	8.09	8.09
Orn	14.47	16.49	7.61	7.72
PEtN	11.51	13.92	7.09	7.25
Phe	9.28	9.71	8.57	8.57
Pro	8.84	9.24	5.82	5.82
PSer	28.71	28.71	10.50	10.50
Sar	10.53	11.25	8.25	8.25
Ser	16.16	18.77	9.06	9.06
Tau	7.23	14.42	3.53	8.36
Thr	9.52	10.24	7.15	8.47
Trp	7.87	9.59	7.54	7.78
Tyr	12.04	14.47	10.76	10.76
Val	10.51	10.91	9.27	9.41

Table 2 Method comparison: IEC versus MS method. Slope and intercept were calculated by means of a nonparametric Passing and Bablok regression

	Slope	Slope 95 % CI[a]	Intercept	Intercept 95 % CI[a]
3MHis	1.01	0.938 to 1.362	3.19	−3.863 to 5.464
Abu	1.17	1.105 to 1.252	−2.94	−5.209 to 0.857
Ala	1.05	1.016 to 1.085	−7.32	−20.1 to 2.336
Arg	1.06	1.045 to 1.083	−0.92	−5.514 to 1.503
Asn	1.19	1.151 to 1.279	5.70	−5.066 to 9.417
Asp	0.99	0.927 to 1.071	1.06	−2.051 to 2.432
Cit	0.96	0.938 to 1.008	1.88	0.449 to 3.583
Cth	1.12	1.005 to 1.156	0.55	−0.428 to 1.388
Cys	1.08	1.011 to 1.167	−3.07	−6.464 to 0.94
Gln	0.92	0.803 to 1.083	3.72	−33.91 to 9.132
Glu	1.08	1.041 to 1.132	3.38	−2.056 to 6.867
Gly	0.98	0.928 to 1.058	1.28	−15.09 to 1.45
His	1.01	0.98 to 1.071	−0.12	−5.099 to 2.776
Hpro	1.14	1.097 to 1.223	−0.39	−4.912 to 2.063
Ile	1.09	0.995 to 1.188	1.19	−2.022 to 5.713
Leu	1.11	1.001 to 1.094	1.16	−5.852 to 6.11
Lys	1.02	1.001 to 1.094	−4.87	−11.99 to 0.824
Met	1.08	1.072 to 1.173	0.20	−5.297 to 0.879
Orn	1.03	0.986 to 1.097	−5.23	−12.84 to 0.285
Phe	1.18	1.051 to 1.294	−4.46	−10.86 to 3.971
Pro	1.18	1.141 to 1.226	6.21	0.419 to 9.499
Ser	1.15	1.087 to 1.246	1.06	−5.565 to 4.681
Tau	1.08	1.022 to 1.154	−10.95	−21.82 to 2.961
Thr	1.01	0.965 to 1.105	4.28	−4.631 to 9.206
Trp	1.02	0.928 to 1.124	3.40	−5.842 to 2.067
Tyr	1.00	0.927 to 1.05	0.64	−3.441 to 7.371
Val	1.07	1.035 to 1.117	−3.31	−22.83 to 4.374

[a] 95 % CI = Confidence interval at 95 % for slope and intercept, respectively

1. The first amelioration referred to the addition of the aTRAQ Internal Standard solution before the evaporation step, and not after as required in the initial method. During this dryness stage, an oxidation phenomenon occurs, which mainly affects methionine and cystathionine. As internal standards were initially added after this step, they were not subjected to this degradation, and Met and Cth were then underestimated. Therefore, adding the Internal Standard solution before desiccation equally affects the metabolites to be quantified and their corresponding internal standards.
2. After hydroxylamine pipetting, an additional 15-min incubation step at room temperature was initiated. The phenolic group of tyrosine is also slowly and

Table 3 Amino acid reference ranges on plasma, urine, and CSF matrices

	Plasma			Urine			CSF
	0–2 years µmol/L	*2–12 years* µmol/L	*>= 12 years* µmol/L	*0–2 years mM/M Creat.*	*2–12 years mM/M Creat.*	*>= 12 years mM/M Creat.*	/ µmol/L
1MHis	0.1–3.7	0.2–15.7	0.5–14	2.7–18.9	2.7–208	3.6–137	0–0.9
3MHis	1.4–5.7	1.3–7.1	2.4–8	7.4–37.5	12.5–35.4	10.2–25.7	0.1–0.4
Aad	0.6–1.8	0.3–1.6	0.4–2	0.9–46.3	1.4–13.3	0.7–7.4	0–0.3
Abu	3.1–16.7	7.6–28	4.4–36.3	0.4–7.4	0.6–4.9	0.4–2.4	1.3–4
Ala	122–426	111–518	153–592	32.1–235	16.8–129	7.4–53.8	19–32.5
Ans	0–0.9	0–1.1	0–0.7	0–8.3	0–41.8	0–19.2	0–12
Arg	14.4–164	18.4–102	11.2–128	0.7–43.3	6.1–61.7	1.1–11.6	10.8–27
Asa[a]	0.3–7.8	0–13.7	0–12.5	0–18.2	1.1–4.2	0.5–3	0.4–6.7
Asn	27.1–123	28.4–102	22.7–115	3.3–136	8.4–48	3.5–36.6	6.6–12.1
Asp	6.1–69.4	4.6–60.3	4.4–65	0.8–20.3	0.3–9.4	0.3–4.6	1–11.6
bAib	0.8–31.8	0.5–3.3	0.3–2.9	3–98.1	2.6–107.2	1.5–27.6	0–0.2
bAla	17.2–67.3	15.8–49.9	18.5–60.7	1.5–116	0.3–15.9	0.2–13.7	17–41.4
Car	0–2.2	0–0.4	0–0.5	1.3–62	2–43.1	0.2–12.1	0–0.1
Cit	7.9–33.6	8.4–40.7	13.5–63.3	0.3–18.5	0.3–2.1	0.1–1.7	1.9–20
Cth	0.3–29.9	0.1–1.2	0.1–1.5	0.7–13	0.3–5	0.3–4.4	0.1–0.5
Cys	6.4–124	0.9–39.1	7.3–58.5	2.5–91.7	2.1–9.8	1.7–10	0–1
EtN	3.8–46.6	4.1–21.9	3.8–24.6	12.3–149	21.7–69.3	15.1–34.8	4.7–41.3
GABA	0.2–57.7	0.2–4.7	0.2–6.5	0.2–5.3	0.2–1.3	0.1–0.7	0.2–2.1
Gln	336–691	300–688	296–884	3–357	32–134	15–90	374–836
Glu	38–353	35–288	41.9–236	2.5–42.6	1.3–37.5	0.9–10.7	0.9–12
Gly	113–458	164.7–402	94.9–463	79.2–1,057	66–417	43–360	9.3–34
Hcit[a]	0.1–0.7	0–0.8	0.1–0.7	0.3–29.4	1–8.1	0.8–3.9	0.1–0.4
Hcy	0–26.3	0–0.4	0–0.3	0–1.8	0–0.2	0–0.2	0–0.5
His	35–117	34.2–114	35.4–136.2	46–379	34.8–290	18–125	9.2–25.3
Hyl	0.1–110	0.1–86.4	0–103.2	1.1–40.3	0.5–11	0.1–1.7	0.1–2
Hyp	10.8–76.2	8.7–31.9	4.8–34.6	1.4–233	0.4–4.2	0.1–2.3	0.3–1.8
Ile	30.3–129	24.7–94.7	28.3–167.8	1–12	1–4.2	0.2–2.6	3.2–12.9
Leu	44.9–198	44.5–158	61.2–203.8	0.6–21.1	2.1–9.9	0.3–6.6	5–10
Lys	64.5–375	75.5–228	105–253	2–274	4.7–105	1.9–23.5	6.3–28.6
Met	9.4–67.6	9.3–31	9.6–44.4	0.2–5.1	0.5–2.3	0–1.3	1.5–4.2
Orn	19.9–181	23.4–165	42.8–186	1.5–52.8	0.9–5.4	0.6–2.6	4.5–10
PEtN	0–6	0–3.8	0.2–2.3	1.8–28.5	2.5–22.1	0.6–4.9	0.8–5.6
Phe	25.5–131	27.7–95.8	23.5–104	1.4–38.2	4.2–19	1.9–10.1	6.3–13.5
Pro	74.9–276	89.2–286	85.8–327.8	1.9–97.2	0.6–9.5	0.3–5	1.4–5.3
PSer	0–0.4	0–0.4	0–0.4	0–1.2	0–0.3	0–0.2	0–0.3
Sar	0.4–3	0.8–4.7	0.5–2.7	0.2–12.4	0–1.2	0–1.3	0–0.2
Ser	62–253	61.8–230	53.7–216	5.3–302	26.4–90.6	11.1–52.6	25.3–67.1
Tau	34.8–309	34.9–266	30.3–223	6–546	14.6–349	4.5–140	4.5–10.1
Thr	41.7–252	51–167	58.3–206	4.8–171	7.5–40.5	4.5–35	15.3–36.1
Trp	17.1–87.3	15.1–58.4	24.6–85.7	2.2–33.7	4–21.1	2.4–11	1.3–3.2
Tyr	24–154	27.3–92.1	34–101	1.3–76.2	6.2–45.5	2.8–17.9	6.9–17.8
Val	72.6–277	94.8–261	99.2–329	1.2–24.7	3.1–12	1–7.9	8.3–21.5

[a] Asa and Hcit concentrations were calculated based upon the corresponding IS concentrations, as they were not included in the five-point external calibration curve

Table 4 Amino acid concentrations measured in different IEM

IEM	Matrix	Amino acid	Concentration (age-related normal range)
MSUD	Plasma	Leu	491 μmol/L (61,0–341,0)
		allo-Ile[a]	115 μmol/L
PKU	Plasma	Phe	1,230 μmol/L (23,5–104,0)
Ornithinemia	Plasma	Orn	660 μmol/L (42.8–346.2)
Treated tyrosinemia type I	Urine	Tyr	86,8 mM/M creatinine (2,8–17,9)
NKHG[b]	Urine	Gly	3971 mM/M creatinine (66,0–416,7)
Cystinuria	Urine	Arg	157,6 mM/M creatinine (6,1–61,7)
		Cys	93,1 mM/M creatinine (2,1–9,8)
		Lys	551,0 mM/M creatinine (4,7–105,0)
		Orn	148,8 mM/M creatinine (0,9–5,4)
Cystathioninuria	Urine	Cth	208 mM/M creatinine (0,3–4,4)

[a] allo-Isoleucine

[b] Non ketotic hyperglycinemia

partially labeled by the aTRAQ Δ8-reagent. Hydroxylamine solution is used to remove this extra label, but as internal standard is added before the drying step, the concentration of hydroxylamine is reduced compared to the original protocol. This dilution slows down the reaction removing the unwanted tag and, therefore, an extra incubation time is required.

3. Finally, the evaporation step under nitrogen stream was reduced to the half mixture volume, and not to dryness as requested by the original proceeding. Indeed, extended drying can result in excessive methionine oxidation.

This latter protocol gives satisfaction for amino acids profiling. Sulfur-containing amino acids generate adequate results with reliable recoveries for Met and Cth. β-Alanine is poorly reproducible on lower concentrations. Because of detector saturation at higher concentrations, the limit of quantification of sarcosine was fixed at 272 μmol/L. Finally, phosphoserine gave precise but inaccurate results at higher concentrations (>341 μmol). Reference medical ranges are equivalent with published intervals (Duran 2008). Results comparison with IEC showed a right concordance, and patients affected by IEM have been readily identified.

Conclusion

The presented method is focused on the targeted identification of about 40 amino acids. The application has been evaluated and offers a valid alternative in a clinical context. Furthermore, the present approach offers certain advantage compared to the IEC method: lower sample volume, time run reduction, and better specificity. Additionally, the use of labeled internal standards for each amino acid confers reliable quantitative results. Neglecting maintenance costs of a devoted IEC-instrument, analytical running expenses are similar between the two methods.

Nevertheless, not everything is idyllic. Although chromatography time drops down from 180 to 18 min, the aTRAQ method requires much more of that time difference for extraction, derivatization, and data processing, this latter step being labor intensive. In addition, some specific ninhydrin-reactive species (i.e., aspartylglucosamine or pipecolic acid), which may be identified with any IEC amino acid analyzer, will remain undetectable with the MRM approach. Nonetheless, implementation of additional analytes in the MS acquisition method should be a future concern. Besides, this latter consideration depicts a certain advantage of the MS technology, as these "extra-analytes" should not involve exclusively ninhydrin-responsive compounds.

Aware that the sensitivity of ultimate generation mass spectrometer is far below major physiological amino acid concentrations, we demonstrate here that these technological advances, which are fundamental for traces detection (on the order of picomol/L or lower), are not incompatible with the reliable quantification of elevated amino acid concentrations (i.e., >100 μmol/L). Therefore, running methods requiring very high sensitivity can be easily combined with less sensitive protocols on the same instruments.

Finally, the aTRAQ kit is a very good alternative to the IEC method, but financial and practical considerations of both technologies have to be counterbalanced before engaging any transition.

Synopsis

Validation of the aTRAQ assay for Amino Acid Analysis in Physiological Fluids.

Compliance with Ethics Guidelines

Disclosure

Romain FILEE, Roland SCHOOS, and François BOEMER declare no conflict of interest.

Grant/Funding Support

None.

References

Dettmer K, Stevens AP, Fagerer SR, Kaspar H, Oefner PJ (2012) Amino acid analysis in physiological samples by GC-MS with propyl chloroformate derivatization and iTRAQ-LC-MS/MS. Methods Mol Biol 828:165–181

Dietzen DJ, Weindel AL, Carayannopoulos MO et al (2008) Rapid comprehensive amino acid analysis by liquid chromatography/tandem mass spectrometry: comparison to cation exchange with post-column ninhydrin detection. Rapid Commun Mass Spectrom (RCM) 22:3481–3488

Duran M (2008) Amino acids. In: Blau N, Duran M, Gibson KM (eds) Laboratory guide to the methods in biochemical genetics. Springer, Berlin, pp 53–89

Gustavo Gonzales A, Angeles Herrador M (2006) Accuracy profiles from uncertainty measurements. Talanta 70:896–901

Harder U, Koletzko B, Peissner W (2011) Quantification of 22 plasma amino acids combining derivatization and ion-pair LC-MS/MS. J Chromatogr B Analyt Technol Biomed Life Sci 879:495–504

Held PK, White L, Pasquali M (2011) Quantitative urine amino acid analysis using liquid chromatography tandem mass spectrometry and aTRAQ reagents. J Chromatogr B Analyt Technol Biomed Life Sci 879:2695–2703

Hubert P, Nguyen-Huu JJ, Boulanger B et al (2004) Harmonization of strategies for the validation of quantitative analytical procedures. A SFSTP proposal–part I. J Pharm Biomed Anal 36:579–586

Hubert P, Nguyen-Huu JJ, Boulanger B et al (2007a) Harmonization of strategies for the validation of quantitative analytical procedures. A SFSTP proposal–part II. J Pharm Biomed Anal 45:70–81

Hubert P, Nguyen-Huu JJ, Boulanger B et al (2007b) Harmonization of strategies for the validation of quantitative analytical procedures. A SFSTP proposal–part III. J Pharm Biomed Anal 45:82–96

Illsinger S, Schmidt KH, Lucke T, Vaske B, Bohnhorst B, Das AM (2010) Plasma and urine amino acid pattern in preterm infants on enteral nutrition: impact of gestational age. Amino Acids 38:959–972

Piraud M, Vianey-Saban C, Petritis K et al (2003) ESI-MS/MS analysis of underivatised amino acids: a new tool for the diagnosis of inherited disorders of amino acid metabolism. Fragmentation study of 79 molecules of biological interest in positive and negative ionisation mode. Rapid Commun Mass Spectrom (RCM) 17:1297–1311

Piraud M, Vianey-Saban C, Bourdin C et al (2005) A new reversed-phase liquid chromatographic/tandem mass spectrometric method for analysis of underivatised amino acids: evaluation for the diagnosis and the management of inherited disorders of amino acid metabolism. Rapid Commun Mass Spectrom (RCM) 19:3287–3297

Rossi R, Danzebrink S, Linnenburger K et al (1994) Assessment of tubular reabsorption of sodium, glucose, phosphate and amino acids based on spot urine samples. Acta Paediatr 83:1282–1286

Rozet E, Morello R, Lecomte F et al (2006) Performances of a multidimensional on-line SPE-LC-ECD method for the determination of three major catecholamines in native human urine: validation, risk and uncertainty assessments. J Chromatogr B Analyt Technol Biomed Life Sci 844:251–260

Rozet E, Wascotte V, Lecouturier N et al (2007) Improvement of the decision efficiency of the accuracy profile by means of a desirability function for analytical methods validation. Application to a diacetyl-monoxime colorimetric assay used for the determination of urea in transdermal iontophoretic extracts. Anal Chim Acta 591:239–247

Waterval WA, Scheijen JL, Ortmans-Ploemen MM, Habets-van der Poel CD, Bierau J (2009) Quantitative UPLC-MS/MS analysis of underivatised amino acids in body fluids is a reliable tool for the diagnosis and follow-up of patients with inborn errors of metabolism. Clin Chim Acta; Int J Clin Chem 407:36–42

WHO (2010) International statistical classification of diseases and related health problems. WHO. http://apps.who.int/classifications/icd10<

JIMD Reports
DOI 10.1007/8904_2013_269

RESEARCH REPORT

Methods of Neurodevelopmental Assessment in Children with Neurodegenerative Disease: Sanfilippo Syndrome

Kathleen A. Delaney · Kyle R. Rudser · Brianna D. Yund · Chester B. Whitley · Patrick A.J. Haslett · Elsa G. Shapiro

Received: 25 January 2013 / Revised: 07 August 2013 / Accepted: 25 September 2013 / Published online: 5 November 2013

Abstract Objectives: (1) Develop a methodology for obtaining reliable cognitive and developmental data in children with neurodegenerative disease and cognitive impairment and in turn monitor disease state and treatment outcomes. (2) Demonstrate validity of age-equivalent scores.

Methods: We present guidelines for obtaining accurate test scores in low-functioning and behaviorally disruptive pediatric patients, followed by a method validation study: (1) using disease-specific protocols to assess salient aspects of the known phenotype, (2) selecting appropriate tests, (3) managing behavior, and (4) using age-equivalent scores on standardized tools. We used the Bayley Scales of Infant Development-III or Kaufman Assessment Battery for Children-II with a group of 25 children with mucopolysaccharidosis type IIIA (MPS IIIA or Sanfilippo syndrome type A) with dementia. To demonstrate concurrent validity, we used the Vineland Adaptive Behavior Scales-II, comparing parent-reported age-equivalent scores (AEs) with those of the cognitive measures.

Results: We were successful in obtaining cognitive age-equivalents for 25 patients with MPS IIIA including those with severe behavioral disruption and a correlation of 0.95 was obtained comparing scores on the parent measure with cognitive age-equivalents validating the age-equivalent approach.

Conclusion: An approach to the assessment of severely impaired children including those with behavioral disruption was implemented and is applicable to children with other severe neurological diseases. This approach will enhance the assessment of disease progression and monitoring of treatment outcome in clinical trials.

Communicated by: Frits Wijburg, MD, PhD

Competing interests: None declared

K.A. Delaney · B.D. Yund · C.B. Whitley · E.G. Shapiro
Department of Pediatrics, University of Minnesota, Minneapolis, MN, USA

K.R. Rudser
Department of Biostatistics, University of Minnesota, Minneapolis, MN, USA

P.A.J. Haslett
Shire, Lexington, MA, USA

K.A. Delaney (✉)
MMC 486 Delaware St., SE Minneapolis, MN 55455, USA
e-mail: delan011@umn.edu

Background

Obtaining reliable and accurate neurocognitive assessment data is a challenge in children with neurodegenerative disorders who have dementia or are very low functioning, have disruptive, noncooperative behavior, or have physical/sensory disabilities. These challenges and the limitations of available measures have been documented previously in patients with lysosomal diseases (Martin et al. 2008). Solutions that will result in precise assessment are essential to assess disease progression and the effects of treatment. We present here an example of how such data can be obtained using a pragmatic, disease-specific approach using age-equivalent scores. Our ultimate goal is to obtain precise data about measurement of disease progression and ultimately treatment outcomes. This becomes a more urgent problem as new treatments emerge for rare neurogenetic diseases.

Standard psychology practice currently does not support the use of age-equivalent scores (AgeEqSs) as their statistical properties are inadequate and can be misleading (Naglieri and Goldstein 2009). AgeEqSs do not consider

the range of normality in contrast to standard scores which establish a range of normal performance (Maloney and Larrivee 2007). Standard deviations vary from age to age and from test to test. The scale units of AgeEqSs are ordinal and the intervals between units are unequal (e.g., an increase of 6 months at one age will differ from an increase at another age) (Lawrence 1992). For these reasons, psychologists have resisted the use of AgeEqSs and have primarily used age-stratified normative data to obtain standard scores. However, those caveats may hold for higher functioning children; for younger more severely impaired children having an ordinal measure that tracks change over time is crucial. Developmental growth curves can be constructed from AgeEqSs to track changes; pediatricians commonly use such curves to monitor height, weight, and head circumference. The difference and challenge here is that, unlike measuring anthropometric measurements (e.g., height, weight, and OFC), uneven skill development within children with neurodegenerative disease challenges the ability to measure their overall development level especially using standard scores.

There are several reasons that standard scores should not be used in very low-functioning children. The standard scores on most tests have a floor; most low-functioning children fall below this floor which makes them insensitive to any change. Furthermore, for a child with dementia, even if a standard score can be obtained at an initial visit, it is very possible that at the next evaluation the child will no longer fall within the range of standard scores available for that measure.

In contrast, AgeEqSs are easily interpretable and allow for precise longitudinal monitoring of illnesses in children with cognitive decline and/or who are very low functioning. Change in rate of growth or decline can be monitored with respect to the disease process or the effects of treatment. One can determine whether a child continues to gain milestones, has reached a plateau, or is losing skills. However, AgeEqSs do not necessarily imply that the child has behavior and development typical of that age, e.g., a child with Sanfilippo syndrome who has an AgeEqSs of 12 months does not necessarily present as a chronologically older child who acts like a 12-month-old child.

In a new development in psychology, the most recent edition of the Bayley Scales of Infant and Toddler Development-III (BSID-III) has added such developmental growth curves to the manual, thus allowing one to track AgeEqSs over time (Bayley 2006). The use of AgeEqSs to assess the development of children with dementia was initially proposed by Shapiro and Klein in 1993 (Shapiro and Klein 1993) and has been endorsed in other discussions of neurodegenerative diseases (Shapiro and Balthazor 1999; Ziegler et al. 2010). As early as 1985, Volkmar et al. recommended the use of age-equivalent scores as a precise measure of function in low-functioning individuals allowing comparisons across domains of function (Volkmar et al. 1987). AgeEqSs have been used in neurodegenerative diseases, primarily the mucopolysaccharidoses, to examine treatment effects using both cognitive (Staba et al. 2004; Peters et al. 1996, 1998; Wraith et al. 2007) and Vineland Adaptive Behavior Scales (Sparrow et al. 2005) age-equivalents. While the use of cognitive AgeEqSs for the BSID II, the Mullen Scales of Early Learning (Mullen 1995), or the Griffiths Mental Development Scales (Huntley 1996) has been common in very low-functioning children, the problems and challenges surrounding cognitive assessment in childhood dementia have not been carefully addressed nor have methods been delineated for obtaining and verifying this information. The validity and sensitivity of AgeEqSs needs to be demonstrated to use them in treatment trials.

We developed a neurodevelopmental assessment approach with applicability to any neurodegenerative disease based on our experience with mucopolysaccharidosis type IIIA (MPS IIIA) or Sanfilippo syndrome. MPS IIIA is associated with dementia and severe behavioral disruption. It is a rare (about 1 in 100,000 births) (Meikle et al. 1999; Poorthuis et al. 1999; Baehner et al. 2005) autosomal recessive lysosomal storage disease caused by absence of enzyme heparan-N-sulfatase (sulfamidase) necessary for degradation of the glycosaminoglycan (GAG) heparan sulfate in lysosomes which then accumulates in the lysosomes of neurons and glial cells. MPS IIIA is a neurodegenerative disease with a variable trajectory in neurocognitive decline with respect to age and time of diagnosis; however, this decline and the variability in decline are not well documented. Deficits in language development, motor skills, and intellectual development have been reported as early as 2 years of age (Cleary and Wraith 1993). Yet precise measurement of the decline of intellectual skills is absent, likely due to the difficulties in testing these children given their tendency toward behavioral noncompliance (Valstar et al. 2011). Abnormal behaviors have been described as aggressive and hyperactive with sleep disturbance (Cleary and Wraith 1993; Valstar et al. 2011; Meyer et al. 2007; Fraser et al. 2002). Autistic-like symptoms and loss of normal fear have also been described (Heron et al. 2011). In a recent study, (Heron et al. 2011) found the average lifespan for MPS IIIA to be 15.4 years (Heron et al. 2011).

In the classic form of MPS IIIA, symptoms appear to arise between 2 to 6 years of age although diagnosis often lags behind the earliest symptoms (Cleary and Wraith 1993). Some MPS IIIA patients, who have clinical onset and diagnosis after age 6, have been described by Hopwood (2007) and by (Heron et al. 2011) with slower decline and an unknown disease progression. Instruments used for assessment need to encompass a wide range of abilities and ages as previously established by Valstar et al. (2011).

Guidelines

Neurocognitive assessment has been a challenge for investigators working with MPS IIIA due to the patients' tendency toward behavioral disruption, their noncompliance, and the lack of disease familiarity of the examiner. Additional challenges include the unavailability of tests/methods sensitive to change in very low-functioning children (Valstar et al. 2011). We sought to develop an approach that would deal with these obstacles using the following four guidelines:

Guideline 1. Protocols and Testing Approaches Must Be Disease Specific

Understanding the disease phenotype is crucial to sensitive testing. We began with clinical behavioral observations of children with MPS III to determine why testing was difficult, and with a goal of finding tasks that they could perform. Disease-specific neurological and medical impediments to testing were defined. Hearing problems were almost universal which affects language-based test results. The use of hearing aids was important in obtaining reliable data. Furthermore, increasing auditory agnosia (inability to comprehend word meaning) is evident as the disease progresses. The child previously understood the word and used the word, but no longer is able to understand its meaning even while continuing to say the word. For these reasons, language-based tests as a measure of cognition were avoided and nonverbal assessment was necessary.

Motor apraxia increases as the neurologic disease progresses. While children with MPS IIIA can spontaneously perform motor activities, they are unable to perform these activities to either verbal instruction or imitation. Consideration of this factor is important as many nonverbal tests require motor output.

Behavioral noncompliance often occurs when the child is unable to do a task or is frustrated. Testing needs to be easy enough for success. Behavioral noncompliance is not the cause of inability to perform, but rather the inability to perform leads to behavioral disruptions and noncompliance which may be typical of the way the MPS IIIA child responds to frustration.

MPS IIIA Testing Challenge: Psychologists with no experience with MPS IIIA assume behavior noncompliance is the cause of the child's poor performance. Parents report the child is able to perform the item at home, but cannot perform it in the clinic; the child seems to lack cooperation on items that appear easy.

Solution: The neurologic conditions of motor apraxia and auditory agnosia in MPS IIIA cause lower scores than the tester might expect when observing spontaneous behavior. Children cannot perform using instruction or imitation. Also, other medical conditions in MPS IIIA can interfere with test performance. Hearing aids and glasses must be brought to the clinic and used. A recent audiology consult to assess hearing status should precede testing. If the child is not well or has a cold, testing should be delayed if possible. Use of pacifiers or "chewies" should be allowed during testing if the child uses them at home. Allow extra time. Children with neurodegenerative disease often have a slower response to requests and it is critical to allow for more time on a task before determining their success. At the same time, spending too much time on any one task or item could lead to frustration during the evaluation.

Do not allow the visit to occur until at least 48 h after sedation or anesthesia or after a recent seizure. Consider whether current medications affect cognition.

Guideline 2. Criteria for Test Selection Includes Appropriate Difficulty Level, Disease-Relevant Domains of Content, and Familiarity with the Test by Psychologists

Our goal is to include tests of cognition, language, motor ability, memory, attention, adaptive function, and behavior. In choosing tests for a protocol, keep the number of measures of any domain to a minimum to increase the validity and comparability of results. In MPS IIIA, the range of cognitive impairment may vary from severe to near-normal in very young children with an age range from infancy to young adulthood. No single measure meeting our criteria covered that range so we needed to use two different measures. Where feasible this should be avoided. No test has standardized scores for very low levels; thus, age-equivalent scores were needed that are psychometrically sound to make the tests comparable.

Because sufficient sample size cannot be accrued in one center if the disease is rare, a protocol should be feasible in multiple centers and in multiple countries. Decreased accuracy and reliability of data in multicenter studies must be offset with precise and simple measurements.

We reviewed many cognitive tests and rejected them. The Mullen Scales of Early Learning (MSEL) (Mullen 1995) is usually our preferred measure because it is comprised of a variety of domains, and each scale begins with birth and is validated up to 7 years of age. However, while used widely in the USA, the MSEL is not familiar to international researchers and is not translated into other languages. The Griffiths Scale of Mental Abilities is unknown in the USA even though it is widely used in the UK and other English-speaking countries (also translated

into Canadian French and German) (Huntley 1996). Another test we considered was the Leiter Scales (Roid and Miller 1997). The age-equivalent scores were not well standardized and it was somewhat outdated. The Stanford Binet Intelligence Scale included too many verbal-based subtests and did not go below an age-equivalent of 2 years and is only available in English (Roid 2003) and the Wechsler Preschool and Primary Scale of Intelligence was too difficult with a high floor, although available in many languages (Wechsler 2002). Most standard IQ tests have a "floor" of a standard score of 40 or 50 (4 or 3.3 standard deviations below the mean). The Differential Abilities Scale-II (DAS-II) (Elliott 2007) is both difficult to administer and to score, and does not have an international presence (although a Spanish translation exists for the preschool level). Also, the DAS II subtests change from one age grouping to another making it difficult to create a developmental growth trajectory for children who straddle those age groups. The Kaufman Assessment Battery for Children – Second Edition is widely used in cross-cultural research because much of the test is nonverbal and it has been translated into more than 15 languages. Although the test is based on psychological theory which may not apply to such severe impairment, it has a nonverbal scale that is widely used with hearing and language impaired children (Kaufman and Kaufman 2004).

MPS IIIA Challenge: Find tests measuring cognitive ability, adaptive function, and other domains that have an appropriate range of difficultly for MPS IIIA which are widely used with age-equivalent scores that are psychometrically sound.

Solution: Two cognitive tests were chosen for MPS IIIA: Bayley Scales of Infant Development – Third Edition (BSID-III) (Lawrence 1992) and Kaufman Assessment Battery for Children – Second Edition (KABC-II) (Elliott 2007) and one adaptive scale, The Vineland Adaptive Behavior Scales – Second Edition (VABS-II) (Wraith et al. 2007) for the following reasons: (1) universality of use, (2) availability of age-equivalent scores for severely impaired children, (3) nonverbal content as on the cognitive scale on the BSID and the nonverbal scale of the KABC-II for higher functioning children, and (4) availability of supplementary language and motor assessment (both domains on the BSID-III and some language on the KABC-II). The VABS-II, a parent-reported outcome, was selected as an adaptive measure for the same reasons.

Here is the algorithm we developed to choose which measure to administer for each MPS IIIA patient: The VABS-II is always given first.

- If chronological age is under 42 months, the BSID-III was selected.
- If chronological age $>$ 42 months and age-equivalent score on the VABS-II $>$ 42 months, the KABC-II is selected. Forty-two months was chosen so that it would allow considerable decline to occur so that, over the study interval of one year, the child would not fall below the base of the test (lowest possible score).
- If chronological age $>$ 42 months and VABS-II age-equivalent is between 36 and 42months, start with the Triangles subtest on the KABC-II; if the child cannot do a total of two items on the Triangles subtest, we try one other nonverbal subtest. If the child cannot successfully perform three items, we fall back to the BSID-III. We always start with item #1 on every KABC-II subtest for this group.
- If chronological age is $>$ 42 months and mental age-equivalent is $<$ 36 months on the VABS-II, the BSID-III is administered with the cognitive age-equivalent score as the primary outcome.

Guideline 3. Testers Must Be Able to Deal Effectively with Behavioral Difficulties and To Understand the Child's Behavior in the Context of the Disease Process

Nothing is better than experience in testing children with very impaired and behaviorally dysregulated behavior. In children with dementia, often commonly utilized behavioral paradigms such as reinforcement contingencies do not work. Many factors contribute to behavioral noncompliance and should be considered such as diurnal variation in behaviors, lack of sleep and fatigue (often from travel to the testing facility), previous medical evaluations, lack of hearing aids and glasses, lack of ability to perform the task for reasons related to the disease, and frustration.

Here is a short list of testing pointers: avoiding much or too complicated verbalization when administering tests, being sensitive to the physical needs of the child (letting the child have a pacifier or chewie), letting the child up out of the chair, letting the child engage in repetitive behaviors (while observing and recording them) but then distracting the child away from these behaviors, and finding behaviors to reward. Having the parent in the testing room may contribute to behavioral disruption or may help prevent it; a parent's presence is a necessity in about a half of children with MPS III.

MPS IIIA Challenge: Accomplishing neurodevelopmental testing in the face of behavioral dysregulation and lack of compliant behavior.

Solution: Our tests apply the principles mentioned before and where possible:

- Test the child at the optimum time, (i.e., mainly in the morning)
- Give the child ample time to respond to items in a child-friendly environment (defined as nonmedical, appropriate furniture, windowless, small and a quiet, relatively stimulus-free room).
- Consult with parents prior to testing about rewards, etc., that may be useful. Contingencies are difficult for these children to understand; you must "catch" the right behavior to reward it.
- Parents are instructed on what to do in the testing room if they observe during the session. Parents can be a big help but, if they interfere, should be told firmly not to do so.
- Make sure that easy items are given first and items increase in difficulty gradually. Always assume that noncooperation reflects frustration from items that are too difficult. Start with something the child can do. This provides an opportunity for the child to become acclimated to testing and also puts the parent at ease. Allow the child to first play with simple and engaging test materials without risking test integrity. If the child is fond of a particular toy and becomes restless, use that toy (assuming it is not to be used later in the testing) as a distracter between tasks or measures.
- Assess and implement strategies based on the child's temperament and approach to testing. For example, if the child is easily overstimluated, e.g., startles easily, cries a lot, avoids eye contact, then use a quiet tone, slower movements, and present one item at a time. If the child is disengaged, then use exaggerated movements, encouragement, and praise to help elicit a response.
- If the child is particularly disturbed by or disinterested in the object, take it away and attempt that item later.

Guideline 4. Tests Must Be Scorable for all Participants Using Age-Equivalents

The BSID-III, KABC-II, and VABS-II have a lower limit for which the test was standardized. For the BSID-III and KABC-II, the lowest standardized score is 40 and for the VABS-II it is 20. Many of the children in this study are considerably below that limit. Consequently we chose to use age-equivalent scores (AgeEqSs) for the reasons outlined in the introduction. Using AgeEqSs we can examine growth rates for treated and untreated children across tests. Of course, there are some caveats to cross-test comparison; the nature of the normative samples and the years since the norming took place may vary across tests.

We can also obtain a developmental quotient (DQ) using AgeEqSs in the numerator and chronological age at testing as the denominator multiplied by 100. This was the method used when IQ tests were first developed, but these ratio IQs were abandoned because the standard deviations vary by age. In modern psychological tests, a standard score is computed with a set standard deviation of 15 and a mean of 100. DQs are useful when an approximation to an IQ is needed demonstrating the gap between the child with a neurodegenerative condition and a typically developing child of the same age. However, AgeEqSs provide more detailed information about changes in rate of development due to disease or treatment.

MPS IIIA Challenge: As no standard score data are available for very low-functioning individuals, we have used AgeEqSs. Any nonstandard approach to scoring neuropsychological tests must be validated.

Solution: We sought to validate the age-equivalent approach to demonstrate that our approach is reliable and yields accurate data. The VABS-II, a parent report measure, yields AgeEqSs making it possible to compare it to scores on a directly administered measure (BSID-III and KABC-II), thus obtaining a measure of concurrent validity. Our results are indicated in the study outlined below:

Methods

Patients

Twenty-five patients with documented Sanfilippo syndrome type A were recruited to this single-center study supported by Shire (A 12-month Longitudinal, Prospective, Natural History Study of Patients with Sanfilippo syndrome type A (MPS IIIA), Clinicaltrials.gov reference number, NCT01047306.

Patients were recruited from our own clinics and through patient advocacy groups and Clinicaltrials.gov. Inclusion criteria were as follows: (1) documented deficiency in HS enzyme activity of less than or equal to 10 % of the lower limit of the normal range as measured in fibroblasts or leukocytes and normal enzyme activity level of at least one other sulfatase (to rule out multiple sulfatase deficiency) as measured in fibroblasts or leukocytes; (2) a developmental age greater than or equal to 1 year of age on the interview

Table 1 Descriptive data

Measure $N = 25$ for all measures	Mean (standard deviation)
Age: mean (S.D.)	75.0 months (53.4) range 13–220 months
Cognitive age-equivalent (BSID or KABC)	23.0 months (12.9) range 7–58 months
Developmental quotient (mean age-equivalent of BSID or KABC/chronological age)	44.6 (28.4) range 3–91
Vineland age-equivalent (mean of subscales except motor domain)	23.8 months (12.8) range 6–61 months
Vineland developmental quotient (mean of age-equivalents except motor domain/chronological age)	44.4 (25.3) range 3–95
Standard score using normative data on the Vineland	63.0 (16.8) range 25–95

form of the VABS-II (Sparrow et al. 2005); and (3) the patient was determined to be medically stable to accommodate the protocol requirements. Relevant exclusion criteria included non-MPS IIIA-related central nervous system impairment or behavioral disturbance, blindness, deafness, poorly controlled seizures, and other treatments (e.g., hematopoietic cell transplant, investigational drugs or devices). This protocol was approved by the Institutional Review Board and all parents of patients signed consents.

Materials and Procedure

Twenty-two patients were administered the Bayley Scales of Infant Development-III (BSID-III) and three had the Kaufman Assessment Battery for Children-II (KABC-II). Decisions were made according to the rules specified above. While the BSID-III has motor and language scales and they were also administered, only scores for the cognitive scale are reported here. The cognitive scale of the BSID-III has a split-half reliability coefficient of 0.91 (Bayley 2006). The KABC II has many subtests and scales. We administered only the Nonverbal Index which includes five different subtests: Story Completion, Triangles, Block Counting, Pattern Reasoning, and Hand Movements. The internal consistency as a measure of reliability of the Nonverbal Index is 0.92 (Elliott 2007).

Parents of all 25 patients were administered the Vineland Adaptive Behavior Scale – Second Edition-Interview format (VABS-II). These data were used to determine eligibility as well as to assess adaptive function.

Procedure: Two independent examiners interviewed parents to administer the VABS-II. The two examiners carried out 16 and 9 VABS-II interviews respectively prior to cognitive testing. Importantly, both examiners who administered the cognitive tests were experienced with MPS and other neurodegenerative diseases. The primary examiner (KD) tested 22/25 patients. She supervised the other examiner who assessed patients who had fewer behavioral difficulties or were older. All scoring was vetted by KD. All testing was carried out at the Center for Neurobehavioral Development, University of Minnesota and was done in the morning of the second day of the patient's visit (to ensure recovery from travel).

Scoring and statistical methods: Either the BSID-III cognitive age-equivalent or the KABC-II nonverbal age-equivalent was calculated for each patient. The mean age-equivalent of the subtests of the Nonverbal Index was calculated as the best measure of language-free cognition on the KABC-II in the older and less impaired children which was most equivalent to the BSID cognitive age-equivalent.

For the VABS-II, we calculated the mean age-equivalent over the subtests, excluding the VABS motor scale, to generate a score as equivalent as possible to those of the cognitive tests. The goal was to establish concurrent validity between the VABS-II and the cognitive tests. Concurrent validity is shown when scores on a test are highly associated with scores on another measure which tests a similar set of skills or abilities. Both tests presumably reflect related constructs. We calculated a correlation coefficient between the cognitive age-equivalent (either BSID-III cognitive or KABC-II nonverbal) and the VABS-II age-equivalent.

However, a high correlation does not necessarily imply that both measures will show agreement in level of scores between the two methods of assessment. A Bland-Altman (Bland and Altman 1986) style plot was used to examine the agreement between these two different tests with the mean of the two assessments on the x-axis and the difference as a percent of the mean on the y-axis.

Results

Both cognitive ability and the VABS-II age-equivalent scores (AgeEqSs) yielded similar mean scores and standard deviations (See Table 1). Cognitive ability as measured by the DQ (ratio of cognitive age-equivalent to chronological age) was discrepant from the Adaptive Behavior Composite standard score but not the DQ (mean of the age-equivalents for all subtests divided by chronological age) on the VABS-II (Table 1).

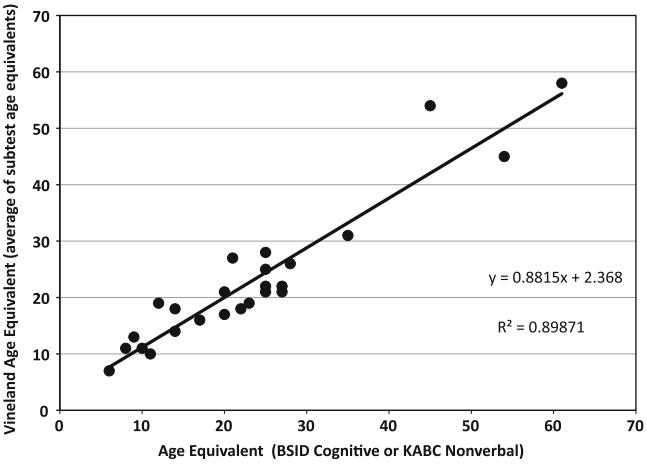

Fig. 1 Association of BSID or KABC age-equivalent score with Vineland age-equivalent score

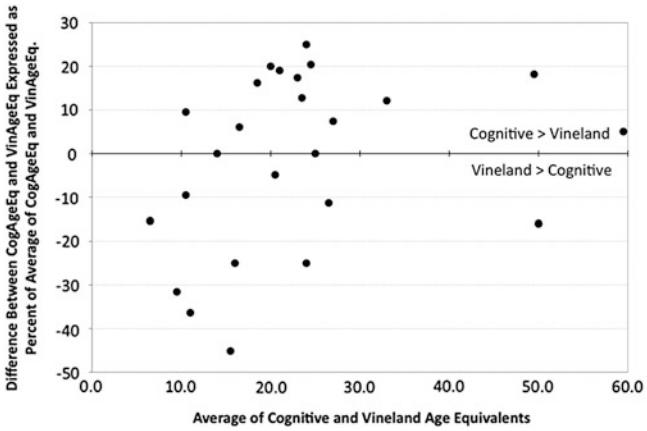

Fig. 2 Percent difference in VABS and cognitive scores by cognitive age-equivalent (Bland-Altman graph)

A correlation of 0.95 was found between AgeEqSs on the cognitive tests and on the VABS-II. See Fig. 1.

From the Bland-Altman graph, we conclude that the parent ratings of the lower functioning children, when compared to the mean of both measures, have a tendency toward more positive scores on the VABS-II. See Fig. 2.

Discussion

The two aims of this study were as follows: (1) to provide guidelines for the clinical collection of neurodevelopmental data in children with severe neurodegenerative diseases and (2) to demonstrate that the accuracy of such data even with the most severely impaired children can be precise, thus making it useful for understanding disease progression as well as for sensitive treatment monitoring. We found that following such guidelines we could measure disease progression with accuracy and precision even in children who are severely impaired.

We have demonstrated the concurrent validity of AgeEqSs. In our results, the positive correlation of the AgeEqSs on the BSID-III/KABC-II with the VABS-II likely is due to several factors. The first is the extensive experience in our clinics with cognitively normal children, and children with lysosomal and other dementing illnesses. Our transplant program and our lysosomal disease program have introduced us to hundreds of children with these diseases. Our tester KD is extraordinarily skilled at getting cooperation and obtaining accurate scores on these tests. It is highly unlikely that a tester never having seen a child like this will be able to achieve that breadth of understanding and accuracy of assessment. The second is the very controlled circumstance of our testing procedures: time of day, testing environment, and organization of the testing experience. Also, we note that in more than half the cases, parent report on the VABS-II was obtained by someone other than the tester with no knowledge of the test results, making those scores in part independent of each other. We conclude that accurate developmental data that is sensitive to change can be obtained, but that adherence to the above guidelines can increase accuracy.

In 1992, Raggio, Massingale, and Bass (Raggio et al. 1994) administered the VABS and the BSID (both first editions of those tests) to a sample of high-risk infants who were suspected of developmental delay to answer the question of whether standard scores or age-equivalents were a better measure. The standard scores obtained on their sample were higher than the age-equivalents and the MDI, and the authors concluded, as did we, that AgeEqSs are more accurate. These authors propose that age-equivalents are better measures for severely impaired children because of the imprecision of very low standardized scores on the VABS. Our results support that finding and extend it to a larger age range and up-to-date tests.

We found a tendency toward more positive scores on the VABS-II. This discrepancy is more pronounced in the most impaired children with the lowest cognitive age-equivalents. Thus, even while using age-equivalents instead of standard scores, getting precise scores may be difficult especially on the VABS-II. Although these results support the use of direct measurement of cognitive function, the easily administered VABS-II could be used to estimate cognitive ability in settings where the BSID-III might be difficult, for lack of availability or expertise.

A specific explanation for the difference in performance between the parent report and direct measurement of the child's performance in low-functioning children could be the motor apraxia and auditory agnosia that were observed in MPS IIIA. These symptoms may prevent the child from performing an item to instruction or imitation, while

spontaneously they may be able to produce this behavior in the home environment; we have reported this elsewhere (Delaney et al. 2013). Although we cannot determine which score is more "correct," a score in a standardized testing situation such as the BSID-III or KABC-II reflects the consequences of the disease and should change over time with disease progression.

Each test assesses different aspects of cognitive development. The lack of overlap of what test items measure is a limitation of tracking from one test to another using AgeEqSs. Tests of infant and toddler development assess primarily visual and motor development; tests that start at age 2 or 3 will have more problem-solving and reasoning tasks (Sigelman et al. 2011). This may result in a discontinuity in what the AgeEqSs are measuring. However, the association with a parent report suggests that even though the items are quite different, a similar developmental trajectory can be identified.

Several papers have been published in the past regarding cognitive methods of assessment in lysosomal storage diseases (Martin et al. 2008; Shapiro et al. 1995). Valstar et al. addressed the issue of methods to assure reliability using familiar environments to decrease behavioral problems as well as tests for different levels of development (Valstar et al. 2011). Previously AgeEqSs have been used in some studies of cognitive and adaptive development (Staba et al. 2004; Peters et al. 1996, 1998; Wraith et al. 2007; Valstar et al. 2011; Bjoraker et al. 2006) despite their lack of acceptability in the psychology literature. What is new here? This study has (1) demonstrated the concurrent validity of AgeEqSs in cognitive ability testing, and (2) provided detailed specific clinical guidelines for testing behaviorally and cognitively impaired children. This is important as precise measurement of functional outcomes will be necessary as treatments for these children are developed.

The approach to testing we have taken with MPS IIIA is also applicable to multicenter studies of children with dementia or severe cognitive impairment in other conditions such as in late infantile Batten disease, Tay-Sachs disease, Krabbe disease, and Niemann-Pick disease type C. An in-depth understanding of how the disease alters the child's limitations should be the basis of test selection. Specific challenges that may arise due to neurological or medical concomitants of these disorders should be the foundation of the testing approach.

New treatments for genetic illnesses of children are now in trials or may soon be available. Enzyme replacement, gene therapy, stem cell therapies, small molecule medications, anti-inflammatories, and chaperone therapies will all require assessment of change over time. This is challenging because many of these children plateau in their development for long periods of time with sudden declines followed by another plateau. It requires natural history studies that trace the developmental growth curves of these patients without treatment to determine whether a treatment might alter the rate of growth or the slope of development. We propose that using guidelines for acquisition of neurodevelopmental data in severely impaired children to obtain AgeEqSs for test scores yields a useful, easily interpretable approach to assessing developmental trajectories and longitudinal change.

Acknowledgements The authors would like to acknowledge the support of Shire Pharmaceuticals and the Lysosomal Disease Network.

The Lysosomal Disease Network (U54NS065768) is a part of the National Institutes of Health (NIH) Rare Diseases Clinical Research Network (RDCRN), supported through collaboration between the NIH Office of Rare Diseases Research (ORDR) at the National Center for Advancing Translational Science (NCATS), the National Institute of Neurological Disorders and Stroke (NINDS) and National Institute of Diabetes and Digestive and Kidney Diseases (NIDDK). The content is solely the responsibility of the authors and does not necessarily represent the official views of the National Institutes of Health.

Summary Statement

A validated method of neurodevelopmental assessment in children with Sanfilippo and other neurodegenerative diseases.

References

Baehner F, Schmiedeskamp C, Krummenauer F et al (2005) Cumulative incidence rates of the mucopolysaccharidoses in Germany. J Inherit Metab Dis 28:1011–1017

Bayley N (2006) Bayley scales of infant and toddler development–third edition. Psychological Corporation, San Antonio

Bjoraker K, Delaney K, Peters C et al (2006) Long term outcomes of adaptive functions for children with MPS I. J Beh Dev Peds 27:290–296

Bland JM, Altman DG (1986) Statistical methods for assessing agreement between two methods of clinical measurement. Lancet 327:307–310

Cleary MA, Wraith JE (1993) Management of mucopolysaccharidosis type III. Arch Dis Child 69:403–406

Delaney K, Nestrasil I, Yund B et al (2013) Motor function decline and motor apraxia in Sanfilippo syndrome. Mol Genet Metab 108:S34

Elliott CD (2007) Differential ability scales-second edition. Psychological Corporation, San Antonio

Fraser J, Wraith JE, Delatycki MB (2002) Sleep disturbance in mucopolysaccharidosis type III (Sanfilippo syndrome): a survey of managing clinicians. Clin Genet 62:418–421

Heron B, Mikaeloff Y, Froissart R, et al (2011) Incidence and natural history of mucopolysaccharidosis type III in France and comparison with United Kingdom and Greece. Am J Med Genet A 155A:58–68

Hopwood J (2007) Sanfilippo syndrome: clinical genetic diagnosis and therapies. In: Barranger J (ed) Lysosomal storage disorders, Ch. 26. Springer, New York, pp 415–432

Huntley M (1996) The Griffiths mental development scales: from birth to 2 years, 2nd ed. The Test Agency Limited, Oxford

Kaufman AS, Kaufman NL (2004) Manual for the Kaufman assessment battery for children—second edition (KABC-II) comprehensive form. American Guidance Service, Circle Pines

Lawrence CW (1992) Assessing the use of age-equivalent scores in clinical management. Lang Speech Hear Serv Sch 23(1):6–8

Maloney ES, Larrivee LS (2007) Limitations of age-equivalent scores in reporting the results of norm-referenced tests. Contemporary Issues Commun Sci Disorder 34:86–93

Martin HR, Poe MD, Reinhartsen D, Pretzel RE, Roush J, Rosenberg A, Dusing SC, Escolar ML (2008) Methods for assessing neurodevelopment in lysosomal storage diseases and related disorders: a multidisciplinary perspective. Acta Pediat 97:69–75

Meikle PJ, Hopwood JJ, Clague AE, Carey WF (1999) Prevalence of lysosomal storage disorders. JAMA 281:249–254

Meyer A, Kossow K, Gal A et al (2007) Scoring evaluation of the natural course of mucopolysaccharidosis type IIIA (Sanfilippo syndrome type A). Pediatrics 120:e1255–e1261

Mullen EM (1995) Mullen scales of early learning. American Guidance Service, Circle Pines

Naglieri J, Goldstein S (2009) Practitioner's to guide assessing intelligence and achievement. Wiley, Hoboken

Peters C, Balthazor M, Shapiro E et al (1996) Outcome of unrelated donor bone marrow transplantation in forty children with Hurler syndrome. Blood 87:4894–4902

Peters C, Shapiro E, Anderson J et al (1998) Hurler Syndrome: II. Outcome of HLA-genotypically identical sibling and HLA-haploidentical related donor bone marrow transplantation in fifty-four children. Blood 91:2601–2608

Poorthuis BJ, Wevers RA, Kleijer WJ et al (1999) The frequency of lysosomal storage diseases in The Netherlands. Hum Genet 105:151–156

Raggio DJ, Massingale TW, Bass JD (1994) Comparison of Vineland adaptive behavior scales- survey form age equivalent and standard score with the Bayley Mental Development Index. Percept Mot Skills 79:203–206

Roid GH (2003) Stanford-Binet intelligence scales (5th ed). Riverside, Itasca, NY

Roid GH, Miller LJ (1997) Leiter international performance scale-revised: examiner's manual. Stoelting Co., Wood Dale

Shapiro E, Balthazor M. Metabolic (1999) and neurodegenerative disorders of childhood. In: G Taylor, D Ris, K Yeates (eds) Pediatric neuropsychology: research, theory and practice. Guilford Press, New York. pp 171–205

Shapiro E, Klein K (1993) Childhood dementia: neuropsychological assessment and treatment of degenerative childhood diseases. In: Tramontana MG, Hooper SR (eds) Advances in child neuropsychology, Volume III. Ch. 4. Springer, New York, pp 119–171

Shapiro EG, Lockman LA, Balthazor M, Krivit W (1995) Neuropsychological outcomes of several storage diseases with and without bone marrow transplantation. J Inherit Metab Dis 18:413–429

Sigelman CK, Rider EA (2011) Life-span human development – sixth edition. Wadsworth Cengage Learning, Belmont

Sparrow SS, Cicchetti DV, Balla DA (2005) Vineland adaptive behavior scales, 2nd edn. Psychological Corporation, San Antonio

Staba SL, Escolar ML, Poe M et al (2004) Cord blood transplants from unrelated donors in patients with Hurler's syndrome. NEJM 350:1060–1969

Valstar MJ, Marchal JP, Grootenhuis M et al (2011) Cognitive development in patients with mucopolysaccharidosis type III (Sanfilippo syndrome). Orphanet J Rare Dis 6:43

Volkmar FR, Sparrow SS, Goudreau D, Cicchetti DV, Paul R, Cohen DJ (1987) Social deficits in autism: an operational approach using the Vineland Adaptive Behavior Scales. J Amer Acad Child Psychiat 26:156–165

Wechsler D (2002) Wechsler preschool and primary scale of intelligence, 3rd edn. Psychological Corporation, San Antonio

Wraith JE, Beck M, Lane R et al (2007) Enzyme replacement therapy for mucopolysaccharidosis I patients less than 5 years old: Results of a multinational study of recombinant human alpha-L-iduonidase (laronidase). Pediatrics 120:e37–e46

Ziegler R, Shapiro E (2010) Metabolic neurodegenerative diseases across the lifespan. In: Donders J, Hunter S (eds) Principles and practice of lifespan developmental neuropsychology, ch. 15. Cambridge University Press, Cambridge, pp 427–448

JIMD Reports
DOI 10.1007/8904_2013_270

RESEARCH REPORT

Aminoglycoside-Induced Premature Stop Codon Read-Through of Mucopolysaccharidosis Type I Patient Q70X and W402X Mutations in Cultured Cells

Makoto Kamei · Karissa Kasperski · Maria Fuller · Emma J. Parkinson-Lawrence · Litsa Karageorgos · Valery Belakhov · Timor Baasov · John J. Hopwood · Doug A. Brooks

Received: 19 April 2013 / Revised: 13 August 2013 / Accepted: 25 September 2013 / Published online: 6 November 2013

Abstract The premature stop codon mutations, Q70X and W402X, are the most common α-L-iduronidase gene (IDUA) mutations in mucopolysaccharidosis type I (MPS I) patients. Read-through drugs have been used to suppress premature stop codons, and this can potentially be used to treat patients who have this type of mutation. We examined the effects of aminoglycoside treatment on the IDUA mutations Q70X and W402X in cultured cells and show that 4,5-disubstituted aminoglycosides induced more read-through for the W402X mutation, while 4,6-disubstituted aminoglycosides promoted more read-through for the Q70X mutation: lividomycin (4,5-disubstituted) induced a 7.8-fold increase in α-L-iduronidase enzyme activity for the W402X mutation; NB54 (4,5-disubstituted) induced a 3.7 fold increase in the amount of α-L-iduronidase enzyme activity for the W402X mutation, but had less effect on the Q70X mutation, whereas gentamicin (4,6-disubstituted) had the reverse effect on read-through for both mutations. The predicted mRNA secondary structural changes for both mutations were markedly different, which may explain these different effects on read-through for these two premature stop codons.

Communicated by: Frits Wijburg, MD, PhD

Competing interests: None declared

Makoto Kamei and Karissa Kasperski are equal first authors.

This work was supported by an NHMRC project grant (NHMRC 511321; DAB and MF) and an NHMRC Senior Research Fellowship (DAB).

M. Kamei (✉) · K. Kasperski · E.J. Parkinson-Lawrence · D.A. Brooks
Mechanisms in Cell Biology and Diseases Research Group, School of Pharmacy and Medical Sciences, Sansom Institute for Health Research, University of South Australia, South Australia 5001, Australia
e-mail: makoto.kamei@sahmri.com

L. Karageorgos · J.J. Hopwood
Lysosomal Diseases Research Unit, South Australian Health and Medical Research Institute, Adelaide, South Australia 5001, Australia

M. Fuller
SA Pathology, North Adelaide, South Australia 5006, Australia

V. Belakhov · T. Baasov
Schulich Faculty of Chemistry, Technion, Israel Institute of Technology, Haifa 32000, Israel

Introduction

Mucopolysaccharidosis type I (MPS I) is an autosomal recessive lysosomal storage disorder caused by a deficiency in the lysosomal exo-hydrolase, α-L-iduronidase (Neufeld and Muenzer 1995). MPS I patients exhibit clinical symptoms that include mental retardation, physical disability, short stature, skeletal deformity, somatic tissue pathology, and coarse facial features. There are three recognized MPS I clinical subgroups, which represent different points in a continuous clinical spectrum: Hurler, Hurler–Scheie, and Scheie syndromes. The majority of MPS I patients (up to 70%) present with Hurler syndrome, and have early onset and rapid disease progression (Bunge et al. 1994; Gort et al. 1998; Brooks 2002).

Molecular genetic studies show that most MPS I patients have a premature stop codon mutation in one or both alleles (Scott et al. 1992b, 1993; Hein et al. 2004;

Brooks et al. 2006). At least 17 different α-L-iduronidase premature stop codon mutations have been detected, and over 90% of Caucasian MPS I patients have at least one of these mutations (Hein et al. 2004). The association of premature stop codon mutations with early onset and rapidly progressive Hurler syndrome is the result of an inability to synthesize a full-length polypeptide and the ensuing dire consequences on enzyme activity (Scott et al. 1992b, 1993; Brooks 2002). The two α-L-iduronidase gene (IDUA) premature stop codon mutations, Q70X and W402X, are the most common mutations in MPS I patients (Scott et al. 1992a, b; Bunge et al. 1994) and this skews the clinical spectrum towards Hurler syndrome.

In people with a genetic disease caused by premature stop codon mutations, ribosomal read-through is a potential treatment strategy (Wilschanski et al. 2003; Lai et al. 2004). In a preclinical study using cultured cells, we demonstrated that gentamicin enhanced the read-through of IDUA premature stop codons and induced the synthesis of significant amounts of active α-L-iduronidase (Keeling et al. 2001; Hein et al. 2004). Aminoglycosides such as gentamicin can induce ribosomal read-through, by binding to the eukaryotic ribosome, causing a conformational change that induces faulty stop codon recognition (Francois et al. 2005). Aminoglycoside binding effectively lowers the docking energy required for the near-cognate transfer RNAs (tRNA), enabling amino acid substitution (Fourmy et al. 1998a, b; Pape et al. 2000). Glutamine and tryptophan have been reported to be the two most common amino acid insertions for mammalian stop codon read-through (Harrell et al. 2002) and these coincidently relate to the high frequency of Q70X and W402X mutations in MPS I (Brooks et al. 2006).

Extended administration of aminoglycosides to patients can cause nephrotoxicity and ototoxicity, a complication that is not ideal for a therapeutic agent (Darlington and Smith 2003; Rougier et al. 2004; Bitner-Glindzicz and Rahman 2007; Touw et al. 2009). Developing compounds with increased read-through capacity and reduced toxicity will therefore improve therapeutic potential. The paromomycin derivatives NB30 (Rebibo-Sabbah et al. 2007) and NB54 (Nudelman et al. 2009) have been reported to have significant read-through capacity and minimal toxicity (Nudelman et al. 2009; ClinicalTrials.gov 2010b). In addition, NB30 and NB54 have recently been shown to exhibit excellent biocompatibility and low toxicity *in vivo* (Goldmann et al. 2010, 2012). Here we evaluated six aminoglycosides (Fig. 1) for their capacity to induce premature stop codon read-through for the IDUA mutations Q70X and W402X established in CHO-K1 cells. We also examined the transcript secondary structure of these mutations to gain an appreciation of the differential efficacy for read-through.

Experimental Procedures

Aminoglycoside compounds for premature stop codon read-through. Amikacin, gentamicin, lividomycin, and paromomycin were purchased as sulfate salts (Sigma-Aldrich, Sydney, Australia).

Cell culture and extract preparation. CHO-K1 cells containing the human MPS I mutations Q70X and W402X (CHO-Q70X and CHO-W402X; with UAG premature stop codons) and the wild-type CHO-IDUA were cultured and harvested as previously described (Hein et al. 2004). The CHO-IDUA, CHO-Q70X, and CHO-W402X cell lines were generated as stably transfected CHO cell lines expressing either the human cDNA coding for α-L-iduronidase or its respective mutant forms, as previously described (Hein et al. 2004). For read-through analysis, the CHO-K1 cells were cultured to confluence in T-75 flasks (Greiner Bio-One, Monroe, NC, USA), harvested and seeded (5×10^5 cells in 2 mL of F12 culture media) into six-well culture plates (Nunc, Rochester, NY, USA). The cells were cultured for 24 h, then incubated with read-through drugs for 96 h (in fresh F12 culture media), before being harvested (Hein et al. 2004).

Human MPS I fibroblasts were established from skin biopsies archived in the National Referral Laboratory for Lysosomal, Peroxisomal and Related Genetic Disorders at SA Pathology, Adelaide, Australia, with the approval of the Children, Youth and Women's Health Service Research Ethics Committee. These fibroblasts were established and maintained as previously described (Ashton et al. 1992). Triplicates of each Q70X, W402X and unaffected fibroblast cell lines were cultured to confluence in T-75 flasks before the addition of the read-through drugs (for 96 h in BME culture media). The cells were then washed twice with PBS, resuspended in 200 μL 20 mM Tris–HCl (pH 7) containing 0.5 M NaCl, and then sonicated for 20 s to yield cell extracts (Myerowitz and Neufeld 1981). To remove cellular debris, fibroblast cell extracts were centrifuged at 17,000*g* for 10 min at room temperature; the supernatant was then stored at −20°C for subsequent analysis of protein and enzyme activity. The protein in cell extracts was determined using a Pierce Micro BCA Protein Assay Kit (Thermo Fisher Scientific, Sydney, Australia); α-L-iduronidase activity was determined by a fluorometric immunobinding assay as previously described (Hein et al. 2003).

Secondary structure predictions of IDUA transcripts. The predicted secondary structures of wild-type (full-length sequence; GenBank Accession Number NM_000203) and mutant IDUA transcripts (Q70X mutation: C to T base change at position 296; W402X mutation: G to A base change at position 1294) were generated using the RNA

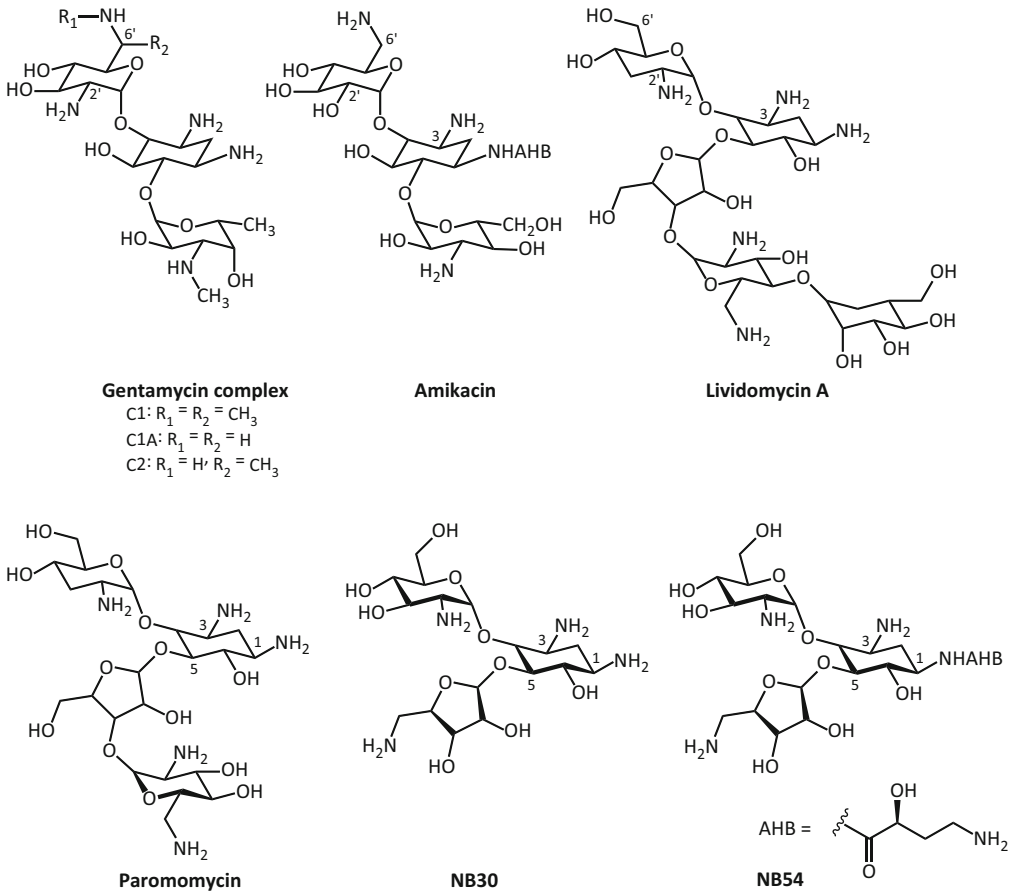

Fig. 1 Structure of the aminoglycosides used in this study, including 4,6-disubstituted compounds gentamicin and amikacin and the 4,5-disubstituted compounds lividomycin, paromomycin, NB30, and NB54

fold web server (http://rna.tbi.univie.ac.at; (Gruber et al. 2008)). The Minimum Free Energy algorithm (Zuker and Stiegler 1981) was used to predict the secondary structure; comparisons were made by overlapping the structures electronically using graphics files to identify landmark structural elements near the mutations. Putative ribozyme structures were detected visually by inspection of the altered secondary structures and by known ribozyme sequence requirements (Reymond et al. 2009).

Results

Aminoglycoside-induced read-through in CHO-K1 cell lines. CHO-K1 cells (no IDUA construct) had no detectable α-L-iduronidase activity either before or after treatment with aminoglycosides (data not shown); which involved detection of only human IDUA activity by specific immune capture (Hein et al. 2003). The maximum read-through response was defined for the aminoglycosides (0.5 mg/mL for gentamicin, amikacin, and paromomycin; and 2.0 mg/mL for lividomycin, NB30, and NB54), using CHO-Q70X and CHO-W402X cells (data not shown). In CHO-Q70X cells, α-L-iduronidase activity increased 3.1-fold with gentamicin, 1.8-fold with amikacin, and 2.2-fold with paromomycin, when compared to an untreated CHO-Q70X control (Fig. 2a). In CHO-W402X cells, α-L-iduronidase activity increased 1.7-fold with gentamicin, 1.8-fold with amikacin, and 3.1-fold with paromomycin, when compared to an untreated CHO-W402X control (Fig. 2b). α-L-Iduronidase activity did not increase in CHO-IDUA cells following treatment with any of the aminoglycosides (data not shown).

There was a significant increase in α-L-iduronidase activity in CHO-Q70X cells treated with 2 mg/mL of either NB30 (1.2-fold) or NB54 (1.7-fold), when compared to untreated CHO-Q70X cells (Fig. 3a). In CHO-Q70X cells, treatment with 0.5 mg/mL gentamicin resulted in higher α-L-iduronidase activity than either NB30 or NB54 (Fig. 3a). Some experimental variability was observed for the amount of IDUA activity in response to gentamicin read-through, for different experiments (Figs. 2, 3). Treatment of CHO-W402X cells with either 0.5 mg/mL or 2 mg/mL NB30 had no significant effect on α-L-iduronidase activity (Fig. 3b)

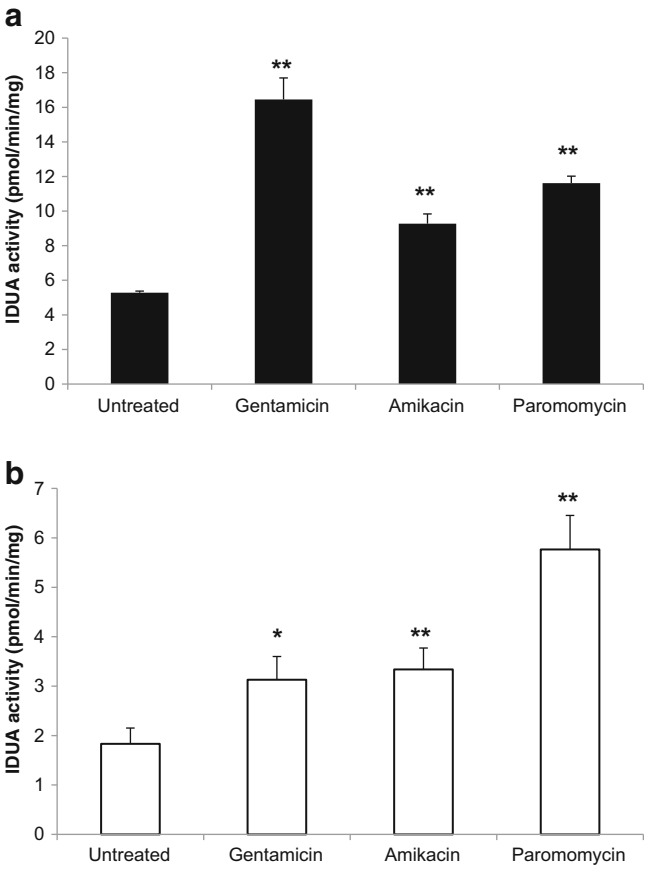

Fig. 2 Aminoglycoside treatment of CHO-Q70X and CHO-W402X cells. CHO-Q70X (Panel **a**) and CHO-W402X (Panel **b**) expression cells were treated with either gentamicin (0.5 mg/mL), amikacin (5 mg/mL), or paromomycin (4 mg/mL) and read-through assessed by analysis of α-L-iduronidase activity relative to an untreated control. Results were expressed in pmol/min/mg of α-L-iduronidase activity, corrected for total cell protein and represented the mean ± SD for three independent replicates. * and ** represent a significant difference from the untreated control at, respectively, $p < 0.05$ and $p < 0.001$

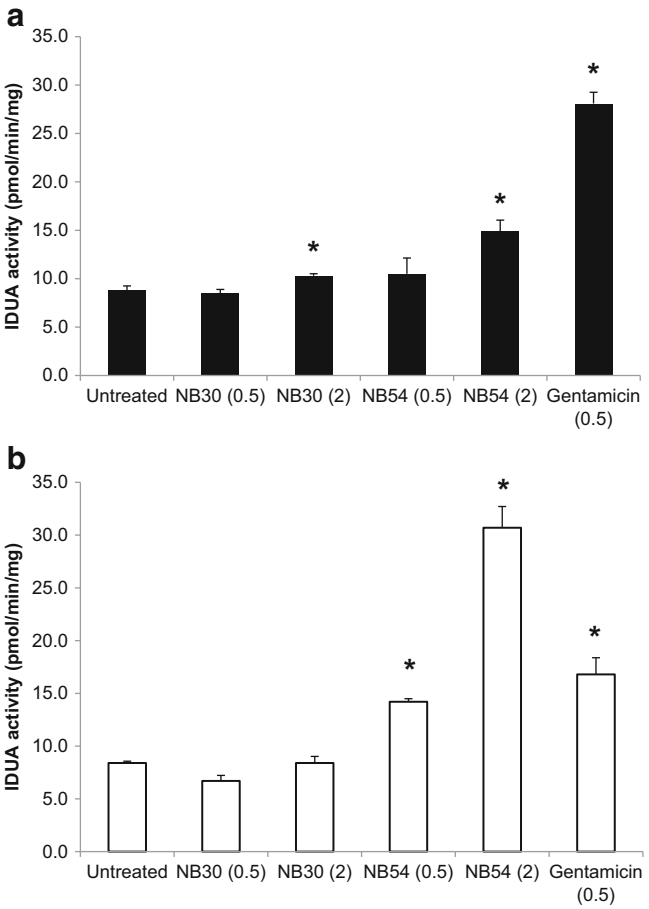

Fig. 3 NB30 and NB54 treatment of CHO-Q70X and CHO-W402X cells. CHO-Q70X (Panel **a**) and CHO-W402X (Panel **b**) expression cells were treated with either NB30 (0.5 or 2 mg/mL) or NB54 (0.5 or 2 mg/mL) and compared with either an untreated control or a 0.5 mg/mL gentamicin-positive control (gold standard). Results were expressed in pmol/min/mg of α-L-iduronidase activity, corrected for total cell protein, and represented the mean ± SD for three independent replicates. * and ** represent a significant difference from the untreated control at, respectively, $p < 0.05$ and $p < 0.001$

but treatment with NB54 resulted in a significant increase (1.7-fold for 0.5 mg/mL and 3.7-fold for 2 mg/mL), when compared to an untreated CHO-W402X control (Fig. 3b). α-L-Iduronidase activity in CHO-W402X cells was higher with NB54 treatment when compared to gentamicin (0.5 mg/mL; Fig. 3b).

In CHO-W402X cells, lividomycin had no effect at 0.5 mg/mL but α-L-iduronidase activity increased 2.9-fold at 1 mg/mL and 7.8-fold at 2 mg/mL (Fig. 4). The lack of availability of lividomycin precluded further testing of this compound.

Treatment of human fibroblasts with gentamicin and NB54. There was little or no detectable α-L-iduronidase activity in Q70X/Q70X or W402X/W402X skin fibroblasts (UAG premature stop codons; data not shown). In Q70X/Q70X fibroblasts, α-L-iduronidase activity increased to 0.27 pmol/min/mg with 2 mg/mL NB54, and to 0.48 pmol/min/mg with 0.5 mg/mL gentamicin (Fig. 5a); in contrast, α-L-iduronidase activity in W402X/W402X fibroblasts increased to 1.04 pmol/min/mg with 2 mg/mL NB54 and to 0.26 pmol/min/mg with 0.5 mg/mL gentamicin (Fig. 5a). NB54 and gentamicin treatment did not significantly change α-L-iduronidase activity in unaffected control fibroblasts (Fig. 5b).

Single base mutations are predicted to cause significant changes in the secondary structure of IDUA transcripts. The Q70X mutation (CAG to TAG) caused changes in the predicted mRNA secondary structure 20 base pairs before and 2 base pairs after the premature stop codon. This resulted in a change from a Q70 stem (Fig. 6a) to a Q70X loop structure (Fig. 6b). In addition, at base positions 413 to 475 there were changes from a relatively simple loop and stem structure to a more complex double stem–loop

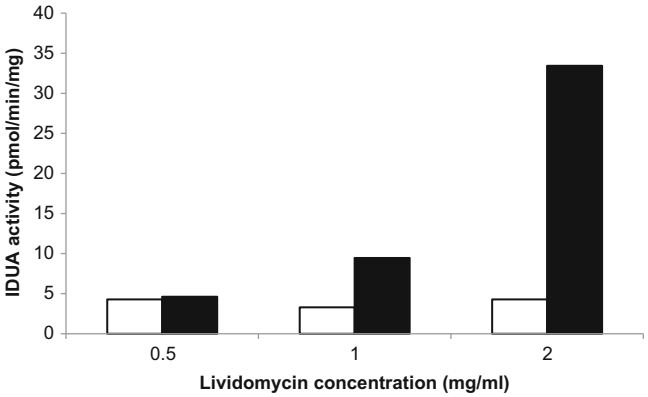

Fig. 4 Lividomycin treatment of CHO-W402X cells. CHO-W402X cells were treated with 0.5, 1.0, or 2 mg/mL of lividomycin (*solid bars*) and read-through assessed by α-L-iduronidase activity relative to an untreated control (*open bars*). Results were expressed in pmol/min/mg of α-L-iduronidase activity, corrected for total cell protein, and represented the mean of duplicate analyses

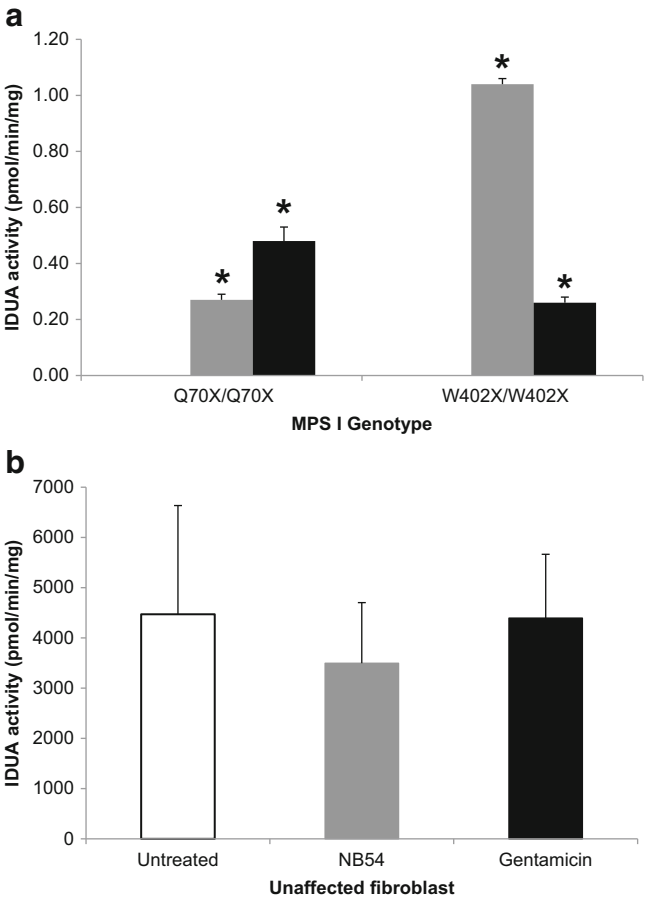

Fig. 5 NB54 and gentamicin treatment of MPS I patient skin fibroblasts. (**a**) MPS I patient skin fibroblasts with either W402X/W402X or Q70X/Q70X genotype (UAG premature stop codons; *open bar*) were treated with either NB54 (*shaded bar*) or gentamicin (*closed bar*). (**b**) Unaffected control fibroblasts (*open bar*) were treated with either NB54 (*shaded bar*) or gentamicin (*closed bar*). Results for **a** and **b** were expressed as pmol/min/mg of α-L-iduronidase activity, corrected for total cell protein and represented the mean ± SD for three independent replicates. * represented a significant difference from the untreated control at $p < 0.05$

structure (Fig. 6a and b). The W402X mutation (TGG to TAG) resulted in mRNA changes 74 base pairs before and 10 base pairs after the premature stop codon (Fig. 6d), causing a predicted shift in the secondary structure from a W402 stem (Fig. 6c) to a W402X stem–loop structure (Fig. 6d). In addition, a stem–loop (base positions 1457 to 1479) was extended (base positions 1470 to 1637) and created a putative hammerhead self-cleaving ribozyme structure (base positions 1607 to 1612 and 1614; Fig. 6b). In addition, "landmark" secondary structures surrounding the area were also significantly changed (Fig. 6a and b). The predicted structural changes were greater for the W402 to W402X transition than the Q70 to Q70X transition.

Discussion

MPS I is a common mucopolysaccharidosis disorder with most patients exhibiting mental retardation. Current therapies for MPS I include enzyme replacement therapy and bone marrow transplantation (Brooks 2002; Moore et al. 2008; D'Aco et al. 2012). While these therapies are effective for somatic tissue pathology, there are limitations with regard to the treatment of neuropathology. Drug-induced premature stop codon read-through is a potential alternative therapy; these drugs can potentially cross the blood–brain barrier from circulation, override premature stop codons, and provide full-length functional protein.

Gentamicin has been investigated as a read-through agent for MPS I (Keeling et al. 2001; Hein et al. 2004), and this aminoglycoside has the capacity to cross the blood–brain barrier. Aminoglycosides are 2-deoxystreptamine derivatives, which can be modified by links at the 4, 5, or 6 positions. These molecules contain at least two ring structures and, depending on modifications, may contain up to 5 rings: rings I and II have been shown to interact with RNA molecules, while rings III and above appear to contribute less to this binding (Carter et al. 2000; Kotra et al. 2000; Cashman et al. 2001; Vacas et al. 2010). The mechanism for aminoglycoside-mediated stop codon read-through is not fully understood: the binding of aminoglycosides to eukaryotic ribosomal RNA is thought to cause a conformation change in the ribosome (Francois et al. 2005), enabling tRNA binding and amino acid substitution (Carter et al. 2000) but aminoglycosides can also stabilize the mRNA of nonsense transcripts (Floquet et al. 2011).

Here, we examined six aminoglycosides for their capacity to induce read-through of the mutations Q70X and W402X. Lividomycin generated the highest W402X

Fig. 6 Predicted secondary structures of wild-type and mutant IDUA transcripts. Predicted secondary structures of both wild-type and mutant transcripts (both Q70X and W402X) were generated electronically using the Minimum Free Energy model and the local differences in the vicinity of the premature stop codon mutations (PTCs) were examined for their alterations. All PTCs and their precursors are indicated by red circles (Q70, Q70X, W402, and W402X). The orientation of the mRNA is indicated (5' and 3'). The first common base between Q70/Q70X (**a** and **b**) and W402/W402X (**c** and **d**) are indicated by *pale blue* and *cyan circles*, respectively. Both Q70X (**b**) and W402X (**d**) mutations cause alterations in mRNA secondary structures compared to their precursors Q70 (**a**) and W402 (**c**), respectively. The putative hammerhead self-cleaving ribozyme structure of the W402X transcript (**d**) is indicated by *green circles* (*RZ*)

read-through but drug availability limited these studies. Of the other drugs investigated, gentamicin had the most effect on Q70X, while NB54 had a greater effect on the W402X mutation. From the literature, the apparent sequence context dependency of aminoglycosides on the efficacy of read-through induction is not clear. We concluded that 4,6-disubstituted 2-deoxystreptamine molecules were more effective at inducing read-through for Q70X, whereas 4,5-disubstituted 2-deoxystreptamine molecules were more effective for W402X.

Direct aminoglycoside-to-RNA interaction depends upon the RNA secondary structure and therefore on the sequence. This was initially shown in short RNA molecules (aptamers) (Wang and Rando 1995) and subsequently in messenger RNA (Voeller et al. 1995; Tok et al. 1999; Walter et al. 1999). Aminoglycoside–RNA interaction has been implicated in gene expression regulation (Suess et al. 2003). Here, lividomycin induced the most efficient read-through for W402X. Lividomycin RNA aptamers can be dissociated using other 4,5-disubstituted aminoglycosides such as paromomycin but not readily with 4,6-disubsituted aminoglycosides such as kanamycin (Lato et al. 1995). This suggested that class-specific aminoglycoside binding might be responsible for the different amounts of read-through that we observed. The predicted secondary structure of wild-type and mutant IDUA transcripts was used to determine whether RNA structure correlated with the capacity to induce read-through. Large differences were apparent in the predicted secondary structures of the mutant transcripts in the vicinity of the altered bases, which may explain the differences in aminoglycoside binding. The W402X G to A base change altered the predicted secondary and tertiary structure, with a Uridine Turn Motif (CTGANGA) being exposed in a loop. To date five ribozymes have been characterized, which catalyze the sequence-specific intramolecular cleavage of RNA: the hammerhead (Prody et al. 1986; Forster and

Table 1 Descriptive data

Measure $N = 25$ for all measures	Mean (standard deviation)
Age: mean (S.D.)	75.0 months (53.4) range 13–220 months
Cognitive age-equivalent (BSID or KABC)	23.0 months (12.9) range 7–58 months
Developmental Quotient (mean age-equivalent of BSID or KABC/ chronological age)	44.6 (28.4) range 3–91
Vineland age-equivalent (mean of subscales except motor domain)	23.8 months (12.8) range 6–61 months
Vineland developmental quotient (mean of age equivalents except motor domain/chronological age)	44.4 (25.3) range 3–95
Standard score using normative data on the Vineland	63.0 (16.8) range 25–95

Symons 1987), hairpin (Buzayan et al. 1986), hepatitis delta virus (HDV) (Sharmeen et al. 1988), Varkud satellite (VS) (Saville and Collins 1990), and *glmS* (Winkler et al. 2004) ribozymes. The Uridine Turn Motif that we observed for the W402X mutation was characteristic of a hammerhead ribozyme.

RNA self-cleavage may help to remove some of the W402X mutant transcript, which is also degraded by nonsense-mediated decay, resulting in the very low mutant mRNA observed in MPS I cells (Menon and Neufeld 1994; Hein et al. 2004). Aminoglycosides can inhibit ribozymes when bound to messenger RNA (Walter et al. 1999; Schroeder et al. 2000) and could potentially act on the W402X-associated ribozyme activity. Novel approaches could be used to address this loss of transcript (e.g., antisense oligonucleotide technology: LNA (Obika et al. 1997; Koshkin et al. 1998); PNA (Egholm et al. 1993) and morpholino (Summerton 1999); or mutant RNA editing (Woolf et al. 1995; Morabito and Emeson 2009).

Extended administration of aminoglycosides is known to cause vestibulotoxicity (Halmagyi et al. 1994; Darlington and Smith 2003) and nephrotoxicity (Rougier et al. 2004) in humans. This has led to the development of less toxic aminoglycoside derivatives and other compounds such as NB30 and NB54 which exhibited read-through for both W402X and Q70X mutations and may be more suitable read-through agents (Hirawat et al. 2007; Du et al. 2009; Nudelman et al. 2009). Potential read-through compounds have been evaluated in preclinical trials; for example, the aminoglycoside G418 was used to prevent proximal renal tubular acidosis and proximal spinal muscular atrophy (Azimov et al. 2008; Heier and DiDonato 2009); NB30 and NB54 have been evaluated for biocompatibility and read-through potential in an animal model of Usher syndrome (Goldmann et al. 2010, 2012) and patients with cystic fibrosis have been treated with PTC124 (Wilschanski et al. 2003; Welch et al. 2007; Du et al. 2008; Kerem et al. 2008; Goodier and Mayer 2009; Peltz et al. 2009; Sermet-Gaudelus et al. 2010); and this drug has been evaluated in a Phase III clinical trial (ClinicalTrials.gov 2010b) in cystic fibrosis patients. Duchenne muscular dystrophy patients have been treated with gentamicin (Malik et al. 2010) and PTC124 (Wilton 2007), although the PTC124 clinical trial was suspended due to lack of efficacy in these patients (ClinicalTrials.gov 2010a).

In this study, different responses to read-through drugs were observed for Q70X and W402X mutation. This may relate to the observed structural changes in these transcripts resulting in either different amounts of residual mutant mRNA and/or different transcript read-through potential. The mechanism controlling the efficacy of aminoglycoside action is not fully clear but may involve a combination of mutant transcript stabilization, modulation of the fidelity of ribosome tRNA selection/amino acid substitution, or even reduced ribozyme activity for certain mutations. In MPS I, premature stop codon read-through therapy may therefore require drugs that are tailored to each patient's specific mutations in order to deliver an optimal therapeutic outcome. The compounds tested here produced relatively small increases in IDUA activity, and it is yet to be determined if this is sufficient read-through for clinical applications.

Synopsis

Examination of aminoglycoside-mediated read-through of premature stop codons present in the Q70X and the W402X mutations in the human α-iduronidase gene provided insights into the difference in efficacies seen in read-through drugs in use.

References

Ashton LJ, Brooks DA, McCourt PA, Muller VJ, Clements PR, Hopwood JJ (1992) Immunoquantification and enzyme kinetics of alpha-L-iduronidase in cultured fibroblasts from normal controls and mucopolysaccharidosis type I patients. Am J Hum Genet 50(4):787–794

Azimov R, Abuladze N, Sassani P et al (2008) G418-mediated ribosomal read-through of a nonsense mutation causing autosomal recessive proximal renal tubular acidosis. Am J Physiol Renal Physiol 295(3):F633–641

Bitner-Glindzicz M, Rahman S (2007) Ototoxicity caused by aminoglycosides. BMJ 335(7624):784–785

Brooks DA (2002) Alpha-L-iduronidase and enzyme replacement therapy for mucopolysaccharidosis I. Expert Opin Biol Ther 2 (8):967–976

Brooks DA, Muller VJ, Hopwood JJ (2006) Stop-codon read-through for patients affected by a lysosomal storage disorder. Trends Mol Med 12(8):367–373

Bunge S, Kleijer WJ, Steglich C et al (1994) Mucopolysaccharidosis type I: identification of 8 novel mutations and determination of the frequency of the two common alpha-L-iduronidase mutations (W402X and Q70X) among European patients. Hum Mol Genet 3(6):861–866

Buzayan JM, Gerlach WL, Bruening G (1986) Non-enzymatic cleavage and ligation of RNAs complementary to a plant virus satellite RNA. Nature 323(6086):349–353

Carter AP, Clemons WM, Brodersen DE, Morgan-Warren RJ, Wimberly BT, Ramakrishnan V (2000) Functional insights from the structure of the 30S ribosomal subunit and its interactions with antibiotics. Nature 407(6802):340–348

Cashman DJ, Rife JP, Kellogg GE (2001) Which aminoglycoside ring is most important for binding? A hydropathic analysis of gentamicin, paromomycin, and analogues. Bioorg Med Chem Lett 11(2):119–122

ClinicalTrials.gov (2010a) Study of Ataluren (PTC124®) in non-ambulatory patients with nonsense-mutation-mediated Duchenne/Becker muscular dystrophy (nmDMD/BMD). In: Study of Ataluren (PTC124®) in nonambulatory patients with nonsense-mutation-mediated Duchenne/Becker muscular dystrophy (nmDMD/BMD). http://clinicaltrials.gov/ct2/show/NCT01009294?term=study+of+ataluren&rank=4

ClinicalTrials.gov (2010b) Study of Ataluren (PTC124™) in cystic fibrosis. In: Study of Ataluren (PTC124™) in Cystic Fibrosis. http://clinicaltrials.gov/ct2/show/NCT00803205?term=study+of+ataluren&rank=6

D'Aco K, Underhill L, Rangachari L et al (2012) Diagnosis and treatment trends in mucopolysaccharidosis I: findings from the MPS I Registry. Eur J Pediatr 171(6):911–919

Darlington CL, Smith PF (2003) Vestibulotoxicity following aminoglycoside antibiotics and its prevention. Curr Opin Investig Drugs 4(7):841–846

Du M, Liu X, Welch EM, Hirawat S, Peltz SW, Bedwell DM (2008) PTC124 is an orally bioavailable compound that promotes suppression of the human CFTR-G542X nonsense allele in a CF mouse model. Proc Natl Acad Sci U S A 105(6): 2064–2069

Du L, Damoiseaux R, Nahas S et al (2009) Nonaminoglycoside compounds induce readthrough of nonsense mutations. J Exp Med 206(10):2285–2297

Egholm M, Buchardt O, Christensen L et al (1993) PNA hybridizes to complementary oligonucleotides obeying the Watson-Crick hydrogen-bonding rules. Nature 365(6446):566–568

Floquet C, Deforges J, Rousset JP, Bidou L (2011) Rescue of non-sense mutated p53 tumor suppressor gene by aminoglycosides. Nucleic Acids Res 39(8):3350–3362

Forster AC, Symons RH (1987) Self-cleavage of plus and minus RNAs of a virusoid and a structural model for the active sites. Cell 49(2):211–220

Fourmy D, Recht MI, Puglisi JD (1998a) Binding of neomycin-class aminoglycoside antibiotics to the A-site of 16 S rRNA. J Mol Biol 277(2):347–362

Fourmy D, Yoshizawa S, Puglisi JD (1998b) Paromomycin binding induces a local conformational change in the A-site of 16 S rRNA. J Mol Biol 277(2):333–345

Francois B, Russell RJ, Murray JB et al (2005) Crystal structures of complexes between aminoglycosides and decoding A site oligonucleotides: role of the number of rings and positive charges in the specific binding leading to miscoding. Nucleic Acids Res 33(17):5677–5690

Goldmann T, Rebibo-Sabbah A, Overlack N et al (2010) Beneficial read-through of a USH1C nonsense mutation by designed aminoglycoside NB30 in the retina. Invest Ophthalmol Vis Sci 51(12):6671–6680

Goldmann T, Overlack N, Moller F et al (2012) A comparative evaluation of NB30, NB54 and PTC124 in translational read-through efficacy for treatment of an USH1C nonsense mutation. EMBO Mol Med 4(11):1186–1199

Goodier JL, Mayer J (2009) PTC124 for cystic fibrosis. Lancet 373 (9673): 1426; author reply 1426–1427

Gort L, Chabas A, Coll MJ (1998) Analysis of five mutations in 20 mucopolysaccharidois type 1 patients: high prevalence of the W402X mutation. Mutations in brief no. 121. Online. Hum Mutat 11(4):332–333

Gruber AR, Lorenz R, Bernhart SH, Neubock R, Hofacker IL (2008) The Vienna RNA websuite. Nucleic Acids Res 36(Web Server issue): W70–74

Halmagyi GM, Fattore CM, Curthoys IS, Wade S (1994) Gentamicin vestibulotoxicity. Otolaryngol Head Neck Surg 111(5):571–574

Harrell L, Melcher U, Atkins JF (2002) Predominance of six different hexanucleotide recoding signals 3' of read-through stop codons. Nucleic Acids Res 30(9):2011–2017

Heier CR, DiDonato CJ (2009) Translational readthrough by the aminoglycoside geneticin (G418) modulates SMN stability in vitro and improves motor function in SMA mice in vivo. Hum Mol Genet 18(7):1310–1322

Hein LK, Hopwood JJ, Clements PR, Brooks DA (2003) The alpha-L-iduronidase mutations R89Q and R89W result in an attenuated mucopolysaccharidosis type I clinical presentation. Biochim Biophys Acta 1639(2):95–103

Hein LK, Bawden M, Muller VJ, Sillence D, Hopwood JJ, Brooks DA (2004) Alpha-L-iduronidase premature stop codons and potential read-through in mucopolysaccharidosis type I patients. J Mol Biol 338(3):453–462

Hirawat S, Welch EM, Elfring GL et al (2007) Safety, tolerability, and pharmacokinetics of PTC124, a nonaminoglycoside nonsense mutation suppressor, following single- and multiple-dose administration to healthy male and female adult volunteers. J Clin Pharmacol 47(4):430–444

Keeling KM, Brooks DA, Hopwood JJ, Li P, Thompson JN, Bedwell DM (2001) Gentamicin-mediated suppression of Hurler syndrome stop mutations restores a low level of alpha-L-iduronidase activity and reduces lysosomal glycosaminoglycan accumulation. Hum Mol Genet 10(3):291–299

Kerem E, Hirawat S, Armoni S et al (2008) Effectiveness of PTC124 treatment of cystic fibrosis caused by nonsense mutations: a prospective phase II trial. Lancet 372(9640):719–727

Koshkin AA, Singh SK, Nielsen P et al (1998) LNA (Locked Nucleic Acids): Synthesis of the adenine, cytosine, guanine, 5-methylcytosine, thymine and uracil bicyclonucleoside monomers, oligomerisation, and unprecedented nucleic acid recognition. Tetrahedron 54(14):3607–3630

Kotra LP, Haddad J, Mobashery S (2000) Aminoglycosides: perspectives on mechanisms of action and resistance and strategies to counter resistance. Antimicrob Agents Chemother 44 (12):3249–3256

Lai CH, Chun HH, Nahas SA et al (2004) Correction of ATM gene function by aminoglycoside-induced read-through of premature termination codons. Proc Natl Acad Sci U S A 101(44): 15676–15681

Lato SM, Boles AR, Ellington AD (1995) In vitro selection of RNA lectins: using combinatorial chemistry to interpret ribozyme evolution. Chem Biol 2(5):291–303

Malik V, Rodino-Klapac LR, Viollet L, et al (2010) Gentamicin-induced readthrough of stop codons in Duchenne muscular dystrophy. Annals Neurol 9999(999A): NA

Menon KP, Neufeld EF (1994) Evidence for degradation of mRNA encoding alpha-L-iduronidase in Hurler fibroblasts with premature termination alleles. Cell Mol Biol (Noisy-le-grand) 40(7):999–1005

Moore D, Connock MJ, Wraith E, Lavery C (2008) The prevalence of and survival in Mucopolysaccharidosis I: Hurler, Hurler-Scheie and Scheie syndromes in the UK. Orphanet J Rare Dis 3:24

Morabito MV, Emeson RB (2009) RNA editing as a therapeutic target for CNS disorders. Neuropsychopharmacology 34(1):246

Myerowitz R, Neufeld EF (1981) Maturation of alpha-L-iduronidase in cultured human fibroblasts. J Biol Chem 256(6):3044–3048

Neufeld EF, Muenzer J (1995) The mucopolysaccharidosis. In: Scriver CR, Beaudet AL, Sly WS, Valle D (eds) The metabolic and molecular bases of inherited disease. McGraw-Hill, New York

Nudelman I, Rebibo-Sabbah A, Cherniavsky M et al (2009) Development of novel aminoglycoside (NB54) with reduced toxicity and enhanced suppression of disease-causing premature stop mutations. J Med Chem 52(9):2836–2845

Obika S, Nanbu D, Hari Y et al (1997) Synthesis of 2'-O,4'-C-methyleneuridine and -cytidine. Novel bicyclic nucleosides having a fixed C3, -endo sugar puckering. Tetrahedron Lett 38 (50):8735–8738

Pape T, Wintermeyer W, Rodnina MV (2000) Conformational switch in the decoding region of 16S rRNA during aminoacyl-tRNA selection on the ribosome. Nat Struct Biol 7(2):104–107

Peltz SW, Welch EM, Jacobson A, et al (2009) Nonsense suppression activity of PTC124 (ataluren). Proc Natl Acad Sci USA 106(25): E64; author reply E65

Prody GA, Bakos JT, Buzayan JM, Schneider IR, Bruening G (1986) Autolytic processing of dimeric plant virus satellite RNA. Science 231(4745):1577–1580

Rebibo-Sabbah A, Nudelman I, Ahmed ZM, Baasov T, Ben-Yosef T (2007) In vitro and ex vivo suppression by aminoglycosides of PCDH15 nonsense mutations underlying type 1 Usher syndrome. Hum Genet 122(3–4):373–381

Reymond C, Beaudoin JD, Perreault JP (2009) Modulating RNA structure and catalysis: lessons from small cleaving ribozymes. Cell Mol Life Sci 66(24):3937–3950

Rougier F, Claude D, Maurin M, Maire P (2004) Aminoglycoside nephrotoxicity. Curr Drug Targets Infect Disord 4(2):153–162

Saville BJ, Collins RA (1990) A site-specific self-cleavage reaction performed by a novel RNA in Neurospora mitochondria. Cell 61 (4):685–696

Schroeder R, Waldsich C, Wank H (2000) Modulation of RNA function by aminoglycoside antibiotics. EMBO J 19(1):1–9

Scott HS, Litjens T, Hopwood JJ, Morris CP (1992a) A common mutation for mucopolysaccharidosis type I associated with a severe Hurler syndrome phenotype. Hum Mutat 1(2):103–108

Scott HS, Litjens T, Nelson PV, Brooks DA, Hopwood JJ, Morris CP (1992b) Alpha-L-iduronidase mutations (Q70X and P533R) associate with a severe Hurler phenotype. Hum Mutat 1 (4):333–339

Scott HS, Litjens T, Nelson PV et al (1993) Identification of mutations in the alpha-L-iduronidase gene (IDUA) that cause Hurler and Scheie syndromes. Am J Hum Genet 53(5):973–986

Sermet-Gaudelus I, Boeck KD, Casimir GJ et al (2010) Ataluren (PTC124) induces cystic fibrosis transmembrane conductance regulator protein expression and activity in children with nonsense mutation cystic fibrosis. Am J Respir Crit Care Med 182(10):1262–1272

Sharmeen L, Kuo MY, Dinter-Gottlieb G, Taylor J (1988) Anti-genomic RNA of human hepatitis delta virus can undergo self-cleavage. J Virol 62(8):2674–2679

Suess B, Hanson S, Berens C, Fink B, Schroeder R, Hillen W (2003) Conditional gene expression by controlling translation with tetracycline-binding aptamers. Nucleic Acids Res 31 (7):1853–1858

Summerton J (1999) Morpholino antisense oligomers: the case for an RNase H-independent structural type. Biochim Biophys Acta 1489(1):141–158

Tok JB, Cho J, Rando RR (1999) Aminoglycoside antibiotics are able to specifically bind the 5'-untranslated region of thymidylate synthase messenger RNA. Biochemistry 38(1):199–206

Touw DJ, Westerman EM, Sprij AJ (2009) Therapeutic drug monitoring of aminoglycosides in neonates. Clinical Pharmacokinetics 48(2):71–88. doi:10.2165/00003088-200948020-200900001

Vacas T, Corzana F, Jimenez-Oses G et al (2010) Role of aromatic rings in the molecular recognition of aminoglycoside antibiotics: implications for drug design. J Am Chem Soc 132 (34):12074–12090

Voeller DM, Changchien LM, Maley GF et al (1995) Characterization of a specific interaction between *Escherichia coli* thymidylate synthase and Escherichia coli thymidylate synthase mRNA. Nucleic Acids Res 23(5):869–875

Walter F, Vicens Q, Westhof E (1999) Aminoglycoside-RNA interactions. Curr Opin Chem Biol 3(6):694–704

Wang Y, Rando RR (1995) Specific binding of aminoglycoside antibiotics to RNA. Chem Biol 2(5):281–290

Welch EM, Barton ER, Zhuo J et al (2007) PTC124 targets genetic disorders caused by nonsense mutations. Nature 447(7140):87–91

Wilschanski M, Yahav Y, Yaacov Y et al (2003) Gentamicin-induced correction of CFTR function in patients with cystic fibrosis and CFTR stop mutations. N Engl J Med 349(15):1433–1441

Wilton S (2007) PTC124, nonsense mutations and Duchenne muscular dystrophy. Neuromuscul Disord 17(9–10):719–720

Winkler WC, Nahvi A, Roth A, Collins JA, Breaker RR (2004) Control of gene expression by a natural metabolite-responsive ribozyme. Nature 428(6980):281–286

Woolf TM, Chase JM, Stinchcomb DT (1995) Toward the therapeutic editing of mutated RNA sequences. Proc Natl Acad Sci USA 92 (18):8298–8302

Zuker M, Stiegler P (1981) Optimal computer folding of large RNA sequences using thermodynamics and auxiliary information. Nucleic Acids Res 9(1):133–148

JIMD Reports
DOI 10.1007/8904_2013_273

RESEARCH REPORT

Dietary Habits and Metabolic Control in Adolescents and Young Adults with Phenylketonuria: Self-Imposed Protein Restriction May Be Harmful

A.M. Das · K. Goedecke · U. Meyer · N. Kanzelmeyer · S. Koch · S. Illsinger · T. Lücke · H. Hartmann · K. Lange · H. Lanfermann · L. Hoy · X.-Q. Ding

Received: 03 June 2013 / Revised: 20 September 2013 / Accepted: 07 October 2013 / Published online: 13 November 2013

Abstract Background: In untreated patients, phenylketonuria (PKU) results in severe encephalopathy with mental retardation. A protein-restricted diet is recommended which can be relaxed in adolescence/adulthood.

Methods: We contacted all 72 adult/adolescent PKU patients who had been treated in our center during early childhood. Some still regularly attended our outpatient clinics, while others were lost for follow-up, giving 51 patients in our study. We asked all patients to complete a dietary protocol as well as a questionnaire on quality of life. Blood and urine were analyzed and body impedance plethysmography and cerebral MRI were performed.

Results: 42 % of the patients followed protein restriction supplemented with amino acid mixtures (AAM), others had a vegan diet with (8 %) or without (14 %) AAM; 36 % said they were eating normally and did not need any AAM. However, based on dietary protocols and blood urea levels, protein intake was restricted in this patient group. None of the patients examined had serious nutritional deficits. Phenylalanine levels were higher in patients not taking AAM. MRI of the brain was not different from those following protein restriction and taking AAM. The lesions score and mood correlated best with the cumulative phenylalanine values during the first 10 years of life.

Conclusion: In summary, 50 % of adult/adolescent patients from our center did not take AAM at the start of our survey although they unknowingly followed self-imposed protein restriction. They had no overt nutritional deficits; however, long-term brain function may be compromised. Our study emphasizes the need for specialized metabolic care in PKU during adulthood.

Communicated by: Anita MacDonald, PhD, BSc

Competing interests: None declared

A.M. Das (✉)
Clinic for Pediatric Kidney-, Liver- and Metabolic Diseases, Hannover Medical School, Carl-Neuberg- Str. 1, D- 30625 Hannover, Germany
e-mail: das.anibh@mh-hannover.de

K. Goedecke · U. Meyer · N. Kanzelmeyer · S. Koch · S. Illsinger · T. Lücke · H. Hartmann
Clinic for Pediatric Kidney-, Liver- and Metabolic Diseases, Hannover Medical School, Hannover, Germany

K. Lange
Medical Psychology, Hannover Medical School, Hannover, Germany

H. Lanfermann · X.-Q. Ding
Institute of Diagnostic and Interventional Neuroradiology, Hannover Medical School, Hannover, Germany

L. Hoy
Institute for Biometrics, Hannover Medical School, Hannover, Germany

Introduction

Phenylketonuria (PKU, MIM #261600) is an inherited disorder of amino acid metabolism leading to the accumulation of phenylalanine and reduction of tyrosine in body fluids. If left untreated, patients develop severe encephalopathy with mental retardation and epilepsy. In many countries, PKU is diagnosed in the first days of life by newborn mass screening. Treatment is exclusively dietary, based on protein restriction supplemented with amino acid mixtures (AAM) free of phenylalanine (and enriched with tyrosine, vitamins, minerals, and trace elements) (Hendriksz and Walter 2004; Blau et al. 2010). Administration of tetrahydrobiopterin (BH4) has been suggested as an adjunct therapy in milder forms of PKU (Oddason et al. 2011), but its role in clinical medicine is still under discussion. "Diet for life" is advocated in this genetically determined disease,

although relaxation of the diet in adolescence and adulthood is thought possible (Burgard 2000; Abadie et al. 2005; de Baulny et al. 2007).

The latter may lead to at least partial loss of compliance, with consequent reduction in metabolic control. Some adult patients eat healthily, while others have an unbalanced diet not necessarily supplemented with an amino acid mixture. Still others may assume that their protein-restricted diet is normal as they are accustomed to protein restriction since early childhood. As a consequence, deficiencies of trace elements, vitamins, minerals, and amino acids may result because diet is not supplemented with AAM (Giovannini et al. 2007; Feillet and Agostoni 2010; MacDonald et al. 2011).

Symptoms of poor metabolic control are concentration deficits, abnormal behavior, and headaches, as well as general weakness, frequently accompanied by poor school or job performance (Hendriksz and Walter 2004; Blau et al. 2010). Skin and hair abnormalities may result from zinc or selenium deficiency.

Although major disabilities can be prevented by early protein restriction, more subtle deficits are common (Bick et al. 1993; Huijbregts et al. 2002; Anderson et al. 2007; Gentile et al. 2010), even in patients with good metabolic control. These health problems may be more pronounced in those patients who do not adhere to dietary recommendations and requirements.

In this study, we examined dietary habits and metabolic control in early-treated adult and adolescent patients, assessed their quality of life, and performed cerebral MRI.

Patients and Methods

Patients

All patients were recruited from one single center. PKU patients with other chronic diseases or chronic use of medication other than amino acid supplementation, pregnant women, and patients not diagnosed and treated in the newborn period were excluded. At the start of our study, 130 patients with PKU were registered in our center. We only invited adult/adolescent patients with classical, early-treated PKU to participate. This gave 72 adolescent and adult patients (45 females, 27 males) who regularly visited our metabolic outpatient clinic and/or were treated in our center as children or infants. Fifty-one PKU patients (age range 16–44 years, mean ± SD 26.6 ± 6.6 years; 32 females, 26.5 ± 6.2 years; 19 males, 26.8 ± 7.7 years) accepted our invitation.

Methods

Participants were asked to compile a dietary protocol, which was analyzed by our metabolic dietician. Additionally, we analyzed body composition and biochemical parameters in blood and urine which may indicate nutritional deficiencies, and offered cerebral MRI scans.

Not all 51 patients completed a dietary protocol. However, as many other parameters were measured, non-completion was not an exclusion criterion in our study.

Dietary protocol: Dietary protocols (3–8 days) were obtained from 36 patients (24 females, 12 males) at the start of our survey.

According to their nutritional habits, assessed by the patients and documented in the protocol, patients were divided into four groups:

1. Normal food (**"normal food"**)
2. Vegan without amino acid mixture **("vegan")**
3. Vegan with amino acid mixture (**"vegan + AAM")**
4. Protein reduced with amino acid mixture which is the recommended form of nutrition **("PKU-diet")**

All patients not taking AAM at the beginning of the study agreed to supplement their original diet with an AAM subsequently.

Body impedance analysis (BIA): BIA was performed using commercially available instrumentation (multifrequency impedance analyzer "Nutriguard-M", Nutriplus software, Data Input GmbH, Darmstadt, Germany). Contents of fat and water were analyzed. Furthermore, body cell mass, lean body mass, extracellular mass, and phase angle assessing the quality of cell membranes were approximated.

Biochemical analyses: At the beginning of our survey, parameters of organ function and nutritional status were determined in blood and urine (see Table 1 for an overview). Acylcarnitine profiles in dried blood were analyzed (assessment of carnitine status, fatty acid oxidation, organic acids) to exclude deficiency of vitamins and cofactors. Results were compared to normal values in our laboratory. Actual phenylalanine concentration in plasma was determined.

As therapeutic target concentrations of phenylalanine are age dependant, three age bands were chosen:

1. 0–10 years (target: < 4 mg/dl $= 240$ μM)
2. 10–15 years (target: < 15 mg/dl $= 900$ μM)
3. Older than 15 years (target: < 20 mg/dl $= 1{,}200$ μM)

Both average phenylalanine levels and variation of phenylalanine levels over lifetime are supposed to influence the outcome of the disease (Burgard 2000; Anastasoaie et al. 2008; Viau et al. 2011). Via retrospective statistical

Table 1 Overview of parameters analyzed in blood and urine

Blood	Parameters
Blood count	Leucocytes
	Thrombocytes
	Haemoglobine
	MCV
	MCH
Coagulation	Quick test
	INR Ratio
	PTT
Electrolytes	Potassium
	Sodium
	Calcium
	Chloride
	Phosphate
Bone	Alkaline phosphatase
Renal function	Urea
	Creatine
Liver function	AST
	ALT
	GLDH
	Alkaline phosphatase
	Gamma GT
	Cholinesterase
	Bilirubine
Additional	Glucose
Metabolic data	Lactate
	Creatine kinase
	Acylcarnitine profile
Iron metabolism	Iron
	Iron binding capacity
	Transferrin saturation
	Ferritin
Other trace elements	Zinc
	Selenium
Water-soluble vitamins	Folate
	Cobalamine
Liposoluble vitamins	Retinole
	Tocopherole
Protein metabolism	Protein
	Amino acids
Lipid metabolism	Cholesterol
Urine	
Organic acids	Methylmalonic acid and others
Additional data	Creatinine
	Albumine
	Alpha-1-microglobuline
	Amino acids

analysis mean phenylalanine concentration in plasma as well as variation of plasma phenylalanine levels during lifetime were calculated.

MR Imaging

Twenty-four out of 51 PKU patients included in the study underwent MRI examination of brain. The other patients did not give consent (claustrophobia, fear of pathological results, etc.) or had to be excluded for medical reasons (interfering material like dental brackets or tattoos).

MRI examinations were conducted using a 1.5 T scanner (Siemens Avanto, Erlangen, Germany). A routine MRI protocol was applied, which included single voxel spectroscopy (TR/TE = 6,000/20) in the parietal white matter.

MR morphological findings were independently interpreted by two experienced neuroradiologists. The images of all subjects were assessed using a standardized structured form (involvement of the lobar white matter (WM), periventricular white matter, centrum semiovale) and rated by using a modified version of the semiquantitative Scheltens scale (Scheltens et al. 1993).

Quality of Life, Mood Status, and Education

Health-related quality of life (HrQoL) and current psychological well-being were assessed using established psychometric questionnaires. The questionnaire "Alltagsleben (AL)" (Bullinger et al. 1993) consists of 45 items summed up to six subscales (general health perception, social role functioning, physical functioning, emotional role functioning, medical care, vitality). Psychological well-being was assessed using the "Profile of Mood States (POMS)" ((McNair et al. 1972), German (Biehl and Landauer 1975)) containing 35 items and four subscales of mood (vigor, irritability, fatigue, numbness). A separate item asked for the highest level of graduation.

Statistical Analysis

For statistical analysis, the IBM SPSS Statistics package 19 was applied (IBM corporation Armank, NY, USA). Data of the four subgroups were compared using the nonparametric Chi-Square test by Kruskal-Wallis to identify statistical significance. Differences were judged significant when $p < 0.05$ (95 % confidence interval).

For the correlation of phenylalanine levels versus MRI score and quality of life items, a Spearman-Rho test was performed.

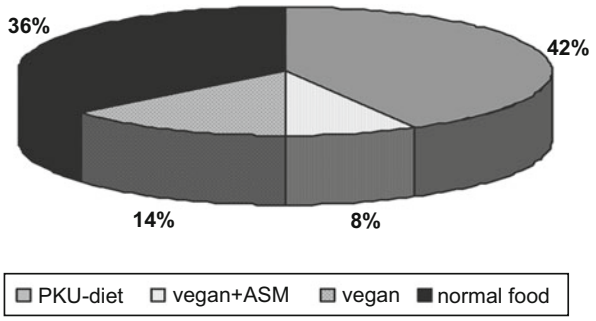

Fig. 1 Distribution of patients in dietary groups at start of the study, AAM = amino acid mixture

Results

The distribution of patients in the four different dietary groups at the start of our study is shown in Fig. 1.

Body mass indices (BMI) were normal in the two groups taking AAM and increased in the vegan (mean ± SD: 27.3 ± 4 kg/m^2) and normal food (25.9 ± 3 kg/m^2) groups, although differences were not significant ($p > 0.1$).

Dietary Protocols and Body Composition

Dietary protocol analysis at the beginning of the study is summarized in Table 2. In all patients, protein and energy intake were too low as judged by the DACH-recommendations (German-Austrian-Swiss dietary association) (DGE 2012). Protein supply was markedly reduced in patients following a vegan diet without AAM and in those who ate normally according to their personal judgment. Energy supply was also lower than recommended in these two groups. Results of follow-up dietary protocols showing normalized protein and energy intake after dietary intervention with AAM-supplementation can be found in Table 3.

Differences were found in the supply of phenylalanine. Patients who lived according to dietary recommendations had a lower intake than the other groups with more relaxed diets. In particular, patients in the normal food group consumed significantly more phenylalanine than vegan patients taking no AAM.

BIA-measurements (fat content, phase angle) were normal in all dietary groups, with no significant differences between groups. Compared to a normal, healthy population, no abnormalities were found for water, carbohydrate, and protein content (results not shown). Fat content in patients following a vegan diet was higher compared to patients following a protein-reduced diet or no diet at all. Body mass index and body cell mass were increased in vegan patients taking amino acids and reduced in vegan patients taking no AAM compared to patients following a diet supplemented with amino acids. Differences for these parameters were not significant. Membrane quality and cell density were not significantly different in the four subgroups as judged by the phase angle.

Biochemical Parameters in Blood and Urine

Although mean phenylalanine levels were within the therapeutic range in all groups, they were significantly higher in patients with presumed normal eating habits, $p < 0.05$ (Fig. 2). Historical data for phenylalanine levels are given in Fig. 3. There was a correlation between historical phenylalanine levels during childhood (0–15 years) and phenylalanine levels during adulthood (r = 0.6, $p < 0.01$, results not shown).

No systematic nutritional differences could be found between the four dietary groups except for levels of the amino acids phenylalanine and valine: patients who followed a strict protein-restricted diet with supplements had significantly lower concentrations of phenylalanine compared to those either without diet restriction or with vegan diets. Concentrations of valine were higher in patients following the recommended diet than in subjects consuming normal food.

Table 4 summarizes the results of the most important biochemical parameters in blood and urine. No statistical differences were found in blood cell count, coagulation, acylcarnitine profile in dried blood spots, organic acids in urine, concentrations of electrolytes, urea, creatine, lactate, glucose, creatine kinase, ALT, AST, GLDH, cholesterol, water- and fat-soluble vitamins, or trace elements such as iron, zinc, or selenium. However, there were single patients who returned to our outpatient clinic in response to the invitation for the study after many years without monitoring who had reduced levels of selenium and zinc. Interestingly, all patients had reduced or low normal urea concentrations in blood reflecting dietary protein restriction.

MRI Morphological Findings

None of the MRI scans showed signs of brain atrophy or signal changes in gray matter. Different grades of signal changes in white matter, typically found in PKU patients, were detected: while some of the patients showed no or only minor abnormalities, distinct signal changes in the parieto-occipital lobar WM and other brain regions were observed in other patients. The estimated semiquantitative Scheltens score varied from 0 (no changes) to 22. As an example, T2-weighted MRI scans of two patients are shown in Fig. 4 demonstrating enormous differences in white matter lesions. Linear regression showed a correlation between the retrospective mean phenylalanine levels in plasma and the lesion scores which was significant in the age period 0–10 years (R = 0.6, $p = 0.037$, Fig. 5). No differences between groups were observed.

Table 2 Supply of energy and basic nutrients at start of study compared to DACH-recommendations (2000) according to dietary protocol (DACH = German – Austrian – Swiss dietary association, * red: above recommended value, * green: below recommended value, AAM = amino acid mixture)

Diet	Total energy [kcal/day]	Carbohydrate [% of energy]	Fat [% of energy]	Protein [g/kg per day]
Protein-reduced with AAM	1830	61	24	1.1
Vegan with AAM	2169	57	31	0.9
Vegan without AAM	1605	57	35	0.5
Normal food	1400	56	34	0.6
DACH (2000)	> 2000	55-60	>30	1.0

Table 3 Follow-up: Supply of energy and basic nutrients compared to DACH-recommendations (2000) according to dietary protocol (* red: above recommended value, * green: below recommended value, AAM = amino acid mixture)

Diet	Total energy [kcal/day]	Carbohydrate [% of energy]	Fat [% of energy]	Protein [g/kg per day]
Protein-reduced with AAM	1716	61	22	1.0
Vegan with AAM	1720	62	25	1.0
Vegan without AAM	1519	54	32	0.7
Normal food	1558	57	28	1.0
DACH (2000)	> 2000	55-60	>30	1.0

Education, Quality of Life, and Mood

Educational performance was slightly better than average with 32 % of PKU patients reaching German secondary school diploma and only 2.6 % leaving school without qualification, compared to 30 % and 6 % in the general population, respectively. There were no significant differences between the dietary groups.

In all 51 patients, the questionnaire on HrQoL revealed no major deficits regarding general health perception, social role functioning, physical functioning, emotional role functioning, medical care, and vitality compared to the general population. Mood was correlated to the retrospective mean phenylalanine levels in the first 10 years of life ($R = 0.446$, $p = 0.037$) with better phenylalanine control leading to better mood. There were no significant differences in quality of life or mood assessment between the four dietary groups. Notably, the patients following the strict protein-restricted diet with amino acid supplementation did not feel worse than those with normal diet (according to their own assessment).

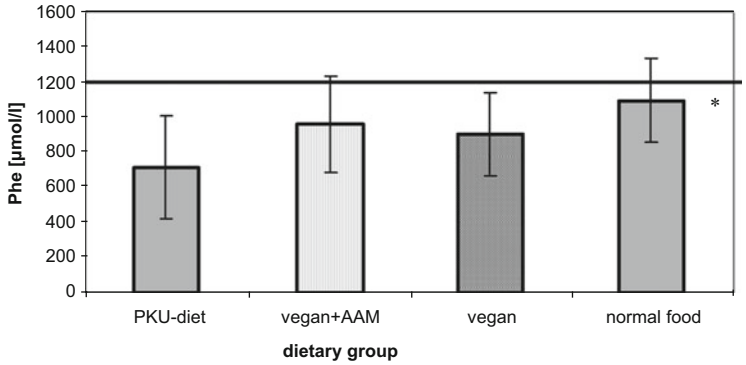

Fig. 2 Mean concentration of phenylalanine [µmol/l] compared to upper therapeutic levels for adults, * $p < 0.05$

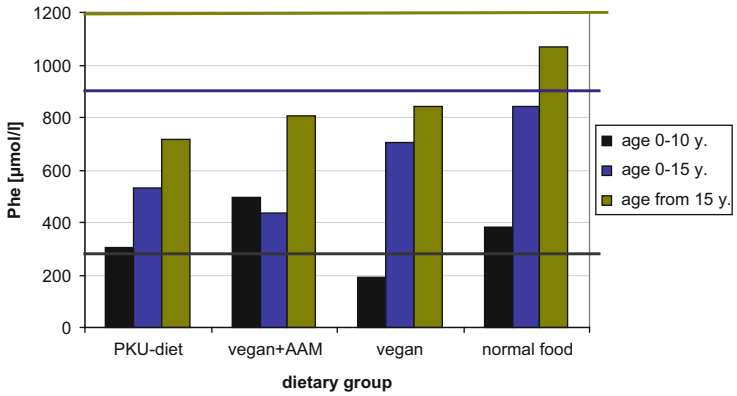

Fig. 3 Mean concentration of historical phenylalanine levels [µmol/l] compared with APS*-recommendations (1997) in three different age bands (*APS = German working group for pediatric metabolic diseases, APS- recommendations: 0–10 y.: 40–240 µmol/l, 10–15 years: 40–900 µmol/l, > 15 years: <1,200 µmol/l)

Discussion

"Diet for life" is recommended in classical PKU. While in the era of newborn screening dietary control is excellent during childhood, in most patients it can deteriorate during adolescence and adulthood (MacDonald et al. 2010). Transition from the pediatric clinic to an adult unit is known to be difficult (Feillet et al. 2010; Yoshino et al. 2010). A considerable number of adults (especially males) are lost for follow-up. Most women of childbearing age are aware of the risk of "maternal PKU" and regularly attend outpatient clinics, but older women – like many men – often think that dietary treatment is no longer necessary. Indeed, some older patients were previously advised by their doctors to discontinue the diet during adolescence and these patients frequently presume that they have normal eating habits. However, based on reduced or low normal urea levels in serum and dietary protocols in our survey, they continue a self-imposed reduction in protein intake. This is also true for the patient group following a vegan diet without AAM. Protein restriction in adulthood is related to that in early childhood, as we found a positive correlation between phenylalanine levels in both age bands.

Serious nutritional deficits may result when patients do not take amino acid supplements (MacDonald et al. 2011). In this study, serious nutritional deficiency was not found based on biochemical parameters in blood and urine. This does not completely rule out deficiencies in tissues. In previous studies on treated PKU patients, vitamin deficiencies (Hoeks et al. 2009) and low normal free carnitine values (Weigel et al. 2008) were found. An increased risk of vitamin B12-deficiency was reported in PKU patients on a relaxed diet in a previous study (Robinson et al. 2000); as methylmalonic acid in urine was negative, vitamin B12-deficiency could be ruled out in our cohort. We only identified reduced selenium and zinc levels in individual patients in the group with presumed normal eating habits without AAM. These rapidly normalized when amino acid mixtures were introduced.

Phenylalanine concentrations in blood were in the therapeutic range in all four groups indicating satisfactory metabolic control. However, phenylalanine levels were

Table 4 Selected biochemical parameters in the four groups, all were within normal range

Diet	Protein [g/l]	Urea [mM]	Tyrosine [μM]	Iron [μM]	Folate [μg/l]	Zinc [μM]	Selenium [μM]	Tocopherol [mg/dl]
Protein-reduced with AAM	73	3.3	58	19	14.1	10.2	0.74	10
Vegan with AAM	76	3.8	54	18	15.7	10.9	0.84	10
Vegan without AAM	76	3.6	56	17	11.2	9.9	0.70	9
Normal food	74	3.8	41	24	9.9	10.3	0.94	11
Reference range	**65–80**	**3.3–6.7**	**28–153**	**14–27**	**5.3–14.2**	**9.0–26.0**	**0.6–1.5**	**5–20**

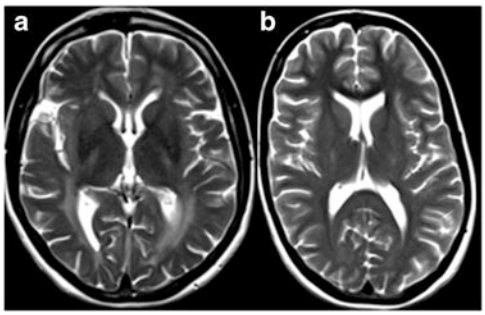

Fig. 4 Typical T2-weighted MRI scans of two PKU patients, where patient A shows diffuse white matter changes (Scheltens score = 10), patient B shows morphologically no white matter abnormalities

highest in those patients assuming to follow a normal diet. This may in principle be related to low energy supply in this group leading to catabolism. Elevation of branched chain amino acids can be used as an indicator of catabolism (Illsinger et al. 2005). However, as valine levels were lower in these patients, a catabolic state seems unlikely.

In line with other studies (Huemer et al. 2007), membrane quality and body composition do not seem to be compromised as judged by BIA-measurements; however, this is only an approximate overall estimation. Others have found correlations between (fat-free) muscle mass and protein intake (Huemer et al. 2007). As in other studies (Albersen et al. 2010; MacDonald et al. 2011), we saw a tendency to obesity in our cohort.

Despite early dietary treatment, MRI findings revealed typical white matter lesions of PKU as previously reported (Bick et al. 1993; Cleary and Walter 2001; Moller et al. 2003; Anderson et al. 2007; Leuzzi et al. 2007; Ding et al. 2008; Anderson and Leuzzi 2010) in many, but not all patients. In an attempt to quantify the white matter lesions, an adapted Scheltens score was used (Scheltens et al. 1993). As in other studies, the MRI lesions score could be correlated with cumulated retrospective phenylalanine levels during the first 10 years of life, while correlation with phenylalanine levels at later age bands was poor (Moller et al. 2003; Anastasoaie et al. 2008). T2-hyperintense white matter lesions are thought to be reversible as they are presumed to reflect intramyelinic edema (Leuzzi et al. 2007; Vermathen et al. 2007; Anderson and Leuzzi 2010). So far, follow-up MRI scans have only been performed in a few patients; therefore, reversibility of lesions in response to improved diet supplemented with AAM cannot be assessed at present.

On the functional level, mood was positively correlated with metabolic control during the first 10 years of life. Variation of phenylalanine levels over lifetime was reported to correlate with IQ (Waisbren et al. 2007; Anastasoaie et al. 2008); however, we could not find a significant correlation of variation of phenylalanine levels with white matter lesions. This indicates that other factors such as the blood-brain barrier or Phe-transporters (Moller et al. 2003) may influence the formation of white matter lesions. Further, secondary factors such as glucose metabolism may also play a role (Wasserstein et al. 2006). In line with these considerations, we did not detect differences in Scheltens' lesion score between the four dietary groups in our survey.

With regard to cognitive function, considerable executive and cognitive dysfunction even in early-treated PKU patients under good metabolic control has been described (Bick et al. 1993; Cleary and Walter 2001; Azadi et al. 2009; Gentile et al. 2010). Results from the questionnaires showed slightly better school performance of the PKU patients compared to the average population, which might be related to better self-management and structured lifestyle of PKU patients.

Quality of life was good. Patients not following a diet did not feel any better than patients on a strict diet with amino acid supplementation. However, the significance of this is limited due to the small sample size.

Previously it has been shown that compliance is not related to the knowledge of disease management in PKU patients (Durham-Shearer et al. 2008). In our view, the process of transition and patient management in the adult metabolic setting should be improved in order to maintain more adult patients on a diet supplemented with AAM.

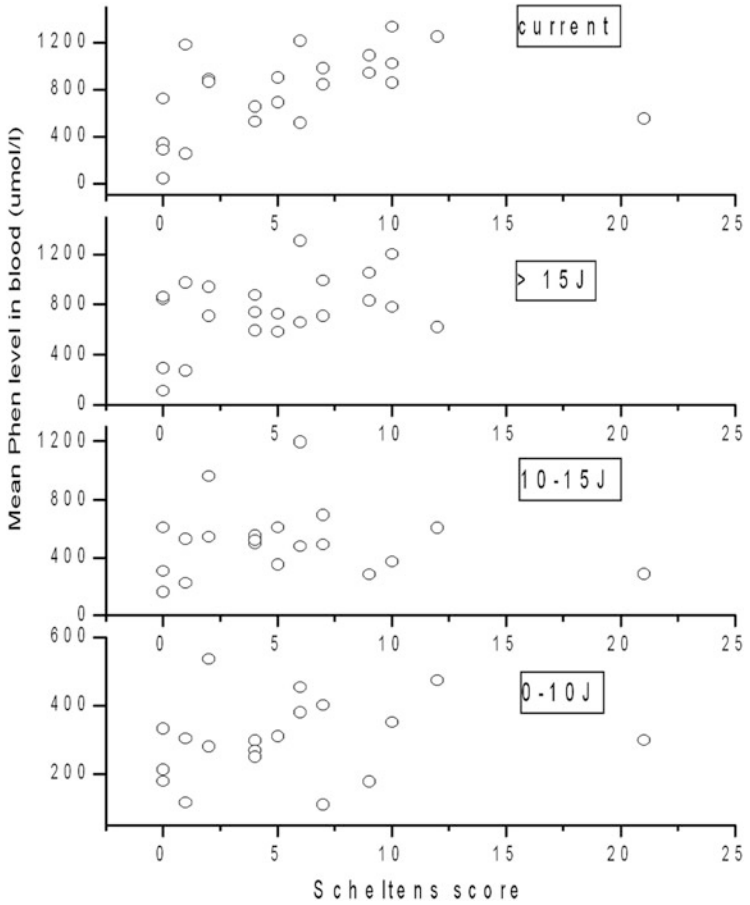

Fig. 5 Relationship between the cerebral lesions score and current as well as historical plasma phenylalanine levels at different age of the patients. There was a significant correlation for the age group 1–10 years (R = 0.6, $p = 0.037$), in all other age groups there were non-significant weak correlations (R = 0.1–0.4, $p = 0.43$–0.06)

Further, costs for AAM should be covered by health insurance companies, even for adults.

We are aware that the results obtained in this survey are of limited value as only a relatively small number of patients could be studied. However, examining patients from a single center had the advantage that patients were well known to us, and counseling, dietary recommendations, and therapeutic monitoring were relatively uniform. Results of our study may have implications for other metabolic diseases treated by protein restriction.

In summary, a considerable number of adult patients with PKU do not adhere to dietary recommendations including supplementation with AAM. Nevertheless, they unknowingly restrict their protein intake, probably as a result of following such a diet during infancy and childhood: protein-restricted eating habits are simply normal for them. Patients following a vegan diet without amino acid supplementation also have reduced protein and energy intake. This does not lead to significant deficits or overt functional deficiencies. However, it seems desirable over time to avoid even subtle nutritional deficits in order to prevent chronic intracellular "toxicity" or deficiency resulting in cellular dysfunction, especially of the brain. MRI lesions score and mood during adolescence/adulthood correlated with metabolic control during the first 10 years of life. There were no significant differences in MRI lesions scores between the different groups in our study population of adolescents/young adults. "Diet for life" does not only mean protein restriction but also supplementation with AAM and regular metabolic monitoring in adults by a unit with expertise in caring for patients with PKU/inborn errors of metabolism. A qualified metabolic dietician should be part of the team. Our study underpins the necessity of "Care for life" in patients with PKU including adequate funding.

Acknowledgment We thank Dr. G. Ulrich for advice regarding the quality-of-life questionnaires.

Take-Home Message

Adult patients with phenylketonuria tend to self-restrict their protein intake, irrespective of taking supplementary amino acid mixtures, and thus risk longer-term nutritional deficiency.

Compliance with Ethics Guidelines

The chairman of the local ethical review board decided that no vote was required as only routine procedures were carried out in order to monitor metabolic control.

Conflict of Interest

Anibh Martin Das, Kristin Goedecke, Uta Meyer, Nele Kanzelmeyer, Stefanie Koch, Sabine Illsinger, Thomas Lücke, Hans Hartmann, Karin Lange, Heinrich Lanfermann, Ludwig Hoy, and Xiao-Qi Ding declare that they have no conflict of interest.

Competing Interests

This study was financially supported by a grant of the German Ministry for Education and Research (BMBF) and by MetaX, Germany.

References

Abadie V, Berthelot J, Feillet F et al (2005) Management of phenylketonuria and hyperphenylalaninemia: the French guidelines. Arch Pediatr 12(5):594–601

Albersen M, Bonthuis M, de Roos NM et al (2010) Whole body composition analysis by the BodPod air-displacement plethysmography method in children with phenylketonuria shows a higher body fat percentage. J Inherit Metab Dis 33: S283–S288

Anastasoaie V, Kurzius L, Forbes P, Waisbren S (2008) Stability of blood phenylalanine levels and IQ in children with phenylketonuria. Mol Genet Metab 95(1–2):17–20

Anderson PJ, Leuzzi V (2010) White matter pathology in phenylketonuria. Mol Genet Metab 99(Suppl 1):S3–S9

Anderson PJ, Wood SJ, Francis DE, Coleman L, Anderson V, Boneh A (2007) Are neuropsychological impairments in children with early-treated phenylketonuria (PKU) related to white matter abnormalities or elevated phenylalanine levels? Dev Neuropsychol 32(2):645–668

Azadi B, Seddigh A, Tehrani-Doost M, Alaghband-Rad J, Ashrafi MR (2009) Executive dysfunction in treated phenylketonuric patients. Eur Child Adolesc Psychiatry 18(6):360–368

Bick U, Ullrich K, Stober U et al (1993) White matter abnormalities in patients with treated hyperphenylalaninaemia: magnetic resonance relaxometry and proton spectroscopy findings. Eur J Pediatr 152(12):1012–1020

Biehl B, Landauer A (1975) Das profile of mood states (POMS). Mannheim, unpublished manuscript

Blau N, Belanger-Quintana A, Demirkol M et al (2010) Management of phenylketonuria in Europe: survey results from 19 countries. Mol Genet Metab 99(2):109–115

Bullinger M, Kirchberger I, von Steinbüchel N (1993) Der Fragebogen Alltagsleben – ein Verfahren zur gesundheitsbezogenen Lebensqualität. Zeitschrift für Medizinische Psychologie 2: 121–131

Burgard P (2000) Development of intelligence in early treated phenylketonuria. Eur J Pediatr 159(Suppl 2):S74–S79

Cleary M, Walter JH (2001) Assessment of adult phenylketonuria. Ann Clin Biochem 38(Pt 5):450–458

de Baulny HO, Abadie V, Feillet F, de Parscau L (2007) Management of phenylketonuria and hyperphenylalaninemia. J Nutr 137 (6 Suppl 1):1561S–1563S, Discussion 1573S–1575S

DGE (2012) Referenzwerte für die Nährstoffzufuhr. DGE-Medien Service, Rostock

Ding XQ, Fiehler J, Kohlschutter B et al (2008) MRI abnormalities in normal-appearing brain tissue of treated adult PKU patients. J Magn Reson Imaging 27(5):998–1004

Durham-Shearer SJ, Judd PA, Whelan K, Thomas JE (2008) Knowledge, compliance and serum phenylalanine concentrations in adolescents and adults with phenylketonuria and the effect of a patient-focused educational resource. J Hum Nutr Diet 21(5):474–485

Feillet F, Agostoni C (2010) Nutritional issues in treating phenylketonuria. J Inherit Metab Dis 33(6):659–664

Feillet F, MacDonald A, Hartung Perron D, Burton B (2010) Outcomes beyond phenylalanine: an international perspective. Mol Genet Metab 99(Suppl 1):S79–S85

Gentile JK, Ten Hoedt AE, Bosch AM (2010) Psychosocial aspects of PKU: hidden disabilities–a review. Mol Genet Metab 99-(Suppl 1):S64–S67

Giovannini M, Verduci E, Salvatici E, Fiori L, Riva E (2007) Phenylketonuria: dietary and therapeutic challenges. J Inherit Metab Dis 30(2):145–152

Hendriksz CJ, Walter JH (2004) Update on phenylketonuria. Curr Paediatr 14:400–406

Hoeks MP, den Heijer M, Janssen MC (2009) Adult issues in phenylketonuria. Neth J Med 67(1):2–7

Huemer M, Huemer C, Moslinger D, Huter D, Stockler-Ipsiroglu S (2007) Growth and body composition in children with classical phenylketonuria: results in 34 patients and review of the literature. J Inherit Metab Dis 30(5):694–699

Huijbregts SC, de Sonneville LM, van Spronsen FJ, Licht R, Sergeant JA (2002) The neuropsychological profile of early and continuously treated phenylketonuria: orienting, vigilance, and maintenance versus manipulation-functions of working memory. Neurosci Biobehav Rev 26(6):697–712

Illsinger S, Lucke T, Meyer U, Vaske B, Das AM (2005) Branched chain amino acids as a parameter for catabolism in treated phenylketonuria. Amino Acids 28(1):45–50

Leuzzi V, Tosetti M, Montanaro D et al (2007) The pathogenesis of the white matter abnormalities in phenylketonuria. A multimodal 3.0 tesla MRI and magnetic resonance spectroscopy (1H MRS) study. J Inherit Metab Dis 30(2):209–216

MacDonald A, Gokmen-Ozel H, van Rijn M, Burgard P (2010) The reality of dietary compliance in the management of phenylketonuria. J Inherit Metab Dis 33(6):665–670

MacDonald A, Rocha JC, van Rijn M, Feillet F (2011) Nutrition in phenylketonuria. Mol Genet Metab 104(Suppl):S10–S18

McNair D, Lorr M, Droppelmann LF (1972) Profile of mood states. Educational and Industrial Testing Service, San Diego

Moller HE, Weglage J, Bick U, Wiedermann D, Feldmann R, Ullrich K (2003) Brain imaging and proton magnetic resonance spectroscopy in patients with phenylketonuria. Pediatrics 112 (6 Pt 2):1580–1583

Oddason KE, Eiriksdottir L, Franzson L, Dagbjartsson A (2011) Phenylketonuria (PKU) in Iceland. Laeknabladid 97(6):349–352

Robinson M, White FJ, Cleary MA, Wraith E, Lam WK, Walter JH (2000) Increased risk of vitamin B12 deficiency in patients with phenylketonuria on an unrestricted or relaxed diet. J Pediatr 136(4):545–547

Scheltens P, Barkhof F, Leys D et al (1993) A semiquantative rating scale for the assessment of signal hyperintensities on magnetic resonance imaging. J Neurol Sci 114(1):7–12

Vermathen P, Robert-Tissot L, Pietz J, Lutz T, Boesch C, Kreis R (2007) Characterization of white matter alterations in phenylketonuria by magnetic resonance relaxometry and diffusion tensor imaging. Magn Reson Med 58(6):1145–1156

Viau KS, Wengreen HJ, Ernst SL, Cantor NL, Furtado LV, Longo N (2011) Correlation of age-specific phenylalanine levels with intellectual outcome in patients with phenylketonuria. J Inherit Metab Dis 34(4):963–971

Waisbren SE, Noel K, Fahrbach K et al (2007) Phenylalanine blood levels and clinical outcomes in phenylketonuria: a systematic literature review and meta-analysis. Mol Genet Metab 92(1–2):63–70

Wasserstein MP, Snyderman SE, Sansaricq C, Buchsbaum MS (2006) Cerebral glucose metabolism in adults with early treated classic phenylketonuria. Mol Genet Metab 87(3):272–277

Weigel C, Kiener C, Meier N et al (2008) Carnitine status in early-treated children, adolescents and young adults with phenylketonuria on low phenylalanine diets. Ann Nutr Metab 53(2):91–95

Yoshino M, Watanabe Y, Ohira T, Harada N (2010) Phenylketonuria–toward a better carry-over care. Nihon Rinsho 68(1):123–126<

JIMD Reports
DOI 10.1007/8904_2013_274

RESEARCH REPORT

Behavioral Responses in Rats Submitted to Chronic Administration of Branched-Chain Amino Acids

Giselli Scaini · Gabriela C. Jeremias · Camila B. Furlanetto · Diogo Dominguini · Clarissa M. Comim · João Quevedo · Patrícia F. Schuck · Gustavo C. Ferreira · Emilio L. Streck

Received: 18 June 2013 / Revised: 27 September 2013 / Accepted: 02 October 2013 / Published online: 9 November 2013

Abstract Maple syrup urine disease (MSUD) is an inborn metabolism error caused by a deficiency of branched-chain α-keto acid dehydrogenase complex activity. This blockage leads to an accumulation of the branched-chain amino acids (BCAA) leucine, isoleucine, and valine, as well as their corresponding α-keto and α-hydroxy acids. Previous reports suggest that MSUD patients are at high risk for chronic neuropsychiatric problems. Therefore, in this study, we assessed variables that suggest depressive-like symptoms (anhedonia as measured by sucrose intake, immobility during the forced swimming test and body and adrenal gland weight) in rats submitted to chronic administration of BCAA during development. Furthermore, we determined if these parameters were sensitive to imipramine and *N*-acetylcysteine/deferoxamine (NAC/DFX). Our results demonstrated that animals subjected to chronic administration of branched-chain amino acids showed a decrease in sucrose intake without significant changes in body weight. We also observed an increase in adrenal gland weight and immobility time during the forced swimming test. However, treatment with imipramine and NAC/DFX reversed these changes in the behavioral tasks. In conclusion, this study demonstrates a link between MSUD and depression in rats. Moreover, this investigation reveals that the antidepressant action of NAC/DFX and imipramine might be associated with their capability to maintain pro-/anti-oxidative homeostasis.

Communicated by: Bruce A Barshop, MD, PhD

Competing interests: None declared

G. Scaini · G.C. Jeremias · C.B. Furlanetto · E.L. Streck (✉)
Laboratório de Bioenergética, Programa de Pós-Graduação em Ciências da Saúde, Universidade do Extremo Sul Catarinense Criciúma, Av. UniversitÄria, 1105, Criciúma 88806-000 SC, Brazil
e-mail: emiliostreck@gmail.com

G. Scaini · G.C. Jeremias · C.B. Furlanetto · D. Dominguini · C.M. Comim · J. Quevedo · E.L. Streck
Instituto Nacional de Ciência e Tecnologia Translacional em Medicina (INCT-TM), Porto Alegre, RS, Brazil

D. Dominguini · C.M. Comim · J. Quevedo
Laboratório de Neurociências, Programa de Pós-Graduação em Ciências da Saúde, Universidade do Extremo Sul Catarinense, Criciúma, SC, Brazil

P.F. Schuck · G.C. Ferreira
Laboratório de Erros Inatos do Metabolismo, Programa de Pós-Graduação em Ciências da Saúde, Universidade do Extremo Sul Catarinense, Criciúma, SC, Brazil

Introduction

Maple syrup urine disease (MSUD; OMIM #248600), or branched-chain ketoaciduria, is an inborn metabolism error caused by a deficiency in the activity of branched-chain alpha-keto acid dehydrogenase complex (BCKDH). This deficiency leads to an accumulation of the branched-chain amino acids (BCAA) leucine, isoleucine, and valine, as well as their associated alpha-keto acids (BCKA) in tissue and body fluids (Chuang and Shih 2001; Treacy et al. 1992). The worldwide frequency is approximately 1:185,000 based on routine screening data from 26.8 million newborns (Chuang and Shih 2001). Individuals with MSUD usually present with poor feeding, convulsions, ketoacidosis, hypoglycemia, coma, ataxia, psychomotor delay, and mental retardation, as well as generalized edema and hypomyelination/ demyelination shown by magnetic resonance imaging studies of the central nervous system (Chuang and Shih 2001; Cavalleri et al. 2002; Ha et al. 2004; Schönberger et al. 2004; Zinnanti et al. 2009).

Neurological sequelae of MSUD are likely caused by several interacting mechanisms. Proposed mechanisms of neurotoxicity include energy deprivation and osmotic dysregulation (Howell and Lee 1963; Land et al. 1976; Danner and Elsas 1989; Yudkoff et al. 1994; Zielke et al. 2002; Pilla et al. 2003; Sgaravatti et al. 2003; Ribeiro et al. 2008) and alterations in the concentrations of the neurotransmitters glutamate, aspartate, and aminobutyric in the brain (Dodd et al. 1992; Prensky and Moser 1967; Tavares et al. 2000; Yudkoff et al. 1994; Hutson et al. 2001). The brain injury in this disorder may also be related to a reduction of brain uptake of essential amino acids (Araújo et al. 2001; Wajner and Vargas 1999; Wajner et al. 2000), apoptosis of neural cells (Jouvet et al. 2000), oxidative stress (Bridi et al. 2003, 2005; Fontella et al. 2002; Barschak et al. 2006; Mescka et al. 2011), increased acetylcholinesterase activity in the brain (Scaini et al. 2012), and alterations of neurotrophin levels (Scaini et al. 2013a, b).

Hereditary disorders that cause neuropsychiatric sequelae provide a window into the biological foundations of mental illness. Anecdotal reports suggest that aging MSUD patients are at high risk for chronic neuropsychiatric problems, such as attention deficit disorder, depression, and anxiety (Strauss et al. 2006; Walterfang et al. 2013). Muelly and colleagues (2013) showed that the neurochemical deficiencies previously demonstrated in MSUD patients and experimental animals may persist in the chronic state, although to a lesser degree, and cumulatively contribute to neuropsychiatric morbidity. Therefore, in this study, we assessed anhedonia, measured by sucrose intake, immobility during the forced swimming test and body and adrenal gland weight in rats submitted to chronic administration of BCAA during development. Because previous observations suggested that oxidative stress may be involved in the pathophysiology of the neurological dysfunction of MSUD (Bridi et al. 2003, 2005; Fontella et al. 2002; Barschak et al. 2006; Mescka et al. 2011) and these variables suggest depressive-like symptoms (Katz et al. 1981b; Gamaro et al. 2003; Lucca et al. 2008), we also investigated the influence of the concomitant administration of *N*-acetylcysteine (NAC) plus deferoxamine (DFX) or imipramine in the behavioral tasks.

Materials and Methods

Animals

Male Wistar rats that were 7 days old (10–15 g) were obtained from the Central Animal House of Universidade do Extremo Sul Catarinense. The rats were weaned at 21 days of age. All rats were caged in groups of five, had free access to food and water, and were maintained on a 12-h light-dark cycle (lights on 7:00 am) at a temperature of 23 ± 1°C. All experimental procedures were conducted in accordance with the National Institutes of Health Guide for the Care and Use of Laboratory Animals and the Brazilian Society for Neuroscience and Behavior recommendations for animal care. All experiments and procedures were conducted after approval from the Ethics Committee of the Universidade do Extremo Sul Catarinense was granted (protocol number 60/2010).

Chronic Administration of the BCAA Pool and Treatment with Antioxidants

The animals were divided into four groups: Group I – control (saline); Group II – Hyper-BCAA (H-BCAA); Group III – H-BCAA treated with a combination of NAC (20 mg/kg) and DFX (20 mg/kg); and Group IV – H-BCAA treated with imipramine (10 mg/kg). The animals received two subcutaneous injections per day of the BCAA pool (15.8 μL/g body weight at 12-h intervals) containing 190 mmol/L Leu, 59 mmol/L Ile, and 69 mmol/L Val in saline solution, administered for 21 days starting at postnatal day (PD) 7 (last injection at PD 27) ($n = 12$, per group) (Bridi et al. 2006). Immediately after administration of the first injection of the BCAA pool, NAC was administered subcutaneously twice a day (at 12-h intervals) and DFX was administered once every two days for a total of 21 days (Di-Pietro et al. 2008). Imipramine, a standard antidepressant, was obtained from Novartis Pharmaceutical Industry (São Paulo, Brazil), and a dose of 10 mg/kg was injected intraperitoneally (i.p.) once a day over 21 days (Tuon et al. 2007). Twelve hours after the last injection of BCAA, the animals were submitted to behavioral testing. The choice of the administered doses and the ages of the rats were based on a previous study (Bridi et al. 2006), which showed that the administration of the BCAA pool to rats (similar doses and ages to those used in this study) resulted in increased levels of Leu, Ile, and Val in the blood and brain. Importantly, the dose of the BCAA pool mimicked the biochemical events observed in MSUD patients during crises, but in this model leucine levels in plasma and brain returned to basal values after 12 h the final BCAA injection, thus, we evaluate the chronic effects of daily episodes of metabolic decompensation.

Sweet Food Consumption (Anhedonia Test)

The consumption of sweet food was measured in all groups to evaluate anhedonia during the 7 days (PD 21–28). For this purpose, the animals were placed in an illuminated lightened rectangular box (40 cm × 15 cm × 20 cm) with a glass ceiling and floor and wooden sidewalls, and the box was divided into nine equal

rectangles by black lines. Ten Froot Loop(s) (Kellogg's® pellets of wheat, cornstarch, and sucrose) were placed in one extremity of the box. The animals were subjected to five 3-min trials, once daily for 5 days, to become familiarized with the food (PD 21–26). After being habituated, the animals were exposed to two test sessions of 3 min each, during which the number of ingested pellets was measured (PD 27–28). This task was performed during the light cycle by an observer who was blinded to the groups. The observer noted if the animal ate 1/4, 1/2, or an entire Froot Loop, in accordance with previous studies (Katz et al. 1981b; Gamaro et al. 2003).

During the first 5 days, the animals were exposed to a 22-h fasting before the count of Froot Loops, after the animals were exposed to standard food for 2 h. However in the test sessions (last 2 days), the animals were not fasting. These evaluations were performed because food deprivation, which is used in many behavior tasks as a motivating stimulus, may also be an acute stressor (Katz et al. 1981a; Gamaro et al. 2003). The behavioral tests were performed by the same person blinded to the experimental group. The number of black line crossings and rearings were measured during the first (PD 21) session to evaluate motor activity.

Body and Adrenal Gland Weight

Body weight was measured before administration of the BCAA pool (day 0) and 22 days (day 22) after the first administration of the BCAA pool. On the 22nd day, after consumption of the sweet food, the rats were anesthetized with a mixture of ketamine (80 mg/kg) and xylazine (10 mg/kg) administered i.p. After death, the adrenal gland was removed through laparotomy and weighed on an analytical scale (Krishnan and Nestler 2008; Katz et al. 1981b; Nestler et al. 2002; Gamaro et al. 2003).

Forced Swimming Test

This test was conducted according to previous reports (Porsolt et al. 1977) and used as a model for depressive behavior. The behavioral tests were performed by the same person blinded to the experimental group. Briefly, the test involves two exposures to a cylindrical water tank in which rats cannot touch the bottom and from which they cannot escape. The tank is made of transparent Plexiglas, is 80 cm tall, is 30 cm in diameter, and is filled with water (22–23°C) to a depth of 40 cm. The water in the tank was changed for each rat. For the first exposure, the rats were placed in the water for 15 min (training session). After 24 h, the rats were placed in the water again for a 5-min session (test session). The time of immobility was analyzed in the test session. The rats were judged to be immobile whenever they stopped swimming and remained floating in the water, with their heads above the surface.

Statistical Analysis

The results are presented as the mean ± the standard deviation. Tests for determining normality and equal variances were performed to examine whether the data qualified for parametric statistical tests. The data were normally distributed (Shapiro–Wilk, $p > 0.05$) with equal variances among samples (equal variances test, $p > 0.05$). Therefore, a one-way analysis of variance (ANOVA) followed by Tukey HSD post hoc tests was used to compare the means. The differences between groups were considered to be significant at $p < 0.05$. All of the analyses were carried out on an IBM-compatible PC computer using Statistical Package for the Social Sciences (SPSS) software (Armonk, New York, USA).

Results

As demonstrated in Fig. 1, chronic administration of BCAA decreased sucrose intake by 45.78% when compared with the control group. Treatment with imipramine and NAC plus DFX partially reversed the reduction of sweet food consumption by 52.83% and 45.78%, respectively, when compared with the H-BCAA group. Figure 2 shows that the chronic administration of BCAA produced no differences in the number of crossings or rearings between groups during the habituation to the open-field training sessions. These results demonstrated that there was no difference in the motor or exploratory activities between groups and that the results observed in Fig. 1 were not secondary to locomotor alterations.

Table 1 illustrates the effects of H-BCAA on body weight. Control animals significantly increased in body weight after the first administration, whereas H-BCAA animals did not. There was a 25.39% increase in adrenal gland weight in H-BCAA animals compared with the control group. Treatment with imipramine and NAC plus DFX prevented the increase in adrenal gland weight by 29.05% and 14%, respectively, compared with the H-BCAA group (Fig. 3).

The effects of H-BCAA administration on immobility time during the forced swimming test are illustrated in Fig. 4. In the H-BCAA group, we observed an increase in immobility time by 260, 61%, compared with the control group. Treatment with imipramine and NAC plus DFX reversed the increase in the immobility time by 55, 69% and 76, 61%, respectively, compared with the H-BCAA group.

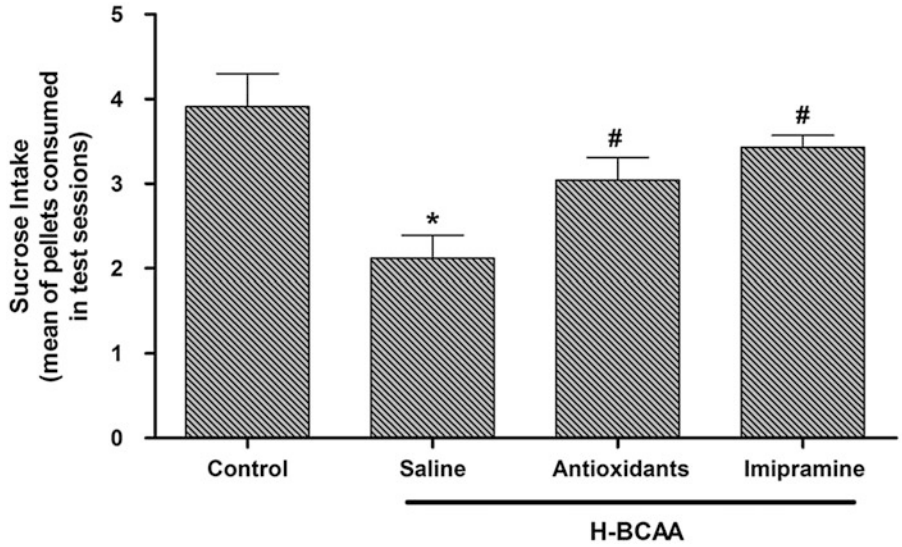

Fig. 1 Effects of chronic administration of hyper branched-chain amino acids (H-BCAA), imipramine (IMI), and antioxidants (ATX) (*N*-acetylcysteine plus deferoxamine) on the consumption of sweet food in the anhedonia test. Data are expressed as the mean ± the standard deviation of 12 rats. $*p < 0.05$ compared with the control group. $\#p < 0.05$ compared with the H-BCAA group

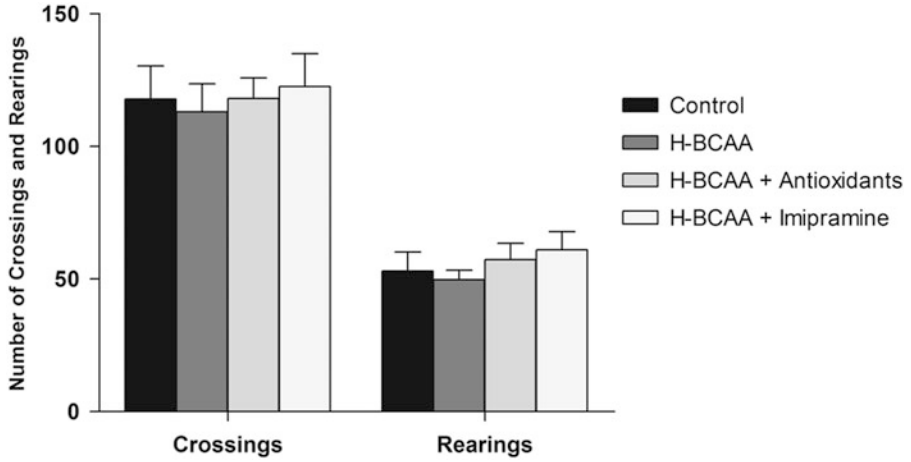

Fig. 2 Effects of chronic administration of hyper branched-chain amino acids (H-BCAA), imipramine (IMI), and antioxidants (ATX) (*N*-acetylcysteine plus deferoxamine) number of crossings and rearings of rats subjected to the open-field test. Data are expressed as the mean ± the standard deviation of 12 rats

Discussion

A number of metabolic disorders that affect the central nervous system can present in childhood, adolescence, or adulthood as a phenocopy of a major psychiatric syndrome, such as psychosis, depression, anxiety, or mania (Walterfang et al. 2013). In this study, we observed that rats submitted to chronic administration of H-BCAA have a decreased sweet food intake and increased adrenal gland weight, without any alteration of body weight compared with the control group. This mimics anhedonia, a key depressive symptom (Katz et al. 1981b; Willner et al. 1987, 1998). We also observed an increase in immobility time in the H-BCAA group during the forced swimming test. Additionally, as described above, the H-BCAA group did not present with any locomotor activity impairments, reinforcing that the decreased sweet food intake and higher immobility time in the H-BCAA group were related to changes in the behavioral tasks (anhedonia and forced swimming tests).

Evidence from the literature shows that the causality of psychiatric illness is the result of two processes: the interruption of childhood/early adulthood neurodevelopmental trajectories in progressive illness, and the acute alteration of monoaminergic or excitatory/inhibitory neurotransmitter systems in acute or episodic illness (Walterfang et al. 2013). Moreover, neurotransmitter deficiency can be a primary

Table 1 Effects of chronic administration of hyper branched-chain amino acids (H-BCAA), imipramine (IMI), and antioxidants (ATX) (*N*-acetylcysteine plus deferoxamine) on body weight on day 0 (A) and day 22 (B). Data are expressed as the mean ± the standard deviation of 12 rats

	Body weight	
	Day 0	Day 22
Control	11.65 (1.06)	48.77 (4.53)
H-BCAA	11.78 (0.918)	48.94 (2.93)
H-BCAA + ATX	11.81 (0.99)	49.86 (3.22)
H-BCAA + IMI	11.63 (1.07)	47.62 (1.42)

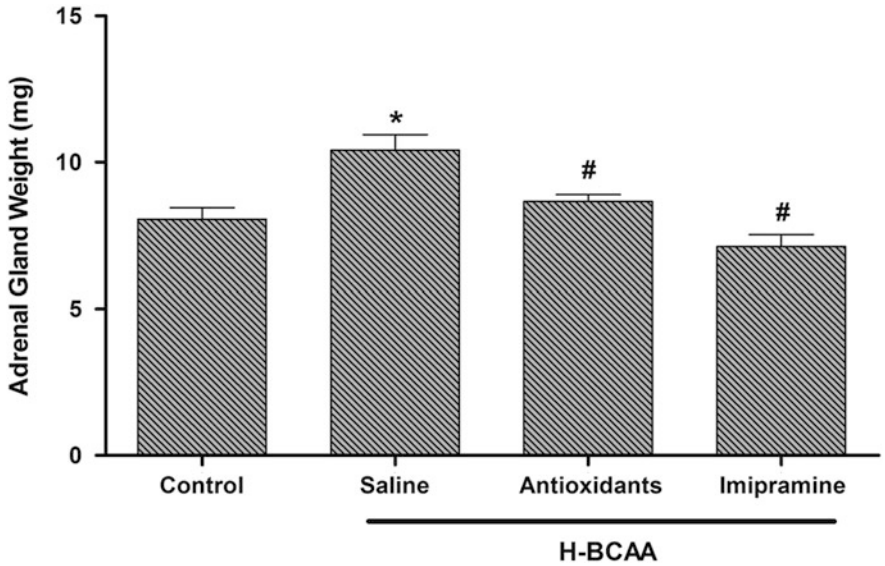

Fig. 3 Effects of chronic administration of hyper branched-chain amino acids (H-BCAA), imipramine (IMI), and antioxidants (ATX) (*N*-acetylcysteine plus deferoxamine) on adrenal gland weight. Data are expressed as the mean ± the standard deviation of 12 rats. $*p < 0.05$ compared with the control group. $\#p < 0.05$ compared with the H-BCAA group

cause of psychiatric disorders or entrain compensatory changes in receptor expression and synaptic structure that affect brain function. Neuronal energy depletion, osmotic dysregulation, and dysmyelination also likely contribute to the development of psychiatric disorders (Jou et al. 2009; Gardner and Boles 2011). Additionally, major depression is characterized by significantly lower plasma concentrations of a number of key antioxidants, such as vitamin E, zinc, and coenzyme Q10. Lowered total antioxidant status, or antioxidant enzyme activity, is another hallmark of depression (Kahnzole et al. 2003; Maes et al. 2000, 2009a, b). Several studies have shown evidence of oxidative damage to lipids, fatty acids, and DNA in depression (Forlenza and Miller 2006; Dimopoulos et al. 2008; Maes et al. 1999). These effects may occur on an ongoing basis or stem from developmental or cumulative aberrations of neurochemistry that lead to persistent modifications of receptor regulation and neurochemistry. In this context, studies have demonstrated that metabolite accumulation in MSUD may affect myelin development (Taketomi et al. 1983; Tribble and Shapira 1983; Treacy et al. 1992) and inhibit the transport of tyrosine, tryptophan, and other essential amino acids across the blood-brain barrier, thereby limiting substrate availability for cerebral catecholamine, serotonin, and protein synthesis (Dodd et al. 1992; Prensky and Moser 1967; Tavares et al. 2000; Yudkoff et al. 1994; Araújo et al. 2001; Hutson et al. 200; Wajner and Vargas 1999; Wajner et al. 2000).

Because the metabolites accumulating in MSUD induce oxidative stress (Fontella et al. 2002; Bridi et al. 2003, 2005; Mescka et al. 2011), which plays a critical role in the pathophysiology of depressive disorders, we also investigated whether free-radical generation could be involved in reduction in sucrose preference and higher immobility time. Corroborating this hypothesis, antioxidant administration prevented the decreased sweet food intake, increased immobility time, and increased adrenal gland weight.

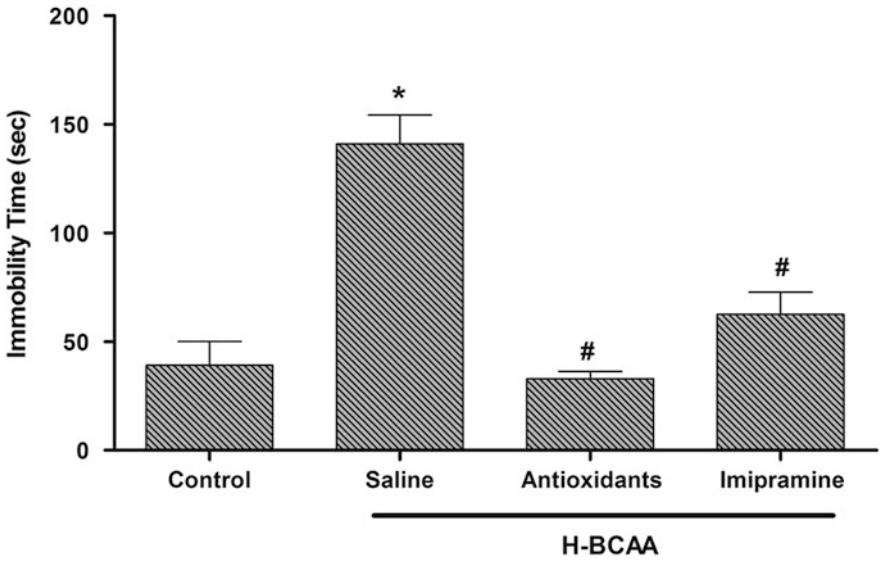

Fig. 4 Effects of chronic administration of hyper branched-chain amino acids (H-BCAA), imipramine (IMI), and antioxidants (ATX) (*N*-acetylcysteine plus deferoxamine) on immobility time during the forced swimming test. Data are expressed as the mean ± the standard deviation of 12 rats. $*p < 0.05$ compared with the control group. $\#p < 0.05$ compared with the H-BCAA group

Though specific trials for antidepressant effects in depression are still lacking, NAC shows antidepressant-like activity in several preclinical models; studies corroborate the antidepressant-like effects of NAC in rats subjected to the forced swimming test (Ferreira et al. 2008) and in mice subjected to the tail suspension test (Linck et al. 2012). Additionally, the chronic administration of NAC resulted in a dose-dependent reduction in immobility time in bulbectomized rats and resulted in a significant increase in cellular antioxidant mechanisms (superoxide dismutase activity) in the frontal cortex, hippocampus, and striatum (Smaga et al. 2012). Arent and colleagues (2012) demonstrated that NAC and DFX, alone or in combination, reversed the stress-induced sweet food consumption decrease and oxidative stress in rats submitted to chronic mild stress. Magalhães and colleagues (2011) reported that adjunctive NAC may be useful for major depressive episodes in bipolar disorder.

NAC contributes to the maintenance of oxidative balance through the actions of the cysteine/cystine cycle. Like glutathione and GSSG, cysteine and cystine are coupled redox partners that help to prevent oxidative cellular dysfunction and injury (Iyer et al. 2009; Banjac et al. 2008; Vene et al. 2011). Hence, the actions of NAC are multifold and interrelated, with the production of glutathione, the cysteine/cystine cycle, and the action of the glutamate/cystine antiporter contributing to the maintenance of oxidative balance and cellular function. Note that NAC also acts on glutamatergic neurotransmission, both directly and indirectly (Berk et al. 2013). NAC is converted to cystine, which in turn facilitates the glutamate/cystine antiporter and the production of glutathione in glial cells (Lafleur et al. 2006). In addition to the regulation of glutamate release, NAC, via GSH or its derivatives, has the capacity to modulate NMDA activity (Gilbert et al. 1991; Leslie et al. 1992; Varga et al. 1997). NAC regulation of the cystine/glutamate antiporter and mGluR2/3, as described above, can also regulate dopamine release from presynaptic terminals (Baker et al. 2002). NAC may also regulate dopamine release via the modulation of the redox status of the cell, via antioxidant effects of GSH and L-cysteine (JanÄky et al. 2007; Gere-Paszti and Jakus 2009). Additionally, Linck and colleagues (2012) have demonstrated that AMPA receptors play a key role in the mechanism of the antidepressant-like action of NAC by indirectly modulating the serotonin and noradrenaline pathways. Consistent with these mechanisms, reduced cerebral dopamine and glutamate levels have been observed in experimental MSUD animals (Dodd et al. 1992; Zinnanti et al. 2009) and postmortem brain tissue from a child who died of leucine intoxication (Prensky and Moser 1996).

Interestingly, we also demonstrated that the tricyclic antidepressant imipramine prevented the changes in the behavioral tasks observed in H-BCAA rats. Imipramine increase the levels of serotonin and/or norepinephrine by blocking reuptake of these neurotransmitters to presynaptic terminals, although an increase in monoamine levels occurs soon after drug administration, the effects of antidepressants emerge gradually over several weeks of continuous application, it is possible that in addition to an increase in monoamine levels, other more temporal neuronal events may be responsible for the action of imipramine (Yagasaki et al. 2006). The immobility is a parameter evaluated in the

forced swimming test and a reduction in sucrose preference in anhedonia test is interpreted as a depression-like behavior (Porsolt et al. 1977; Katz et al. 1981b; DellaGioia and Hannestad 2010; Réus et al. 2011), suggesting an imbalance in the noradrenergic and serotoninergic neurotransmission. In fact, human and animal studies have showed low levels of dopamine and serotonin associated with high levels of BCAA (Wajner and Vargas 1999; Wajner et al. 2000; Araújo et al. 2001). In this context, we suggest that the alterations in monoamine metabolism evoke adaptive changes in intracellular signal transduction and prevent these changes in the behavioral tasks. In addition, previous studies reported that antidepressant treatments present an antioxidant action. Imipramine treatment reversed the lipid peroxidation in brain of Sprague Dawley rats induced by chronic ozone (Mokoena et al. 2010). Réus and colleagues (2010) recently showed that imipramine also presents antioxidant properties, reducing oxidative damage and increasing superoxide dismutase and catalase activity in the rat brain. Additionally, imipramine (10 and 20 mg/kg) restored depleted reduced glutathione levels and catalase activity and attenuated raised lipid peroxidation and nitrite concentrations in sleep-deprived mice compared to untreated sleep-deprived mice (Kumar and Garg 2009). Thus, the effects of imipramine in preventing the changes in the behavioral tasks observed in H-BCAA rats might be also associated with its capability to maintain pro-/anti-oxidative homeostasis.

Some limitations of this study should be taken into consideration, such as the fact that the antioxidant drugs and the antidepressants were given from the start of the BCAA administration and this will not be possible in humans unless it is known before birth that they have MSUD. Besides, we cannot rule out a possible effect of the branched-chain alpha-keto acids that were also produced considering an in vivo model of MSUD, since the analyses of plasma and brain levels branched-chain alpha-keto acids were not performed. However, the present findings demonstrate a link between H-BCAA and depression in rats. Moreover, this investigation revealed that the antidepressant action of NAC/DFX and imipramine might be associated with its capability to maintain pro-/anti-oxidative homeostasis. Besides, NAC/DFX and imipramine interact with distinct receptor systems, such as the glutamatergic and monoaminergic systems, which could produce synergic effects on brain pathways involved in the modulation of depressive-like behavior.

Acknowledgments This research was supported by grants from Programa de Pós-graduação em Ciências da Saúde – Universidade do Extremo Sul Catarinense (UNESC) and Conselho Nacional de Desenvolvimento Científico e Tecnológico (CNPq).

Author Contribution

Giselli Scaini, Emilio L. Streck, and João Quevedo designed the study and wrote the protocol. Giselli Scaini, Gabriela C. Jeremias, Camila B. Furlanetto, and Diogo Dominguini conducted the experiments. Giselli Scaini and Clarissa M. Comim undertook the statistical analysis; and Giselli Scaini and Emilio L. Streck wrote the first draft of the manuscript. All authors contributed to and have approved the final manuscript.

Conflicts of Interest

Giselli Scaini, Gabriela C. Jeremias, Camila B. Furlanetto, Diogo Dominguini, Clarissa M. Comim, João Quevedo, Patrícia F. Schuck, Gustavo C. Ferreira, and Emilio L. Streck declare that they have no conflict of interest.

Informed Consent and Animal Rights

All institutional and national guidelines for the care and use of laboratory animals were followed. All experimental procedures were conducted in accordance with the National Institutes of Health Guide for the Care and Use of Laboratory Animals and the Brazilian Society for Neuroscience and Behavior recommendations for animal care.

References

Araújo P, Wassermann GF, Tallini K et al (2001) Reduction of large neutral amino acid levels in plasma and brain of hyperleucinemic rats. Neurochem Int 38:529–537

Arent CO, Réus GZ, Abelaira HM et al (2012) Synergist effects of n-acetylcysteine and deferoxamine treatment on behavioral and oxidative parameters induced by chronic mild stress in rats. Neurochem Int 61:1072–80

Baker DA, Xi ZX, Shen H, Swanson CJ, Kalivas PW (2002) The origin and neuronal function of in vivo nonsynaptic glutamate. J Neurosci 22:9134–9141

Banjac A, Perisic T, Sato H et al (2008) The cystine/cysteine cycle: a redox cycle regulating susceptibility versus resistance to cell death. Oncogene 27:1618–1628

Barschak AG, Sitta A, Deon M et al (2006) Evidence that oxidative stress in increased in plasma from pacients with maple syrup urine disease. Metab Brain Dis 21:279–286

Berk M, Malhi GS, Gray LJ, Dean OM (2013) The promise of N-acetylcysteine in neuropsychiatry. Trends Pharmacol Sci 34:167–177

Bridi R, Araldi J, Sgarbi MB et al (2003) Induction of oxidative stress in rat brain by the metabolites accumulating in maple syrup urine disease. Int J Dev Neurosci 21:327–332

Bridi R, Fontella FU, Pulrolnik V et al (2006) A chemically-induced acute model of maple syrup urine disease in rats for neurochemical studies. J Neurosci Methods 155:224–230

Bridi R, Latini A, Braum CA et al (2005) Evaluation of the mechanisms involved in leucine induced oxidative damage in cerebral cortex of young rats. Free Radic Res 39:71–79

Cavalleri F, Berardi A, Burlina AB, Ferrari F, Mavilla L (2002) Diffusion-weighted MRI of maple syrup urine disease encephalopathy. Neuroradiology 44:499–502

Chuang DT, Shih VE (2001) Maple syrup urine disease (branched-chain ketoaciduria). In: Scriver CR, Beaudet AL, Sly WS, Valle D (eds) The metabolic and molecular bases of inherited disease. McGraw-Hill, New York, pp 1971–2005

Danner DJ, Elsas LJ (1989) Disorders of branched chain amino acid and keto acid metabolism. In: Scriver CR, Beaudet AL, Sly WS, Valle D (eds) The metabolic basis of inherited disease. McGraw-Hill, New York, pp 671–692

DellaGioia N, Hannestad J (2010) A critical review of human endotoxin administration as an experimental paradigm of depression. Neurosci Biobehav Rev 34:130–143

Dimopoulos N, Piperi C, Psarra V, Lea RW, Kalofoutis A (2008) Increased plasma levels of 8-iso-PGF2alpha and IL-6 in an elderly population with depression. Psychiatry Res 161:59–66

Di-Pietro PB, Dias ML, Scaini G et al (2008) Inhibition of brain creatine kinase activity after renal ischemia is attenuated by N-acetylcysteine and deferoxamine administration. Neurosci Lett 434:139–143

Dodd PR, Williams SH, Gundlach AL et al (1992) Glutamate and gamma-aminobutyric acid neurotransmitter systems in the acute phase of maple syrup urine disease and citrullinemia encephalopathies in newborn calves. J Neurochem 59:582–590

Ferreira FR, Biojone C, Joca SRL, Guimarães FS (2008) Antidepressant-like effects of N-acetyl-L-cysteine in rats. Behav Pharmacol 19:747–50

Fontella FU, Gassen E, Pulrolnik V et al (2002) Stimulation of lipid peroxidation in vitro in rat brain by the metabolites accumulating in maple syrup urine disease. Metab Brain Dis 17:47–54

Forlenza MJ, Miller GE (2006) Increased serum levels of 8-hydroxy-2'-deoxyguanosine in clinical depression. Psychosom Med 68:1–7

Gamaro GD, Manoli LP, Torres IL, Silveira R, Dalmaz C (2003) Effects of chronic variate stress on feeding behavior and on monoamine levels in different rat brain structures. Neurochem Int 42:107–114

Gardner A, Boles RG (2011) Beyond the serotonin hypothesis: mitochondria, inflammation and neurodegeneration in major depression and affective spectrum disorders. Prog Neuro Psychopharmacol Biol Psychiatry 35:730–743

Gere-Paszti E, Jakus J (2009) The effect of N-acetylcysteine on amphetamine-mediated dopamine release in rat brain striatal slices by ion-pair reversed-phase high performance liquid chromatography. Biomed Chromatogr 23:658–664

Gilbert KR, Aizenman E, Reynolds IJ (1991) Oxidized glutathione modulates N-methyl-D-aspartate- and depolarization-induced increases in intracellularCa2+ in cultured rat forebrain neurons. Neurosci Lett 133:11–14

Ha JS, Kim TK, Eun BL et al (2004) Maple syrup urine disease encephalopathy: a follow-up study in the acute stage using diffusion-weighted MRI. Pediatr Radiol 34:163–166

Howell RK, Lee M (1963) Influence of a-keto acids on the respiration of brain in vitro. Proc Soc Exp Biol Med 113:660–663

Hutson SM, Lieth E, LaNoue KF (2001) Function of leucine in excitatory neurotransmitter metabolism in the central nervous system. J Nutr 131:846S–850S

Iyer SS, Jones DP, Brigham KL, Rojas M (2009) Oxidation of plasma cysteine/cystine redox state in endotoxin-induced lung injury. Am J Respir Cell Mol Biol 40:90–98

JanÄky R, Dohovics R, Saransaari P, Oja SS (2007) Modulation of [3H]dopamine release by glutathione in mouse striatal slices. Neurochem Res 32:1357–1364

Jou SH, Chiu NY, Liu CS (2009) Mitochondrial dysfunction and psychiatric disorders. Chang Gung Med J 32:370–379

Jouvet P, Rustin P, Taylor DL et al (2000) Branched chain amino acids induce apoptosis in neural cells without mitochondrial membrane depolarization or cytochrome c release: implications for neurological impairment associated with maple syrup urine disease. Mol Biol Cell 11:1919–1932

Katz RJ, Roth KA, Carroll BJ (1981a) Acute and chronic stress effects on open field activity in the rat: implications for a model of depression. Neurosci Biobehav Rev 5:247–251

Katz RJ, Roth KA, Carroll BJ (1981b) Animal models and human depressive disorders. Neurosci Biobehav Rev 5:231–246

Khanzode SD, Dakhale GN, Khanzode SS, Saoji A, Palasodkar R (2003) Oxidative damage and major depression: the potential antioxidant action of selective serotonin re-uptake inhibitors. Redox Rep 8:365–370

Krishnan V, Nestler EJ (2008) The molecular neurobiology of depression. Nature 455:894–902

Kumar A, Garg R (2009) Possible role of trazodone and imipramine in sleep deprivation-induced anxiety-like behavior and oxidative damage in mice. Methods Find Exp Clin Pharmacol 31:383–387

Lafleur DL, Pittenger C, Kelmendi B et al (2006) N-Acetylcysteine augmentation in serotonin reuptake inhibitor refractory obsessive–compulsive disorder. Psychopharmacology 184:254–256

Land JM, Mowbray J, Clark JB (1976) Control of pyruvate and h-hydroxybutyrate utilization in rat brain mitochondria and its relevance to phenylketonuria and maple syrup urine disease. J Neurochem 26:823–830

Leslie SW, Brown LM, Trent RD et al (1992) Stimulation of N-methyl-D-aspartate receptor-mediated calcium entry into dissociated neurons by reduced and oxidized glutathione. Mol Pharmacol 41:308–314

Linck VM, Costa-Campos L, Pilz LK, Garcia CRL, Elisabetsky E (2012) AMPA glutamate receptors mediate the antidepressant-like effects of N-acetylcysteine in the mouse tail suspension test. Behav Pharmacol 23:171–177

Lucca G, Comim CM, Valvassori SS et al (2008) Chronic mild stress paradigm reduces sweet food intake in rats without affecting brain derived neurotrophic factor protein levels. Curr Neurovasc Res 5:207–213

Maes M, De Vos N, Pioli R et al (2000) Lower serum vitamin E concentrations in major depression. Another marker of lowered antioxidant defences in that illness J Affect Disord 58(3):241–246

Maes M, Galecki P, Chang YS, Berk M (2011) A review on the oxidative and nitrosative stress (O&NS) pathways in major depression and their possible contribution to the (neuro) degenerative processes in that illness. Prog Neuropsychopharmacol Biol Psychiatry 35:676–92

Maes M, Mihaylova I, Kubera M, Uytterhoeven M, Vrydags N, Bosmans E (2009a) Increased 8-hydroxy-deoxyguanosine, a marker of oxidative damage to DNA, in major depression and myalgic encephalomyelitis/chronic fatigue syndrome. Neuro Endocrinol Lett 30:715–722

Maes M, Mihaylova I, Kubera M, Uytterhoeven M, Vrydags N, Bosmans E (2009b) Lower plasma Coenzyme Q10 in depression: a marker for treatment resistance and chronic fatigue in depression and a risk factor to cardiovascular disorder in that illness. Neuro Endocinol Lett 30:462–469

Magalhães PV, Dean OM, Bush AI et al (2011) N-acetyl cysteine add-on treatment for bipolar II disorder: a subgroup analysis of a randomized placebo-controlled trial. J Affect Disord 129:317–20

Mescka C, Moraes T, Rosa A et al (2011) In vivo neuroprotective effect of L-carnitine against oxidative stress in maple syrup urine disease. Metab Brain Dis 26:21–28

Mokoena ML, Harvey BH, Oliver DW, Brink CB (2010) Ozone modulates the effects of imipramine on immobility in the forced

swim test, and nonspecific parameters of hippocampal oxidative stress in the rat. Metab Brain Dis 25:125–133
Muelly ER, Moore GJ, Bunce SC et al (2013) Biochemical correlates of neuropsychiatric illness in maple syrup urine disease. J Clin Invest 123(4):1809–20
Nestler EJ, Gould E, Manji H et al (2002) Preclinical model: status of basic research in depression. Biol Psychiatry 52:503–528
Pilla C, Cardozo RF, Dutra-Filho CS, Wyse AT, Wajner M, Wannmacher CM (2003) Creatine kinase activity from rat brain is inhibited by branched-chain amino acids in vitro. Neurochem Res 28:675–679
Porsolt RD, Le Pichon M, Jalfre M (1977) Depression: a new animal model sensitive to antidepressant treatments. Nature 21:266–730
Prensky AL, Moser HW (1966) Brain lipids, proteolipids, and free amino acids in maple syrup urine disease. J Neurochem 13:863–874
Prensky AL, Moser HW (1967) Changes in the amino acid composition of proteolipids of white matter during maturation of the human nervous system. J Neurochem 14:117–121
Réus GZ, Stringari RB, de Souza B et al (2010) Harmine and imipramine promote antioxidant activities in prefrontal cortex and hippocampus. Oxid Med Cell Longev 3:325–331
Réus GZ, Stringari RB, Ribeiro KF et al (2011) Ketamine plus imipramine treatment induces antidepressant-like behavior and increases CREB and BDNF protein levels and PKA and PKC phosphorylation in rat brain. Behav Brain Res 221:166–171
Ribeiro CA, Sgaravatti AM, Rosa RB et al (2008) Inhibition of brain energy metabolism by the branched-chain amino acids accumulating in maple syrup urine disease. Neurochem Res 33:114–124
Scaini G, de Rochi N, Jeremias IC et al (2012) Evaluation of acetylcholinesterase in an animal model of maple syrup urine disease. Mol Neurobiol 45:279–86
Scaini G, Comim CM, Oliveira GM et al (2013a) Chronic administration of branched-chain amino acids impairs spatial memory and increases brain-derived neurotrophic factor in a rat model. J Inherit Metab Dis 36:721–730
Scaini G, Mello-Santos LM, Furlanetto CB et al (2013b) Acute and chronic administration of the branched-chain amino acids decreases nerve growth factor in rat hippocampus. Mol Neurobiol. doi:10.1007/s12035-013-8447-1
Schönberger S, Schweiger B, Schwahn B, Schwarz M, Wendel U (2004) Dysmyelination in the brain of adolescents and young adults with maple syrup urine disease. Mol Genet Metab 82:69–75
Sgaravatti AM, Rosa RB, Schuck PF et al (2003) Inhibition of brain energy metabolism by the a-keto acids accumulating in maple syrup urine disease. Biochim Biophys Acta 1639:232–238
Smaga I, Pomierny B, Krzyżanowska W et al (2012) N-acetylcysteine possesses antidepressant-like activity through reduction of oxidative stress: behavioral and biochemical analyses in rats. Prog Neuropsychopharmacol Biol Psychiatry 39:280–87
Strauss KA, Puffenberger EG, Morton DH (2006) Maple syrup urine disease. In: Pagon R, Bird T, Dolan C, Stephens K, Adam M (eds) GeneReviews. University of Washington, Seattle, Washington, USA
Taketomi T, Kunishita T, Hara A, Mizushima S (1983) Abnormal protein and lipid compositions of the cerebral myelin of a patient with maple syrup urine disease. Jpn J Exp Med 53:109–116
Tavares RG, Santos CE, Tasca CI, Wajner M, Souza DO, Dutra-Filho CS (2000) Inhibition of glutamate uptake into synaptic vesicles of rat brain by the metabolites accumulating in maple syrup urine disease. J Neurol Sci 181:44–49
Treacy E, Clow CL, Reade TR, Chitayat D, Mamer OA, Scriver CR (1992) Maple syrup urine disease: interrelationship between branched-chain amino-, oxo- and hydroxyacids; implications for treatment; associations with CNS dysmyelination. J Inherit Metab Dis 15:121–135
Tribble D, Shapira R (1983) Myelin proteins: degradation in rat brain initiated by metabolites causative of maple syrup urine disease. Biochem Biophys Res Commun 114:440–446
Tuon L, Comim CM, Antunes MM et al (2007) Imipramine reverses the depressive symptoms in sepsis survivor rats. Intensive Care Med 33:2165–2167
Varga V, Jenei Z, JanÄky R, Saransaari P, Oja SS (1997) Glutathione is an endogenous ligand of rat brain N-methyl-D-aspartate (NMDA) and 2-amino-3-hydroxy-5-methyl-4-isoxazolepropionate (AMPA) receptors. Neurochem Res 22:1165–1171
Venè R, Castellani P, Delfino L, Lucibello M, Ciriolo MR, Rubartelli A (2011) The cystine/cysteine cycle and GSH are independent and crucial antioxidant systems in malignant melanoma cells and represent druggable targets. Antioxid Redox Signal 15:2439–2453
Wajner M, Coelho DM, Barschak AG et al (2000) Reduction of large neutral amino acid concentration in plasma and CSF of patients with maple syrup urine disease during crises. J Inherit Metab Dis 23:505–512
Wajner M, Vargas CR (1999) Reduction of plasma concentrations of large neutral amino acids in patients with maple urine disease during crises. Arch Dis Child 80:579
Walterfang M, Bonnot O, Mocellin R, Velakoulis D (2013) The neuropsychiatry of inborn errors of metabolism. J Inherit Metab Dis 36(4):687–702
Willner P, Benton D, Brown E et al (1998) “Depression” increases “craving” for sweet rewards in animal and human models of depression and craving. Psychopharmacology 136:272–283
Willner P, Towell A, Sampson D, Sophokleous S, Muscat R (1987) Reduction of sucrose preference by chronic unpredictable mild stress, and its restoration by a tricyclic antidepressant. Psychopharmacology 93:358–364
Yagasaki Y, Numakawa T, Kumamaru E, Hayashi T, Su TP, Kunugi H (2006) Chronic antidepressants potentiate via sigma-1 receptors the brain-derived neurotrophic factor-induced signaling for glutamate release. J Biol Chem 281:12941–12949
Yudkoff M, Daikhin Y, Lin ZP et al (1994) Interrelationships of leucine and glutamate metabolism in cultured astrocyts. J Neurochem 62:1192–1202
Zielke HR, Zielke CL, Baab PJ, Collins RM (2002) Large neutral amino acids auto exchange when infused by microdialysis into the rat brain: implications for maple syrup urine disease and phenylketonuria. Neurochem Int 40:347–54
Zinnanti WJ, Lazovic J, Griffin K et al (2009) Dual mechanism of brain injury and novel treatment strategy in maple syrup urine disease. Brain 132:903–918